Volume n° 2 - from B16 to B33

32nd INTERNATIONAL GEOLOGICAL CONGRESS

PALEOZOIC OROGENIES IN THE FRENCH MASSIF CENTRAL A CROSS SECTION FROM BÉZIERS TO LYON

Leader: M. Faure

Associate Leaders: J.M. Lardeaux, P. Matte

Field Trip Guide Book - B22

Florence - Italy
August 20-28, 2004

Pre-Congress **B22**

The scientific content of this guide is under the total responsibility of the Authors

Published by:
APAT – Italian Agency for the Environmental Protection and Technical Services - Via Vitaliano Brancati, 48 - 00144 Roma - Italy

Series Editors:
Luca Guerrieri, Irene Rischia and Leonello Serva (APAT, Roma)

English Desk-copy Editors:
Paul Mazza (Università di Firenze), Jessica Ann Thonn (Università di Firenze), Nathalie Marléne Adams (Università di Firenze), Miriam Friedman (Università di Firenze), Kate Eadie (Freelance indipendent professional)

Field Trip Committee:
Leonello Serva (APAT, Roma), Alessandro Michetti (Università dell'Insubria, Como), Giulio Pavia (Università di Torino), Raffaele Pignone (Servizio Geologico Regione Emilia-Romagna, Bologna) and Riccardo Polino (CNR, Torino)

Acknowledgments:
The 32nd IGC Organizing Committee is grateful to Roberto Pompili and Elisa Brustia (APAT, Roma) for their collaboration in editing.

Graphic project:
Full snc - Firenze

Layout and press:
Lito Terrazzi srl - Firenze

Volume n° 2 - from B16 to B33

32nd INTERNATIONAL GEOLOGICAL CONGRESS

PALEOZOIC OROGENIES IN THE FRENCH MASSIF CENTRAL A CROSS SECTION FROM BÈZIERS TO LYON

AUTHORS:
M. Faure (University of Orléans - France)
P. Ledru (BRGM, Orléans - France)
J.M. Lardeaux (University of Nice - France)
P. Matte (CNRS, University of Montpellier - France)

Florence - Italy
August 20-28, 2004

Pre-Congress

B22

Front Cover:
View of gneiss-migmatite of the Montagne Noire axial zone (visited during D2) looking to the north. The village of Olargues is located in the micaschist envelope of the dome. The picture is taken from the northernmost part of the recumbent folds of the Montagne Noire southern side (visited during D1).

Leader: M. Faure
Associate Leaders: J.M. Lardeaux, P. Ledru, P. Matte

1. Introduction

The formation of the continental substratum of Medio-Europa occurred in Paleozoic times. The names of "Hercynian" or "Variscan" are used to deal with the geodynamic processes that took place from Cambrian to Carboniferous. It is now widely accepted that this Paleozoic Belt that crops out from Iberia to Bohemia (Fig. 1) results from a complex interplay of rifting, convergence and collision between three large continents, namely Laurentia, Baltica and Gondwana and several microcontinental stripes such as Avalonia or Armorica (Matte, 2001). Continental drifting and welding resulted in the opening and closure of several oceans such as Iapetus, Rheic and Medio-European. There is however a wide range of opinions concerning the location and width of these oceanic domains and the number, kinematics and timing of collisional processes (e. g. Autran and Cogné, 1980; Franke, 1989, 2000; Ledru et al., 1989; Matte, 1991; 2001; Faure et al., 1997).

The French Massif Central is one of the largest pieces of the Variscan Belt. The whole Massif Central provides a reference cross section throughout the north Gondwana margin deformed and metamorphozed during the Paleozoic. During the last two decades, and recently through the GéoFrance 3D program, developments made in the areas of geochronology, structural geology, metamorphic and magmatic petrology, allow us to draw a comprehensive structural map of the Massif Central and to discuss a possible scenario accounting for the Paleozoic tectono-thermal evolution.

This field trip presents representative lithological, structural, magmatic, metamorphic and geochronological data of the French Massif Central from unmetamorphozed kilometer-scale recumbent folds to UHP metamorphic rocks. Most of the controversial aspects of collisional orogens such as continental subduction and exhumation

Figure 1 - Location of the French Massif Central in the frame of the Paleozoic belt of Medio-Europa (Matte, 1991).

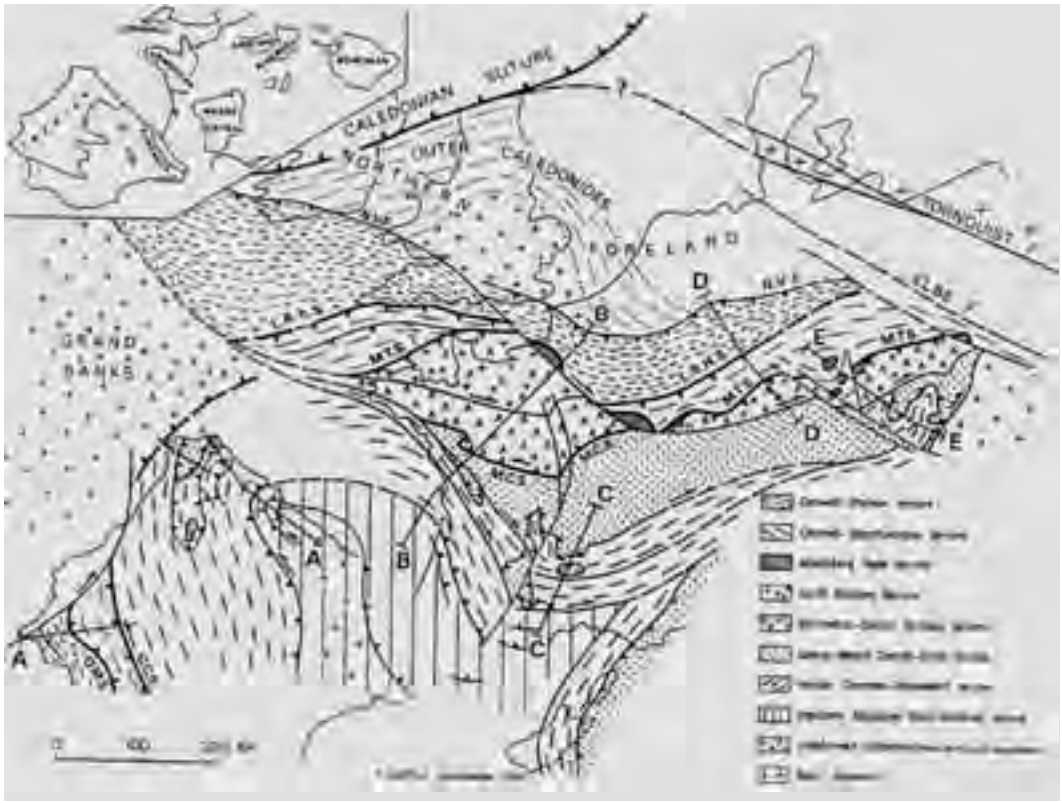

Volume n° 2 - from B16 to B33

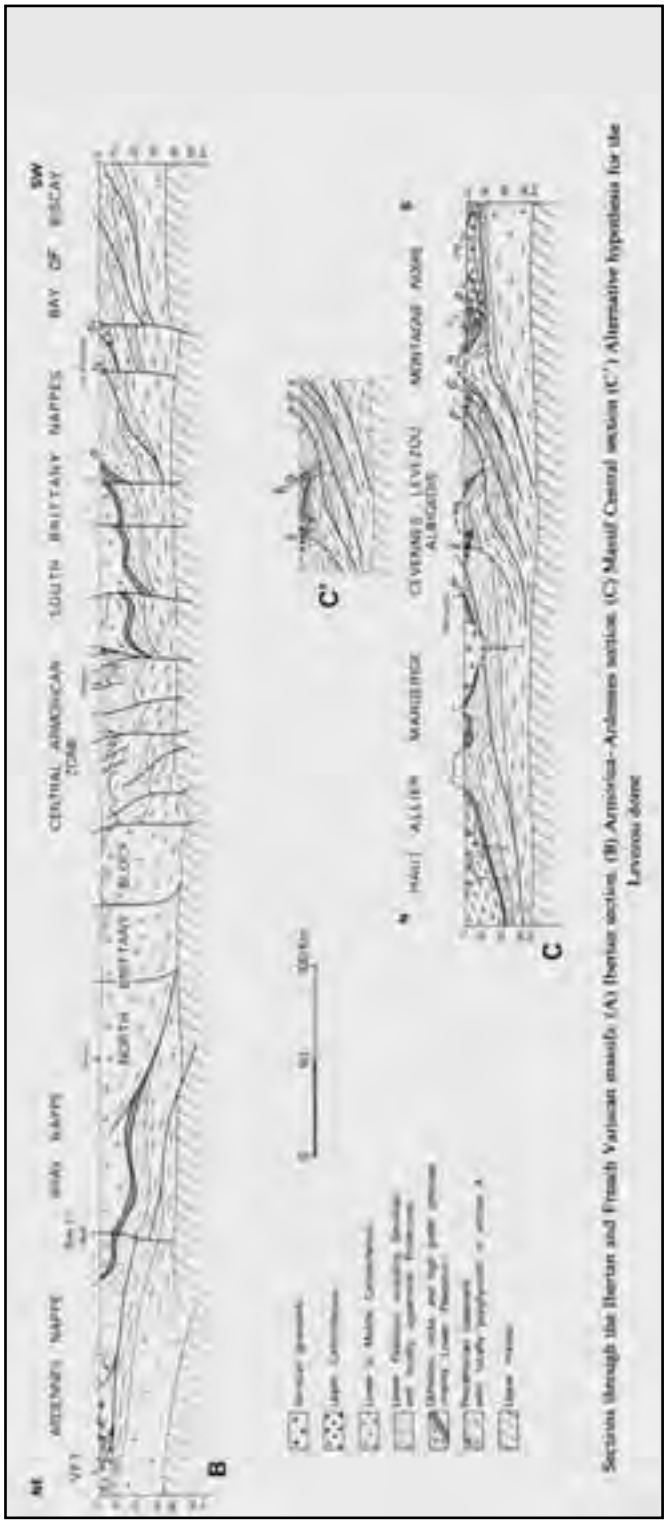

Figure 2 - Cross-sections from the Massif Armoricain to Ardenne (B) and through Massif Central (C). C' is an alternative section through the Lèvezou klippe (Matte, 1991).

of ultrametamorphic rocks, nappe kinematics, inverted metamorphism, syn- to post-orogenic extensional tectonics, crustal melting and tectonic setting of pluton emplacement will be addressed.

Field References

Topographic maps IGN 1/100 000: n°65 Béziers-Montpellier; n°58 Rodez-Mende; n°59 Privas-Alès; n°50 St-Etienne-Le Puy; n°51 Lyon-Grenoble.
Geologic maps BRGM 1/50 000: n°1014 St-Chinian; n°988 Bédarieux; n°862 Mende; n°863 Le Bleymard; n°839 Langogne; n°840 Burzet; n°792 Yssingeaux; n°745 St-Etienne; n°721 St-Symphorien-sur-Coise; n°697 Tarare.

2. Regional geological setting

2.1. A structural map of the French Massif Central.

It is now widely accepted that the structure of the French Massif Central is a stack of nappes (Ledru et al., 1989, 1994 Fig. 3). From top to bottom and also from south to north, six main tectonic units are distinguished.

i) The Southern Palaeozoic Fold and Thrust Belt involves a set of continental margin/platform series recording a more or less continuous sedimentation spanning from Early Cambrian to Early Carboniferous. The series is deformed within kilometer-scale recumbent folds well observed in the Montagne Noire area (Arthaud, 1970).

ii) The Para-autochthonous Unit that overthrusts the previous unit consists of a thick metapelite-metagrauwacke series (also called "Cévennes micaschists") with some quartzite beds and volcanic rocks. Although stratigraphic ages are lacking, a Neoproterozoic to Ordovician age is

Figure 3 - Structural map of the Massif Central (adapted from Ledru et al., 1989).

generally accepted.

iii) The Lower Gneiss Unit (LGU) is lithologically quite similar to the Para-autochthonous Unit. Early Cambrian and Early Ordovician alkaline granitoids, now transformed in augen orthogneiss, are also widespread. Both the Para-autochthonous Unit and Lower Gneiss Unit are interpreted as Proterozoic-Early Paleozoic remnants of the northern Gondwana margin that experienced crustal thinning and rifting in Ordovician times.

iv) The Upper Gneiss Unit (UGU) is made up of a bi-modal association called "leptynite-amphibolite" sequence which is a peculiar assemblage of mafic and felsic rocks. This unit experienced a higher metamorphic pressure under eclogite and HP granulite facies (ca. 20Kb). Ultra high-pressure metamorphism is reached locally near Lyon, coesite-eclogite facies rocks crop-out (Lardeaux et al., 2001). The protoliths of the UGU also include metasediments and granitoids. The upper part of the UGU consists of migmatites formed by the partial melting of pelitic and quartzo-feldspathic rocks within which amphibolite block are preserved as restites. Radiometric dates show that the magmatism occurred in Early Ordovician times (ca. 480 Ma) and the high-pressure metamorphism in Late Silurian (ca. 420-410 Ma, Pin and Lancelot, 1982; Ducrot et al., 1983). Due to the occurrence of rare metagabbros and serpentinized ultramafics, the UGU is considered by some authors as a remnant of an oceanic domain, the Medio-European Ocean, that opened in Early Paleozoic times during the rifting that led to the separation of Armorica from North Gondwana (e. g. Dubuisson et al., 1989; Matte, 1991). However, it is worth noting that the Upper Gneiss Unit is not a true ophiolitic sequence since oceanic sedimentary rocks such as radiolarites or siliceous shales are lacking and ultramafics or serpentinites are rare. A likely interpretation would be to consider that the UGU is a transitional crust between true continental and oceanic ones.

v) The Thiviers-Payzac Unit that crops out in the south Limousin, is the highest tectonic unit of the allochthonous stack in the French Massif Central. It is formed by Cambrian metagraywackes, rhyolites and quartzites intruded by Ordovician granite. Conversely to the underlying UGU, the Thiviers-Payzac Unit never experienced the high-pressure metamorphism. As revealed by seismic reflection line (Bitri et al., 1999), these relatively low grade rocks tectonically overly the UGU.

vi) In the NE Massif Central, near Lyon, the Brevenne Unit consists of mafic magmatic rocks (pyroclastites, pillow basalts, diabases, gabbros), serpentinized ultramafics, acidic volcanic rocks,

and siliceous sediments (radiolarites, siltites). The acidic rocks are dated of 366 ± 5 Ma (U/Pb method on zircon, Pin and Paquette, 1998). Petrology and geochemistry show that the Brevenne Unit and its extension in the Beaujolais area is a Middle Devonian oceanic sequence formed within an oceanic or a back-arc basin opened within the UGU (Sider and Ohnenstetter, 1986; Pin, 1990; Pin and Paquette, 1998). The Brevenne Unit records an early thrusting to the NW over the UGU followed by a NE-SW dextral strike-slip (Feybesse et al., 1988; Leloix et al., 1999). The precise age of the thrusting is unknown but since the metamorphic rocks are concealed below the Early Visean calcareous sandstone of the famous unconformity of Le Goujet (east of Lyon) an Early Carboniferous age is likely (see below).

2.2. The tectono-metamorphic evolution.

Structural information related to the high-pressure metamorphism and the prograde metamorphic evolution is poorly documented since these rocks are known only as relics. It is therefore quite difficult to draw a general view of this event. Moreover, three main synmetamorphic ductile events are recognized.

The earliest deformation found in the UGU, D1, is characterized by a NE-SW trending lineation with a top-to-the-SW shearing developed coevally with an intermediate pressure/intermediate temperature metamorphism and anatexis dated around 385-380 Ma (e. g. Floc'h, 1983; Quenardel and Rolin, 1984; Costa, 1992; Boutin and Montigny, 1993; Duthou et al., 1994; Roig and Faure, 2000; Figs. 4, 5). Since the D1 event is found in the migmatites that form the upper part of the UGU, it occurred during or at the end of the exhumation of the high-pressure metamorphic rocks. The radiometric dates comply with the Devonian stratigraphic age of the unmetamorphozed rocks (e. g. Villedé d'Ardin, Génis, Somme, Belfort

Figure 4 - Structural and geochronologic features related to the Late Silurian-Middle Devonian D1 event.

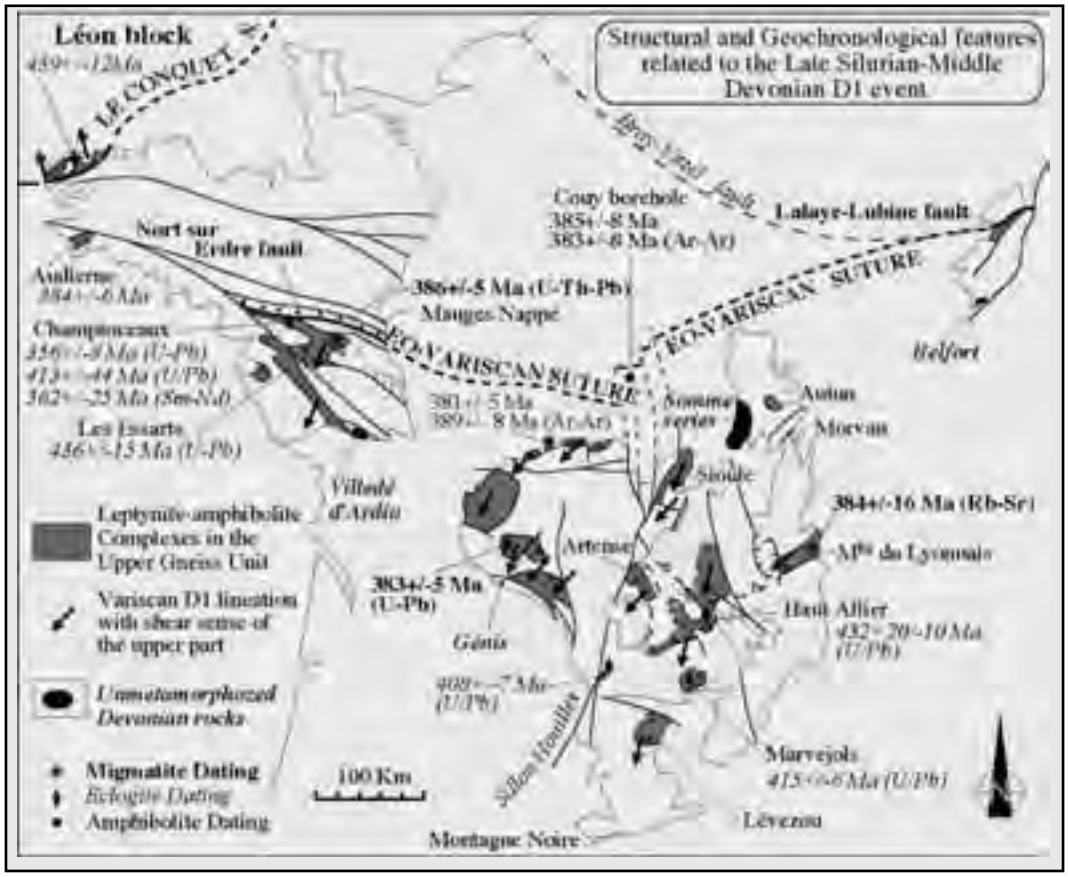

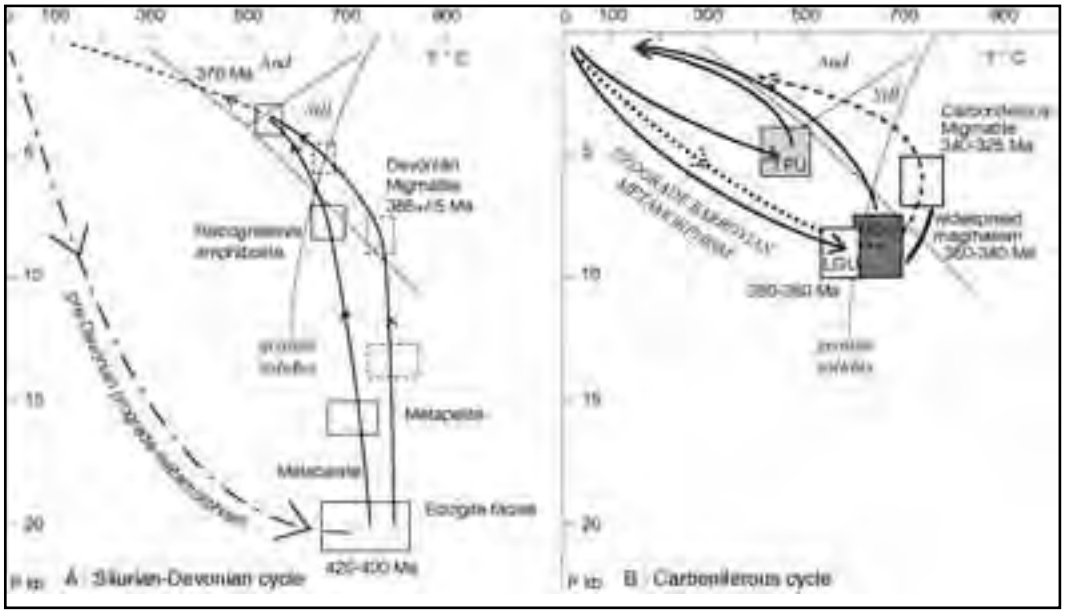

Figure 5 - P-T paths of the Silurian-Devonian and Carboniferous events for the different units.

areas, Fig. 4). Although a direct unconformity is never observed, field relationships suggest that D1 is older than Middle Devonian.

The second event, D2, is characterized by a NW-SE trending lineation coeval with a barrovian type metamorphism (Figs. 5, 6). $^{40}Ar/^{39}Ar$ dates on biotite, muscovite and amphibole range around 360-350 Ma. Most of the shear criteria developed along the NW-SE lineation indicate a top-to-the-NW shearing. In the Rouergue area, the Naucelle thrust is related to this event (Duguet and Faure, in press). The last increment of the ductile deformation in the metamorphic series is associated with the emplacement of peraluminous cordierite bearing granitoids such as the Guéret pluton that is the largest massif of this type. These granitoids exhibit magmatic to sub-solidus fabrics that comply with the synkinematic character of these plutons (e. g. Roig et al., 1998). A similar tectonic-metamorphic-magmatic pattern is also recognized in the south part of the Massif Armoricain. The closure of the Brevenne oceanic basins is chronologically and kinematically in agreement with the D2 event (Leloix et al., 1999). The geodynamic significance of the NW-SE lineation parallel to the belt is not clearly understood yet. Several hypotheses have been proposed (e. g. Burg et al., 1987; Bouchez and Jover, 1986; Mattauer et al., 1988) but none of them appears fully convincing. As discussed in section 2.4, this Early Carboniferous deformation is coeval with the closure of the Rheic Ocean and collision between Gondwana and Laurussia.

The third event, D3, is restricted to the southern part of the Massif Central. In the Para-autochthonous Unit of Cévennes-Albigeois, upper greenschist to amphibolite facies rocks are deformed by top-to-the-south ductile shearing along a submeridian lineation (Fig. 7). Available $^{40}Ar/^{39}Ar$ dates on the metamorphic minerals yield Visean ages around 340 Ma (Monié et al., 2000; Faure et al., 2001). This thrusting propagates southward in the Fold and Thrust Belt where kilometer-scale recumbent folds develop from Visean to Namurian. Although in the South Massif Central south-directed compressional regime lasts from Visean to Namurian (345 to 325Ma), conversely, in the northern part of the massif, the Late Visean (ca. 340 Ma) is a turning point in the tectonic evolution.

From Morvan to Limousin, the Late Visean time corresponds to the onset of syn-orogenic extension caracterized by a huge crustal melting. Structural studies indicate that the syn-orogenic extension is controled by a NW-SE maximum stretching direction (Fig. 7). The NW-SE spreading of the inner part of the Massif Central is also partly accommodated by ductile wrench faults well developed in Limousin (e. g. La Courtine or S. Limousin faults, Fig. 7) and in the Massif Armoricain. In the scale of the whole

Figure 6 - Structural, magmatic and geochronologic features related to the Late Devonian-Early Carboniferous D2 event (AMBP: Magnetic Anomaly of Paris Basin).

belt, the Late Visean to Namurian compression is also responsible for the development of north-directed thrusts in Ardenne and SE England.
The last ductile deformation events (ca. 320 Ma and younger ones) took place during the collapse of the belt. Since they are closely associated to magmatism, they will be considered in the next section.

2.3. A magmatic outline.
Like all the Variscan massifs, the Massif Central is also characterized by a voluminous magmatism mainly derived from crustal melting. Several generations of migmatites and granitoids are recognized (e. g. Duthou et al., 1984).

2.3.1. The pre-orogenic magmatism is not presented in detail here. The Early Ordovician bimodal magmatism, responsible for the formation of the leptynite-amphibolite complex in the UGU, and the Cambrian or Ordovician magmatic rocks are ductilely deformed, metamorphozed and included in the stack of nappes.

2.3.2. The Middle to Late Devonian calc-alkaline volcanic and volcaniclastic rocks that crop out in the Morvan area (called the Somme series) belong to a magmatic arc (Fig. 8; Pin et al., 1982; Delfour, 1989). In the south part of the Massif Armoricain, Eifelian-Givetian basaltic pillow lavas form the Meilleraie series. These rocks are interpreted as the aerial part of a magmatic arc. Moreover, mafic calk-alcaline rocks well known for a long time in the Limousin (Didier and Lameyre, 1971), are interpreted as the deep part of the same Devonian arc. Its geodynamic significance will be discussed in section 2.4.

2.3.3. The Tournaisian late-collisional magmatism is represented by the Guéret-type granites peraluminous plutons. Their magmatic fabric suggests that those plutons emplacement was controlled by the same strain field than the D2 deformation (Fig. 6) .

2.3.4. The Visean magmatism is well developed in the north and west part of the massif Central (Fig. 7). It consists in aerial products with lava flows, ignimbrites, pyroclastic deposits, called "Tufs anthacifères series", rhyolitic to dacitic dykes and hypovolcanic microgranites. Geochemistry indicates that crustal melting was triggered by heat imput from the mantle. Moreover, a mantle contribution as the source of magma is also likely (Pin and Duthou, 1990). The structural control of dyke intrusion complies with a NW-SE stretching related to the early stage of orogenic collapse. In the northern Cévennes, the Para-autochthonous Unit is underlain by migmatitic ortho- and paragneiss called " the Masméjean Unit " or pre-Velay migmatites (Faure et al., 2001). The anatexis is dated between 333 and 324 Ma by the Chemical U/Th/Pb method on monazite (Be Mezème, 2002). The migmatites and cordierite granites of the

Figure 7 - Structural and geochronologic features related to the Visean-Namurian D3 tectonics and Late Visean magmatism (AMBP: Magnetic Anomaly of Paris Basin).

Montagne Noire Axial Zone (cf D2 field itinerary in section 3) yield similar ages. In the present state of knowledge, this Late Visean event is still poorly studied. It is likely that other pre-Velay migmatites are not yet recognized also within the Velay dome.

2.3.5. The Namurian-Westphalian plutonism corresponds to the main period of magma production in the French Massif Central. It is well acknowledged (Didier and Lameyre, 1971) that this magmatism is represented by two types of granitoids, namely porphyritic monzogranites, such as the Margeride or Pont-de-Montvert-Borne plutons, and biotite-muscovite leucogranites such as the Brame or Millevache

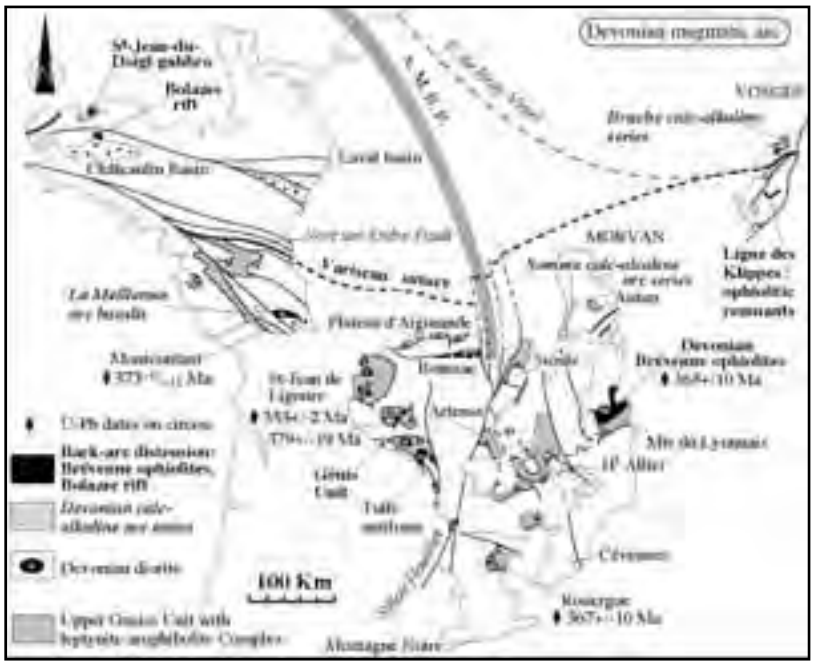

Figure 8 - Map showing the distribution of the Devonian plutons and volcanic rocks related to the magmatic arc and ophiolites (Brè venne, Ligne Klippes) interpreted as back arc basins (adapted from Faure et al., 1997).

Figure 9 - Distribution of the main granitic plutons coeval with the stretching lineation and kinematics related to theNamurian-Westphalian extensional tectonics. During this event, the pre-Visean GuÈret pluton behaves as a rigid body.

massifs (Fig. 9). Although both granite types crop out throughout the Massif Central, the former type is best represented in the central and southern parts of the massif and the later type is more abundant in the north and west parts. The two types were derived from different magmas, but field relationships and geochronology show that these two magmatic types emplaced coevally. Petro-structural and AMS studies of the Namuri-Westphalian plutons show that these bodies are characterized by a conspicuous NW-SE trending mineral, stretching and magnetic lineation. The same trend is also observed in biotite ans andalusite contact minerals in the pluton host rocks (Fig. 9). In the north Limousin, the Brame pluton is bounded to the west by the Nantiat ductile normal fault that also exhibits a NW-SE trending hot slickenline. A similar kinematics is also found along the Argentat ductile normal fault. This structural pattern is interpreted as the consequence of the syn-orogenic extensional tectonics of the Massif Central (Faure, 1995).

2.3.6. The Stephanian magmatism is represented by cordierite granite and migmatites of the Velay dome, and also by acidic tuf, ash layers and more rarely alkaline basalts interlayers with terrigeneous formations in the coal basins. The Velay dome is bounded to the north by a detachment fault, the Pilat ductile normal fault (Malavieille et al., 1990). Gneiss and micaschists belonging to the LGU that crop out north of the Pilat fault form the substratum of the Late Carboniferous St-Etienne basin.

2.4. A possible geodynamic scenario.

The above-presented data allow us to discuss a geodynamic evolution model. Presently, two scenari for the evolution of the French Massif Central are proposed. The first one emphasizes a continuous convergence between Gondwana and Laurussia from Silurian to Early Carboniferous (e. g. Matte, 1991, Lardeaux et al., 2001). The second one points out a polycyclic evolution (Pin, 1990; Faure et al., 1997). According to this model, an Early Paleozoic cycle, (Cambrian to Early Devonian), is related to the opening and closure of the Medio-European Ocean and correlatively drifting and rewelding of Armorica to Gondwana. A second orogenic cycle ranging from Middle Devonian to Carboniferous accounts for which the closure of the Rheic Ocean and the collision of Gondwana and Laurussia. Whatever the preferred model, the following stages are acknowledged.

2.4.1. The breaking of the north Gondwana margin.

From Cambrian to Early Silurian, the Massif Central belongs to the northern passive margin of Gondwana which extends from South America to China. From the study of Montagne Noire, the Cambrian-Ordovician corresponds to a terrigeneous environment, followed in Devonian by a carbonate platform. The lack of Late Ordovician and Silurian deposits is interpreted as the result of erosion on tilted blocks (Robardet et al., 1994). Evidence of an Ordovician rifting is also inferred from magmatism. In the Para-autochthonous Unit, alkaline mafic volcanics (sometimes with pillow lava), diabase dykes, gabbro intrude the grauwacke-pelite series (Pin and Marini, 1993). In LGU, the alkaline Ordovician granitoids also comply with continental rifting. It is worth noting that “pseudo-calc-alkaline” geochemistry of these granitoids is due to crustal contamination (Duthou et al., 1984; Pin and Duthou, 1990). In the UGU, crustal thinning due to continental rifting is coeval with the emplacement of the leptynite-amphibolite complexes. As a matter of

Figure 10 - Devonian geodynamic reconstruction (map and section) showing the closure of the Rheic Ocean by southward subduction below Gondwana and related microcontinents (from Faure et al., 1997).

fact, the Cambrian-Ordovician period is characterized by the formation of continental stripes, such as the Armorica microcontinent drifted from the north Gondwana margin. The question of the maximum width of the intervening Medio-European Ocean has not been not settled yet (see discussion in Robardet, 2003). A rough estimate suggests that this oceanic area was of limited extension (i. e. between 500 and 1000 km).

2.4.2. The closure of the Medio-European Ocean.
On the basis of available dates on the high-pressure metamorphism, the closure of the Medio-European Ocean started in Silurian. All authors accept a northward subduction of the Gondwana margin, however, structural constraints (i. e. kinematics coeval with the development of high-pressure assemblages) or geodynamic evidence (i. e. relics of a magmatic arc) are lacking. By Middle Devonian time, the Armorica microcontinent is rewelded to Gondwana. In NE Massif Central, (North of Lyon), undeformed and unmetamorphozed Givetian sedimentary rocks unconformably cover the migmatites and high pressure rocks (Delfour, 1989; Godard, 1990). Subduction of oceanic and continental rocks is followed by their exhumation in Early to Middle Devonian, around 390-385 Ma. The lack of large volumes of Devonian clastic rocks suggests that exhumation was tectonically assisted. Exhumation results in the extensive retrogression of the high-pressure rocks of the UGU and migmatisation of the pelitic parts.

2.4.3. Mid-Devonian magmatic arc-back arc system.
Frasnian-Fammenian calc-alkaline volcanism in the NE Massif Central and Vosges argue for subduction. In addition, the 380-370 Ma calc-alkaline diorite, tonalite, granodiorite plutons that crop out in NW Massif Central are interpreted as the deep part of this magmatic arc. However, in their present position, these plutons are rootless and tectonically included into the Hercynian nappes. Southward subduction of the Rheic Ocean is viewed as the cause of the calc-alcaline magmatism. At the same time, distension also occurred in the upper plate, giving rise to limited oceanic zones such as the Brévenne in the Massif Central or other areas in the Massif Armoricain and Vosges. Therefore, an arc-back arc pattern appears as the most likely geodynamic setting for Devonian times (Fig. 10). However a discussion of the Léon and microcontinents is beyond the scope of this presentation.

2.4.4. The closure of the Rheic Ocean and the Tournaisian collision.
Since the Late Fammenian, a complete closure of the Rheic Ocean led to a collision between the North European continent made by the assembly of Laurentia, Baltica and Avalonia during the Caledonian orogeny and Gondwana, including Armorica microcontinent rewelded to it. Intracontinental shortening follows the Lizard ophiolite obduction

Volume n° 2 - from B16 to B33

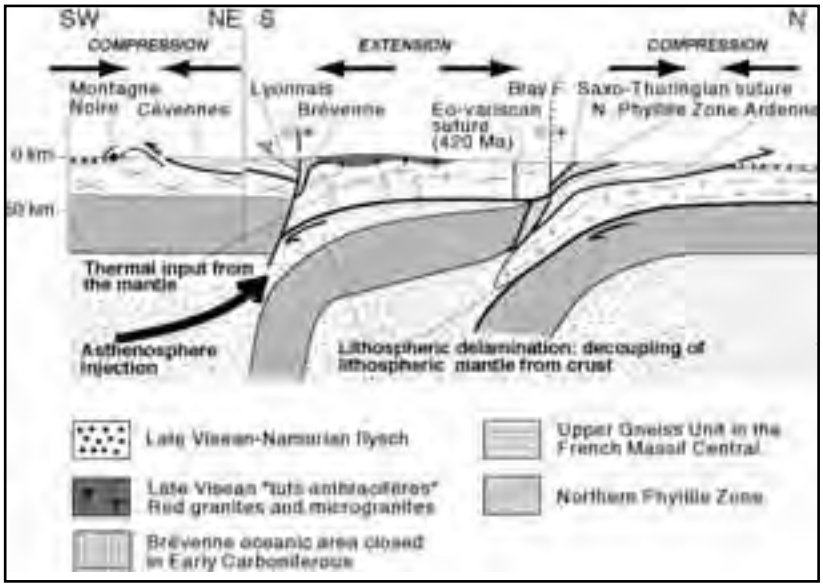

Figure 11 - Interpretative lithosphere scale cross section through the French Hercynian Belt in Late Visean. Mantle lithosphere delamination may account for the contrasted tectonic regimes (extensional and compressional), magmatism and heat flow in the central part of the belt (modified from Faure et al., 2002).

(which probably extends along the Magnetic Anomaly of Paris Basin). North-directed thrusts develop from the South of England to the Ardennes. In the northern Massif Central, the closure of the Brévenne oceanic area is characterized by top-to-the-NW shearing under upper greenschist-lower amphibolite facies in the mafic rocks. Top-to-the-NW ductile shearing coeval with middle temperature / middle pressure metamorphism, and dated around 360 Ma is also widespread in western and northern Massif Central. In the southern part of the Massif Central, southward shearing and recumbent folding develops with a progressively younging southward: ca. 345-340 Ma in the Para-autochthonous Unit to 330-325 Ma in the Fold and Thrust Belt.

2.4.5. Late Visean-Namurian syn-convergence extension.

As soon as Late Visean (ca 335 Ma), the northern Massif Central experienced crustal melting responsible for the "tufs anthracifères" acidic volcanism and related plutonism. The structural analysis of the Late Visean plutons and dykes emplacement is controlled by a NW-SE maximum stretching direction and argue for an incipient stage of syn-orogenic collapse in the inner part of the belt (Fig. 7). However, the southern and northern external zones of the Hercynian Belt, such as Montagne Noire and Ardenne respectively, are still under compression as shown by the development of kilometer-scale recumbent folds and thrusts.

In the Central and southern Massif Central, the thermal overprint is reponsible for migmatite and cordierite granite formation. The ca 330 Ma migmatites that crop out in the Montagne Noire Axial Zone and south of the late Carboniferous Velay massif belong to this event. However, in the present state of knowledge, the tectonic setting (namely extensional or compressional tectonic regime) is not settled yet. Decoupling of lithospheric mantle from crust, i. e. lithospheric delamination, is likely to play a significant role to account for the magmatism (Fig. 11).

From Namurian to Westphalian (ca 325-310 Ma), orogen parallel extension is well recorded by emplacement fabrics of leucogranites and granodiorites in the Massif Central (Fig. 9). In the Massif Armoricain, leucogranitic are also widespread. There, they are syn-kinematic plutons coeval with dextral wrenching (e. g. Berthé et al., 1978). However, it is worth noting that both in the Massif Armorican and Massif Central the wrench or extension controlled synkinematic plutons exhibit the same NW-SE maximum stretching direction. This tectonic stage corresponds also to the main metallogenetic epoch for mesothermal gold deposits.

2.4.6. Stephanian post-orogenic NNE-SSW extension

The last stage of the Hercynian orogeny in the French Massif Central corresponds to the collapse of the whole belt. Extensional regime is well recorded by the tectonic setting of intra-mountain Stephanian coal basins. Two structural types of basins are recognized : 1) half-graben bounded by pure normal faults or normal faults with a

Figure 12 - Massif Central map showing the Carboniferous extensional structures: coal basins, Velay granite-migmatite dome.

Figure 13 - Structural map of the Montagne Noire modified from Gèze (1949) and Arthaud (1970).

strike-slip component or 2) pull-apart controlled by wrench faults (Fig. 12). Among these intra-mountain basins, the St-Etienne coal basin is one of the most famous since it corresponds to the para-stratotype of the Stephanian stage. Nevertheless the structural control, either as a left-lateral pull apart or a half-graben is not settled yet (Mattauer and Matte, 1998). In the scale of the Massif Central, the deformation pattern of Stephanian extension is characterized by NE-SW stretching, NW-SE and vertical shortening. The amount of extension increases from west to east. NE-SW extension and correlatively coal basins are widespread in eastern Massif Central but are rare in western Massif Central and almost lacking in the Massif Armoricain. Several N-S to NNE-SSW trending wrench faults such as the Sillon Houiller and Argentat fault are interpreted as transfer faults that accommodate different amounts of extension. Magmatism and mid-crustal deformation associated to Late Carboniferous extension are less developed than during syn-convergence extension. The most spectacular structure is the 100 km diameter migmatitic-granitic Velay dome (Ledru et al., 2002). Heat imput from the mantle is responsible for high temperature granulitization of the lower crust (Pin and Vielzeuf, 1983).

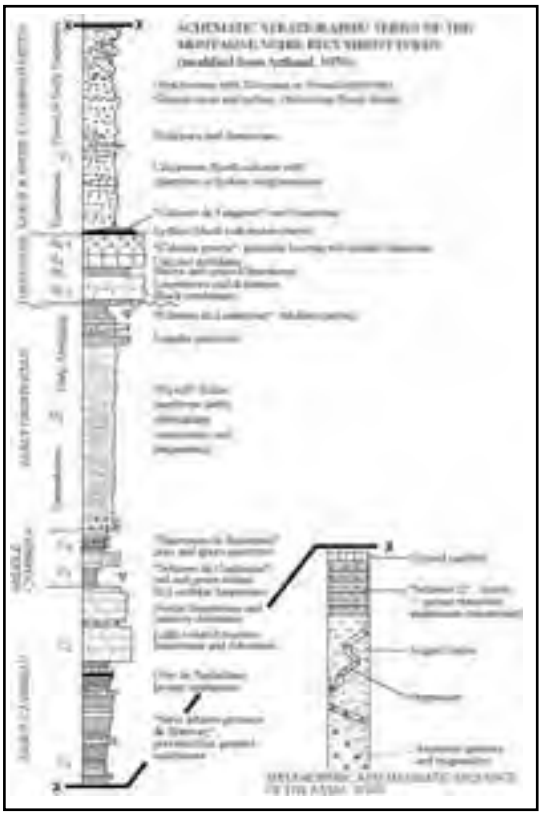

Figure 14 - Schematic stratigraphic column of the Paleozoic series found in the Montagne Noire southern side recumbent folds (adapted from Arthaud, 1970).

3. Field itinerary

DAY 1

Recumbent folding in the Montagne Noire Southern Side

Montpellier--> Béziers --> Cessenon D 136 to St-Nazaire de Ladarez

A. Geologic setting

Following Gèze (1949) and Arthaud (1970), the Montagne Noire area is classically divided from South to North, into a Southern Side, an Axial Zone and a Northern Side (Fig. 13). This last area is less studied than the previous two. The geology of the Axial Zone will be presented during D2. The Southern Side is worldwide famous for Paleozoic stratigraphy (Lower Cambrian,

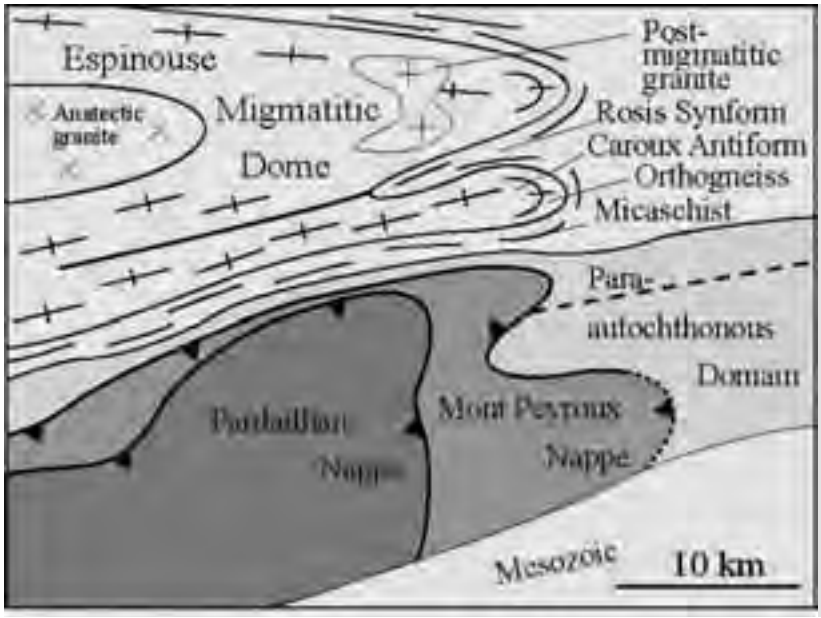

Figure 15 - Sketch of the main units observed in the eastern part of the Montagne Noire.

Lower Ordovician, Devonian, Carboniferous) and the development of kilometer-scale recumbent folds (or nappes). The stratigraphic column is schematically summarized in Fig. 14.

Five tectonic units are recognized in the southern side of the Montagne Noire, namely from top to bottom (Fig. 15):

i) The Pardailhan Nappe (or recumbent fold)

ii) The Mont Peyroux Nappe

iii) The Monts de Faugères Unit

iv) The Cabrières Unit

v) The Para-autochthonous domain

The Pardailhan Nappe consists of folded and overturned Cambrian to Devonian rocks. The Mont Peyroux Nappe includes Ordovician to Visean rocks. The Monts de Faugères Unit consists of several overturned folds of Devonian to Visean rocks. The Cabrières Unit is an olistostrome, with large-scale olistoliths of Carboniferous and Devonian limestones, Silurian volcanites and Ordovician turbidites are resedimented within a wild-flysch matrix corresponding to the foreland basin of the belt (Engel et al., 1980).

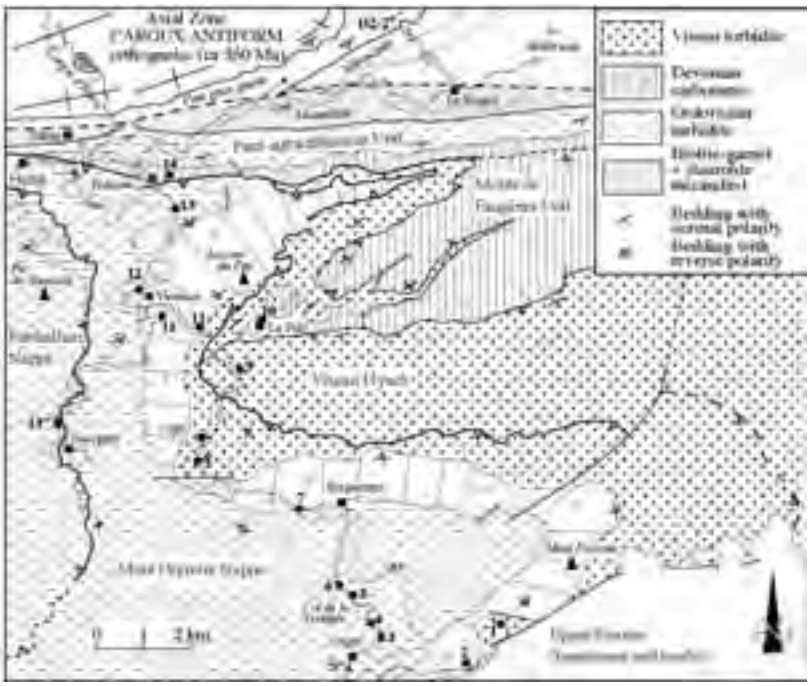

Figure 16 - D1 route map.

The Pardailhan Nappe exhibits a conspicuous axial planar cleavage, whereas in the Mont Peyroux Nappe, the transition between ductile deformation with axial planar cleavage folds and synsedimentary structures can be observed. On the basis

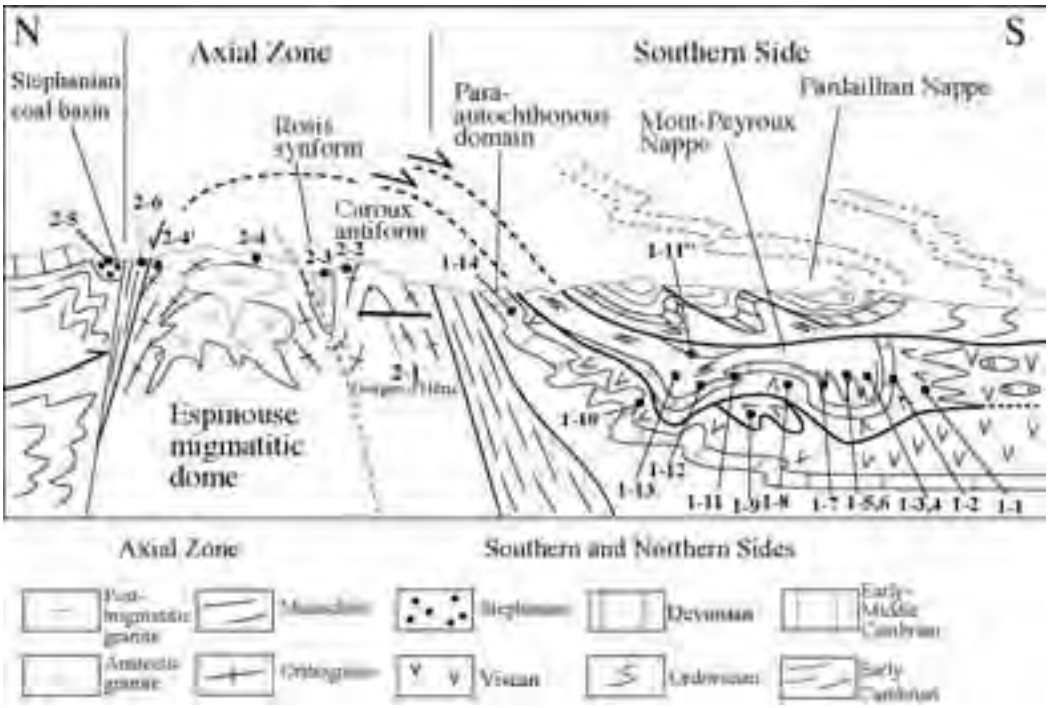

Figure 17 - Synthetic cross section of the Montagne Noire with location of the D1 and D2 stops.

of stratigraphy, those nappes were emplaced in Visean-Namurian times (around 330-325Ma).

The aim of this first day is to present the polyphase deformation of the Mont Peyroux recumbent fold through a South to North cross section along the Orb river (Fig. 16). There, the stratigraphic succession ranges from Early Ordovician (Tremadoc-Arenig) to Middle Carboniferous (Visean). Along this route, deformation and metamorphism increase from South to North, however most of the observed structures develop after recumbent folding during an upright deformation linked with the formation of the Axial Zone dome (cf. D2).

B. Stop description

The stops will show most of the lithological and structural aspects of the Mont Peyroux nappe and Para-autochthonous domain underneath (Figs. 16, 17).

Stop D1.1:

Visean flysch with limestone blocks.

The landscape shows Eocene limestone unconformably overlying at low angle Paleozoic rocks. The S. part of the section exposes Visean flysch with continuous sandstone beds dipping east (20E 60). The northern part that is folded and sheared exposes disrupted beds with sandstone lenses and limestone blocks. Devonian limestone overlying the Visean turbidite is seen on the other side of the valley and nearly 200m to the north of this stop.

Stop D1.2:

Coumiac quarry (protected area)
-Frasnian/Famennian boundary.

This old quarry was mined for red nodular limestone exported all over the world (e. g. the White House in Washington, or the Maison de la France in Rio de Janeiro). The vertical beds (N 30. 90) are Late Devonian (365 Ma) Goniatite limestone called “Griotte marble” (griotte is a type of cherry). This section has been chosen as the Global Stratotype Section for the Frasnian/Famennian boundary. This series corresponds to the “Famenian Biological Crisis” responsible for one of the most severe mass extinction in the Earth history (Kapper et al., 1993).

Stop D1.3:

Early Ordovician turbidite. NE of Lugné.

In the landscape, looking to the SE, the vertical cliffs are Early Devonian limestones continuous with those seen in the previous stop (D1-2) in the Coumiac quarry.

Sandstone-mudstone alternations lie subhorizontally, however graded bedding and load cast show that the sequence is upside down. Folds are apparently overturned to the north but correspond in reality to the inverted limb of the Mont Peyroux recumbent fold. This Early Ordovician turbidite is interpreted as deposited along the northern passive margin of Gondwana.

Stop D1.4:

Early Ordovician turbidite.

A few hundred meters from the previous stop.

The subvertical to north dipping upside down of the beds exhibits numerous load casts, ripple marks and bioturbation evidence (worm burrows). Locally Lingula shells can be abundant. Sandstones contain abundant floatted muscovite and heavy minerals. In this outcrop, like the previous one, cleavage is lacking.

Stop D1.5:

Panorama on Roquebrun synform and the Orb River. Col de la Vernède.

Below the road, the vineyards and Orb river are located in the Ordovician turbidites which form the core of the Roquebrun synform. Looking northward, above the Roquebrun village, the white cliffs are Devonian limestones. In the background, the hills with bushes are Visean flysch and in the distance, the last hills are made of Devonian limestone belonging to the Monts de Faugères Unit. To the West (left), the highest mountain is the Pic de Naudech made of inverted Cambrian rocks overlying inverted Ordovician turbidites belonging to the Pardailhan Nappe. Lastly, the farthest mountain to the NW is the Mt Caroux composed of orthogneiss belonging to the Axial Zone.

Along the other side of the road, the Ordovician turbidite is complexly folded. Superimposed folds are observed in the next stop.

Stop D1.6:

Superimposed folds in Ordovician turbidite. 200 m down to Roquebrun.

The Ordovician turbidite experienced two folding phases. Recumbent isoclinal folds (F1) are deformed by upright open folds (F2) with axes plunging 50° NW. F1 are related to the Mont Peyroux recumbent fold and F2 belong to the kilometer-scale upright folding responsible for the Roquebrun synform, Vieussan synform, and Axial Zone antiform (Fig. 17).

Stop D1.7:

Ordovician-Devonian contact. North of Roquebrun.

This stop shows the inverted stratigraphic contact between Ordovician detritals and Devonian carbonates in the northern limb of the Roquebrun synform. From south to north: Ordovician turbidite with top-to-the-S base (with load casts) dipping southward is underlain by Devonian calcareous sandstone, followed by limestone and dolomite. At the northern end of the outcrop, undeformed crinoid stems can be observed in the Devonian carbonates.

Stop D1.8:

Visean flysch. Chapelle St-Poncian, S. of Ceps.

Looking to the NW, the white rocks above the village of Ceps are inverted Devonian limestone, and to the W and SW, the vineyards are located in the Ordovician turbidite. The highest white cliff in the background (La Tour du Pin summit) is the northern extension of Devonian formations. Below the cliff and up to Ceps, the lowest parts of the mountains are made of Visean flysch, belonging to several tectonic units.

The outcrop exposes Visean mudstone-sandstone with limestone intercalations dipping south-westwards (S0-1: 130 SW 50). Contrasting with the Visean rocks observed at the first stop (point D1-1), here the Visean pelites are slightly metamorphosed (sericite) and exhibit a N70E trending crenulation lineation. Chevron folds and south-directed brittle shear zones with quartz veins deform S0-1. Along the road, Devonian rocks are not observed, a late fault separates the Visean and Devonian rocks.

Stop D1.9:

Monts de Faugères Unit. Large curve of Orb River below Chapelle St-Geminian.

Tournaisian (?)-Visean limestone and sericite metapelite present a westward (170W40) dipping foliation and a well marked mineral, stretching and crenulation lineation trending N 70E. Pressure-solution is the dominant deformation mechanism. S0-1 is also cut at high angle by west dipping tension

gashes filled by fibrous calcite.

Stop D1.10:

Para-autochthonous Domain. Le Pin and Le Lau anticlines.

Turning right to the road of Le Pin, we can observe the underlying Para-autochthonous Domain. North of Le Pin, this outcrop exposes the deepest part of the Orb section. From North to South, the upside down sequence consists of the Upper Devonian red nodular limestone (griotte marble) with goniatites (S0: 60NW60) with an inverted limb subhorizontal cleavage; Tournaisian radiolarian black cherts (lydiennes) and nodular limestones (calcaires de Faugères) and Visean flysch. North of this outcrop, the succession becomes normal from Devonian limestone to Visean flysch from bottom to top, respectively. This S-SE verging fold is called "Le Pin " anticline. Bedding-cleavage relationships with cleavage refraction in sandstone beds comply with the anticline geometry. A N70E composite lineation due to elongated nodules and goniatites, crenulation and intersection develops. Regionally, this para-autochthonous series is folded by two anticlines (Le Pin and le Lau folds) overturned to the South.

Back to the main road, the contact between the Para-autochthonous series and the Mont Peyroux nappe is marked by numerous quartz veins (no stop).

Stop D1.11:

Recumbent fold in Devonian limestone. Moulin de Graïs.

This famous outcrop (Color Plate 1, A) exposes a folded Late Devonian limestone (partly dolomitized). Bedding-cleavage relationships show a southward overturning. The horizontal part of the outcrop is the normal limb. To the south, radiolarian chert (Color Plate 1, B) and limestone are involved in isoclinal folds belonging to the same large-scale structure. It is worth noting that stretching lineation trends close to the fold axis and thus at high angle to the transport direction. In XZ section, pressure shadows indicate top-to-the-NE sense of shear.

Stop D1.11':

Optional. Landscape on the Vieussan antiform.

Turning left on D177, to Berlou, the large curve to the right provides a clear panorama of the northern limb of the Vieussan antiform, well marked in the Devonian limestones.

Stop D1.11»:

Basal thrust contact of the Pardailhan recumbent fold "Queue de cochon (pig's tail)".

Southward, the road goes through the Ordovician turbidite of the Mont Peyroux recumbent fold deformed both by isoclinal and upright folds. The contact between Ordovician turbidite belonging to the Mont Peyroux recumbent fold and the Devonian limestone boudins marking the basal thrust contact of the Pardailhan recumbent fold can be observed in the tight curve north of Escagnès. In spite of intense shearing, the limestone is weakly or undeformed. Back to Vieussan by the same road.

D1.12:

Ordovician/Devonian contact. N. of Vieussan.

Looking West, the hill slope shows several white masses corresponding to Devonian limestone boudins along the basal thrust contact of the Pardailhan recumbent fold (Fig. 18). The outrop exposes inverted stratigraphic contact between Ordovician turbidite to the left and Early Devonian sandstone to the right. Isoclinal folds with curved hinges can be observed in the Ordovician sandstone. The angular unconformity between Ordovician and Devonian formations, and the lack of Late Ordovician-Silurian rocks in most of the Montagne Noire southern side can be interpreted as a sedimentary consequence of a remote tectonic-metamorphic event that took place more to the north in the internal zone of the Belt. It is worth noting that sedimentology of eo-Devonian rocks indicates a northern source of the terrigeneous sediments. Detrital volcanic quartz grains, mica, garnet, zircon, rutile, tourmaline support a pre-Devonian metamorphic event occurring in the hinterland.

Stop D1.13:

Ordovician turbidite in the north part of the Mont Peyroux recumbent fold. N of Vieussan.

Looking to the north, the landscape presents the Axial Zone gneiss and the entrance of Gorges d'Heric visited on D2. The village of Tarassac is built on Devonian marbles (D1-14), the front view is Ordovician turbidite at the western pericline of the Vieussan antiform.

At the outcrop scale, the Ordovician rocks are black pelite and sandstone deformed by upright N80E trending folds (F2) and N50E isoclinal folds (F1). A few biotite grains can be observed in the vertical S2 foliation axial planar to F2.

Stop D1.14:

para-autochthonous Devonian marble. Tarassac, parking of VVP.

Muscovite bearing Devonian marble with pink calcite crystals corresponding to deformed crinoid stems exhibit a southward dip (70S60) and well marked subhorizontal mineral and stretching lineation. This marble is separated from the overlying Ordovician turbidite by a major thrust contact corresponding to the basal thrust surface of the Mont Peyroux recumbent fold. The Devonian marble and the underlying metapelites attributed to Ordovician (not seen here) are a normal sequence belonging to the Para-autochthounous Unit. $^{40}Ar/^{39}Ar$ date on muscovite gives 297 ± 3 Ma which is interpreted as the age of a Late Carboniferous gravity sliding event related to the formation of the Axial Zone (Maluski et al., 1991).

End of the 1st day. Overnight stay in Olargues

Figure 18 - Panoramic view of the contact between the Pardaillhan (top) and Mont-Peyroux nappe (bottom) marked by Devonian limestone boudins called " pig's tail ".

DAY 2

Migmatite dome of the Montagne Noire Axial Zone

A. Geological setting

The Montagne Noire Axial Zone remains one of the most controversial area in the geology of Massif Central (cf extensive references in Soula et al., 2001). The Late Visean-Early Namurian recumbent folds examined during D1 are overprinted by metamorphic and structural features related to a granite-migmatite gneiss dome developed in the Axial Zone (Figs. 13, 17). The foliation of micaschists and gneiss defines a NE-SW long axis elliptical dome whose western part is disturbed by the Eocene Mazamet thrust. Some authors argued that the Axial Zone metamorphic rocks correspond to the Precambrian basement of the Paleozoic series observed in the recumbent folds. In the present state of knowledge, there is no argument to support the existence of a Neo-Proterozoic (i. e. Cadomian) orogen in the Massif Central. Therefore, the reality of a Precambrian basement in the Montagne Noire Axial Zone is not supported by the data. The augen orthogneiss seen in the gorges d'Heric, are porphyritic granites intruding a Neo-Proterozoic to Paleozoic metasedimentary series of micaschists and gneiss and transformed into augen gneiss during Hercynian tectonics. Recent U/Pb dating supports an Early Paleozoic age for the magmatism. The presence of penninic style recumbent folds overturned to the north has also been assumed (Demange, 1975). Although possible, this interpretation cannot be demonstrated, mainly due to poor outcrop conditions.

The Axial Zone gneiss experienced a HT/LP type metamorphism up to partial melting giving rise to migmatites and anatectic cordierite granites (e. g. Laouzas granite). U/Pb dating on single grain zircon and monazite give a ca 330 age. Isograds of this HT/LP metamorphism define the same domal geometry as the foliation. Within the micaschist enveloppe, kyanite relics are locally found (K in Fig. 13). P-T paths for the gneiss core and metamorphic envelope have been proposed (e. g. Soula et al;, 2001; Fig. 19). It is worth noting that some amphibolites included in the gneiss are retrogressed eclogites (E in Fig. 13) with estimated pressure and temperature around 9 ± 2

Volume n° 2 - from B16 to B33

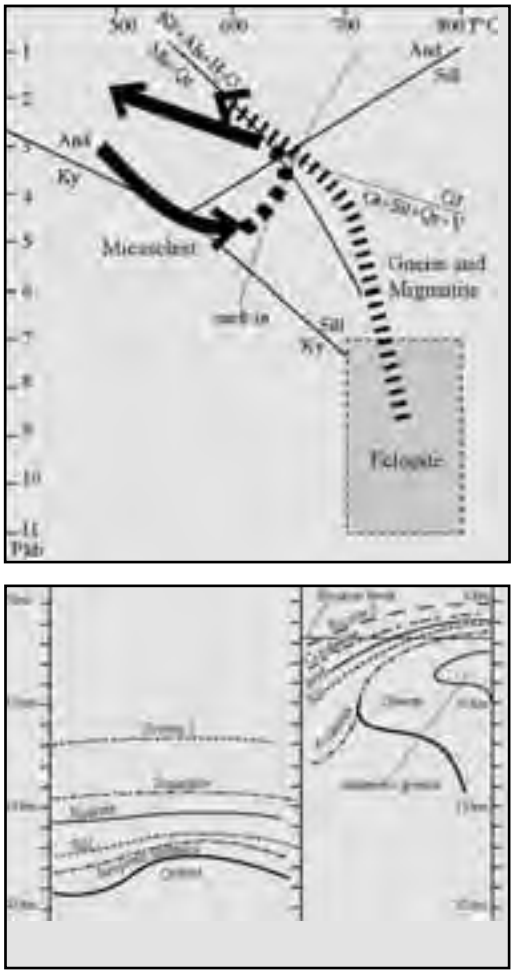

Figure 19 - P-T paths inferred for the Montagne Noire Axial Zone micaschist and migmatitic gneiss (modified from Soula et al., 2001 and Demange, 1985).

Figure 20 - Interpretation of the present-day geometry of the Montagne Noire Axial Zone. During upward doming of the migmatitic core, early isograds are deformed and new HT metamorphic minerals crystallize (from Soula et al., 2001).

kbar and 750 ± 50°C respectively (Demange, 1985). These high-pressure rocks suggest that the tectonic units situated under the recumbent fold were buried at ca 25-30 km depth. Although no radiometric date is available for the eclogites, a possible interpretation is that the high-pressure metamorphism and a part of the ductile deformation of the gneiss is related to compressional tectonics coeval with recumbent folding of the Paleozoic sedimentary sequence.

The Axial Zone is characterized by a conspicuous NE-SW trending stretching lineation which in the southern and northern sides overprints the recumbent folds (cf. stop D1-14). The kinematic analysis provides contrasted shear criteria. Around the dome northeastern and southwestern terminations, shearing is down dip, i. e. top-to-the-NE and SW respectively. However, along the subvertical dome long limbs, shear criteria are ambiguous, as seen along the famous section of "gorges d'Héric" visited in D2 morning.

The present shape of the isograds results from a combination of the tectonic and thermal structures due to the uplift of the migmatitic core (Fig. 20). However, the tectonic significance of the Montagne Noire doming remains disputed. Several interpretations are proposed, namely: i) NE-SW ductile wrench zone (Nicolas et al., 1977; Echtler et Malavieille, 1990); ii) NE-SW antiformal stack (Mattauer et al. 1996, Matte et al., 1998 ; iii) interference between migmatitic diapir and regional NE-SW shortening (Schuilling, 1960, Faure et Cotterau, 1988) ; iv) "metamorphic core complex" (Van den Driessche et Brun, 1991-92). A recent discussion of this problem can be found in Soula et al. (2001).

Although extensional tectonics plays an important role to account for the Late Carboniferous (Stephanian) tectonics (e. g. syntectonic infill of the Graissessac coal basin); the extensional gneiss dome hypothesis cannot account for the bulk structure of the Axial Zone. Indeed, the Vialais granite (Fig. 21) that crosscuts the migmatite foliation is dated by U/Pb on zircon and monazite at 327 ± 5 Ma (Matte et al., 1998).

B. Stop description (Fig. 21)

Stop D2.1:

Cross section of the Caroux Massif along the gorges d'Héric track, 1.5 km, an easy walk.

The morning is dedicated to the observation of the SE part of the Axial Zone, called "Caroux Massif". The Heric augen orthogneiss and paragneiss septa are the most common rock-types. Tourmaline-garnet pegmatitic dykes obliquely cut the foliation. At the entrance of the gorges d'Héric, most of the dykes dip southwards whereas near the top of the mountain, the dykes are flat lying.

After the second bridge, the foliation flattens but the lineation keeps the same N60-70E trend. Further north, the development of a NE-SW crenulation, strengthens

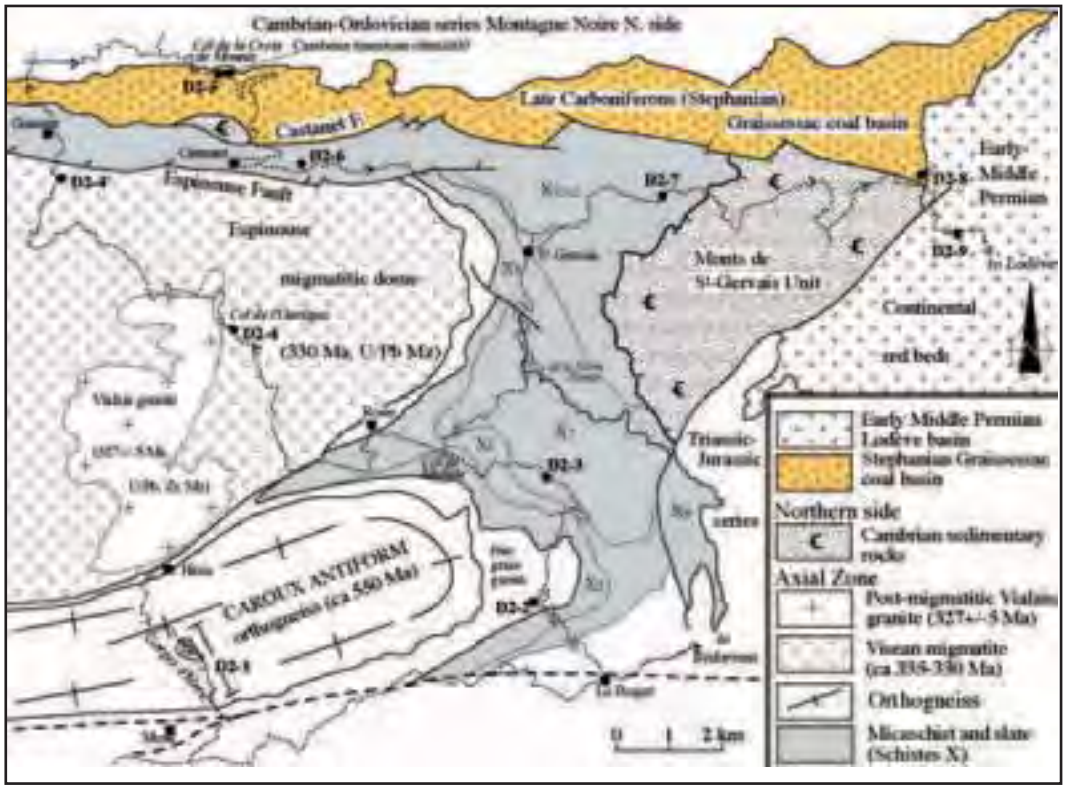

Figure 21 - D2 route map

the gneissic linear fabric. In the paragneiss, meter scale isoclinal folds are refolded by NE-SW trending upright folds.

Pegmatites dykes are also deformed by upright ptygmatitic folds and veins parallel to the fold axes are boudinated. Along the stream, amphibolite boulders (containing garnet locally) including retrogressed eclogites, boulders of migmatites and migmatized augen gneiss, sometimes containing sillimanite nodules are widespread. Outcrop of migmatite will not be visited along this route.

In spite of a clear stretching and mineral lineation, the sigma-type porphyroclast systems exhibit both dextral and sinistral asymmetry at the outcrop scale. The ambiguous sense of shear might be due to superimposed deformation (namely doming overprinted upon low angle shearing) or to strain partitioning with a significant component of pure shear (Color Plate 1, C) during doming.

The bulk structure of the Heric section is a gneiss antiform overturned to the north (Figs. 13, 17). The antiform hinge zone is parallel to upright folds in augen gneiss and meter to millimeter-scale crenulation.

Stop D2.2:

Augen gneiss and sheare pegmatite veins at the eastern part of the Caroux dome. Le Vernet .

From gorges d'Héric → east to Le Poujol → north (left) to Combes.

Fine grain augen gneiss (Sx 40SE 30) with a N70E trending stretching lineation at the eastern termination of the Caroux antiform. Sigmoidal K-feldspath indicates a down-dip, top-to-the East sense of shear. Pegmatite dykes cross cutting the foliation are also sheared to the East. Along the road next curves, many asymmetric pegmatite boudins can be observed within weathered gneiss (no stop).

Stop D2.3:

Biotite-Garnet-staurolite micaschists. Crossing of the road to Forêt des Ecrivains Combattants.

The gneiss-micaschist series experienced a high-

temperature and low-pressure metamorphism characterized by biotite, garnet, andalousite, staurolite tight isograds. The eastward dipping foliation (160E15) bears a composite crenulation, mineral and stretching lineation trending N70E along which top-to-the-E shear criteria develops. In thin section, quartz pressure shadows, helicitic garnet and staurolite, and shear bands indicate a top-to-the East shearing (Color Plate 1, D).

After the Col de Madale, the road runs within the Rosis synform which consists of crenulated and folded HT/LP micaschists between the Caroux antiform and the Espinouse dome.

Stop D2.4:

Migmatitic orthogneiss. Col de l'Ourtigas.

Partial melting develops at the expense of the Heric orthogneiss but MFK and gneissic fabric are still preserved. Migmatisation is dated at 330 Ma. After the pass, the road crosses the northern border of the Vialais granite, however due to poor exposure quality and parking difficulties, the excursion will not stop there.

Optional
Stop D2.4':

Sheared augen gneiss and migmatite.
S. of Ginestet.

The migmatitic orthogneiss experiences a ductile shearing, the NW-SE trending foliation dips 50NE and bears a N60E trending slickenline corresponding to the Espinouse normal fault. $^{40}Ar/^{39}Ar$ dates on muscovite and biotite indicate 297 ± 3 Ma (Maluski et al., 1991).

North of Ginestet, begins the Montagne Noire Northern Side. In spite of globally poor exposure quality, Early Cambrian carbonates can be observed on top of the mountains.

Stop D2.5:

Stephanian conglomerate. Falaise d'Orques.

At the pass of Croix de Mounis, the road enters into the Stephanian Graissessac coal basin. In the northern landscape, the Early Cambrian limestone cliffs are exposed.

The Late Carboniferous conglomerate contains cm to m size blocks of Early Cambrian sandstone and limestone. Along the road, a decameter-scale Cambrian limestone block that is probably an olistolith can be observed too. Stephanian beds dipping 110S10 unconformably cover the Paleozoic (Cambrian-Ordovician) sedimentary rocks of the Northern Side. Thus strictly speaking, the southern border fault of the Graissessac basin (Castanet fault) is reactivated after the deposition of the Stephanian rocks.

At the crossing with D22E road to Castanet-le-Haut, the landscape to the east shows the foliation of the Espinouse gneiss dome dipping north-eastward. The ductile dextral-normal Espinouse fault separates the Espinouse dome from the Stephanian Graissessac basin.

Stop D2.6:

Sheared rocks along the Espinouse fault.
N. of Nougayrols.

The Graissessac basin substratum (i. e. early Paleozoic rocks of the Northern Side) is sheared by the Espinouse fault. Quartz veins are well developed.

Stop D2.7:

Weakly metamorphosed schists. West of Castanet-le-Bas.

Weakly deformed and weakly metamorphosed greenish sandstone-pelite series correspond to the outermost part of the metamorphic rocks surrounding the Axial Zone. Centimeter- to meter-scale folds overturned to the SE can be observed at this outcrop.

East of Verenoux, the road goes through unmetamorphosed and undeformed greenish sandstone and pelite corresponding to the Early Cambrian (grès de Marcory). This Unit (called Monts de St-Gervais Unit) belongs to the Northern Side, and forms an extensional allochthon emplaced upon the Axial Zone micaschists. No stop.

Stop D2.8:

Stephanian massive sandstone and coal mesures. East of La Mouline.

The Late Carboniferous rocks belong to the Graissessac coal basin. They are fluviatile deposits dipping 120NE30 with coal intercalations. Decollement surfaces may develop along coal mesures. In the ancient open pit of the Graissessac mine (not visited) synsedimentary folds overturned to the South can be observed. These Late Carboniferous rocks are unconformably covered by Early Permian conglomerates, sandstones and pelites dipping 0E20, but unfortunately the contact cannot be observed there.

Stop D2.9:

Permian (Autunian) conglomerate.

West of La Tour-sur-Orb.
Continental conglomerates with quartz, sandstone pebbles.

Stop D2.10:

Permian extensional tectonics.
Mas d'Alary quarry.
In the ancient open pit formerly mined for uranium, continental red beds are cut by north dipping normal faults. Alike other early Permian basins in S. France (e. g. St-Affrique, Rodez), the Lodève basin is a half-graben bounded to its southern margin by normal faults.

End of the 2nd day. Drive to Millau (ca 60 km), overnight.

DAY 3

The stacking of Upper and Lower Gneiss Units and post-nappe crustal melting
Millau→ Highway to La Canourgue Exit n° 39

Leaving Millau to the North, the road crosses the Jurassic limestone plateau called Causse de Sauveterre. Near Séverac-le-Château, Toarcian black shales were mined for oil. The Jurassic sedimentary series observed along the road, is deformed by decameter to kilometer-scale wave-length upright folds and reverse faults. These structures are related to the Eocene compression due to the Pyrenean orogeny.

A. Geological setting

The Marvejols area (Fig. 22) is a famous place in the geology of the French Massif Central since it is one of the first places where Variscan syn-metamorphic nappe thrusting has been documented on the basis of geochronology, metamorphism and tectonics (Pin, 1979). The metamorphic inversion with HP rocks of the Upper Gneiss Unit upon the Lower Gneiss Unit was used as an argument for tectonic superposition (Fig. 23). The contact between the two units is a high temperature mylonitic zone (Faure et al., 1979). Moreover, radiometric dates document the tectonic

Figure 22 - D3 route map

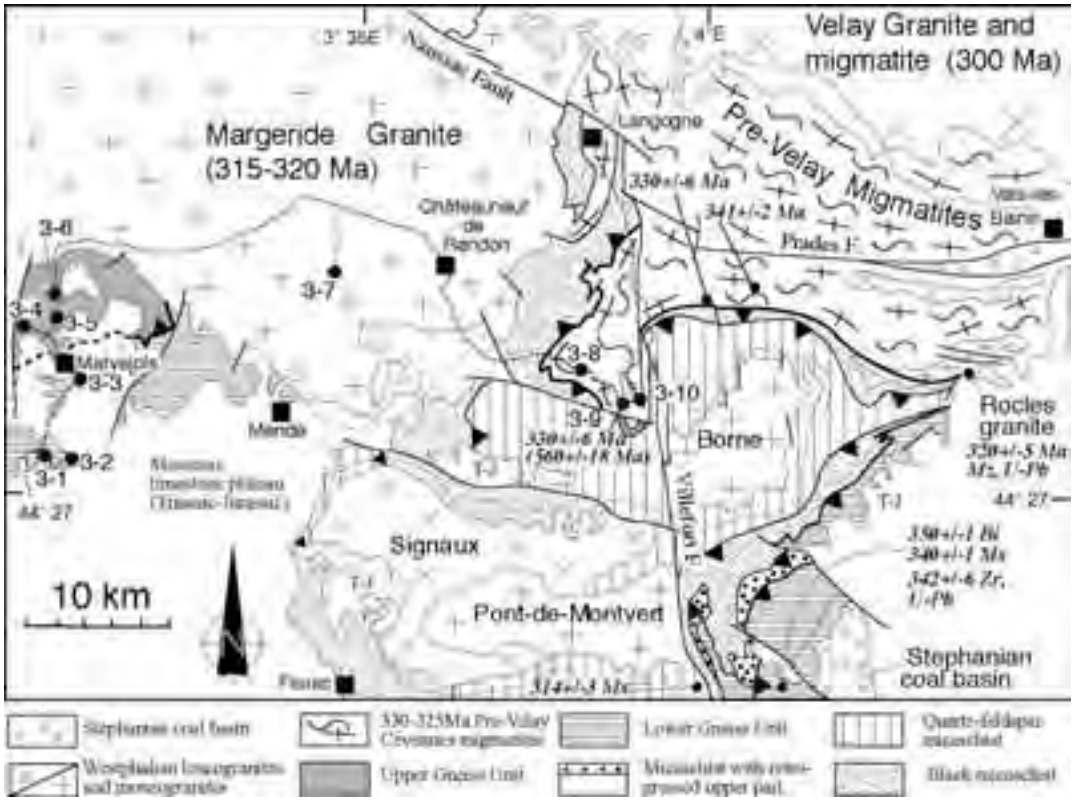

evolution of the area. The Lower Gneiss Unit, called locally the Lot Series, consists of a monotonous succession of metapelite and metagrauwacke intruded by various magmatic bodies:

1. Quartz-diorite orthogneiss is dated at 540 ± 12 Ma by U/Pb isotopic dilution method on zircon populations (Pin and Lancelot, 1978). This rock exhibits a well marked post-solidus planar and linear structure. 40Ar/39Ar dating on biotite gives 352 ± 1 Ma (Costa, 1989).
2. Pink K-feldspar orthogneiss of alkaline composition is not well dated due to inherited zircons. By comparison with the Mendic orthogneiss in the Montagne Noire northern side, an Early Cambrian age is generally accepted.
3. An acidic augen orthogneiss with mylonitic zones crops out immediately below the Upper Gneiss-Lower Gneiss Unit contact. An U/Pb age on zircon populations gives a lower intercept age of 346 ± 8 Ma (Pin, 1981). Due to its tectonic setting, and radiometric age this orthogneiss is interpreted as a synkinematic pluton coeval with the thrusting of the Upper Gneiss Unit. However, this conclusion does not comply with microstructural data and particularly with the NW-SE stretching lineation developed in the Lower Gneiss Unit (cf below). A preliminary chemical U/Th/Pb age of 370 ± 12 Ma is obtained on monazite (A. Joly unpublished data).
4. Other small gneiss masses are recognized in the Lower Gneiss Unit, some of them are considered as hypovolcanic granites or volcaniclastic metasediments (Pin, 1981).

As seen in the first stops of D3 day, the Lot Series of the Lower Gneiss Unit is characterized by a subhorizontal foliation and a conspicuous NW-SE trending mineral and stretching lineation. This ductile deformation is coeval with an intermediate temperature-intermediate pressure metamorphism. Biotite, garnet, staurolite, andalousite and muscovite are widespread in the metapelites. The Marvejols area is often taken as an example of the inverted metamorphism developed in the footwall of the Upper Gneiss Unit overthrust (Fig. 24). $^{40}Ar/^{39}Ar$ dates on biotite and muscovite from the Lot Series micaschist yields 351 ± 4 Ma and 342 ± 4 Ma respectively (Costa, 1989). The tectonic significance of the NW-SE trending stretching lineation which is widespread throughout the Massif

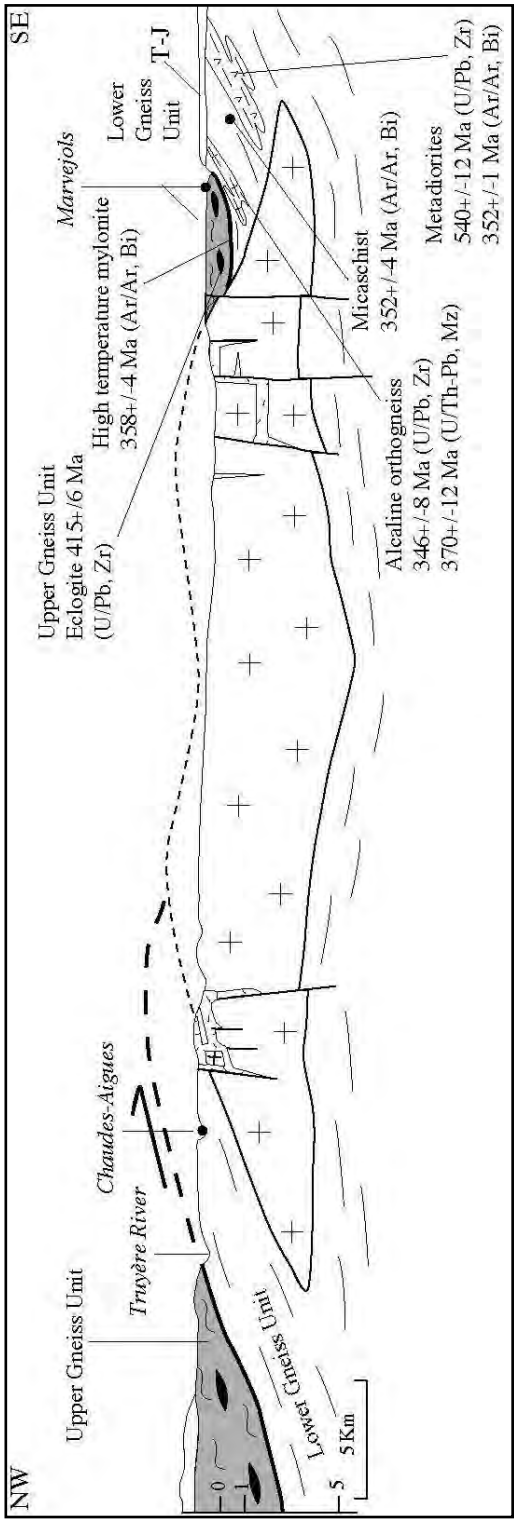

Figure 23 - General cross section from Marvejols to the Truyère area showing the tectonic superposition of the Upper Gneiss Unit upon the Lower Gneiss Unit and the shape of the Margeride pluton

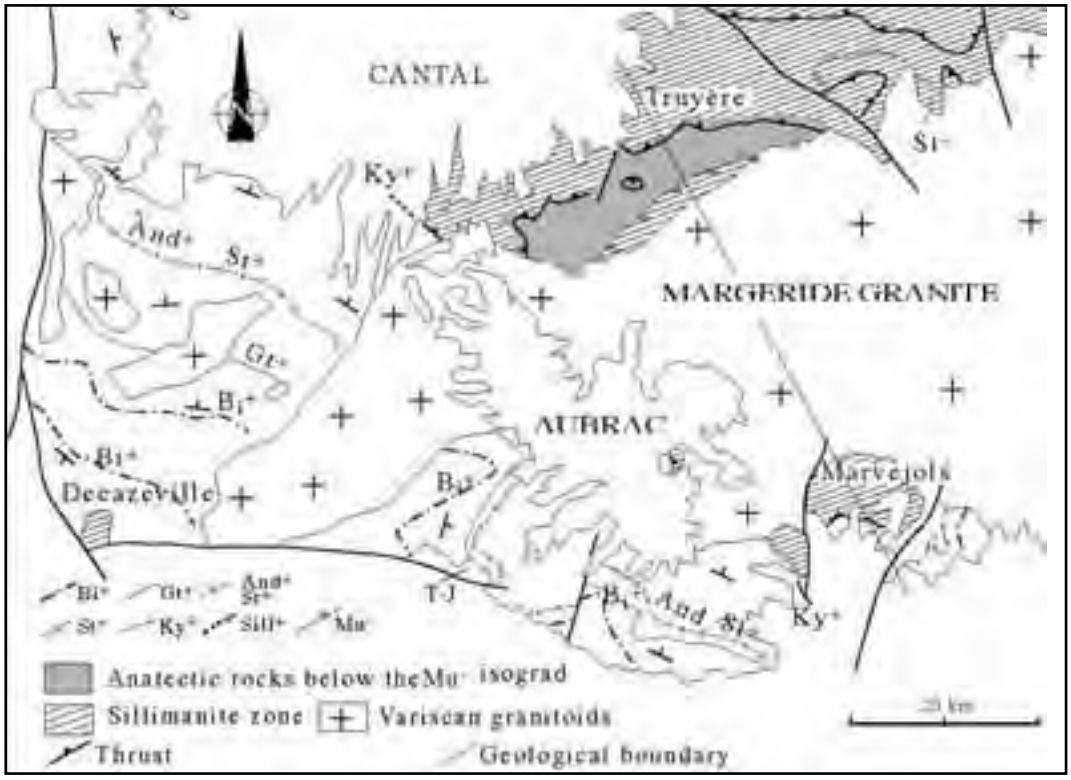

Figure 24 - Metamorphic map of the Lower Gneiss Unit around the west part of the Margeride pluton (Marvejols, Truyère, Châtaigneraie) showing the inverted metamorphism (adapted from Burg et al., 1984).

Central is not clearly settled yet.

The mylonitic zone at the base of the Upper Gneiss Unit is characterized by a N-S trending mineral and stretching lineation. In spite of intense recrystallization and post-kinematic annealing, top-to-the-south shearing can be observed. $^{40}Ar/^{39}Ar$ dating of synfolial biotite gives 358 ± 4 Ma interpreted as the age of thrusting. Moreover, a late muscovite developed upon the early foliation is dated at 340 ± 4 Ma (Costa, 1989).

In the Marvejols area, the Upper Gneiss Unit consists of a lower part called "leptynite-amphibolite" sequence and an upper part with migmatitic gneiss and micaschist. The leptynite-amphibolite sequence contains metamorphosed mafic rocks of magmatic or sedimentary origin such as metagabbro, metabasalt, amphibolite rare serpentinites and acidic rocks (i. e. leptynites) Meter to centimeter scale acidic-mafic alternations are probably of volcani-clastic origin. Several U/Pb ages on zircon populations are available (Pin and Lancelot, 1982). Namely, an amphibolite boudin is dated at 487 ± 6 Ma, and a coronitic metagabbro at 484 ± 7 Ma. An orthogneiss intrusive in the paragneiss gives 478 ± 6 Ma. These dates are interpreted as the evidence for an Ordovician magmatism related to the rifting of Armorica from Gondwana. Moreover, the 415 ± 6 Ma age of zircon populations from a high-pressure trondhjemite is considered as the age of melting coeval with eclogite facies metamorphism. Pressure and temperature constraints on this rock are 16 ± 4 kb and 800 ± 50°C respectively.

Upper and Lower Gneiss Units stacking was followed by huge crustal melting produced under distinct P-T conditions (Fig. 25). The second part of the D3 and the whole D4 days are devoted to the observation of some manifestations of the Middle to Late Carboniferous crustal melting. From older to younger, three stages are distinguished.

1. Pre-Velay Cévennes migmatites, dated between 333 to 324 Ma by chemical U/Th/Pb method on monazite (Be Mezème, 2002).
2. Namurian-Westphalian plutonism dated around

Volume n° 2 - from B16 to B33

320-315 Ma. This magmatism is characterized by porphyritic monzogranite (Margeride or Pont-de-Montvert-Borne plutons) and also by leucogranite (Signaux and Rocles plutons). Although distinct massifs derived from different magmas, field relationships show that these two magmatic types are coeval.

3. Velay migmatites and cordierite granite dated around 300Ma. This large massif will be examined during D4.

B. Stop description

Stop D3.1:

Cambrian quartz-diorite. N88, East of Pont des Ajustons, S. of Marvejols.

A fine-grained biotite-hornblende quartzdiorite originally intrudes micaschists (stop D3-2) belonging to the Lower Gneiss Unit. U/Pb dating on zircon populations gives a 540 ± 12 Ma age (Pin and Lancelot, 1978) for the emplacement of this pluton. $^{40}Ar/^{39}Ar$ dates on biotite provide a 352 ± 1 Ma age corresponding to the tectonic event (Costa, 1989). This well foliated and lineated rock experienced a NW-SE deformation.

Stop D3.2:

Lower Gneiss Unit of the Lot series.

The Lot series are composed of biotite-garnet ± staurolite micaschists originally intruded by porphyric granite and metadiorite. The flat lying foliation bears a conspicuous NW-SE mineral and stretching lineation, indicating a top to NW sense of shear (Color Plate 1, E). Biotite and muscovite $^{40}Ar/^{39}Ar$ ages are respectively 351 and 342 ± 4 Ma (Costa, 1989). In the background, Early Jurassic limestones unconformably overly the metamorphic rocks.

Stop D3.3:

Augen orthogneiss within the Lot series. Pont de Pessil.

The Lower Gneiss Unit includes augen orthogneiss with mylonitic fabric. In sections perpendicular to the foliation and parallel to the NW-SE lineation, asymmetric K-feldspar augen indicate a top-to-the-SE sense of shear. U/Pb date on zircon populations gives a lower intercept age of 346 ± 8 Ma (Pin, 1981). An U/Th/Pb chemical age on monazite gives 370 ± 12 Ma (Joly, unpublished data).

Stop D3.4:

Coronitic metagabbro belonging to the Upper Gneiss Unit. Le Croisier.

The Upper Gneiss Unit outcrops North of

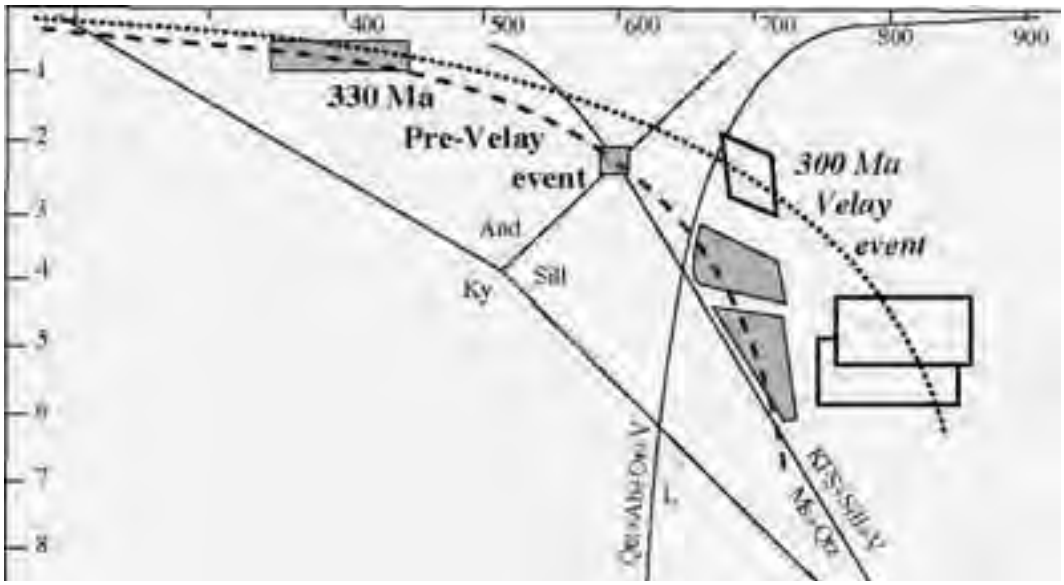

Figure 25 - P-T paths of pre-Velay and Velay events constructed from metamorphic rocks sampled in the south part of the Velay area (simplified from Montel et al., 1992).

Marvejols city. Metabasites, locally with mylonitic fabric, underwent the Eovariscan high-pressure metamorphism (Color Plate 1, F). However, due to the heterogeneity of deformation, magmatic textures are still preserved. This rock is dated by U/Pb method on zircon populations (upper intercept) at 484 ± 7 Ma (Pin and Lancelot, 1982).

Stop D3.5:

Leptynite-amphibolite complex
(Upper Gneiss Unit). Along the main road (N9).

This outcrop exposes a typical section of the "leptynite-amphibolite complex" made of alternations of mafic and acidic rocks considered as a volcaniclastic formation. The foliation exhibits meter to decameter-size amphibolite boudins (Color Plate 2, A). Zircon populations from an amphibolite give a U/Pb age of 487 ± 6 Ma age (upper intercept) interpreted as the rock formation age (Pin and Lancelot, 1982). The lower intercept at 340 ± 4 Ma is close to the thermal event (ca. 345-330 Ma) that overprints the tangential tectonics.

Stop D3.6:

Early Variscan migmatisation.
Gorges du Val d'Enfer.

The road runs from South to North in the leptynite-amphibolite complex which becomes migmatized northward. The migmatite is not dated here. By comparison with other places in the Massif Central, a ca 380 Ma age can be inferred.

Stop D3.7:

Middle Carboniferous Margeride pluton.
Truc de Fortunio.

Drive to St-Amans → Estables

The Margeride massif is one of the largest granitic plutons in the French Massif Central (3200 km^2). It consists mainly of a porphyritic monzogranite with large (up to 10cm) K-feldspar megacrysts. On the basis of biotite content, three facies, namely dark, intermediate and light facies, are distinguished

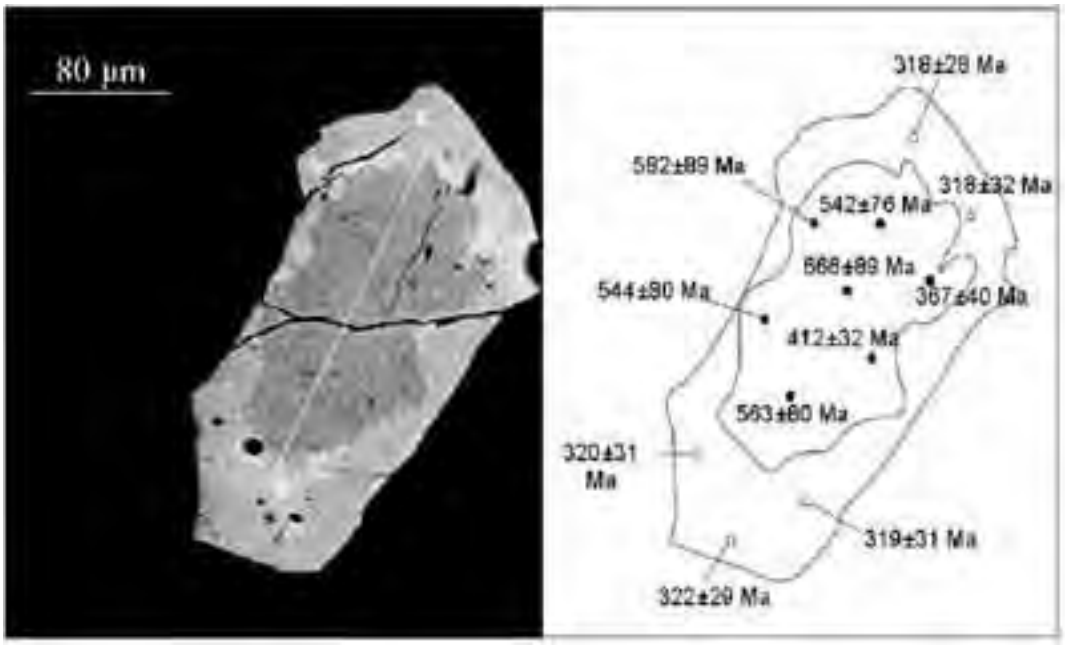

Figure 26 - Example of ponctual dating on monazite single grain by U/Th/Pb chemical method (Be Mezème et al., 2003).

(Couturier, 1977). Nevertheless, more than 80% of the massif is made of the intermediate facies. Moreover, muscovite-K-feldspar leucogranite intrude the monzogranite. Most of the leucogranites are meter-scale dykes, but east of the massif the Grandrieu leucogranite represents a kilometer-sized pluton. The monzogranite yields a Rb-Sr whole rock age of 323 ± 12 Ma (Couturier, 1977) and an isotopic

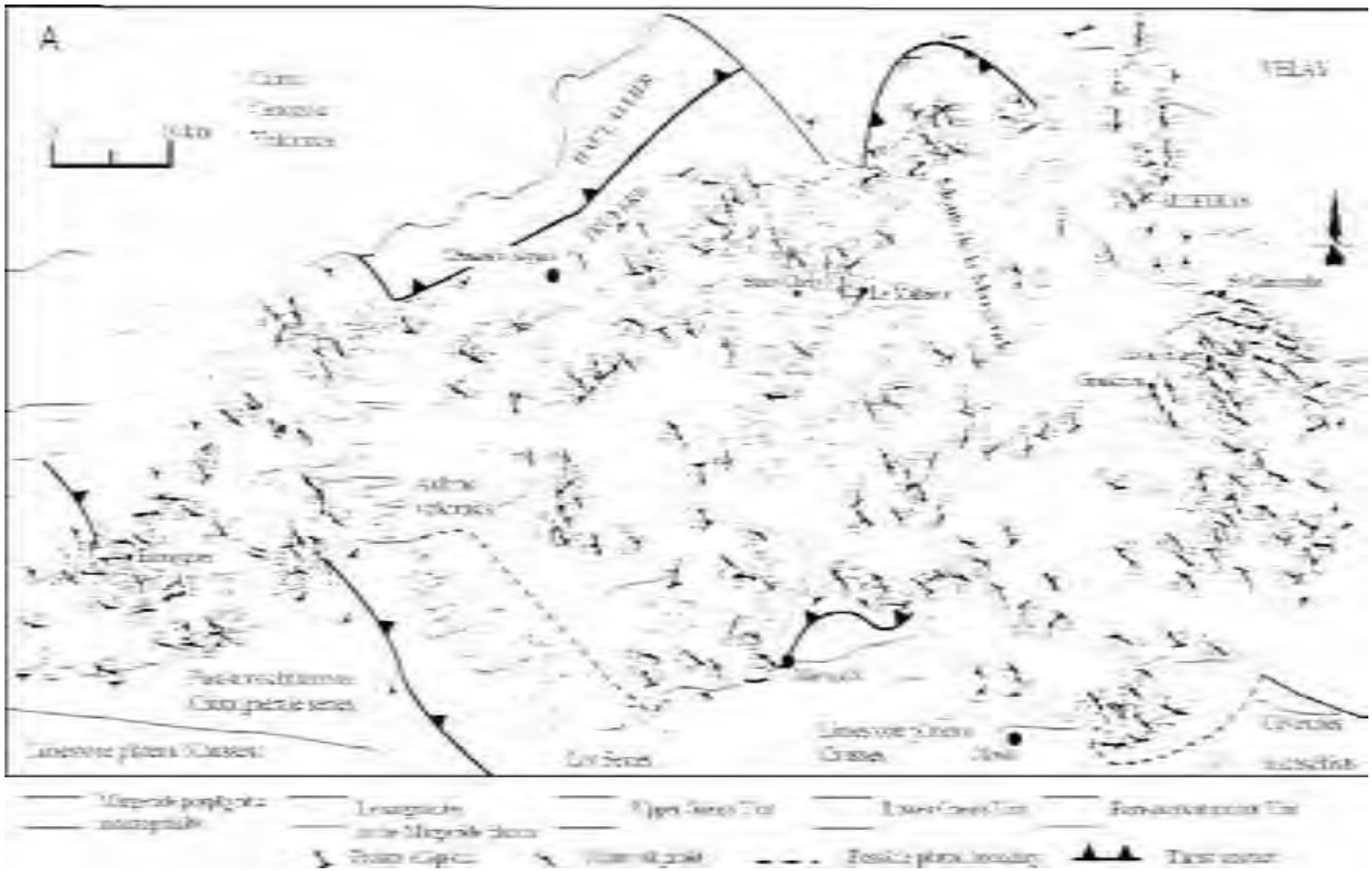

Figure 27 - A: Map of the planar and linear structures in the Margeride pluton inferred from AMS study (from J-Y. Talbot, unpublished).
B: Stereograms represent the magnetic lineation (K1) and the pole of foliation (K3).

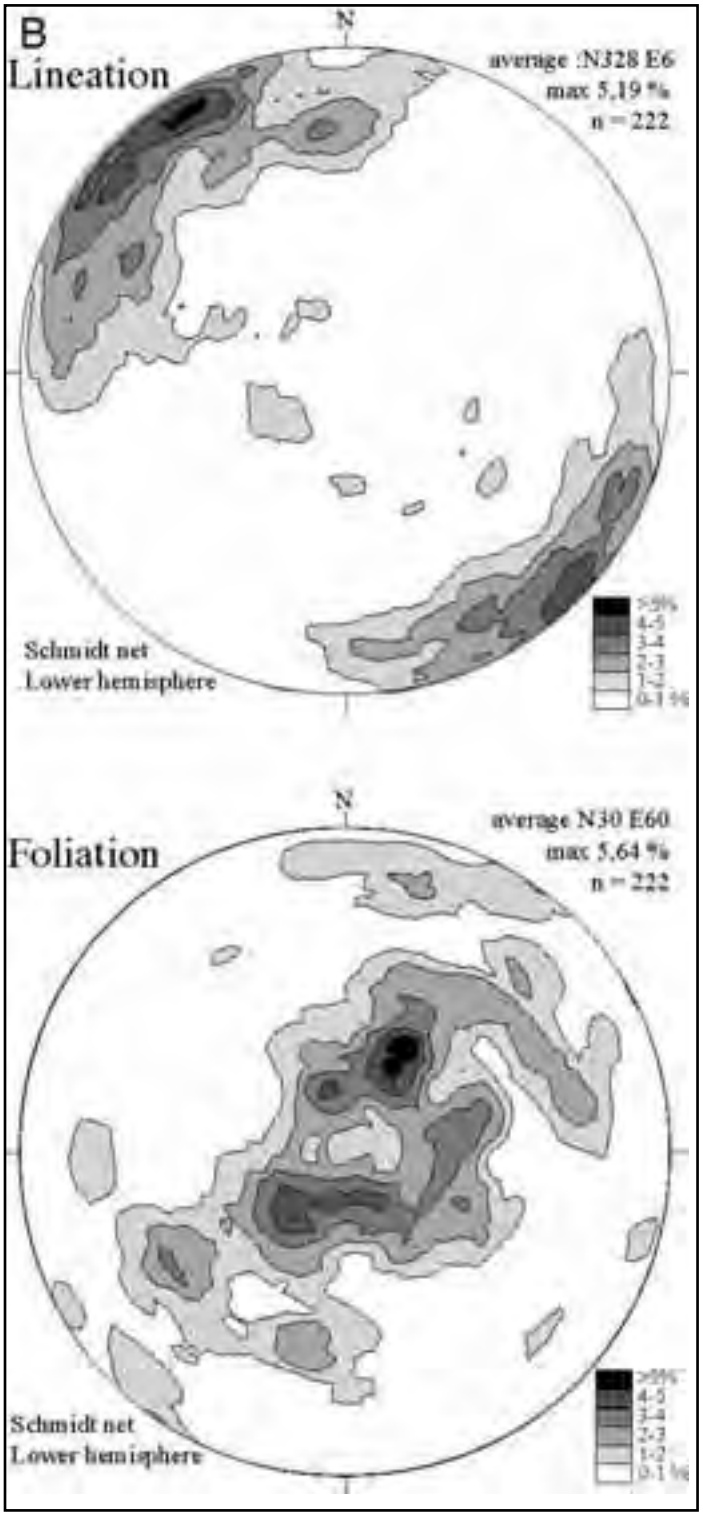

dilution U/Pb monazite age of 314 ± 3Ma (Pin, 1979); the Grandrieu leucrogranite is dated at 305 ± 4 Ma (U/Pb method, Lafont and Respaut, 1988). The Margeride pluton is a subhorizontal of 4 to 8 km thick (Fig. 23). Petrostructural and AMS studies (J-Y. Talbot, work in progress, Fig. 27) show a complex pattern of the foliation trajectories. Although the foliation trajectories do not show a consistent shape, at the scale of the whole pluton, the foliation presents a flat lying attitude. The lineation pattern exhibits a well-defined NW-SE trend. It is worth noting that such a trend is widespread throughout the whole Massif Central and corresponds to the maximum stretching direction of the Namurian-Westphalian syn-orogenic extension (Faure, 1985).

Stop D3.8:

Augen orthogneiss below the Para-autochthonous Unit.

Drive to Châteauneuf-de-Randon → Montbel → NE of Belvezet

SE of the Margeride pluton, the Cévennes area exposes the para-autochthonous Unit of the Massif Central. Below the unconformity of the Mesozoic sedimentary rocks, an augen orthogneiss and its host rocks crop out in a tectonic window below the Para-autochthonous Unit (Cévennes micaschists). The augen orthogneiss exhibits a subhorizontal foliation and NE-SW trending stretching lineation. The age of the granitic magmatism is not determined here but assumed to be Early Cambrian (ca 550 Ma) by comparison with other orthogneiss in the Massif Central. The chemical U/Th/Pb age of 560 ± 18 Ma in the core of monazites grains from migmatitic orthogneiss supports this interpretation (cf. Stop D3-9)

Stop D3.9:

A few kilometers eastward, biotite, garnet (± cordierite) paragneiss and quartz-micaschist correspond to the orthogneiss host rock.

Stop D3.10:

Migmatitic orthogneiss. Barrage de Puylaurent.

To the east, the orthogneiss experiences a partial melting giving rise to diatexites. Locally the orthogneiss fabric remains well preserved. A chemical U/Th/Pb dates on monazite give 560 ± 18 Ma and 324 ± 6 Ma for the grains core and rim respectively (Be Mezème, 2002, Cocherie et al., in press). The latter is interpreted as the age of migmatization.

Boudinaged dykes of leucogranites.

Pink granite dykes and leucogranite dykes intrude the metamorphic rocks. Muscovite dyke is dated by chemical U/Th/Pb method on monazite at 316 ± 5 Ma (Be Mezème et al., 2003; fig. 26).

In Prévenchères, turn to the north (left) to Langogne. The road follows the brittle left-lateral Villefort fault of Permian age. South of La Bastide-Puylaurent, the road is located in the Para-autochthonous Unit (Schistes des Cévennes). From La Bastide Puylaurent, to Langogne, the migmatitic orthogneiss crops out again along the Allier river.

End of the 3rd day. Overnight in Langogne

DAY 4

The Velay dome (French Massif Central): melt generation and granite emplacement during orogenic evolution

The generation of large granite-migmatite complexes by crustal melting during orogeny is a process still discussed in particular because of the deep, inaccessible location of their production sites (Clemens, 1990; Brown, 1994). Moreover, the development of a partially molten middle crust during collision tectonics implies a major change in the rheology of the thickened crust and largely control its behaviour during orogenic collapse (Vanderhaeghe and Teyssier, 2001). Thus, the Variscan belt which exposes numerous granitic intrusions and large migmatitic complexes is of great interest to study the role of partial melting during orogenic evolution (Brown and Dallmeyer, 1996; Gardien et al., 1997; Vanderhaeghe et al., 1999). The Velay migmatite-granite dome located in the SE Massif Central (Fig. 28, 29, 30) offers a unique opportunity to examine the thermal conditions required for widespread crustal anatexis and the consequences of the presence of the generation of a large volume of partially molten rocks on the evolution of the Variscan orogenic crust.

The aim of the fourth day is to illustrate the melt generation and granite emplacement of the Velay dome in connection with the tectonic evolution of the Variscan belt, by showing:

- incipient stages of melting in the Late Neoproterozoic pre-tectonic granite and metasediments on the southern margin;
- the cordierite-bearing granites and migmatites;
- the relation between granite emplacement, extensional tectonics and formation of the St Etienne Stephanian basin on the northern flank of the Velay dome.

A. Geological setting

The Velay dome (Fig. 28,29), about 100 km in diameter, is composed of peraluminous granites (about 70%) characterized by abundance of nodular and prismatic cordierite and by enclaves of gneisses (25%) and granites (5%) of various nature and size (Didier, 1973; Dupraz and Didier, 1988). Previous work in this area provided the following results and models

- Montel et al. (1992) describe two successive stages of anatexis, first under water-saturated conditions with biotite stable followed by melting under biotite dehydration conditions.
- Burg and Vanderhaeghe (1993) proposed that the amplification of the Velay dome cored by migmatites and granites reflects gravitational instabilities within a partially molten middle crust during late-orogenic extension.
- Lagarde et al. (1994) suggested that the deformation pattern of the Velay dome records southward lateral expansion of the granites below the detachment zone of the Pilat, one of the major normal faults developed during the collapse of the Variscan belt (Malavielle et al., 1990)
- Geochemical and petrological data published by Williamson et al. (1992), Montel et al. (1992) and Barbey et al. (1999), indicate that the Velay dome has followed a clockwise P-T-time evolution overprinted by a thermal peak due to the underplating of mafic magmas (Fig. 31).

Figure 28 - Simplified geologic map of the eastern margin of the Massif Central, Day 4 and Day 5 localities

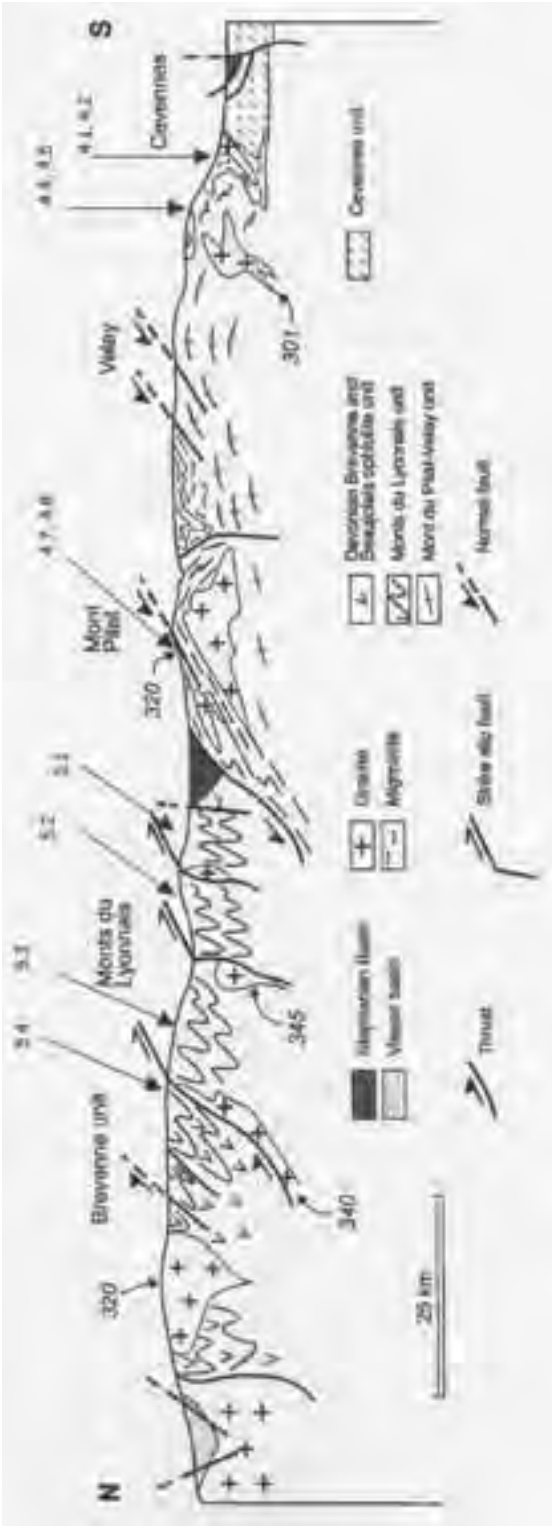

Figure 29 - Simplified cross section through the eastern margin of the Massif Central showing the main tectonic units and their structural relationships, Day 4 and Day 5 localities. Ages of some granites are indicated as specific geochronological markers.

According to Ledru et al., 2001, structural, petrologic and geochronological data indicate that the formation of the Velay migmatite-granite dome results from the conjunction of several phenomena.

- Partial melting of the thickened crust started at about 340 Ma, while thrusting in the hinterland of the Variscan belt was still active, and ended during collapse of the orogenic crust at ~300 Ma. Crustal anatexis responsible for the generation of the rocks forming the Velay dome hence lasted about 40 My.
- Partial melting took place within a dominantly metasedimentary crustal layer dominated by fertile pelitic compositions. Melting reactions evolved from the water-saturated granitic solidus to destabilization of hydrous minerals and indicate that melting started at the end of the prograde metamorphic path and ended during decompression associated with exhumation of the migmatite-granite dome.
- Thermal relaxation and increased radioactive heat production following crustal thickening likely caused a rise in temperature during the evolution of the Variscan orogenic crust. However, it is proposed that heat advection from mantle-derived magmas and also asthenospheric upwelling coeval with orogenic collapse have provided the extra heat source required to melt a large volume of the thickened crust and generate the migmatites and granites of the Velay dome.

The formation of the Velay dome, coeval with the activation of crustal-scale detachements, potentially corresponds to flow of a partially molten crustal layer in response to gravitational collapse.

Four main structural zones, that will be partially illustrated during this fourth day, are defined (Fig. 28, 30):

1. The host rocks. The Velay granite-migmatite dome is hosted by gneissic units stacked during the collision history of the Variscan belt (Ledru et al., 1994a, b):

- the Upper Gneiss Unit, that contains remnants of Early Paleozoic oceanic or marginal basins is presently in an upper geometric position, this unit

Figure 30 - Extension of Meso and Neovariscan metamorphism and foliation trends within the host rocks of the Velay migmatite-granite dome

Volume n° 2 - from B16 to B33

contains dismembered basic-ultrabasic complexes at its base overlain by gneisses derived from granites, microgranites, acid and basic volcanics, tuffs and grauwackes. Numerous eclogitic relics are preserved within basic layers marking an Eovariscan stage of lithospheric subduction (450-400 Ma). Structural and radiometric data show these rocks were exhumed from 90 km at 420-400 Ma to less than 30 km at 360-380 Ma while subduction was still active (Lardeaux et al., 2001).

- The north Gondwana continental margin is represented by (a) a Lower Gneiss Unit composed of metasediments derived from pelites and argilites, and augen orthogneiss (the "Arc de Fix") originating from peraluminous porphyric granite dated at 528 ± 9 Ma (Rb-Sr whole rock, R'Kha Chaham et al., 1990), and (b) a mainly sedimentary parautochthonous sequence. This margin underwent a general medium-pressure metamorphism attributed to the thrusting of the Upper Gneiss Unit which occurred during Devonian, prior to 350 Ma in the internal zone (Mesovariscan period). The Lower Gneiss Unit is intruded by syn tectonic granites precursor of the Velay dome emplaced between 335 - 315 Ma, including magnesio-potassic plutons, the so-called "vaugnerite". In the south (Fig. 2), the Cévennes micaschists are interpreted as the parautochthonous domain. Maximum P-T conditions during the metamorphic evolution are there estimated at 500 °C, 5 kbar, with the muscovite-chlorite-garnet parageneses being synchronous with southward thrusting and a thickening estimated at about 15 km (Arnaud and Burg, 1993; Arnaud, 1997). The closure of micas to Ar diffusion has been dated at 335-340 Ma ($^{40}Ar/^{39}Ar$, Caron et al., 1991).

2. The gneiss-migmatite zone, at the periphery and at the roof of the Velay dome. In the migmatites and in the gneissic hosts, the following melting reactions are identified (Fig. 31):

- The first melting stage developed under P-T conditions exceeding those for water-saturated quartz-feldspathic rocks, with biotite remaining stable: around 700 °C, 4 kbar within the metamorphic envelope, 5 kbar in the granitic core (M3 stage of Montel et al., 1992). The presence of corundum paragneiss enclaves confirms the initial presence of muscovite and the prograde character of this melting event (Aït Malek et al., 1995). A U-Pb monazite date indicates a minimum age of 314 ± 5 Ma (Mougeot et al., 1997). High-K magnesian monzodiorite, with mantellic affinity are also dated at 313 ± 3 and 314± 3 Ma (207Pb-206Pb and U-Pb respectively on zircon, Aït Malek, 1997). They contain peraluminous

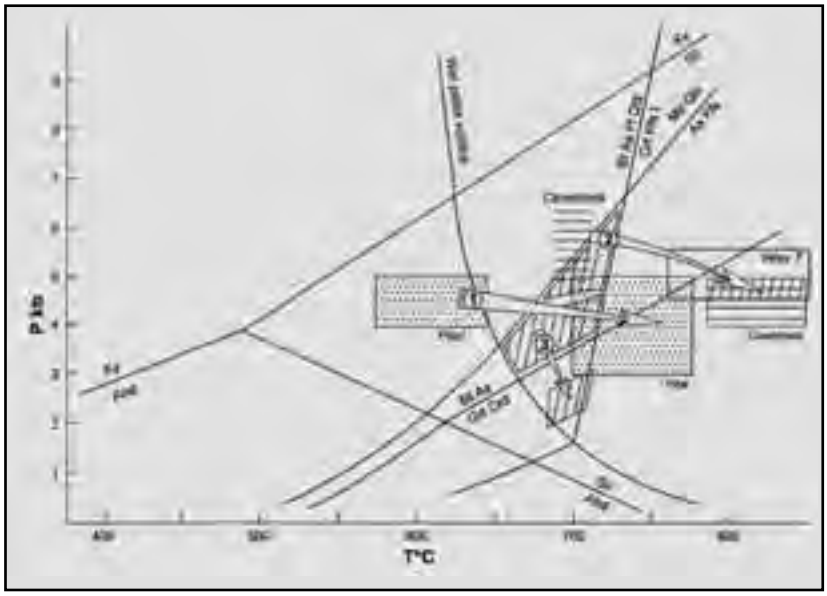

Figure 31 - Pressure-temperature evolution from the gneisses to the Velay granite
Mineral abbreviations: Ky = kyanite; Sil = sillimanite; And = andalusite; Cd = cordierite; Grt = garnet; Ms = muscovite; Qtz = quartz; Kfs = potassium feldspar; Pl = plagioclase; Bt = biotite; As = aluminium silicate; L = liquid. The transition from the M3 to the M4 metamorphic stage is indicated by arrows (1) in the Pilat micaschist (after Gardien et al., 1990), (2) in the migmatitic orthogneiss and granite in the southern part of the dome (oblique- and horizontal-ruled boxes, after Gardien et al., 1997, and Montel et al., 1992), (3) in the migmatitic part of the southern host rocks of the Velay granite (oblique-ruled boxes, after Montel et al., 1992)

xenoliths that record a first stage of isothermal decompression at 700-800 °C, 8-10 kb, consistent with a source located more than 30 km deep, followed by a stage at 5-6 kb (Montel, 1985). In view of the water-saturated conditions, it is unlikely that large quantities of granite (i.e. < 10-20%) were produced and extracted at this stage (Patiño Douce and Johnston, 1990).

- The second stage of melting is characterized by high-temperature metamorphism in the cordierite stability field, with biotite destabilized: 760-850 °C, 4.4-6.0 kbar (stage M4 of Montel et al., 1992). Leucosomes were dated at 298 ± 8 Ma based on Rb-Sr whole rock isochron (Caen-Vachette et al., 1982), and Rb-Sr whole rock-biotite isochrons yield ages between 305 and 276 Ma (Williamson et al., 1992). An age of 301 ± 5 Ma was obtained for the homogeneous parts of the granite using the U-Pb monazite method (Mougeot et al., 1997). Therefore, this second melting stage is considered to be generally synchronous with emplacement of the main cordierite-bearing granites. The volume of cordierite-bearing granites generated makes a case for massive partial melting at this stage, associated to destabilization of hydrous minerals.

3. The migmatite-granite domain. The various granites that appear in the Velay dome define a suite, with 3 main granite types distinguished according to age, structure, homogeneity, mineralogy and geochemistry:

- A heterogeneous banded biotite granite, found mainly on the western margin of the dome and locally on the southern and eastern margin. It corresponds to the first generated granite of the Velay suite. Foliation trajectories are in continuity with porphyric granites in the external rim of the dome suggesting continuity between these precursor granites and the development of the heterogeneous banded biotite granite.
- A main biotite-cordierite granite, in which several sub-types may be distinguished, in particular according to the cordierite habitus (Barbey et al., 1999).
  - a heterogeneous banded granite with abundant enclaves. Most of these enclaves represent incorporated and partly assimilated pieces of the Lower Gneiss unit and precursor plutons originating from the host rocks, although some enclaves with refractory composition or granulite facies metamorphism have a lower crustal origin (Vitel, 1985). Cordierite may be prismatic, cockade-type or mimetic overprinting previous biotite - sillimanite assemblages. Most of the heterogeneous granites indicate mixing between melts of lower-crustal origin and melts from the para- and ortho-derived host rock (Williamson et al., 1992).
  - a homogeneous leucocratic biotite-cordierite granite with mainly cockade-type cordierite. Its emplacement has been dated at 301 ± 5 Ma using the U-Pb method on monazite (Mougeot et al., 1997).
  - a homogeneous granite with biotite and prismatic cordierite as a primary ferromagnesian phase, with few enclaves. The heterogeneous and homogeneous granites with prismatic cordierite, with a high Sr content, have a mixed isotopic signature between the host rocks and a lower-crustal origin. The deep source is considered to be the melting of the lower mafic/felsic plutonic crust (Williamson et al., 1992).
  - a leucocratic granite with cockade-type cordierite, without enclaves. The cordierite-quartz aggregates posdate primary biotite bearing assemblages and probably prismatic cordierite.
- The late magmatic activity that includes:
  - homogeneous granite with K-feldspar porphyrocrysts and common prismatic cordierite, basic and micaceous inclusions (the Quatre Vios massif) (Fig. 10d). These granites are defined as late-migmatitic and are considered to originate from the melting of aluminous sediments at 4.5-5.5 kbar and 750-850 C, under water-undersaturated conditions and have a significant mafic component (Montel et al., 1986; Montel and Abdelghaffar, 1993). Ages at 274 ± 7 Ma (Rb/Sr whole rock, Caen Vachette et al., 1984) are considered to be partially reset during Permian or Mesozoic hydrothermal event.
  - Stephanian leucogranites, microgranite and aplite-pegmatite dykes, Permian rhyolites. Microgranite dykes have been dated at 306 ± 12 and 291 ± 9 Ma and a Permian hydrothermal event at 252 ± 11 and 257 ± 8 Ma (microprobe dating of monazite, Montel et al., 2002).

4. The Stephanian intracontinental basin of St-Etienne. This basin is formed along the hanging wall of the Mont Pilat extensional shear zone (Malavieille et al, 1990). The Mont Pilat unit, attributed to the lower gneissic unit at the scale of the French Massif Central

consists of aluminous micaschists, metapelites, orthogneisses and amphibolites. This unit has a gently north-dipping foliation plane bearing a north-south stretching lineation. Numerous leucogranitic pods outcrop more or less parallel to this main foliation plane and have been dated at 322 ± 9 Ma (Rb/Sr whole rock, Caen-Vachette et al., 1984). Shear criteria, observed at different scales, are compatible with a top-north extension dated between 322 and 290 Ma (39Ar/40Ar, Malavieille et al., 1990). This event was coeval with the progressive development of low pressure - high temperature metamorphic conditions (3- 5 Kbar and 700 - 780 °C, Gardien et al., 1997).

B. Stop description (Fig. 28, 29)

Stop D4.1:

Meyras, Road from Le Puy-en-Velay to Aubenas, N102, Road cut.

Stop D4.1 shows the incipient stage of melting within the orthogneiss of the Lower Gneissic Unit. An augen orthogneiss (the "Arc de Fix"), originating from peraluminous porphyric granite dated at 528 ± 9 Ma (Rb-Sr whole rock, R'Kha Chaham et al., 1990), constitutes an almost continuous rim around the Velay granite-migmatite dome. The melting is marked by the segregation of cordierite-free melts along the main inherited foliation and locally discordant cordierite-bearing granitic patches (Color Plate 2, B). Large phenocrists of K-feldspar attest of the porphyric type of the granite protolith while the foliation is marked by the elongation and crystallization of the quartzofeldspathic aggregates and biotite-rich melanosome. Magnesio-potassic dykes (the so-called "vaugnerite") are intrusive and boudinated within the orthogneiss.

The progressive development of the anatexis and textural evolution in the transition from subsolidus annealing to melting process has been studied in detail in this zone by Dallain et al. (1999). Anatexis first develops with the resorption of quartz along the existing foliation. The breakdown of muscovite is then accompanied by the growth of sillimanite. Quartz-plagioclase aggregates are replaced by assemblages that are in equilibrium with the granite eutectic point, although K-feldspar aggregates are preserved. The breakdown of biotite is responsible for the production of melt beyond 30-50 %, the value of the Rheological Critical Melt Percentage (Arzi, 1978). Leucosomes with cockade-type cordierite produced during this second melting stage tend to be discordant with the inherited structure. Structural orientations then become more varied as the leucosome proportion increases, with folds becoming abundant and randomly oriented.

Stop D4.2:

Pont de Bayzan, Road from Le Puy-en-Velay to Aubenas, N102, River banks of the Ardèche river.

Stop D4.1 shows the incipient stage of melting within paragneiss of the Lower Gneissic Unit. The metagranite observed at the stop 4.1. is originally intrusive in sediments (pelites and argillites, including refractory quatz-rich and calcic layers) The location of early melting is controlled by foliation anisotropy (Macaudière et al., 1992) and folding (Barraud et al., 2003).

Numerous resisters from refractory layers preserve microstructure developed during the pre-migmatitic tectonic evolution that resulted in a composite foliation (named regionally S2) and polyphased folding (Color Plate 2, C). The outcrop is characterized by open folds that play an active role in the segregation of anatectic melts: cordierite-free leucosomes accumulate in saddle reef and axial planes of the folding that is attributed to S3 (Barraud et al., 2003).

Stop D4.3:

Ucel, Road from Aubenas to Mezilhac, Road-cut.

Stop D4.3 shows the unconformity of the Mesozoic sandstone over altered granite and biotite-sillimanite migmatitic paragneiss. The exhumation of the Velay granite-migmatite dome occurred during the Stephanian as boulders of granites and gneisses are found in the conglomerates of the Stephanian basin in the North and Prades basin in the South. Apatites in granite and migmatites yield a U-Pb age at 289 ± 5 Ma that is interpreted as a cooling age during the uplift of the Vealy region (Mougeot et al., 1997). Finally, a regional unconformity is characterized at the base of the Trias sandstone and conglomerate. A recent and fresh road cut provides a spectacular illustration of this unconformity.

Stop D4.4:

Volane river, Road from Aubenas to Mezilhac, D578, Road-cut.

Stop D4.4 shows an hololeucocratic granite, with cockade-type cordierite, that represents one of the petrographic type of the Velay migmatite-granite dome (Color Plate 2, D). Detailed observation indicates that cordierite is formed at the expense of biotite, in the presence of a melt phase. Cordierite is formed from the early phase of melting to the end of the magmatic

evolution of the Velay granite. However some garnets are present in cordierite nodules, indicating that, in that area, melting started in the garnet stability field.

Stop D4.5:

Volane river, Road from Aubenas to Mezilhac, D578, Road-cut.

Stop D4.5 shows a late-migmatitic homogeneous granite and relations with migmatitic gneisses and heterogeneous cordierite-bearing granite. In the upper part of the outcrop, a late-migmatitic granite, the Quatre-Vios granite, is intruding the heterogeneous banded granite: it is a coarse grained peraluminous granite with prismatic cordierite and frequently oriented feldspar phenocrysts. It contains abundant mafic microgranular enclaves and surmicaceous enclaves including biotite, garnet, cordierite, sillimanite, hercynite, ilmenite and rare plagioclase. This unusual mineralogy (absence of quartz and potash feldspar) and the corresponding chemical composition indicate that these enclaves are restites. P-T conditions calculated from this mineralogy yielded water-undersaturated conditions estimated at 4.5-5.5 kbar and 750-850 C. The mafic microgranular (biotite+plagioclase) enclaves correspond to frozen blobs of mafic magma. Locally, another type of late-migmatitic fine-grained granite, with typical acicular biotite and devoid of enclaves, crosscuts the Quatre-Vios granite.

In the lower part of the outcrop, another dyke of late-migmatitic granite is intrusive within migmatitic orthogneiss in which the second stage of melting is well marked by the biotite breakdown that produces Fe-rich garnet and cordierite. This zone is itself enclosed within the heterogeneous banded granite that contains a lot of enclaves of migmatitic paragneiss.

Stop D4.6:

Mont Gerbier-de-Jonc, Road from Mezilhac to Le Puy-en-Velay, D378, Sight as seen from the road.

The Velay volcanism is made up of an eastern chain of Mio-Pliocene basaltic to phonolitic volcanoes and a western Plio-Quaternary basaltic plateau (Mergoil et al., 1993). The road to Le Puy-en-Velay shows nice sightseeing of this phonolitic chain that extends over more than 55 km with more than 180 points of extrusion, emplaced between 14 and 6 Ma.

The Mont Gerbier-de-Jonc is known as the spring of the Loire river. It is a phonolitic protrusion that displays a rough prismatic jointing.

Stop D4.7:

Moulin de Sezigneux, Road from St Chamond to Le Bessat, D2, Road cut.

The cordierite-andalusite-bearing micaschist of the Pilat Unit, seen at stop D4.7, displays extensional tectonics and HT-LP metamorphism within the Pilat series (Lower Gneissic Unit). This outcrop offers a good example of a low-pressure metamorphic unit, with micaschists and paragneisses intruded by syn-tectonic pegmatite dykes and pods. The main foliation plane is gently dipping to the North and shear criteria are well marked mainly around the pegmatitic pods indicating top to the North extensional tectonics. In the metamorphic rocks, the common mineralogy is: quartz + feldspars + biotite + andalusite and /or cordierite ± muscovite.

D4.8: Moulin de Sezigneux, Road from St Chamond to Le Bessat, D2, River banks.

Structure and metamorphism of the orthogneiss of the Lower Gneissic Unit are illustrated at stop D4.8. Ultramylonite and pseudotachylite textures are developed within the orthogneiss and S-C-C' structures indicate top to the North shear criteria compatible with extensional tectonics. Shear bands are underlined by syntectonic recrystallized biotites dated around 320-300 Ma ($^{40}Ar/^{39}Ar$). In the highly sheared parts of the outcrop ultramylonite bands and pseudotachylites are observable. The main foliation plane bears a north-south oriented stretching lineation. The metamorphic mineralogy is characterized by the association of quartz + feldspars + biotite + muscovite. Rare small-sized cordierites can also be observed.

End of the 4th day. Overnight stay in St Etienne

DAY 5

High to ultra-high pressure metamorphism and arc magmatism: records of subduction processes in the French Massif Central

The main goal of Day 5 is to present the geological and petrological records of subduction processes in the eastern Massif Central that preceeded the development of the Velay migmatite-granite dome illustrated during Day 4. These records are: remnants of high to ultra-high pressure metamorphism in both crustal and mantle-derived lithologies in the Mont du Lyonnais unit, a partially preserved back-arc derived ophiolitic sequence, the Brévenne unit.

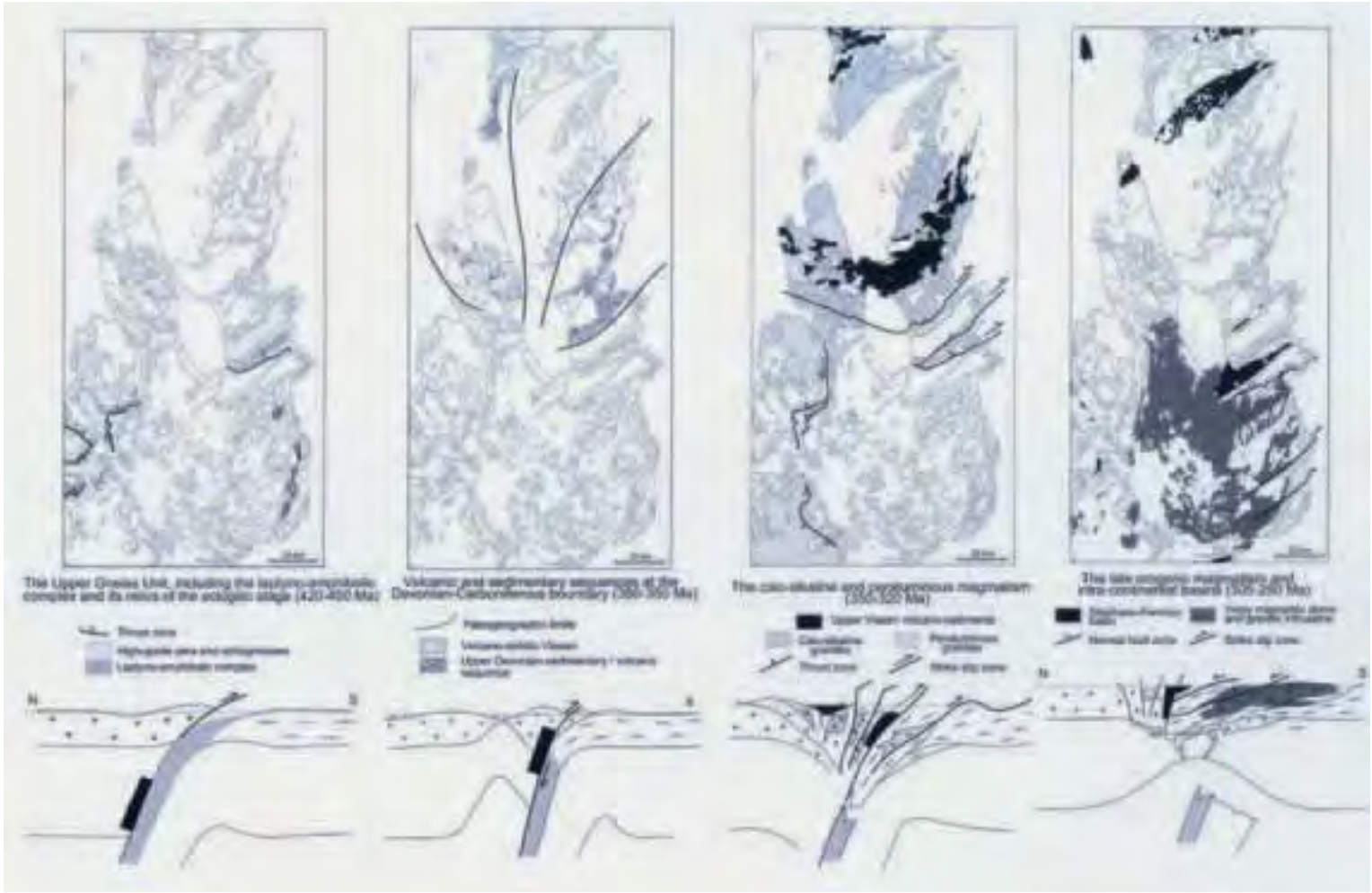

Figure 32 - Geological maps of the eastern margin of the Massif Central through time showing the progressive edification of the belt. The geodynamic cartoons show the possible position of the Monts du Lyonnais eclogites during the four critical periods illustrated (a to d).

A. Geological setting

1. Eclogites and garnet peridotite from The Monts du Lyonnais unit (Fig. 32a)

The Monts du Lyonnais unit belongs to the upper gneissic unit (Lardeaux, 1989; Ledru et al., 1994a). It comprises metasediments, orthogneisses (with protoliths of Ordovician age), leptynites (i.e. meta rhyolites), amphibolites and minor marbles. This unit also contains lenticular relics of either crustal (mafic and acid granulites, eclogites, Lasnier, 1968; Coffrant and Piboule,1971; Dufour,1985; Dufour et al.,1985; Lardeaux et al.,1989) or mantle origin (garnet and / or spinel bearing peridotites, Gardien et al., 1988, 1990). Eclogites outcrop, in close association with garnet-bearing peridotites, in the southernmost part of the Monts du Lyonnais unit. Eclogites and related garnet amphibolites also occur in a similar structural situation farther north (in the Morvan unit, Godard, 1990) and also southeast of the Monts du Lyonnais unit (in the Maclas-Tournon area, Gardien and Lardeaux, 1991). In the Monts du Lyonnais unit, three ductile strain patterns were distinguished (Lardeaux and Dufour, 1987; Feybesse et al., 1996) and related to high pressure and medium pressure metamorphic conditions:

- The relictual high-pressure structures
- A main deformation imprint, contemporaneous with amphibolite facies conditions, corresponds to a NW -SE crustal shortening with a finite NNE-SSW stretching direction (Fig. 32b)
- A deformation event developed under a transpressional regime dated between 335 and 350 Ma (Rb/Sr whole rock, Gay et al., 1981; $^{40}Ar/^{39}Ar$, Costa et al., 1993) which is correlated to the main deformation within the Brévenne ophiolite in relation with its overthrusting. (Fig. 32c)

With respect to this transpressive strain pattern, in the southern part of the Monts du Lyonnais unit, the eclogites outcrop exclusively in the strongly folded domains where they behave as rigid bodies in a deformed ductile matrix. We never found any eclogitic body within the shear zones.

2. The uppermost part of the magmatic arc: the Brévenne ophiolite (Fig. 32b)

The Devonian Brévenne ophiolitic unit consists of an association of metabasalts and metarhyolites together with intrusive intruded by trondhjemitic bodies (Peterlongo, 1970; Piboule et al., 1982,1983). The ophiolitic unit was initially emplaced in a submarine environment (Pin et al., 1982; Delfour et al., 1989). These intercalations are cut and overlain by intrusive gabbros and dolerites and by submarine basaltic lavas that, finally, are overlain by siltstones with pyroclastic intercalations (Milési et Lescuyer, 1989; Feybesse et al., 1996). A prograde greenschist to lower amphibolite facies metamorphism is recorded (Peterlongo, 1960; Fonteilles, 1968; Piboule et al., 1982; Feybesse et al., 1988). The Brévenne ophiolite underwent a polyphase deformation. An early event, well developed in the northern part of the unit, is characterized by a NW-SE stretching lineation with top to the NW shearing (Leloix et al., 1999). During the second event, the ophiolitic unit is overthrusting the Monts du Lyonnais along a dextral transpressional zone in which syntectonic granites emplaced between 340 and 350 Ma (Fig. 32c, Gay et al, 1981; Feybesse et al., 1988; Costa et al., 1993). Subsequently, monzonitic granites of Namurian- Westphalian age and a contact metamorphism aureole postdate this tectonics (Delfour, 1989).

3. The development of the Velay migmatite granite dome and the collapse of the orogen (Fig. 32b)

The tectonic evolution of the eastern Massif Central is achieved during Westphalian and Stephanian. The formation of the Velay dome, coeval with the activation of crustal-scale detachements, potentially corresponds to flow of a partially molten crustal layer in response to gravitational collapse.

B. Stop description (Fig. 28, 29)

Stop D5.1:

The Bois des Feuilles, Road from St Symphorien-sur-Coise to Rive de Gier, D2.

This outcrop consists of garnet bearing peridotites and eclogites occuring as boudins within garnet sillimanite paragneisses. The coesite-bearing eclogite occurs in the southern part of the Monts du Lyonnais unit, near St Joseph in the Bozançon valley (1/50.000 geological map " St Symphorien Sur Coise ", Feybesse et al., 1996) in association with "common" eclogites and serpentinites. In the whole area, eclogites are preserved in low-strain lenses (meter scale boudins) wrapped by amphibolites or amphibolite facies paragneisses. For practical reasons (difficult access), we shall observe only garnet-peridotites and "common eclogites".

Well-preserved peridotites occur as metric to decametric scale bodies within the paragneisses. In the less retrogressed samples, garnets in equilibrium with olivine, clinopyroxenes and orthopyroxenes can be observed. Frequently, garnets contain inclusions of spinels and pyroxenes, while in some samples

spinels are replaced by coronas of garnet. These microstructures indicate an evolution from spinel to garnet lherzolite facies during a prograde metamorphic P-T path involving a strong pressure increase associated to a moderate temperature increase (Gardien et al., 1990). In many samples, garnets are partly replaced by spinel and orthopyroxene while the porphyroclasts of olivine and pyroxenes are transformed into talc, amphibole, chlorite and serpentine. These mineralogical transformations document a retrograde evolution characterized first by a strong isothermal pressure decrease followed by both pressure and temperature decrease.

As a general rule, the eclogites from the Monts du Lyonnais unit are strongly retrogressed under granulite and amphibolite facies conditions, and in 80% of the cases, the mafic boudins are composed of garnet bearing amphibolites with relics of eclogitic minerals. Petrographically, three types of eclogite facies rocks can be distinguished:

- fine-grained dark-colored kyanite-free eclogites
- fine-grained light-colored, often kyanite-bearing eclogites
- coarse-grained meta-gabbros (with coronitic textures) only partly re-equilibrated under eclogite facies conditions.

As pointed out by various authors (Coffrant and Piboule, 1971; Coffrant, 1974; Blanc, 1981; Piboule and Briand, 1985), dark-coloured eclogites are iron and titanium rich (Fe0 + Fe_2O_3 near 13 % and TiO_2 > 2%), Al-poor metabasalts (Al_2O_3 near 13-15 %), while light-coloured eclogites have higher aluminium contents (Al_2O_3 near 17-20 %), and higher average magnesium values but lower titanium contents (TiO_2 < 1,3 %). Detailed geochemical investigations (Blanc, 1981; Piboule and Briand, 1985) have shown that these eclogites can be regarded as the variably

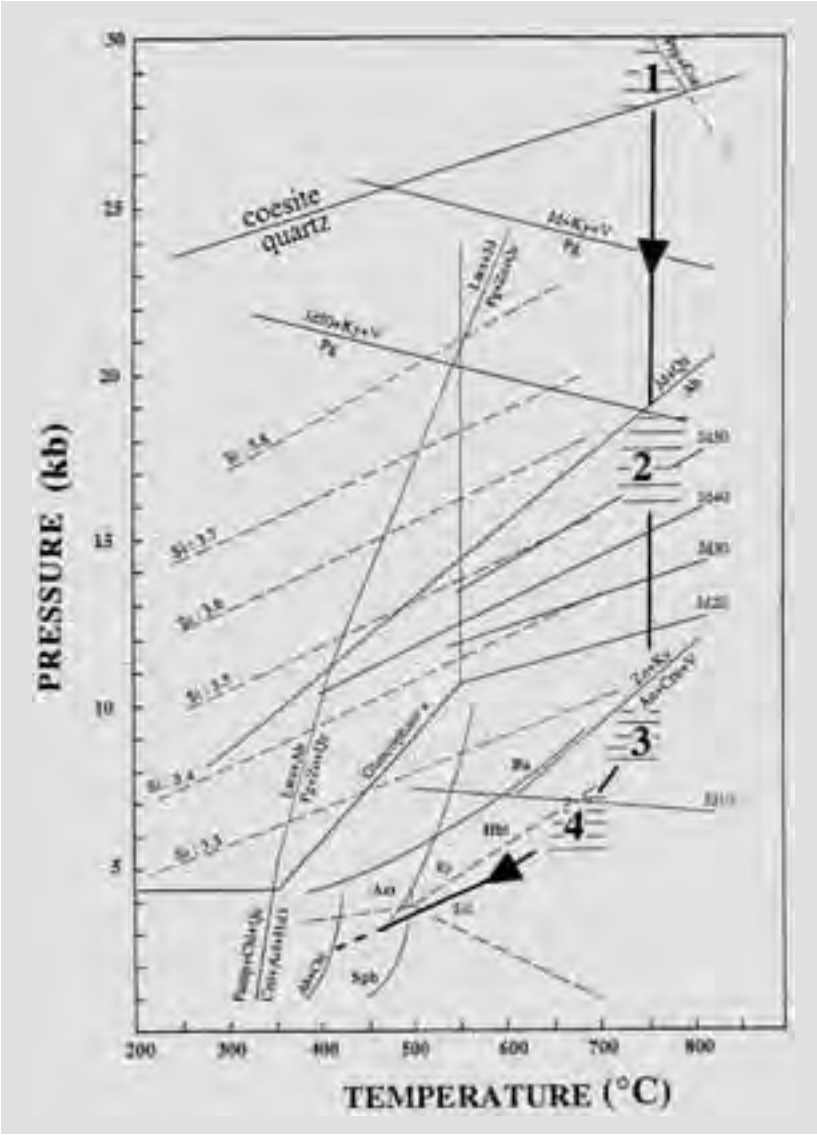

Figure 33 - P-T path of the Monts du Lyonnais coesite-bearing eclogite (see detailed legend of the reactions in Lardeaux et al., 2001).

fractionated members of a volcanic tholeiitic suite.

In the less retrogressed samples, the following mineral assemblages, representing the relicts of eclogite facies metamorphism, are recognized in the dark (1-2) and light (3-4) eclogites from the Monts du Lyonnais (Fig. 33):

- Garnet - omphacite - quartz - zoisite - rutile - apatite - sulfides,
- Garnet - omphacite - quartz - zoisite - colourless amphibole - rutile - sulfides,
- Garnet - omphacite - quartz (or coesite) - zoisite - kyanite - colorless amphibole - rutile,
- Garnet - omphacite - quartz - zoisite - kyanite - phengite - rutile.

Coesite and quartz pseudomorphs after coesite were exclusively detected as inclusions in two garnet grains within one sample of kyanite-bearing eclogite (Color Plate 2, E, F). SiO2 polymorphs were distinguished optically, i.e. coesite was first positively identified relative to quartz by its higher refractive index, and then confirmed by Raman spectroscopy, by observation of the characteristics Raman lines 177, 271, 521 cm-1. Only two coesite grains are preserved as relics and, generally, coesite is otherwise completely transformed into polycrystalline radial quartz (palisade texture) or into polygonal quartz surrounded by radiating cracks. The extremely rare preservation of coesite in the Monts du Lyonnais eclogites is clearly the result of the high temperature conditions (near 750°C, see details in Dufour et al., 1985 and Mercier et al., 1991) reached during decompression as well as the consequence of fluid influx (hydration) during retrogression. Indeed, the kinetics of the coesite ---> quartz transformation are strongly temperature and fluid dependent (Gillet et al., 1984; Van der Molen and Van Roermund, 1986; Hacker and Peacock, 1995; Liou and Zhang, 1996) and consequently in the studied area, coesite has been almost entirely transformed into quartz.

Stop D5.2:

St-André-la-Côte, Road from St-André-en-Haut to Mornant.

Migmatites and granulitic rocks outcrop in the northern part of the Monts du Lyonnais. Near St-André-la-Côte village, mafic and acid granulite facies rocks are well exposed. In mafic granulites the following metamorphic assemblages are described (Dufour, 1985; Dufour et al., 1985):

- Garnet + plagioclase + orthopyroxene + ilmenite,
- Garnet + plagioclase + amphibole + ilmenite,
- Clinopyroxene + orthopyroxene + plagioclase ± amphibole + ilmenite,
- Garnet + clinopyroxene + othopyroxene + plagioclase ± amphibole + ilmenite.

In acid granulites (Dufour, 1982; Lardeaux et al., 1989), the common mineralogy consists of quartz + plagioclase + K-feldspar + garnet + sillimanite ± spinel ± biotite. Kornerupine - bearing granulites have been also locally recognized in this outcrop (Lardeaux et al., 1989).

In this northern part of the Mont du Lyonnais unit, the metamorphic imprint is typical for Intermediate Pressure granulite facies and there is no trace of eclogitic high-pressure facies metamorphism.

Stop D5.3:

The Yzeron quarry, Road from Ste-Foy-l'Argentière to Craponne, D489.

Stop D5.3 shows the migmatitic orthogneisses from the northern Monts du Lyonnais. These rocks are metamorphosed and strongly foliated under amphibolite facies conditions. Their typical mineralogy is an association of quartz + plagioclase + K-feldspar + biotite ± sillimanite. Muscovite and chlorite are developed during retrogression. In the Yzeron quarry, superposed fold systems have been described in relation with progressive deformation under amphibolite and greenschist facies metamorphic conditions. The main foliation observed in the orthogneisses is folded and / or reworked in the ductile strike-slip shear zones related to the development of a regional scale transpressive regime.

The northern Monts du Lyonnais area, with intermediate–pressure granulite and amphibolite facies metamorphic rocks can be interpreted as remnants of the upper overriding continental crust on which the magmatic arc and the Brévenne back-arc were emplaced. In this model, the southern part of the Monts du Lyonnais unit corresponds to a subduction complex (remnant of subduction channel) located on the top of the lower plate (i.e. Pilat – Velay units).

Stop D5.4:

Brévenne valley, road cut: bimodal magmatic sequence.

Stop D5.4 shows different lithologies, like metabasalts, metarhyolites, metapyroclastites and metasediments, typical for the Brévenne ophiolitic unit. All the lithologies are metamorphosed under greenschist facies conditions. In mafic lithologies, the common mineralogy corresponds to an association of

plagioclase + actinolite + chlorite + sphene ± calcite ± quartz.
The different lithologies are also deformed and involved into a regional scale fold system with sub-vertical axial planes. These folds are related to the regional transpressive regime which affects also the Monts du Lyonnais unit at around 350 – 340 Ma.
Recent geochemical investigations support the origin of the Brévenne ophiolitic sequence, during Devonian, in a back-arc basin developed upon the upper plate of a subduction system.

End of the 5th day in Lyon (airport and railway station)

Acknowledgements

O. Monod is thanked for his review of the first draft of this guidebook. Mrs S. Matrat and D. Quiniou provided a great help during the final stages for preparing this guidebook.

References cited

Arzi, A.A. (1978). Critical phenomena in the rheology of partially melted rocks. *Tectonophysics* 44, 173-184.
Ait Malek, H. (1997). Pétrologie, Géochimie et géochronologie U/Pb d'associations acide-basiques: exemples du SE du Velay (Massif central français) et de l'anti-Atlas occidental (Maroc). Thèse doctorat de l'INPL, Univ. Nancy, 297 pp.
Ait Malek, H., Gasquet, D., Marignac, C. and Bertrand, J.M. (1995). Des xénolites à corindon dans une vaugnérite de l'Ardèche (Massif central français) : implications pour le métamorphisme ardéchois. *C. R. Acad. Sci. Paris* 321, 959-966.
Arnaud, F. (1997). Analyse structurale et thermo-barométrique d'un système de chevauchements varisque : les Cévennes centrales (Massif Central français). Microstructures et mécanismes de déformation dans les zones de cisaillement schisteuses. Thèse 3ème cycle, Institut National Polytechnique de Lorraine, Documents du BRGM, 286, 351 pp.
Arnaud, F. and Burg, J.P. (1993). Microstructures des mylonites schisteuses: cartographie des chevauchements varisques dans les Cévennes et détermination de leur cinématique. *C. R. Acad. Sci. Paris* 317, 1441-1447.
Arthaud, F. (1970). Etude tectonique et microtectonique comparée de deux domaines hercyniens : les nappes de la Montagne Noire (France) et l'anticlinorium de l'Iglesiente (Sardaigne). Thèse d'Etat, Univ. Montpellier, France, 175pp.
Arthaud F. and Matte P. (1977) - Late Paleozoic strike slip faulting in southern Europe and northern Africa: result of right lateral shear zone between Appalachians and the Urals. *Geol. Soc. Am. Bull*. 88, p. 1305 -1320.
Autran, A. and Cogné, J. (1980). La zone interne de l'orogenèse varisque dans l'Ouest de la France et sa place dans le développement de la chaîne hercynienne. (J. Cogné J. and M. Slansky M. Eds.), Géologie de l'Europe du Précambrien aux bassins sédimentaires post-hercyniens, 26ème Cong. Géol. Int., Coll. C6, Paris 1980. *Ann. Soc. géol. Nord*, Lille XCIX, 90-111.
Barbey, P., Marignac, C., Montel, J.M., Macaudière, J., Gasquet, D. and Jabbori, J. (1999). Cordierite growth texture and the conditions of genesis and emplacement of crustal granitic magmas: the Velay granite complex (Massif Central, France*). J. Petrology* 40, 1425-1441.
Barraud, J., Gardien, V., Allemand, P. and Grandjean, P. (2003). Analog models of melt-flow in folding migmatites. *J. Struct. Geol*. in press.
Be Mezème, E. (2002). Application de la méthode de datation à la microsonde électronique de monazite de migmatites et de granitoïdes tardi-hercyniens du Massif Central français. Master thesis, Univ. Orléans, 40 pp.
Bernard-Griffiths, J., Cantagrel J.M. and Duthou J.L. (1977) - Radiometric evidence for an Acadian tectono-metamorphic event in western Massif Central français. *Contrib*. *Mineral. Petrol*. 61, 199-212.
Berthé, D., Choukroune, P and Jegouzo, P. (1978). Orthogneiss mylonite and non coaxial deformation of granite: the exemple of the South armorican shear zone. *J. Struc. Geol.* 1, 31-42.
Bitri, A., Truffert, C., Bellot, J.P., Bouchot, V., Ledru, P., Milési, J.P. and Roig J.Y. (1999) - Imagerie des paléochamps hydrothermaux As-Sb d'échelle crustale et des pièges associés dans la chaîne varisque : sismique réflexion verticale (GéoFrance 3D : Massif central français). *C. R. Acad. Sci. Paris* 329, 771-777.
Blanc, D. (1981). Les roches basiques et ultrabasiques des monts du Lyonnais. Etude pétrographique, minéralogique et géochimique. Thèse Doctorat 3ème cycle, Univ. Lyon 1, 152 p.
Bouchez, J.L., and Jover, O. (1986). Le Massif Central : un chevauchement de type himalayen vers l'ouest-nord-ouest. *C. R. Acad. Sci. Paris* 302, 675-680.
Boutin, R. and Montigny, R. (1993). Datation

39Ar/40Ar des amphibolites du complexe leptyno-amphibolique du plateau d'Aigurande : collision varisque à 390 Ma dans le Nord-Ouest du Massif central français. *C. R. Acad. Sci. Paris* 316, 1391-1398.

Brown, M. (1994). The generation, segregation, ascent and emplacement of granite magma: the migmatite-to-crustally-derived granite connection in thickened orogens. *Earth Science Reviews* 36, 83-130.

Brown, M. and Dallmeyer, R.D. (1996). Rapid Variscan exhumation and the role of magma in core complex formation: southern Brittany metamorphic belt. *J. metamorphic Geol*. 14, 361-379

Burg, J.P., Leyreloup, A., Marchand, J. and Matte, P. (1984). Inverted metamorphic zonation and large-scale thrusting in the Variscan belt: an example in the French Massif Central. *In:* " Variscan tectonics of the North-Atlantic region " (D.H.W. Hutton, and D. J. Sanderson,, Ed.),. pp. 47-61, Spec. Publ. Geol. Soc. London, 14,.

Burg, J.P. Bale, P., Brun, J.P. and Girardeau, J. (1987). Stretching lineation and transport direction in the Ibero-Armorican arc during the siluro-devonian collision. *Geodinamica Acta* 1, 71-87.

Burg J.P., Brun, J.P. and Van Den Driessche, J. (1991) - Le Sillon Houiller du Massif central français : faille de transfert pendant l'amincissement crustal de la chaîne varisque. *C. R. Acad. Sci. Paris* 311, II, 147-152.

Burg, J.P. and Vanderhaeghe, O. (1993). Structures and way-up criteria in migmatites, with application to the Velay dome (French Massif central). *J. Struct. Geol.* 15, 1293-1301.

Burg, J.P., Van Den Driessche, J. and Brun, J.P. (1994). Syn- to post-thickening extension: mode and consequences. *C. R. Acad. Sci. Paris* 319, 1019-1032.

Caen Vachette, M., Couturié, J.P. and Didier, J. (1982). Age radiométrique des granites anatectiques et tardimigmatitique du Velay (Massif Central français). *C. R. Acad. Sci. Paris* 294, 135-138.

Caen Vachette, M., Gay, M., Peterlongo, J.M., Pitiot, P. and Vitel, G. (1984). Age radiométrique du granite syntectonique du gouffre d'Enfer et du métamorphisme hercynien dans la série de basse pression du Pilat (Massif Central Français). *C. R. Acad. Sci. Paris* 299, 1201-1204.

Caron, C., Lancelot, J.R., and Maluski, H. (1991). A paired 40Ar-39Ar and U-Pb radiometric analysis applied to the variscan Cévennes, french Massif central. EUG Strasbourg, *Terra abstracts* 3, 205.

Clemens, J.D. (1990). The granulite-granite connexion. *In:* "Granulites and Crustal Evolution" (D. Vielzeuf and Ph. Vidal, Eds.), Kluwer Acad. Publ., pp. 25-36.

Coffrant, D. (1974). Les éclogites et les roches basiques et ultrabasiques associées du massif de Sauviat-sur-Vige, Masssif central français. *Bulletin de la Société Française de Minéralogie Cristallographie* 97, 70-78

Coffrant, D. and Piboule, M. (1971). Les éclogites et les roches associées des massifs basiques de Saint-Joseph (Monts du Lyonnais, Massif Central français). *Bull. Soc. Géol. Fr.* 7, XIII, 283-291

Couturier, J.P. (1969). Le massif granitique de la Margeride. Thèse d'Etat, Univ. Clermont-Ferrand, France, 190 pp.

Costa, S. (1989). Age radiometrique $^{39}Ar/^{40}Ar$ du métamorphisme des séries du Lot et du charriage du groupe leptyno-amphibolique de Mavejols. *C. R. Acad. Sci. Paris* 309, 561-567.

Costa S. (1992). East-West diachronism of the collisional stage in the French Massif Central: implications for the european variscan orogen. *Geodinamica Acta* 5, 51-68.

Costa, S., Maluski, H. and Lardeaux, J.M. (1993). 40Ar-39Ar chronology of Variscan tectono-metamorphic events in an exhumed crustal nappe: the Monts du Lyonnais complex (Massif Central, France). *Chem. Geol.* 105, 339-359.

Dallain, C., Schulmann, K. and Ledru, P. (1999). Textural evolution in the transition from subsolidus annealing to melting process, Velay dome, French Massif Central. *J. Metamorphic Geol*. 17, 61-74.

Delfour, J. (1989). Données lithostratigraphiques et géochimiques sur le Dévono-Dinantien de la partie sud du faisceau du Morvan (nord-est du Massif Central français). *Géologie de la France* 4, 49-77.

Demange, M. (1975). Style pennique de la zone axiale de la Montagne Noire entre Saint-Pons et Murat-sur-Vèbre (Massif Central). *Bull. BRGM* 2, 91-139.

Demange, M. (1985). The eclogite facies rocks of the Montagne Noire, France. *Chemical Geol.* 50, 173-188.

Didier, J. (1973). Granites and their enclaves. The bearing of enclaves on the origin of granites, 2, Developments in *Petrology Series*, Amsterdam, Elsevier, 3, 37-56.

Didier, J. and Lameyre, J. (1971). Les roches granitiques du Massif central. *In*: Symposium J. Jung : "Géologie, géomorphologie et structure profonde du Massif central français", pp. 17-32,

Clermont-Ferrand, Plein Air Service.

Dubuisson, G., Mercier, J.C.C., Girardeau, J. and Frison, J.Y. (1989). Evidence for a lost ocean in Variscan terranes of the western Massif Central, France. *Nature* 337, 23, 729-732.

Ducrot, J., Lancelot, J.R. and Marchand, J. (1983). Datation U-Pb sur zircons de l'éclogite de la Borie (Haut-Allier, France) et conséquences sur l'évolution anté-hercynienne de l'Europe Occidentale. *Earth Planet. Sci. Lett.* 18, 97-113.

Dufour, E. (1982). Pétrologie et géochimie des formations orthométamorphiques acides des Monts du Lyonnais (Massif Central français). Thèse Doctorat de 3ème cycle, Univ. Lyon 1, 241 p.

Dufour, E. (1985). Granulite facies metamorphisme and retrogressive evolution of the Monts du Lyonnais metabasites (Massif Central France) *Lithos* 18, 97-113

Dufour, E., Lardeaux, J.M. and Coffrant, D. (1985). Eclogites and granulites inthe Monts du Lyonnais area: an eo-Hercynian plurifacial metamorphic evolution. *C. R. Acad. Sci, Paris* 300, 141-144

Dupraz, J. and Didier, J. (1988). Le complexe anatectique du Velay (Massif Central français) : structure d'ensemble et évolution géologique. *Géologie de la France* 4, 73-87.

Duthou, J.L, Cantagrel, J.M., Didier, J. and Vialette, Y. (1984). Paleozoïc granitoïds from the French Massif Central: age and origin studied by 87Rb/87Sr system. *Phys. Earth Planet. Int.* 35, 131-144.

Duthou, J-L., Chenevoy, M. and Gay M. (1994). Age Rb/Sr Dévonien moyen des migmatites à cordiérite du Lyonnais (Massif Central français). *C. R. Acad. Sci. Paris.* 319, 791-796.

Echtler, H. and Malavieille, J. (1990). Extensional tectonics, basement uplift and Stephano-Permian collapse basin in a Late Variscan metamorphic core complex (Montagne Noire, Southern Massif Central). *Tectonophysics* 177, 125-138.

Engel, W., Feist, R. and Franke, W. (1980). Le Carbonifère anté-stéphanien de la Montagne Noire : rapports entre mise en place des nappes et sédimentation. *Bull. BRGM* 2, 341-389.

Faure, M. (1995). Late orogenic carboniferous extensions in the Variscan French Massif Central. *Tectonics* 14, 132-153.

Faure, M., Pin, C. and Mailhé, D. (1979). Les roches mylonitiques associées au charriage du groupe leptyno-amphibolique sur les schistes du Lot dans la région de Marvejols (Lozère). *C. R. Acad. Sci. Paris* 288, 167-170.

Faure, M. and Cotterau, N. (1988). Données cinématiques sur la mise en place du dôme migmatitique carbonifère moyen de la zone axiale de la Montagne Noire (Massif Central, France). *C. R. Acad. Sci. Paris* 307, Il, 1787-1794.

Faure, M., Leloix, C. and Roig, J.Y. (1997). L'évolution polycyclique de la chaîne hercynienne. *Bull. Soc. Geol. France* 168, 695-705.

Faure, M., Monié, P., Maluski, H., Pin, C. and Leloix, C. (2001). Late Visean thermal event in the northern part of the French Massif Central. New $^{40}Ar/^{39}Ar$ and Rb-Sr isotopic constraints on the Hercynian syn-orogenic extension. *Int. J. Geol* 91, 53-75.

Feist, R. and Galtier, J. (1985). Découverte de flores d'âge namurien probable dans le flysch à olistolithes de Cabrières (Hérault). Implications sur la durée de la sédimentation synorogénique dans la Montagne Noire (France Méridionale), *C. R. Acad. Sci. Paris* 300, 207-212.

Feybesse, J.L., Lardeaux, J.M., Johan, V., Tegyey, M., Dufour, E., Lemiere, B. and Delfour, J. (1988). La série de la Brévenne (Massif Central Français): une unité dévonienne charriée sur le complexe métamorphique des Monts du Lyonnais à la fin de la collision varisque. *C. R. Acad. Sci. Paris* 307, 991-996.

Feybesse, J.L., Lardeaux, J.M., Tegyey, M., Kerrien, Y., Lemiere, B., Mercier, F., Peterlongo, J.M. and Thieblemont, D. (1996). Carte géologique de France (1/50000), feuille St Symphorien-sur-Coise (721). BRGM Orléans.

Floc'h, J-P. (1983). La série métamorphique du Limousin central. Thèse d'Etat, Univ. Limoges, France, 445pp.

Fonteilles, M. (1968). Contribution à l'nanalyse du processus de spilitisation. Etude comparée des séries volcaniques paléozoïques de la Bruche (Vosges) et de la Brévenne (Massif Central français). *Bull. BRGM* 2, (3), 1-54

Franke, W. (1989). Tectonostratigraphic units in the Variscan belt of central Europe. *In* " Terranes in the circum-Atlantic Paleozoic orogens " (R.D. Dallmeyer Ed.), pp. 67-90. Special paper, Geological Society of America, 230.

Franke,W. (2000). The mid-European segment of the Variscides: tectonostratigraphic units, terrane boundaries and plate tectonic evolution, in Orogenic Processes. *In* " Quantification and Modelling in the Variscan Belt "(W. Franke, V. Haak, O. Oncken, D. Tanner, Eds.) pp. 35-61. Special Publications, 179, Geological Society of London.

Gardien, V., Lardeaux, J.M. and Misseri, M. (1988). Les péridotites des Monts du Lyonnais (Massif Central français) : témoins privilégiés d'une subduction de lithosphère paléozoique. *C. R. Acad. Sci. Paris* 307, 1967-1972.

Gardien, V. (1990). Reliques de grenat et de staurotide dans la série métamorphique de basse pression du Mont Pilat (Massif Central français): témoins d'une évolution tectonométamorphique polyphasée. *C. R. Acad. Sci. Paris* 310, 233-240.

Gardien, V., Tegyey, M., Lardeaux, J.M., Misseri, M. and Dufour, E. (1990). Crustal-mantle relationships in the french Variscan chain: the example of the Southern Monts du Lyonnais unit (eastern French Massif Central*). Journ. Metam. Geol.* 8, 477-492.

Gardien, V. and Lardeaux, J.M. (1991). Découvertes d'éclogites dans la synforme de Maclas: extension de l'Unité Supérieure des Gneiss à l'Est du massif central. *C. R. Acad. Sci. Paris* 312, 61-68.

Gardien, V., Lardeaux, J.M., Ledru, P., Allemand, P. and Guillot, S. (1997). Metamorphism during late orogenic extension: insights from the French Variscan belt. *Bull. Soc. Géol. Fr*. 168, 271-286.

Gèze, B. (1949). Etude Géologique de la Montagne Noire et des Cévennes Méridionales*. Mem. Soc. Géol. France* 24, 215.

Gay, M., Peterlongo, J.M. and Caen-Vachette, M. (1981). Age radiométrique des granites en massifs allongés et en feuillets minces syn-tectoniques dans les Monts du Lyonnais (Massif Central français*). C. R. Acad. Sci. Paris* 293, 993-996.

Gillet, P., Ingrin, J. and Chopin, C. (1984). Coesite in subducted continental crust: *P-T* history deduced from an elastic model. *Earth Planet. Sci. Lett.* 70, 426-436

Godard, G. (1990). Découverte d'éclogites, de péridotites à spinelle et d'amphibolite à anorthite, spinelle et corindon dans le Morvan. *C. R. Acad. Sci. Paris* 310, 227-232.

Hacker, B.R. and Peacock, S.M. (1995). Creation, preservation, and exhumation of UHPM rocks. *In:* "Ultra-high-Pressure Metamorphism". (Coleman, Wang, Eds.), Cambridge University Press, Cambridge, pp. 159-181

Lagarde, J.L., Dallain, C., Ledru, P. and Courrioux, G. (1994). Deformation localization with laterally expanding anatectic granites: Hercynian granites of the Velay, French Massif Central. *J. Struct. Geol*. 16, 839-852.

Lardeaux, J.M. (1989). Les formations métamorphiques des Monts du Lyonnais *Bull. Soc. Géol. Fr.* 4, 688-690

Lardeaux, J.M. and Dufour, E. (1987). Champs de déformation superposés dans la chaîne varisque. Exemple de la zone nord des Monts du Lyonnais (Massif Central français). *C. R. Acad. Sci. Paris* 305, 61-64.

Lardeaux, J.M., Reynard, B. and Dufour, E. (1989). Granulites à kornérupine et décompression post-orogénique des Monts du Lyonnais. *C. R. Acad. Sci. Paris* II 308, 1443-1449

Lardeaux, J.M., Ledru, P., Daniel, I. and Duchène, S. (2001). The variscan French Massif Central - a new addition to the ultra-high pressure metamorphic «club»: exhumation processes and geodynamic consequences. *Tectonophysics* 323, 143-167.

Lasnier, B. (1968a). Découverte de roches éclogitiques dans le groupe leptyno-amphibolique des Monts du Lyonnais. *Bull. Soc. Géol. Fr.* 7, 179-185

Ledru, P., Lardeaux, J.M., Santallier, D., Autran, A., Quenardel, J-M., Floc'h, J-P., Lerouge, G., Maillet, N., Marchand, J. and Ploquin, A. (1989). Où sont les nappes dans le Massif Central français ? *Bull. Soc. Géol. France* 8, 605-618.

Ledru, P., Autran, A. and Santallier, D. (1994a). Lithostratigraphy of Variscan terranes in the French Massif Central. A basic for paleogeographical reconstruction. *In:* "Pre-Mesozoic geology in France and related areas", (J. D. Keppie, Ed.). pp. 276-288. Springer Verlag.

Ledru, P., Costa, S. and Echtler, H. (1994b). Structure. *In*: "Pre-Mesozoic geology in France and related areas", (J. D. Keppie, Ed.). pp. 305-323, Springer Verlag.

Ledru, P., Courrioux, G., Dallain, C., Lardeaux, J.M., Montel, J.M., Vanderhaeghe, O., and Vitel, G. (2001). The Velay dome (French Massif Central): melt generation and granite emplacement during orogenic evolution. *Tectonophysics* 332, 207-237.

Leloix, C., Faure, M. and Feybesse, J.L. (1999). Hercynian polyphase tectonics in north-east French Massif Central : the closure of the Brévenne Devonian-Dinantian rift. *Int. J. Earth. Sci.* 88, 409-421.

Liou, J.G. and Zaang, R.Y. (1996). Occurrences of intergranular coesite in ultrahigh-P rocks from the Sulu region, eastern China: implications of lack of fluid during exhumation. *Am. Mineralogist* 81, 1217-1221

Macaudière, J., Barbey, P., Jabbori, J. and Marignac, C. (1992). Le stade initial de fusion dans le développement des dômes anatectiques : le dôme du Velay (Massif Central français*). C. R. Acad. Sci. Paris* 315, 1761-1767.

Volume n° 2 - from B16 to B33

Malavieille, J., Guihot, P., Costa, S., Lardeaux, J.M., and Gardien, V. (1990). Collapse of the thickened Variscan crust in the French Massif Central: Mont Pilat extensional shear zone and St Etienne upper Carboniferous basin. *Tectonophysics* 177, 139-149.

Mattauer, M., Brunel, M. and Matte, P. (1988). Failles normales ductiles et grands chevauchements : une nouvelle analogie entre l'Himalaya et la chaîne hercynienne du Massif français. *C. R. Acad. Sci. Paris* 306, 671-676.

Mattauer, M., Laurent P. and Matte P. (1996). Plissements hercyniens synschisteux post-nappe et étirement subhorizontal dans le versant Sud de la Montagne Noire. *C. R. Acad. Sci. Paris.* 322, 309-315.

Mattauer, M. and Matte, P. (1998). Le bassin stéphanien de St-Etienne ne résulte pas d'une extension tardi-hercynienne généralisée : c'est un bassin pull-apart en relation avec un décrochement dextre. *Geodinamica Acta* 11, 23-31.

Matte, P. (1991). Tectonics and plate tectonics model for the variscan belt of Europe. *Tectonophysics* 126, 329-374.

Matte, P. (2001). The Variscan collage and orogeny (480-290 Ma) and the tectonic definition of the Armorica microplate : a review. *Terra Nova* 13, 122-1128.

Matte, P., Lancelot, J-R. and Mattauer, M. (1998). La zone axiale hercynienne de la Montagne Noire n'est pas un " metamorphic core complex "extensif mais un anticlinal post-nappe à cœur anatectique. *Geodinamica Acta* 11, 13-22.

Maluski, H., Costa, S. and Echler H. (1991). Late Variscan tectonic evolution by thinning of an earlier thickened crust. An $^{40}Ar/^{39}Ar$ study of the Montagne Noire, southern Massif central, France. *Lithos* 26, 287-304.

Mercier, L., Lardeaux, J.M. and Davy, P. (1991). On the tectonic significance of the retromorphic P-T paths of the french Massif Central eclogites. *Tectonics* 10, 131-140.

Milési, J.P. and Lescuyer J.L. (1989). The Chessy Zn-Cu-Ba massive sulphide deposit and the Devonian Brévenne volcano-sedimentary belt (eastern Massif Central, France). Project: identification of diagnostic markers of high-grade massive sulphide deposits of of their enriched zones in France and in Portugal. CEE contrat MA IM-0030-F(D). Rapp. BRGM 89 DAM 010 DEX (final report)

Mergoil, J., Boivin, P., Blès, J.L., Cantagrel, J.M. and Turland M. (1993). Le Velay. Son volcanisme et les formations associées, notice de la carte à 1/100000. *Géologie de la France* 3, 3-96.

Monié, P., Respaut, J.-P., Brichaud, S., Bouchot, V., Faure, M. and Roig, J.-Y. (2000). $^{40}Ar/^{39}Ar$ and U-Pb geochronology applied to Au-W-Sb metallogenesis in the Cévennes and Châtaigneraie districts (Southern Massif Central, France). *In*: "Orogenic gold deposits in Europe", (V. Bouchot, Ed.), pp. 77-79. Document BRGM 297, Bureau de Recherches Géologiques et Minières, Orléans.

Montel, J.M., 1985. Xénolithes peralumineux dans les dolérites du Peyron, en Velay (Massif Central français). Indications sur l'évolution de la croute profonde tardihercynienne. *C. R. Acad. Sci. Paris* 301, 615-620.

Montel, J.M., Weber, C., Barbey, P. and Pichavant, M. (1986). Thermobarométrie du domaine anatectique du Velay (Massif Central français) et conditions de genèse des granites tardi-migmatitiques. *C. R. Acad. Sci. Paris* 302, 647-652.

Montel, J.M. and Abdelghaffar, R. (1993). Les granites tardi-migmatitiques du Velay (Massif Central): principales caractéristiques pétrographiques et géochimiques. *Géologie de la France* 1, 15-28.

Montel, J.M., Bouloton, J., Veschambre, M., Pellier, C. and Ceret, K. (2002). Age des microgranites du Velay (Massif Central Français). *Géologie de la France* 1, 15-20.

Montel, J.M., Marignac, C., Barbey, P. and Pichavant, M. (1992). Thermobarometry and granite genesis : the Hercynian low-P, high-T Velay anantectic dome (French Massif Central). *J. Metam. Geol.* 10, 1-15.

Mougeot, R., Respaut, J.P., Ledru, P. and Marignac, C. (1997). U-Pb chronology on accessory minerals of the Velay anatectic dome (French Massif Central). *Eur. J. Mineral*. 9, 141-156.

Nicolas, A., Bouchez, J-L. Blaise, J. and Poirier, J-P. (1977). Geological aspects of deformation in continental shear zones. *Tectonophysics* 42, 55-73.

Patiño Douce, A.E. and Johnston, A.D. (1990). Phase equilibria and melt productivity in the pelitic system: implications for the origin of peraluminous granitoids and aluminous granulites. *Contrib*. *Mineral. Petrol*. 107, 202-218.

Peterlongo, J.M. (1960). Les terrains cristallins des monts du Lyonnais (Massif Central français). *Ann. Fac. Sci.* Univ. Clermont-Ferrand 4, (1), 187

Peterlongo, J.M. (1970). Pillows-lavas à bordure variolitique et matrice basique dans la série métamorphique de la Brévenne (Rhône, Massif Central Français). *C. R. Acad. Sci. Paris* 2, 190-194

Piboule, M., Briand, B. and Beurrier, M. (1982). Géochimie de quelques granites albitiques dévoniens de l'Est du Massif Central (France). *Neues Jb. Miner. Abh.,* 143, 279-308.

Piboule, M., Beurrier, M., Briand, B. and Lacroix, P. (1983). Les trondhjemites de Chindo et de St-Veran et le magmatisme kératophyrique associé. Pétrologie et cadre géostructural de ce magmatisme Dévono-Dinantien. *Géologie de la France* I, 2, (1-2), 55-72

Piboule, M. and Briand, B. (1985). Geochemistry of eclogites and associated rocks of the southeastern area of the French Massif Central: origin of the protoliths. *Chem. Geol.* 50, 189-199

Pin, C. (1979). Géochronologie U-Pb et microtectonique des séries métamorphiques anté-stéphaniennes de l'Aubrac et de la région de Marvejols (Massif Central). Thèse 3° cycle, Univ. Montpellier, France, 220pp.

Pin, C. (1981). Old inherited zircons in two synkinematic variscan granitoids: the "granite du Pinet" and the "orthogneiss de Marvejols" (southern French Massif Central). *N. Jb. Miner. Abh*. 142, 27-48.

Pin, C. (1990). Variscan oceans: ages, origins and geodynamic implications inferred from geochemical and radiometric data. *Tectonophysics* 177, 215-227.

Pin, C. and Lancelot, J. (1978). Un exemple de magmatisme cambrien dans le Massif Central : les métadiorites quartzites intrusives dans la série du Lot. *Bull. Soc. Géol. France* 7, 203-208.

Pin, C. and Lancelot, J. (1982). U-Pb dating of an early paleozoïc bimodal magmatism in the French Massif Central and of its further metamorphic evolution. *Contrib. Mineral Petrol,* 79, 1-12.

Pin, C., Dupuy, C. and Peterlongo, JM. (1982). Répartition des terres rares dans les roches volcaniques basiques dévono-dinantiennes du nord-est du Massif central. *Bull. Soc. Géol. Fr.* 7, 669-676.

Pin, C. and Vielzeuf, D. (1983). Granulites and related rocks in Variscan median Europe: a dualistic interpretation. *Tectonophysics* 93, 47-74.

Pin, C. and Duthou, J.L. (1990). Sources of Hercynian granitoids from the French Massif Central: inferences from Nd isotopes and consequences for crustal evolution. *Chemical Geology* 83, 281-296.

Pin, C. and Marini, F. (1993). Early Ordovician continental break-up in Variscan Europe: Nd-SR isotope and trace element evidence for bimodal igneous associations of the southern Massif Central, France. *Lithos* 29, 177-196.

Pin, C and Paquette, JL (1998). A mantle-derived bimodal suite in the Hercynian Belt: Nd isotope and trace element evidence for a subduction-related rift origin of the Late Devonian Brévenne metavolcanics, Massif Central (France). *Contrib Mineral Petrol* 129, 222-238.

Quénardel, J.M. and Rolin, P. (1984). Paleozoic evolution of the Plateau d'Aigurande (N-W. Massif Central, France). *In* "Variscan tectonics of the North Atlantic region" (D. Hutton and D. Sanderson, Eds.), pp. 63-77, Geol. Soc. London Spec. pub, 14.

R'Kha Chaham, K., Couturié, J.P., Duthou, J.L., Fernandez, A. and Vitel, G. (1990). L'orthogneiss oeillé de l'Arc de Fix : un nouveau témoin d'âge cambrien d'un magmatisme hyper alumineux dans le Massif Central français. *C. R. Acad. Sci. Paris* 311, 845-850.

Robardet, M., Verniers, J., Feist R. and Paris, F. (1994). Le Paléozoïque anté-varisque de France, contexte paléogéographique et géodynamique. *Géol. de la France* 3, 3-31.

Robardet, M. (2003). The Armorica 'microplate': fact or fiction? Critical review of the concept and contradictory palaeobiogeographical data. *Palaeogeography, Palaeoclimatology, Palaeoecology* 195, 125-148.

Roig, J-Y. and Faure M. (2000). La tectonique cisaillante polyphasée du Sud-Limousin (Massif Central français) et son interprétation dans un modèle d'évolution polycyclique de la chaîne hercynienne. *Bull. Soc. Géol. Fr.* 171, 295-307.

Roig, J-Y., Faure, M. and Truffert, C. (1998). Folding and granite emplacement inferred from structural, strain, TEM, and gravimetric analyses: the case study of the Tulle antiform, SW French Massif Central. *J. Struct. Geol.* 20, 1169-1189.

Sider, J-M. and Ohnenstetter, M. (1986). Field and petrological evidence forfor the development for an ensialic marginal basin related to the Hercynian orogeny in the Massif Central, France. *Geol. Rundschau* 75, 421-443.

Soula, J.C., Debat, P., Brusset, S., Bessière, G., Christophoul, F. and Déramond, J. (2001). Thrust related, diapiric and extensional doming in a frontal orogenic wedge: example of the Montagne Noire, southern French Hercynian Belt. *J. Struct. Geol.* 23, 1677-1699.

Van den Driessche J. and Brun, J-P. (1991-92). Tectonic evolution of the Montagne Noire (French Massif Central): a model of extensional gneiss dome. *Geodinamica Acta* 5, 85-99.

Vanderhaeghe, O., Burg, J.P. and Teyssier, C. (1999).

Exhumation of migmatites in two collapsed orogens: Canadian Cordillera and French Variscides. *In:* "Exhumation processses: normal faulting, ductile flow and erosion" U. Ring, M.T. Brandon, G.S. Lister and S.D. Willett (Eds.) 181-204, *Geological Society, London*, Special Publications, 154,

Vanderhaeghe, O. and Teyssier, C. (2001). Partial melting and flow of orogens. *Tectonophysics* 342, 451-472.

Van der Molen, I. and Van Roermund, H.L.M. (1986) The pressure path of soild inclusions in minerals: the retention of coesite inclusions during uplift. *Lithos* 19, 317-324

Vitel, G. (1985). La transition faciès granulite faciès amphibolite dans les enclaves basiques du Velay. *C. R. Acad. Sci. Paris* 300, 407-412.

Williamson, B.J., Downes, H. and Thirlwall, M.F. (1992). The relationship between crustal magmatic underplating and granite genesis: an example from the Velay granite complex, Massif Central, France. *Trans. Royal Soc. Edinburgh*, *Earth Sciences* 83, 235-245.

Back Cover:
field trip itinerary

FIELD TRIP MAP

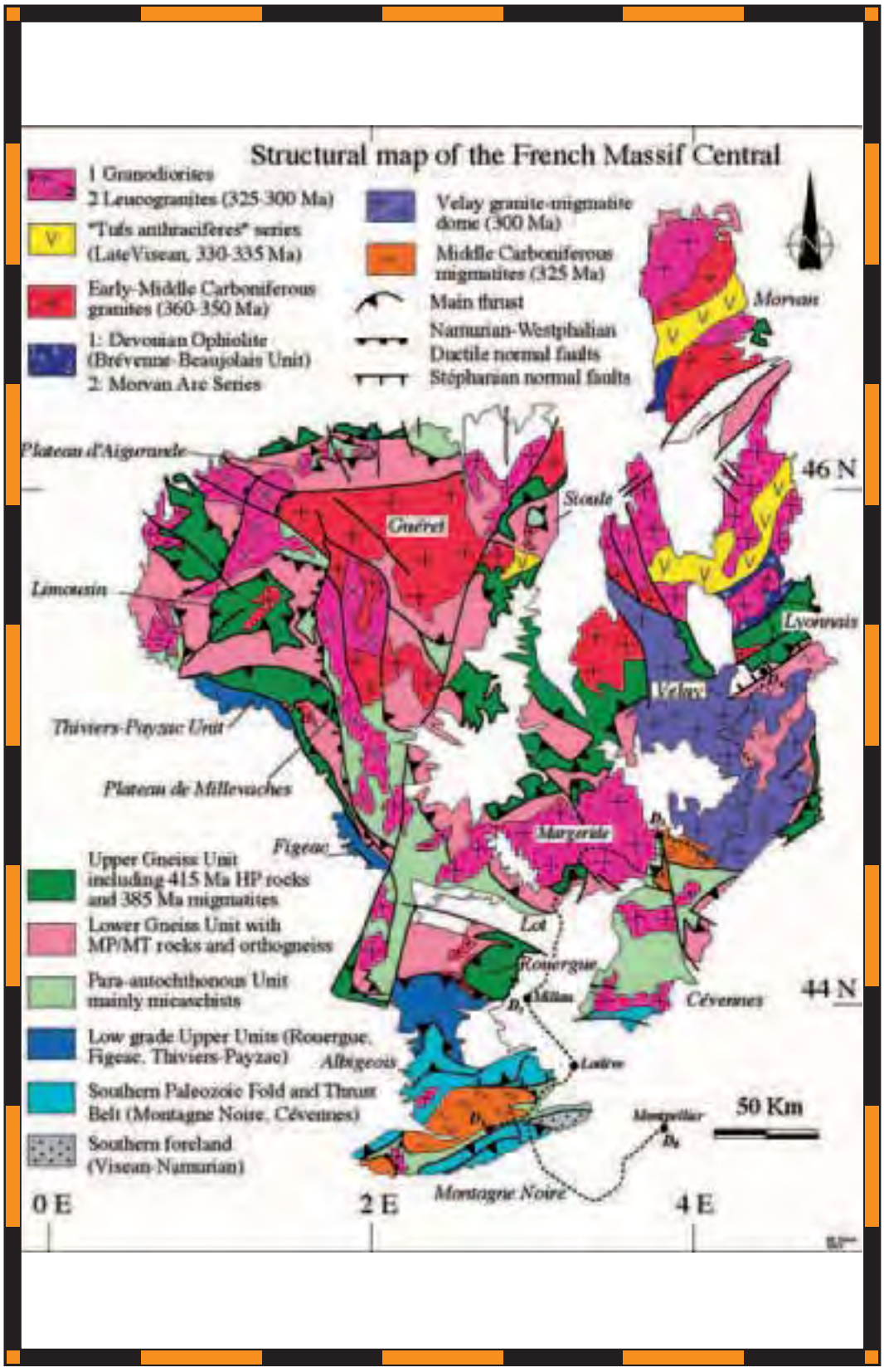

Edited by APAT

Volume n° 2 - from B16 to B33

32nd INTERNATIONAL GEOLOGICAL CONGRESS

LATE QUATERNARY EVOLUTION OF THE PO PLAIN FROM SURFACE AND SUBSURFACE DATA: A TRAVERSE FROM THE APENNINES TO THE ADRIATIC SEA

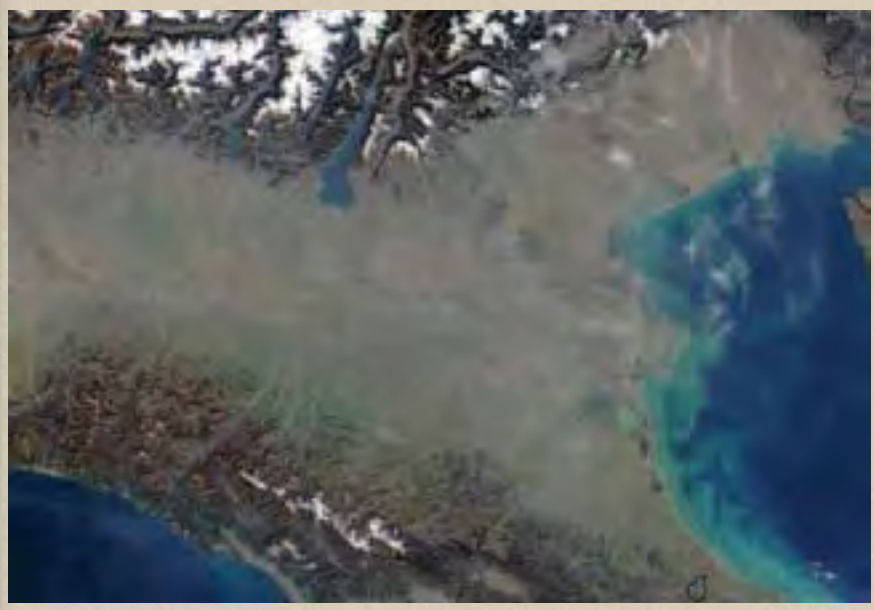

Leaders: A. Amorosi, U. Cibin, P. Severi, M. Stefani

Field Trip Guide Book - B24

Florence - Italy
August 20-28, 2004

Pre-Congress **B24**

The scientific content of this guide is under the total responsibility of the Authors

Published by:
APAT – Italian Agency for the Environmental Protection and Technical Services - Via Vitaliano Brancati, 48 - 00144 Roma - Italy

Series Editors:
Luca Guerrieri, Irene Rischia and Leonello Serva (APAT, Roma)

English Desk-copy Editors:
Paul Mazza (Università di Firenze), Jessica Ann Thonn (Università di Firenze), Nathalie Marléne Adams (Università di Firenze), Miriam Friedman (Università di Firenze), Kate Eadie (Freelance indipendent professional)

Field Trip Committee:
Leonello Serva (APAT, Roma), Alessandro Michetti (Università dell'Insubria, Como), Giulio Pavia (Università di Torino), Raffaele Pignone (Servizio Geologico Regione Emilia-Romagna, Bologna) and Riccardo Polino (CNR, Torino)

Acknowledgments:
The 32nd IGC Organizing Committee is grateful to Roberto Pompili and Elisa Brustia (APAT, Roma) for their collaboration in editing.

Graphic project:
Full snc - Firenze

Layout and press:
Lito Terrazzi srl - Firenze

Volume n° 2 - from B16 to B33

32nd INTERNATIONAL GEOLOGICAL CONGRESS

LATE QUATERNARY EVOLUTION OF THE PO PLAIN FROM SURFACE AND SUBSURFACE DATA: A TRAVERSE FROM THE APENNINES TO THE ADRIATIC SEA

AUTHORS:
A. Amorosi[1], U. Cibin[2], P. Severi[2], M. Stefani[3]
G. Gabbianelli[1], U. Simeoni[3], S. Vincenzi[3]

[1]Dipartimento di Scienze della Terra e Geologico-Ambientali, Bologna - Italy
[2]Servizio Geologico, Sismico e dei Suoli, Bologna - Italy
[3]Dipartimento di Scienze della Terra, Ferrara - Italy

Florence - Italy
August 20-28, 2004

Pre-Congress

B24

Front Cover:
Satellite image of the Po Plain, surrounded by the Alps and Apennines chains and by the Adriatic Sea.

Leader: A. Amorosi, U. Cibin, P. Severi, M. Stefani
Associate Leaders: G. Gabbianelli, U. Simeoni, S. Vincenzi

Introduction

The depositional architecture of alluvial plain and delta deposits is quite valuable, harboring a detailed stratigraphic archive, highly sensitive to both eustatic and climatic fluctuations. Climate plays a major role by modulating both the marine dynamics and the riverine supplies; relative sea level in turn controls the river base level and the accommodation space availability. The impressive Quaternary fluctuations of these parameters broadly affected the depositional dynamics of the alluvial and deltaic units, offering a good opportunity to test the sequence stratigraphy concepts against actual case histories, framed within a high-resolution chronological context. The alluvial Po plain and delta areas provide excellent examples of such terrigenous systems, as well as being the sites of Italy's main economic activity, despite their being subject to major environmental risks. The geological study of these deposits is therefore valuable from both scientific and applied points of view.

Since the late eighties, the Geological Survey of the Emilia-Romagna Region has being carrying out an extensive interdisciplinary research effort, aimed at understanding these complex successions, within the framework of the Geological Mapping Protocol of Italy, at the 1:50,000 scale. The research integrates outcrop and subsurface studies, both in the northern Apennines foothills and in the adjacent subsurface, in order to reconstruct the Po Basin depositional history during Pliocene and Quaternary times, through the hierarchical identification of genetically-related depositional units. Detailed surface geological mapping is integrated by shallow-subsurface 3D modeling, based on stratigraphic coring, a large number of digital cone-penetration tests, and geophysics, the latter being particularly valuable in the offshore areas.

This trip is intended to provide an introduction to the late Quaternary evolution of the Po Plain in the Emilia-Romagna region, through the examination of: (i) outcropping continental deposits and fluvial terraces near the Apennine foothills, (ii) stratigraphic cores from upper and lower Po Plain areas, (iii) outcropping Holocene sedimentary bodies in the present-day coastal plain, and (iv) modern delta bay depositional environments. This paper is a collective effort by academic and public administration geologists; individual authorship is indicated at specific paragraphs, the final editing was mainly carried out by M. Stefani.

The Po Plain is the surface expression of a peri-sutural basin, bounded to the south by the Apennines and to the north by the Alps, with its southern prolongation forming the Adriatic Sea (Fig. 1). The region therefore largely corresponds to a foredeep basin, developed during Neogene times and subject to active tectonic deformation. The active tectonic framework of the basin is characterized by ramp and flat structures, propagating toward northern areas. The subsurface geology has mainly become known through the hydrocarbon exploration of this area (Fig. 2), site of natural gas and geothermal exploitation, the latter by the town of Ferrara. Because of the active structural framework, the Quaternary deposits show a comparatively reduced thickness in the discontinuous basin margin outcrops, but they can exceed 2,000 m in the Po Plain depocentres. Great thickness variations have been identified in the subsurface, between subsiding syncline areas and ramp anticline zones. The Quaternary foredeep successions record an overall shallowing evolution, from deep marine environments to alluvial plain conditions, a trend dramatically punctuated by the Quaternary glacio-eustatic fluctuations. This evolution records the sharp predominance of the sediment influx over the accommodation increase rate. The strong sediment input was related to the fast erosion of the surrounding high relief, through glacial and interglacial phases.

The younger portions of the Po Plain stratigraphic succession are dominated by Po river sediments, grading southward into its tributaries deposits. During the first excursion day, fluvial deposits and morphological terraces will be examined in the Modena (Tiepido river valley) and Bologna (Reno river valley) areas. Some geographic and hydrologic information on these rivers is useful in helping the understanding of their depositional dynamics. We have, however, to keep in mind that these data are strongly influenced by both anthropic alteration and the present-day climatic conditions. The Tiepido river (a name literally meaning "lukewarm") is a small stream flowing from the Apenninic argillaceous hills and reaching the Po through the Panaro river; it is almost dry in summer, but it can experience impressive floods in autumn-winter time (when lukewarm it is not!). The Reno river has presently a length of 211 km, a hydrographic basin of 1,015 km^2, and a mean discharge of about 26 m^3/sec, at its entry point into the alluvial plain. Due to the high relief and the terrigenous lithological composition

Volume n° 2 - from B16 to B33

of the Reno drainage basin, the river sediment load during flood episodes is very large, supporting a high sedimentation rate both along its plain course and at its wave-dominated mouth. The Reno river acted for a long period as a Po tributary, even as late as in the XVI Century, but the combined action of the Po riverbed aggradation and of large hydraulic engineering works then forced it to independently reach the Adriatic Sea, through a former Po delta distributary channel mouth.

The Po is by far the largest river of Italy, albeit being a small one if considered from a global point of view. It has a length of 652 km, a catchment area of about 70,100 km^2, displaying a very complex and heterogeneous geological framework, and a mean annual discharge estimated at about 1,515 cubic metres per second, over the 1918-1981 interval, with flood peaks of over 10,000 m^3/sec and low water levels of just a few hundreds m^3/sec. The largest floods normally take place in November, the lowest level is in late summer. The flux variations are now largely emphasized by human activity impact, such as deforestation, urban growth and continuous river embankment; they were therefore much lower during the Holocene. Throughout the Holocene, active sedimentation was nevertheless essentially confined to autumn-winter flood episodes. The Po northern tributaries, often flowing out of large glacially-induced lakes and from crystalline areas, are generally much poorer in sediment load than their southern counterparts, sourced by the flysch-dominated Apennines. The Po flows into the Adriatic Sea through a complex delta system, the modern one being the youngest out of several generations of highstand wave-dominated deltas. The delta dynamics was obviously influenced also by the oceanographic dynamics of the Adriatic Sea, a semi-enclosed basin subject to strong salinity variations and rich in continental-derived nutrients. Very calm under average conditions, the Adriatic Sea is subject to significant winter storm wave activity, and a tidal range exceeding 130 cm in the Po Delta region. The Po sedimentary evolution will be mainly examined in its historic delta area, during the second day of the trip.

Figure 1 - Location map of the study area, showing section traces of Figures 2, 3, 7, 8 and 10.

Geological setting

The stratigraphic interpretation of the depositional units outcropping at the Po Basin margin is based upon recent field work and previously published papers (Ricci Lucchi et al., 1981, 1982; Gasperi et al., 1986; Vai & Castellarin, 1992; Pini, 1999). Subsurface research at the basin scale (Pieri & Groppi, 1981; Castellarin et al., 1985; Dondi & D'Andrea, 1986; Dalla et al., 1992; Regione Emilia-Romagna and ENI-AGIP, 1998; Regione Lombardia & Eni Divisione Agip, 2002) include: i) the analysis of 30,000 km of seismic reflection profiles provided by ENI-AGIP, ii) sedimentological-stratigraphic interpretation of over 11,000 km of continuously-cored boreholes, and iii) logging measurements (electric logs, spontaneous potential, and, where available, sonic logs) from approximately 600 boreholes.

As already pointed out, an overall shallowing-upward trend characterizes the upper portion of the Apennine foredeep basin fill (Ricci Lucchi, 1986). The distinction of two laterally-extensive stratigraphic discontinuities ("B" and "F" in Fig. 2) enables the identification of three third-order depositional sequences. These sequences coincide with the depositional cycles P2 (middle-late Pliocene), Qm

(Quaternary marine), and Qc (Quaternary continental), recognized at the basin margin by Ricci Lucchi et al. (1982). These discontinuities record important changes in the foredeep accommodation potential, changes generated by basin-modification events which were related to the structural framework reorganization. These structural events forced the marginal area to uplift and the depocentres to migrate northward, generating denudation surfaces, both at the basin margin and on structural highs. Basin margin tilting resulted in the formation of angular unconformities, associated with strong erosion. Diminishing accommodation triggered the development of fast-prograding units, in the central part of the basin, generating the rapid basinward shifting of the offlap breaks. The main tectonic events were separated by subsidence periods, increasing the accommodation potential. This evolution resulted in the piling up of aggrading packages, with the prominent onlap of seismic reflectors onto the sequence bounding unconformities (Fig. 2). The subsurface correlation of the thin stratigraphic packages recognized in outcrop is prevented by the reduced seismic differentiation potential in the subsurface; detailed calibration of well-log and core data, based upon micropalaeontological analysis, pollen and strontium isotope stratigraphy, however, quite often generates reliable correlation lines from proximal to relatively distal areas.

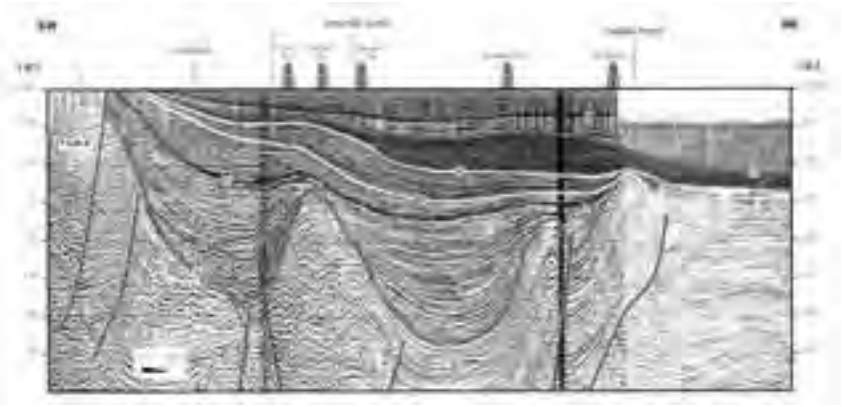

Figure 2 - Seismic line across the southern Po Plain (see section trace in Fig. 1), with sequence-stratigraphic interpretation of the Pliocene-to-Quaternary basin fill, involved into the Apennines front compressive deformation. The "F" unconformity corresponds to the lower boundary of the Emilia-Romagna Supersynthem; the "G" one separates the Lower Emilia-Romagna Synthem from the overlying Upper Emilia-Romagna Synthem. From Regione Emilia-Romagna & Eni-Agip (1998).

An upward transition from deep marine clays ("Argille Azzurre") to littoral sands (Imola Sands of Amorosi et al., 1998; see also Ruggieri, 1962, 1995) represents the diagnostic feature of the Qm cycle in the northern Apennines piedmont belt. The Imola Sands outcrop discontinuously, representing the last marine episode recorded in the outcropping foredeep succession, which was deformed and uplifted during Late Pliocene and Pleistocene times.

Tectonic influence progressively decreases from the strongly deformed Pliocene strata to the relatively undisturbed Late Quaternary deposits (Qc sequence, above unconformity "F" in Fig. 2). In the Geological Map of Italy at a 1:50,000 scale, the Qc cycle is referred to as the Emilia-Romagna Supersynthem. Identification of a laterally extensive unconformity within this unit ("G" in Fig. 2) allows the Emilia-Romagna Supersynthem to be subdivided into two lower-rank units (Lower and Upper Emilia-Romagna Synthems, respectively). The Lower Emilia-Romagna Synthem predominantly consists of alluvial and coastal plain deposits at the basin margin, grading basinward into delta front and shallow-marine deposits (high-amplitude, laterally continuous reflectors, Ori, 1993). This unit is capped by the Upper Emilia-Romagna Synthem, consisting entirely of alluvial fan and alluvial plain alternations in marginal areas, grading basinward into cyclic alternations of alluvial and deltaic/shallow-marine deposits. This sequence is characterized by poorly-defined subsurface reflectors, but it can be carefully studied through core analysis and geologic log interpretation.

A marked cyclicity typifies the Upper Emilia-Romagna Synthem. Beneath the present coastal plain, the repeated alternation of coastal and alluvial deposits enables the splitting up of this unit into

Volume n° 2 - from B16 to B33

stacked transgressive-regressive sequences (T-R), showing an average thickness of about 100 m and spanning over time intervals of about 100 ka (Fig. 3). These sequences are characterized by a peculiar internal architecture and correspond to 4th-order depositional cycles. Lower parts of T-R sequences record fast coastal-plain aggradation and rapid shoreline transgression, through the development of retrograding barrier-lagoon-estuary systems, forming thin transgressive systems tracts (TST). The transgressive deposits are overlain by characteristic shallowing-upward successions, related to delta and strandplain progradation, forming highstand systems tracts (HST). The subsequent long-lasting phases of sea-level fall are recorded by exceptionally thick (up to 60 m) successions of interbedded alluvial and coastal-plain deposits, falling-stage (FST) and lowstand (LST) systems tracts (Amorosi et al., 1999b; Amorosi and Colalongo, in press).

At landward locations, within non-marine strata, the rhythmic alternation of coarse-grained bodies and thick, locally-pedogenized, clay horizons occurs at various scales, providing the basic cyclic theme of the alluvial plain facies associations. In this framework, bounding surfaces of T-R sequences are marked by abrupt facies changes, from amalgamated fluvial-channel gravel and sand, deposited mostly at lowstand conditions, to mud-dominated floodplain sediments, with isolated channel bodies and organic-rich, paludal clays (transgressive alluvial deposits - TST). These successions grade upward into thick alluvial plain deposits, showing increased channel clustering and sheet-like geometry (regressive alluvial deposits, including HST, FST, and LST).

The sharp lower boundaries of T-R sequences, identified within the alluvial sections, can be physically traced into the transgressive surfaces recognized at seaward locations (Fig. 3). Given the unconformable nature of the basal transgressive surfaces, the T-R sequences identified within the Upper Emilia-Romagna Synthem can be regarded as subsynthems. Examining the stratigraphic architecture from top to bottom, we may observe that the base of the Ravenna Subsynthem (AES8) corresponds to the onset of the recent Flandrian transgression (Oxygen Isotope Stage 1 in the curve of Martinson et al., 1987); this unit mainly consists of Holocene deposits. The lower boundary of the underlying Villa Verucchio Subsynthem (AES7) is assigned to O.I.S. 5e, i.e. the Tyrrhenian transgression, whereas the base of the older Bazzano Subsynthem (AES6) is thought to reflect transgression at the onset of O.I.S. 7.

Pollen distribution within T-R sequences shows distinctive cyclic changes, which parallel facies architecture. Arboreal pollen (AP) displays maximum values within coastal sediments, floodplain clays, and inland swamp peats, at the base of T-R sequences, suggesting the development of mixed, broad-leafed vegetation, during warm-temperate climatic phases (Amorosi et al, 1999b; 2001). AP percentages sharply decrease in the middle and upper parts of T-R cycles, dominated by amalgamated fluvial-channel bodies, where pollen spectra record a cold-climate vegetation, dominated by NAP (non-arboreal pollen) and Pinus. Transgressive surfaces correlate with the onset of warm-temperate, interglacial phases (Amorosi et al., 2004). The close match between stratigraphic architecture and pollen distribution suggests that sedimentation in the Po Basin was predominantly driven by combined eustatic sea-level changes and climatic variations. Correlation with the marine oxygen-isotope record documents strict relationships between T-R sequences and glacial/

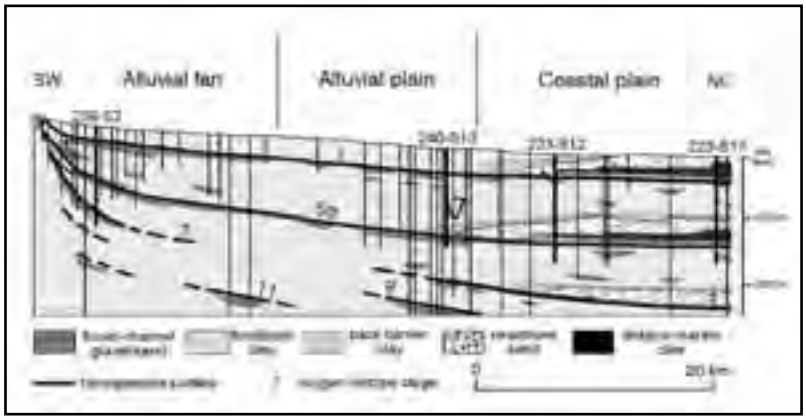

Figure 3 - Stratigraphic overview of the Upper Emilia-Romagna Synthem (see section trace in Fig. 1), showing the subdivision into transgressive-regressive sequences (subsynthems) and the geometric linkage between updip fluvial strata and downdip deltaic and coastal-marine deposits. From Amorosi & Colalongo (in press).

interglacial eustatic cycles.
A peculiar sedimentary cyclicity can also be observed within the intramontane valley deposits, at the northern Apennines margin. Individual cycles there consist of the regular alternation of sections displaying high and low terrace preservation, which are likely to reflect alternating interglacial/glacial phases. Radiocarbon dating (Amorosi et al., 1996) supports the correlation of the well-preserved fluvial terraces, spanning a few tens of metres above the present rivers (terraces 1-14 in Fig. 7), with the Ravenna Subsynthem. Dating of older units is in progress, in order to generate a detailed stratigraphic framework for the whole of the Po Basin. Refined geological mapping of the youngest terraces, together with their radiometric and archaeological dating, document a very close spacing between individual terrace sequences, in the range of 2-5 m, recording a periodicity of 1000-1500 yrs. This study enables their correlation with thin, palaeosol-bounded floodplain cycles, reflecting higher-frequency climatic fluctuations (Fig. 4).
The 3D depositional architecture of Subsynthem AES8 (Ravenna) and the Holocene sedimentary evolution in the Po delta area have been recently reconstructed through interdisciplinary integration of sedimentological, stratigraphic, palaeontological and geotechnical investigations (Amorosi et al., 1999a; 2003; Amorosi & Marchi, 1999; Bondesan et al., 1999). This transgressive-regressive cycle corresponds to the youngest fourth-order depositional sequence, related to the post-glacial eustatic rise. Several evolutionary stages can be schematically identified through the sequence, while only the youngest of these is recorded by outcropping sediments:
a) During the last glacial interval (Würmian), the present day coastal region saw the development of a comparatively-coarse fluvial sedimentation, in a cold, middle alluvial plain setting, about 300 km inland. Amalgamated sand bodies, bearing large mammal remains (e.g., Mammoth), were quite probably deposited into braided river environments, and can be correlated across the entire axial portion of the Po Plain. From a stratigraphic point of view, this unit belongs to the uppermost part of Subsynthem AES7 (Villa Verrucchio).
b) The latest Pleistocene was characterized by a non-depositional and erosional evolution, cutting a system of shallow valleys and fluvial terraces, with elevation differences in the order of 20 m. This evolution resulted in the formation of a laterally extensive hiatal surface, marking the boundary between Subsynthems AES7 and AES8.
c) During the climax of the eustatic rise (O.I.S. 1), coastal sedimentation was negligible, and transgression very fast, producing a widespread ravinement surface, which still bottoms large portions of the Adriatic Sea. Sedimentation was still spotty in the present day coastal area.
d) At about 10,000 yr B.P., the last phases of eustatic rise triggered a renewed fast sedimentation in the area, under lower alluvial plain and coastal marsh conditions. Deposition was unable to counteract the relative sea-level rise and, therefore, further transgression took place, triggering the development of a back-stepping deltaic-estuarine system, characterized by flat, laterally-extensive sand bodies, grading seawards into a condensed bioclastic clay level (TST).
e) At about 5,500 yr B.P., sedimentation managed to compensate the sea-level rise, at the maximum transgression line. This line has been identified 25 km eastward from the present coast in the visited region.
f) High sedimentation rates then took over the reduced sea-level rise, and coastal progradation started. During early highstand times, large coastal bays were closed by the lateral growth of sandy spits

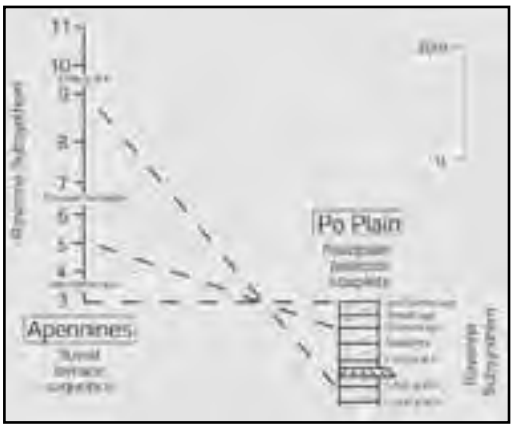

Figure 4 - Stratigraphic correlations between fluvial-terrace and floodplain deposits within the Ravenna Subsynthem. Note how single terrace sequences (numbered on left) correlate into the subsurface with floodplain units bounded by very low-maturity palaeosols (black lines on the right). The correlation line between terrace n. 3 and the post-Roman age palaeosol, based on geometric and pedologic evidence, is assumed as datum. Terraces n. 1 and 2 are not reported in the figure since they are artificial, having been produced by human activity. From Amorosi et al. (1996).

and barrier islands. An environmental innovation phase then generated a deltaic system that was to survive until the recent land reclamation works, through the development of succeeding generations of partially-overlapping delta lobes. Progradation continued to coexist with localised marine transgression onto abandoned distributary systems. The growth of the different lobe generations produced thick regressive sequences (HST). The interpretation of the last 3,000-yr interval becomes more and more accurate, being recorded by outcropping sediments. Through this period, the delta distributary channels migrated laterally, over more than 90 km (Fig. 5). The cold and moist climatic phases saw higher fluvial system instability and faster delta progradation rates than drier periods. The average shoreline migration rate over the last 3,000 yrs was in the order of 4-5 m/yr, peaking at over 100 m in a few months, during the early stages of the present day delta growth. During the same interval, delta front deposits record high sedimentation rates, with an average value of 5 mm/yr and peaks of several m/yr at the distributary mouths.

Over the last 3,000 yrs the sedimentary dynamics have been subject to an increasing anthropic impact. Delta dynamics (Fig. 5) strongly influenced the development of an affluent Etruscan port (Spina), as well as the last capital of the Roman Empire (Ravenna). Eventually, the sedimentary dynamics were totally altered by hydraulic engineering works. The present day delta is an almost artificial structure, induced in the early XVII Century by the Republic of Venice to avoid the silting up of the Venetian Lagoon. The delta is presently characterised by five active distributary channels, namely: Po di Maistra, Pila, Tolle, Gnocca, and Goro, the major one being the Pila channel. During the last 50 years erosion has largely taken over sedimentation as the dominating coastal process, and so delta progradation has ceased, due to the severe reduction of the sediment flux. At present, only large coastal protection works and artificial damming prevent the delta area, largely lying beneath sea level, from being vanquished by the sea.

The modern delta environmental framework

G. Gabbianelli & U. Simeoni

The present day delta territory has been extensively modified by human activity. Hydraulic works were carried out by the monks of the Pomposa Abbey (6th-10th Centuries AD); extensive land reclamation was performed during the XVI Century, but the reclaimed areas were soon to return to their initial marsh condition, because of the fast subsidence, the rapid coastal progradation, the strong sea storms and the river flooding characterizing the so-called “Little Ice Age”, as well as due to human heedlessness. A new cycle of reclamation works began during the second half of the XIX Century, and at the beginning of 1900 ca, 800 km^2 of marshes were reclaimed for agriculture, by means of huge water-scooping machines. The last works were carried out during the 1970s; the marshy areas were eventually reduced to their present 120 km^2 extension, less than a quarter of their 19th Century extension.

The present bowl-shaped form of the delta region, featuring higher borders seaward and a wide depression in the middle, well below sea level (Bondesan, 1989; Simeoni et al., 2000), is mainly due to the artificial subsidence and to the lengthening of the constrained delta distributary channels. During flood events, the levee-retained waters can rise up to 6-8 m above the surrounding floodplain. During the last decades, a deepening trend of the Po distributary channels was recorded, increasing the risk of piping and breaching through artificial levees, grounded on instable soils. The distributaries’ natural tendency of breaching and wandering triggered large flooding even in recent times (1951, 1957 and 1966). This dangerous situation is forcing the managing administrations to constantly reshape the hydraulic works, at a major economic cost. The reclamation works largely enhanced the natural subsidence speed of about 1-2 mm/yr, but the main accelerating factor was the extraction of methane- bearing waters from deposits, carried out between 1938 and 1961 (Bondesan and Simeoni, 1983). Caputo et al. (1970) and Borgia et al. (1982) report subsidence rates of up to 250 mm/yr in the central area of the present day delta, during the 1951-57 interval, and up to 180 mm/yr between 1958 and 1962. After the extraction stopping, subsidence slowed down to mean rates of 33 mm/yr, during the 1962-67 interval, and to 37.5 mm/yr between 1967 and 1974 (Bondesan and Simeoni, 1983). These latter data witness the fading out of the benefits derived from the ending of the water extraction, as early as the early ‘70s. Fast subsidence accelerated shoreline retreat along the delta coasts, already suffering from the sharp decrease of the sediment supply. This evolution also increased the slope angle of beaches. Both the subsidence-triggered lagoon deepening and the sediment occlusion of tidal inlets induced a sensible slackening of internal hydrodynamic energy. The result is a finer-grained sedimentation inside lagoons

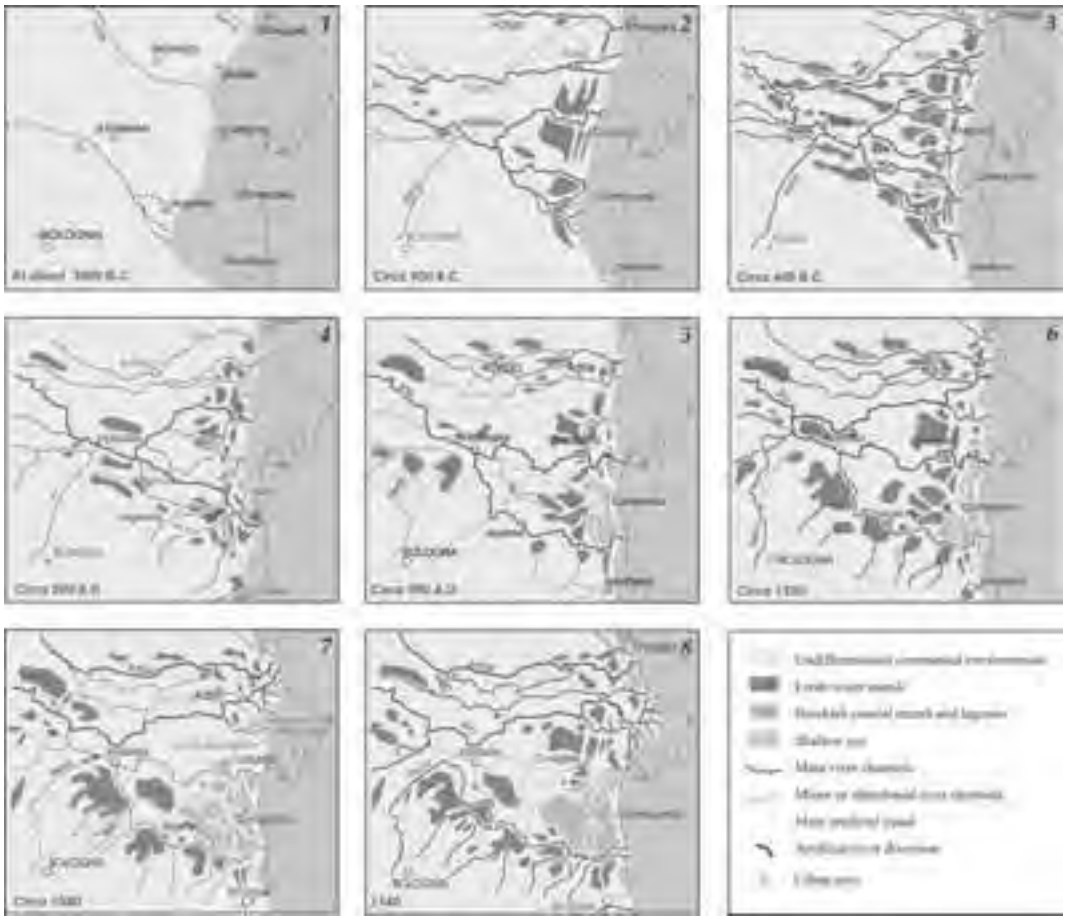

Figure 5 - The complex highstand evolution of the Po delta distributary channels. Palaeogeographic reconstruction becomes progressively more reliable and accurate for the last 3,500 ysr; during this time interval, the delta lobes migrated over more than 90 km and the coastline prograded up to 25 km to the east. The arrows indicate major man-induced fluvial diversions, which had a dramatic impact on the Reno and Po river evolution, the present-day lobe being an almost artificial structure, induced at the very beginning of the XVII Century to prevent the silting up of the Venice lagoon (Cf. Figs. 10 and 11).

and bay areas, which are subject to the progressive benthic fauna depopulation and to increasing anoxia phenomena, also supported by the increasing load of human-produced organic nutrients.

DAY 1

A. Amorosi, U. Cibin, & P. Severi

The first day of trip will be focused on the Late Quaternary deposits of the Po Basin (Emilia-Romagna Supersynthem), along a proximal to distal transect traced from surface to subsurface successions. In the morning, we will observe the fluvial sequences outcropping at the Apennine margin (Modena and Bologna piedmont area). In the afternoon, we will examine the correlative downdip sedimentary successions of the Po Basin, through detailed analysis of continuous cores. Our overall objective is to discuss a stratigraphic traverse stretching across the Po Basin, focusing our attention on the linkage between the updip fluvial strata, partly exposed at the Apennines foothills, and the downdip coastal deposits, buried beneath the Po Plain.

Stop A1:

Quaternary fluvial deposits of the Tiepido River

Volume n° 2 - from B16 to B33

valley (Lower Emilia-Romagna Synthem)

Our trip will start at the southern margin of the Po Basin, in the Modena area. The lower Quaternary fluvial succession (the Lower Emilia-Romagna Synthem), which is several hundreds metres thick in the subsurface of the Po Plain, wedges out toward the basin margin (Figs. 2, 3, and 8) and is generally not exposed along the Apennine foothills, with the exception of a very few sections. In the Tiepido River valley, the Lower Emilia-Romagna Synthem crops out extensively, consisting of a cyclic alternation of fluvial-channel gravel bodies and mud-dominated floodplain deposits. The overall Quaternary succession is punctuated by two major unconformities, which are thought to reflect two distinct episodes of tectonic uplift which affected the Apennine chain. A prominent unconformity separates the Lower Emilia-Romagna Synthem from the underlying littoral Imola Sands (Qm sequence). The base of the Upper Emilia-Romagna Synthem is characterized by an angular unconformity, overlain by an almost horizontal succession of terraced fluvial deposits. As a whole, the Lower Emilia-Romagna Synthem shows a coarsening- and thickening-upward trend, marked by the progressive increase in the gravel content, leading to frequently-amalgamated gravel bodies. Mature palaeosols can be identified in the upper part of the succession.

Stop A2:

Late Quaternary fluvial terraces of Reno River valley (Upper Emilia-Romagna Synthem)

A few stops in the Reno River valley, nearby Bologna, will provide us with the opportunity to discuss the general aspects of fluvial terrace sedimentation at the Po Basin margin. In this area, a hierarchy of fluvial terrace sequences can be identified by successively thinner groupings of genetically-related fluvial terraces. Unfortunately, outcrops are rare in this area, and our discussion will therefore mainly have to follow a geomorphic approach.

A first stop, south of Sasso Marconi, will provide an overview (Fig. 6) of the entire Late Quaternary fluvial terrace succession (the Upper Emilia-Romagna Synthem). We will be standing on top of the Holocene terrace. Two groups of older, well-preserved fluvial terraces are clearly visible at higher topographic levels. In the valley landscape the various terrace groups show up, split by steep escarpments many tens of metres high, displaying very poor terrace preservation and including outcrops of much older bedrock units (Fig. 7).

A close inspection of the topographic bands displaying higher terrace preservation will be possible later in the day, south of Casalecchio di Reno, where individual terraces of Holocene age can be walked on, and minor escarpments, a few m thick, more closely observed.

The alluvial terrace deposits consist of fining-upward successions, generally 2-4 m thick, bounded by erosional basal unconformities, cut into the underlying bedrock. Channel-related facies are mainly represented by massive, horizontally- or cross-stratified gravels. The lens-shaped sand bodies topping gravel units are thought to represent lower energy deposits, formed in chutes or abandoned channels. Coarse-grained sediments are generally abruptly overlain by tabular silty and clay bodies, considered to be overbank deposits, or by localized organic-rich layers. Terrace sequences are generally capped by colluvial deposits, the thickness of which increases moving from the younger to the older units. Pedogenesis typically took place at the top of the overbank fines. Soil formation was triggered by renewed incision, preventing the further flooding of the newly formed terraces. Soils occur at various stratigraphic levels within the colluvium, reflecting distinct episodes of subaerial exposure.

Stop A3:

Late Quaternary stratigraphic architecture in the Po Plain subsurface:

Core examination and stratigraphic imaging

This stop will illustrate the subsurface stratigraphic architecture of the Emilia-Romagna Supersynthem in the Po Plain (Fig. 8), focusing on the youngest transgressive-regressive cycle, of Holocene age (the Ravenna Subsynthem), through fresh core examination. The Ravenna Subsynthem shows a complex stacking pattern of alluvial, coastal, deltaic, and shallow-marine deposits (Rizzini, 1974; Bondesan et al., 1995; Amorosi et al., 1999a). The Late Quaternary facies architecture of the Po Plain reflects the last eustatic cycle of sea-level fall and rise, from the glacial maximum to the present (Figs. 8, 10). Fluvial sedimentation characterized the long-lasting phase of falling sea level, which occurred during the last glacial period.

Lowstand fluvial deposition was restricted to broad, shallow, incised valleys, and to the basin axis, whereas soil development occurred on the interfluves. The Bølling-Allerød interstadial and the

subsequent Younger Dryas cold event, were only recorded in fast-subsiding areas, and even there as scattered spots only. Transgressive sedimentation in the present coastal plain mostly started during the early Holocene. The backstepping evolution of sedimentary facies and coastal onlaps led to the landward migration of the shoreline, up to 25 km west of its present-day position. Detailed facies analysis of cores and interpretation of piezocone penetration tests provide a complex scenario of transgressive depositional environments, including coastal plain/lagoon and estuary systems, either wave-dominated or tide-influenced in nature. Highstand deposition, developed during the last 6 ka BP, was characterized by progradation of several generations of ancient, wave-dominated Po deltas, under the combined influence of climate and subsidence.

There will be ample opportunity to discuss the Late Pleistocene-Holocene depositional history of the Po Plain, through detailed examination of two continuous cores, approximately 35 m long, recovered in updip (alluvial) and downdip (coastal) areas. The comparison of the depositional evolution at proximal versus distal locations will be framed by a series of stratigraphic cross-sections and 3D images, documenting the depositional architecture of non-marine and marine sediments. Facies analysis will include close inspection of fluvial-channel sands, floodplain clays, swamp peats, lagoonal clays, transgressive-barrier sands, inner shelf or prodelta clays, and delta front sands. It will be shown how the interdisciplinary integration of the palaeoecological, pollen, petrographic and geochemical characterization of these facies greatly improves their stratigraphic understanding.

Several sequence-stratigraphic surfaces will be shown on core. The transgressive surface (TS – subsynthem lower boundary in Fig. 8) can be easily recognized as a sharp facies change, separating overconsolidated, stiff floodplain clays from overlying swamp and lagoonal (coastal plain and back-barrier), organic-rich deposits. The tidal ravinement surface (TRS) is locally identified within back-barrier, estuarine deposits of the incised-valley fill. The wave ravinement surface (WRS) is a readily-identifiable, regionally extensive surface, marking an abrupt lithological change from back-barrier clays to transgressive barrier, bioclast-rich sands.

The maximum flooding surface (MFS) is located a short distance above TS and RS, and is generally indistinguishable through conventional sedimentological techniques, but it can be placed, based upon palaeoecological information, at the turnover point of the benthic foraminifera associations. The microfaunal assemblages record a palaeoenvironmental evolution leading from open-marine to shallower water, and eventually to schizohaline environments, thus recording a shallowing trend and an increasing riverine influence.

Finally, the very high-resolution stratigraphic outline reconstructed for the Po Plain will be discussed as a nice case history for distillating a generalized sequence stratigraphy model and for testing the opportunity to use transgressive surfaces, rather than sequence boundaries, as stratigraphic bounding surfaces.

After the discussion we will begin our afternoon drive to Ferrara.

Figure 6 - Highly and poorly preserved terraces along the western flank of the Reno River valley, at Sasso Marconi (15 km south of Bologna). Highly-preserved river terraces are numbered (compare with Fig. 7). Terrace n. 10 belongs to the Ravenna Subsynthem, whereas terraces 21 and 27-28 are assigned to the Villa Verucchio Subsynthem and Bazzano Subsynthem, respectively.

Depositional history and the urban growth of Ferrara

M. Stefani

The overnight stay in Ferrara will provide us with the opportunity to discuss the dynamic relationships between a river depositional evolution and the coeval urban growth. Whereas the majority of the Italian towns shares a pre-Roman origin, Ferrara is a comparatively "new" city,

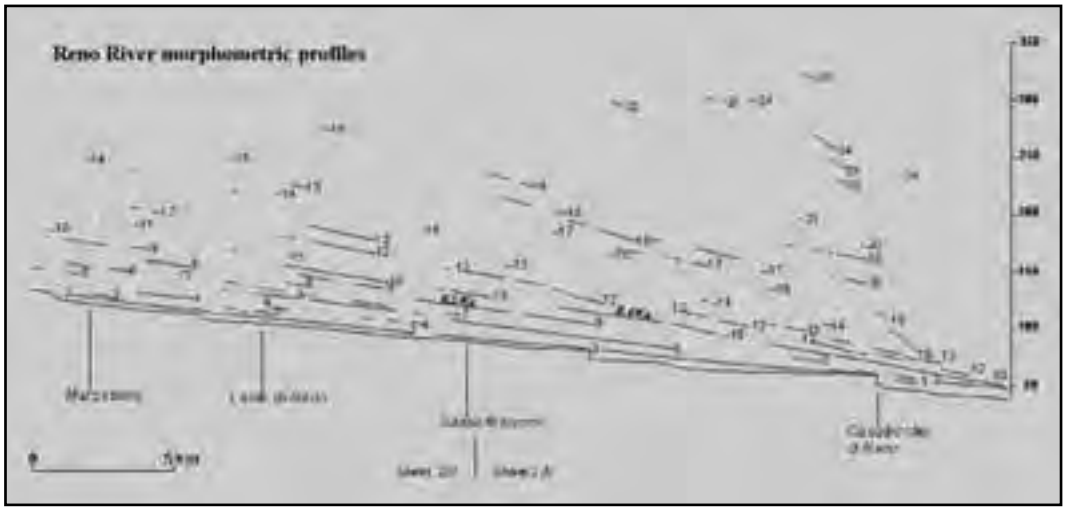

Figure 7 - Longitudinal morphometric profiles through the intramontane valley of the Reno River (see section trace in Fig. 1). Sections with high terrace preservation, corresponding to terraces 1-14, 17-21 and 22-24, are separated by steep escarpments, showing poor (terraces 15-16) or no terrace preservation (see Fig. 6). The escarpments are thought to reflect fluvial channel incision at the onset of glacial periods.

being born in early medieval times (about 1300 yrs B.P.). The early settlers elected the sandy river levees as their dwelling place of choice, since they provided drier and much firmer ground than the surrounding muddy depressions. The town nucleated at two separate sites, the southern one at the very diverging point of the two main Po distributary channels (Primaro and Volano, Fig. 9), where the first cathedral was erected, and the northern one, where a castle was built, near the border between the Byzantine and Longobard areas of influence. The ancient castle area still stands out as the "highest point", so to speak, of the old town. The southern nucleus experienced a reduced expansion, while the northern one enjoyed a steady growth, initially through a linear expansion, on top of an elongate fluvial sand body. Oxford University archeological research has revealed the repeated interbedding of crevasse deposits with anthropic surfaces. At a latter stage, the town grew northward, into the interfluvial depression, through a long series of land reclamation works and discrete town expansions. The environmental constraint, however, still forced the town to keep an elongated shape, parallel to the river. During the XII Century, the Episcopal seat was moved into the Romanesque cathedral, built at the northern limit of the growing town, in a former marsh area. From 1,000 to 500 yrs B.P., the main Po river flow progressively shifted northward, triggering the development of a new delta system (Fig. 5); the water flux at the southern border of the town therefore progressively faded out and a further urban expansion was therefore able to encompass the former fluvial island of St. Anthony. Extensive land reclamation works, starting in 1465, then supported a further huge expansion (the so-called Addizione Erculea, Herculean Addition) into northern interfluvial, morphologically depressed areas, where the poor geotechnical properties generated significant construction problems, witnessed by impressive building deformation. This town expansion started in 1492, but the new areas have still not been completely filled up by constructions (let us hope that they never will be). After a long period of economic and demographic decay, massive urban expansion restarted only after the Second World War, in a chaotic way, utterly unaware of any natural constraint, exposing the town to significant environmental hazards.

The tight scheduling constraints will prevent us from making a comprehensive tour of the town. We will, however, probably be able to get a taste of the "town stratigraphy" by walking through a north-south section, stretching from interfluvial to levee and riverbed areas, eventually reaching remnant distributary channels. We will move from a morphological depression known as Borgo di Sotto (Lower Burg), characterized by organic rich clay and by a very shallow phreatic level, to the sandy levee crest, where 1,000 old buildings are partially buried by slightly younger fluvial sands. We then

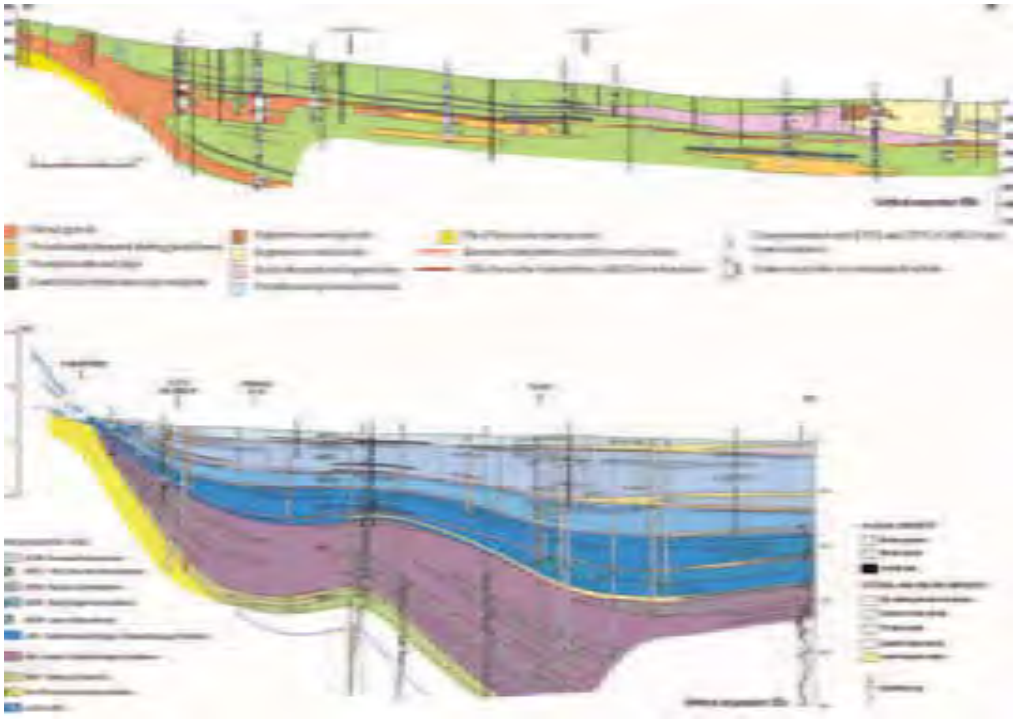

Figure 8 - Geologic cross-sections stretching from the Romagna Apennine foothills to the Adriatic Sea (see section trace in Fig. 1), depicting the subsurface stratigraphy of the Emilia-Romagna Supersynthem (below) and the facies architecture in the uppermost 40 m (above). Compare with the stratigraphic evolution illustrated in Fig. 10. Stratigraphic correlations based upon well geophysical log, core and CPTU data. From the Geological Map of Italy at scale 1:50,000, Sheet 240.

will descend into the ancient sandy river bed (Via XX Settembre), preserving a significant river flank dip (Via Porta d'Amore), and walk through the old town walls and moat, to reach the present day Volano Canal, facing the Po di Primaro distibutary channel diverging area.

DAY 2

M. Stefani and S. Vincenzi

The second day of excursion has aimed at three main goals: (i) exposing the Holocene stratigraphy of the central portion of the Po delta system (Fig. 10); (ii) examining some outcropping coastal units, showing spectacular fossil aeolian dunes, channel-levee complexes, flood erosional structures, etc.; (iii) observe modern depositional environments, during a boat trip into an interdistributary bay. The morning will be aimed at examining some outcropping examples of depositional and erosional processes, which developed over the last 3,000 yrs, a time interval subject to a growing degree of anthropic influence (Fig. 5). This prompts us to put in some remarks on human activity, even in a guide like this one essentially focused on natural processes. Due to the environmental features of the visited area, we recommend trip participants take anti-mosquito precautions.

Stop B1:

Channel-levee complex
of the Volano distributary channel

We will leave the Town of Ferrara heading eastward, following for a while the Po di Volano palaeochannel, gently winding through the lower alluvial plain. The sandy palaeoriverbed morphology often stands out above the surrounding argillaceous depressions. The elevation difference is often in the order of 3-5 m and was enhanced, at a late evolutionary stage of the river, by an early artificial embankment. About 1,000 yrs ago, this was the main distributary channel of the Po system, but then it progressively faded into a minor

Figure 9 - The town of Ferrara has grown on the northernmost natural levee of the Po River, at the diverging point of its medieval-era distributary channels. The stratigraphic architecture strongly influenced the ancient town shape.

role, due to the northward shifting of the water and sediment fluxes. The system eventually experienced a sudden demise, because of an ill-fated attempt to force the Reno River to reach the sea through the Volano; the reduced morphological gradients and the Reno's huge sediment load suddenly choked the Po channel with sediment, preventing any further water flow. The channel axis was therefore filled up with low permeability, fine-grained organic rich sediments, resting on middle-grained fluvial sand. During the XX Century, an artificial canal was dug into the palaeoriverbeds, kept open for navigation and irrigation purposes.

Stop B2:

Reclaimed interdistributary marsh area at the east of Iolanda di Savoia

We will leave the Volano palaeochannel, to enter into a former marsh area, at Tresigallo. Sedimentological reconstruction and archaeological data suggest that the interdistributary area was mainly under subaerial conditions during Roman times, but then evolved into a broad, fresh-water, marshy zone, above sea level. The region then experienced two superimposed land reclamation phases. The first was attempted between 1564 and 1572 (Grande Bonificazione Estense), over more than 400 km^2: a large, 330-km-long canal system was dug, and waters were forced to reach the sea through two canal mouths, under purely gravitational force. Compaction of dried and oxidized peats and organic clays, however, rapidly induced a fast subsidence, which was soon to reverse the topographic gradients, making any effort to keep the region dry totally futile. It was only during the second half of the XIX Century that land reclamation was re-attempted, reaching success through the massive use of steam water pumping and a good injection of British money and know-how. The visited area now shows a completely artificial landscape, with very open spaces, always lying well below sea level. The differential compaction of sediments emphasizes the ancient sandy riverbeds and strongly deforms the rectilinear road-bed driven along during our trip.

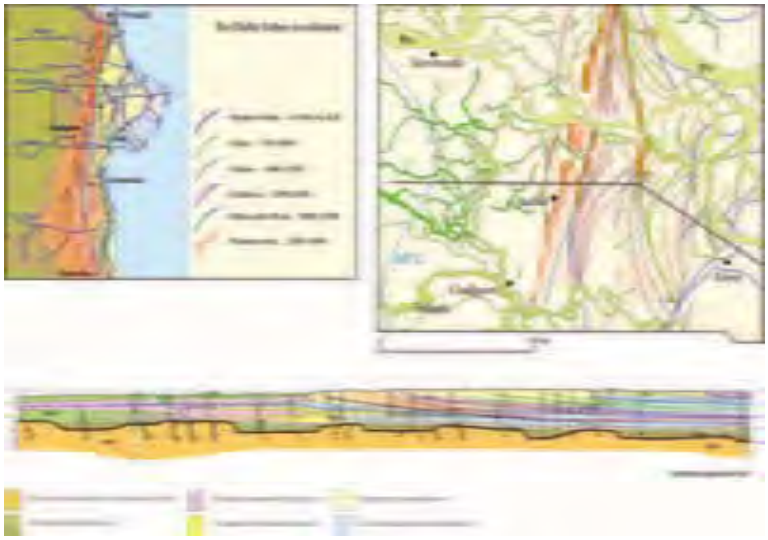

Figure 10 - The visited coastal plain area derived from the superposition of several Po delta lobe generations (a, cf. Fig. 5), the depositional evolution of which is witnessed by outcropping sediments (b) and by the depositional architecture reconstructed in the related subsurface (c, location in Fig. 1). In the profile, a vertical amplification of 1/50 is used and a selection of the analysed cone penetration tests and stratigraphic logs is depicted. While the outcropping units span over the last 3,000 yrs only, the subsurface profile records the evolution from the last glacial maximum to the present. In the stratigraphic profile, note the disconformable superposition of transgressive sediments over eroded continental sands, and the large highstand progradation; in the synthetic surface map, observe the arcuated coastal sand-ridge pattern and the complex palaeoriverbed patterns, showing up in the western portion of the area.

Stop B3:

The Holocene maximum transgression in the northeastern Ferrara Province

Even if nothing catches the eye at the surface, it is worthy to point out the area reached by the Holocene maximum transgression, at about 6,000-5.500 yr B.P., as located by the 3D reconstruction of the depositional geometry and facies (Fig. 10). The maximum transgression line is here located at about 10 m below sea level, and at 25 km to the west of the present day coast line. Such a huge progradation is really impressive, considering the shortness of the time span elapsed and the comparatively reduced dimension of the river system involved.

Stop B4:

Stratigraphic legacy and human alteration on an anomalous delta channel

The trip will perpendicularly cross a peculiar north-south striking palaeoriverbed, the Gaurus. This structure is noteworthy in its being almost perpendicular to all other distributary channels, a trend reflecting the inland wedging out of the transgressive and early highstand coastal sands. This structure was also influenced by the impact of artificial works, carried out during early Roman Empire times, in order to open a continuous navigation canal (Fossa Augusta) linking the ports of Altinum, to the north of Venice, to Classae, near Ravenna. The winding palaeoriverbed stands out above the surrounding reclaimed marsh because of the differential compaction of sand and clay, as well as due to the moistening action of the surviving canal.

Stop B5:

Fossil aeolian dune field near Massenzatica

Major dune field growth was matched with phases of delta lobe abandoning and erosive coast-line retrogradation and stabilization. Some of these aeolian sands show mineralogical features pointing to a northern Adige sediment source, even in this Po dominated area. Among the dune fields preserved throughout the entire Adriatic coast, the visited area stands out for both its good preservation and large dimensions. The dunes date back to about 3,000 yrs B.P., (early Bronze Age) since then, progradation has brought the coastline back an impressive 20 km. The dune field is overall elongated parallel to the ancient coastline, with a N 10° azimuth, but the individual dune ridge direction has a main 50° strike, recording the action of the NE winter winds, in the Adriatic known as "Bora". The internal forsets are mainly dipping at about 230°, again pointing to the NE wind action. The development of this dune field was probably influenced by the stratigraphic inheritance, which made the area less subsiding than the surrounding ones. This site, indeed, corresponds to the seaward edge of the transgressive coastal sand body and to

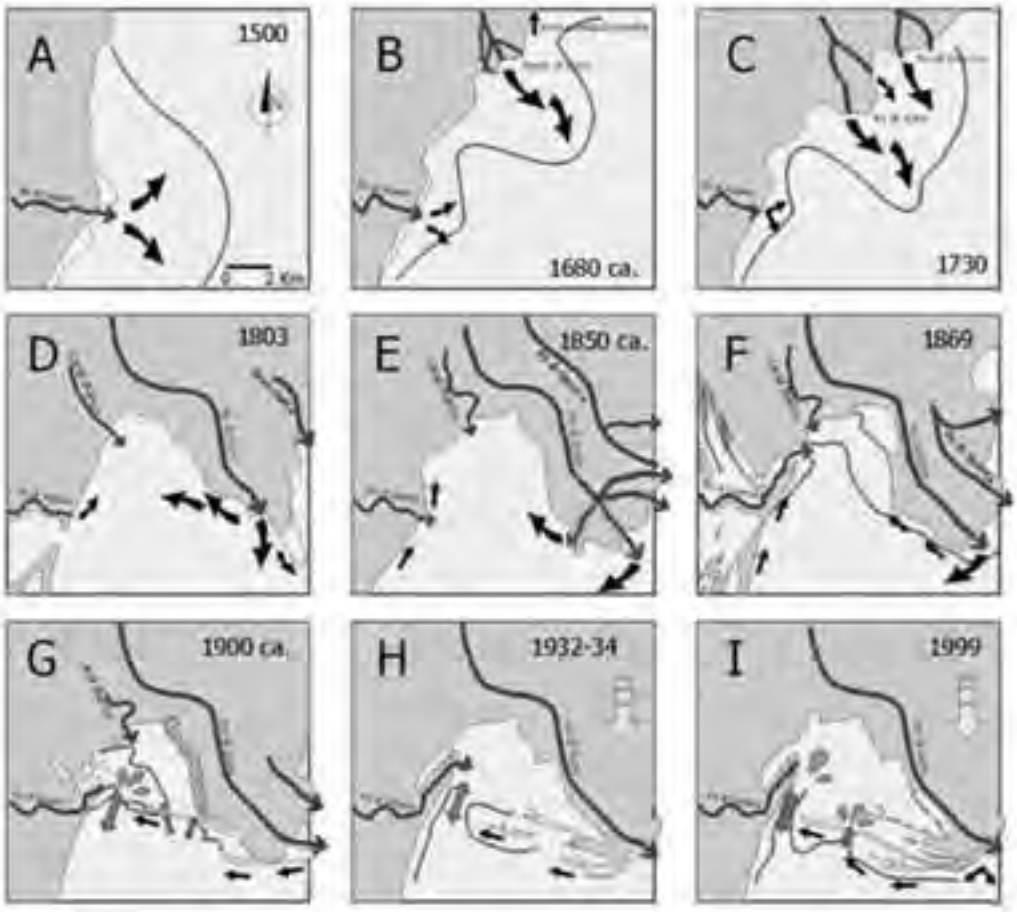

Figure 11 - Environmental evolution of the Po di Goro area from the end of the XVI century to the present day. Bathymetry is depicted by dashed lines (Fontolan et al., 2000). The former marine area was progressively enclosed by the fast modern delta progradation.

an older erosive palaeohigh, curved into Pleistocene sands. The dunes still reach an elevation of about 9 m and are colonized by peculiar xerophilous vegetation. The good preservation of the dune field is also related to the high permeability of these fine-grained, well sorted sands, which prevents rain water from eroding at the surface. At the north, the dune field is suddenly cut by the Po river erosion, near an ancient distributary mouth. At a much more recent time, the dunes barely escaped destruction through illegal sand excavation, a sad fate unfortunately shared by the majority of the surrounding aeolian fields, even where they were harboring major archaeological remains, as in the adjacent San Basilio area.

Stop B6:

Erosive depression cut by flood waters into coastal sands (Gorgo dello Stradone)

The highly turbulent flood waters pouring out from the delta channels interacted in a dramatic way with the coastal sand bodies. The dune alignments played an important role by constraining the flood flux and thus raising up the water level, but the permeable coastal sands were much easier to rework than their finer-grained cohesive marsh counterparts. The fluvial floods were therefore able to pierce through the dune bodies, producing crevasse splays and erosive depressions, locally known as Gorghi, either elongated or sub-circular in shape. The depressions were then filled by the phreatic waters, becoming the site of peculiar, isolated, pond ecosystems. The majority of these depressions was recently filled up by man, generally through their use as waste dumping sites, putting the phreatic waters to a great risk of pollution.

Figure 12 - Satellite image of the modern Po Delta area; the visited Sacca di Goro lagoon is depicted by the dot.

Stop B7:

(optional) Delta distributary palaeochannel mouth and large Renaissance hydraulic works

About 800 yrs ago, the Goro distributary channel bifurcated at Mesola and reached the sea through two independent mouths, in an actively prograding lobe. A Renaissance castle marks the diverging point of the two distributaries. During the second half of the XVI Century, the southern channel was artificially cut off from the active river flow and used as the final draining canal of the large, gravity-driven, land reclamation work, discussed in a previous stop. The interruption of the sediment influx triggered an erosional coastal retrogradation and, to prevent the high tide salty water from flooding the dried-up land, a peculiar bridge-like Renaissance building was erected, as a site of tide-operated locks.

Stop B8:

Depositional evolution of the Goro Lagoon

G. Gabbianelli & U. Simeoni

The afternoon will be mainly spent on a boat trip into the Goro interdistributary lagoon and spit. At the SW of the Goro distributary channel, the homonymous lagoon (Sacca di Goro, Fig. 12) extends over about 2,000 hectares, with an average depth of 1.2–1.5 m only. Its bottom is quite flat and largely consists of bioturbated loam muds, showing a higher clay content in the northern and central zones; sand is, on the contrary, more abundant near the southern lagoon mouth. The evolutionary phases of the Sacca di Goro are depicted in Fig. 11, deduced from ancient cartographic data.

Until the 1500s (A), the open marine area was almost exclusively supplied with sediments by the Po di Volano mouth. The large artificial canal cut in 1604 induced the modern delta formation, that was soon to generate the branches of Goro, Gnocca and Donzella (B). During the early 1700s, the delta lobes of the Po di Goro and of Gnocchetta began to delimitate a protected interdistributary bay (C), which further developed through the following century (D, E). During the second half of the XIX Century (F), a distributary channel mouth deviated into the bay, building up a small deltaic apparatus and feeding sandy spits. At the beginning of the last century (G), the bay was therefore largely occluded by a growing system of sandy spits, turning itself into a semi-enclosed lagoon; the hydraulic exchanges with the sea were mainly supported by tidal currents (bi-directional arrows), through a few remaining tidal mouths. At around 1930 (H), the renewed "sea-flooding" of the Sacca di Goro began, due to the rapid human-induced subsidence (vertical arrow). The deepening evolution still continues today, even if at a reduced speed (I).

The visited lagoon is quite significant from both economic and naturalistic points of view. Following the Ramsar Convention on nature conservation, in 1971, the Goro lagoon was classified as wetland of international importance; in 1982 it was declared a natural reserve, and in 1988 it was included into the Po Delta regional park. These conservation efforts, aimed at enhancing the environmental value of the area, have to unfortunately cope with the strong economic exploitation and ecological degradation of the lagoon: activities connected to clam fishing in the areas involve about 1,000 people, generating an income largely exceeding 50 million Euros per annum. In the last decades, the frequency of eutrophication and anoxia phenomena has had a strong economic impact; the fishery crisis gave rise to an ill-conceived intervention policy, purposely aimed at improving the hydraulic exchanges between the lagoon and the surrounding river and sea waters. The works carried out, however, were performed without any respect for the natural morphodynamics, thus compromising the sedimentary evolution of the area and jeopardizing

Figure 13 - BW reproduction of the nice 1814 watercolour topographic map of the Codigoro area. Before the massive XIX Century land reclamation works, the fluvial and coastal sand ridges spectacularly stood out as emerging topographic highs between fresh water (NW) and brackish (SE) marshes.

the very survival of the Scanno di Goro spit, which provides the only natural protection of the lagoon from the winter sea storms. The impressive lack of sedimentological knowledge showing up in this project was soon to make it utterly useless, because of the lack of any forecasting of the morphological

scenario it would trigger.

Stop B9:

Coastal sand ridges in the Mesola Wood

In our way back to Ferrara, we will cross Bosco Mesola, a mesophyll ilex-dominated wood, grown on well-preserved coastal ridges, largely formed by small, back-beach aeolian dunes. The arcuated and elongated coastal bodies accurately record the prograding evolution of two interfering wave-dominated delta lobes, which developed between 800 and 600 yrs B.P. These ridges record a very high-frequency sedimentary cyclicity, reflecting the climate-driven flood amplitude variations. The careful morphological study of these sedimentary bodies was made more complex by the thick vegetation cover, making the use of GPS and trigonometric techniques difficult.

We will then follow the Romea Road, built on a beach sand ridge, marking the late Roman coastline, at about 1700 yrs B.P. Passing by the Romanesque bell tower of the Pomposa Abbey, we will turn eastward, perpendicularly crossing prograding coastlines formed between 2,000 and 3,000 yrs ago.

Stop B10:

(optional) Subsidence impact at Codigoro

The visited region is subject to a fast natural subsidence, recorded by very thick Quaternary successions (see Introduction). The subsidence has lately been much accelerated by the combined effect of widespread land reclamation works and massive subsurface water pumping. A graphic depiction of the high subsidence speed and of the problematic management of this fragile coastal area is provided by the Po di Volano bank, within the small town of Codigoro. 50 years ago the high tide level was well below the foot path and boats freely docked at the pavement's edge; now two superimposed generations of walls try to barely protect the town from the combined effects of the large subsidence, high autumn and winter tides and the massive water influx, brought in by the largest water-scooping plant of Italy. The nearby plant delivery peaks of over 120 m^3/sec, making it one of the largest river of Italy, albeit a completely artificial one.

Leaving Codigoro, we will follow the northern natural levee of the Volano distributary channel, until entering a freeway near Migliarino. The trip will end in Florence, after driving through the northern Apennines, via Motorway A1.

Acknowledgements

We thank the Geological Survey of the Regione Emilia-Romagna and Dr. Raffaele Pignone for their support during the field trip preparation.

References

Amorosi A. and Marchi N., 1999. High-resolution sequence stratigraphy from piezocone tests: an example from the Late Quaternary deposits of the SE Po Plain. Sedimentary Geology, 128, 69-83.

Amorosi A. and Colalongo M.L, in press. The linkage between alluvial and coeval marginal-marine successions: evidence from the Late Quaternary record of the Po River Plain, Italy. In: M. Blum and S. Marriott (Eds.), IAS Special Publication.

Amorosi A., Farina M., Severi P., Preti D., Caporale L. and Di Dio G., 1996. Genetically related alluvial deposits across active fault zones: an example of alluvial fan-terrace correlation from the upper Quaternary of the southern Po Basin, Italy. Sedimentary Geology 102, 275-295.

Amorosi A., Caporale L., Cibin U., Colalongo M.L., Pasini G., Ricci Lucchi F., Severi P. and Vaiani S.C., 1998. The Pleistocene littoral deposits (Imola Sands) of the northern Apennines foothills. Giornale di Geologia 60, 83-118.

Amorosi A., Colalongo M.L., Pasini G. and Preti D., 1999a. Sedimentary response to Late Quaternary sea-level changes in the Romagna coastal plain (northern Italy). Sedimentology 46, 99-121.

Amorosi A., Colalongo M.L., Fusco F., Pasini G. and Fiorini F., 1999b. Glacio-eustatic control of continental-shallow marine cyclicity from Late Quaternary deposits of the south-eastern Po Plain (Northern Italy). Quaternary Research 52, 1-13.

Amorosi A., Forlani L., Fusco F. and Severi P., 2001. Cyclic patterns of facies and pollen associations from Late Quaternary deposits in the subsurface of Bologna. GeoActa, 1, 83-94.

Amorosi A., Centineo M.C., Colalongo M.L., Pasini G., Sarti G. & Vaiani S.C., 2003. Facies architecture and latest Pleistocene-Holocene depositional history of the Po Delta (Comacchio area), Italy. Journal of Geology, 111, 39-56.

Amorosi A., Colalongo M.L., Fiorini F., Fusco F., Pasini G., Vaiani S.C. and Sarti G., 2004. Palaeogeographic and palaeoclimatic evolution of the Po Plain from 150-ky core records. Global and Planetary Change, 40, 55-78.

Bondesan M., 1989 Geomorphological hazards in the Po Delta and adjacent areas. Geografia Fisica e Dinamica quaternaria, Sup. 2, 25-33.

Bondesan M. and Simeoni U., 1983. Dinamica ed analisi morfologico-statistica dei litorali del Delta del Po e delle foci dell'Adige e del Brenta. Memorie di Scienze Geologiche, v. 36, 1-46.

Bondesan M., Favero V., and Viñals, M.J. 1995. New evidence on the evolution of the Po-delta coastal plain during the Holocene. Quat. Int. 29/30: 105-110.

Bondesan M., Calderoni G., Cattani L., Ferrari M., Furini A.L., Serandrei Barbero, R., and Stefani, M. 1999. Nuovi dati stratigrafici, paleoambientali e di cronologia radiometrica sul ciclo trasgressivo-regressivo olocenico nell'area deltizia padana. Annali dell'Università di Ferrara, 8: 1-34.

Borgia G.C., Brighenti G., Vitali D., 1982, I giacimenti di gas del Delta del Po: criteri per una nuova valorizzazione. Atti Convegno sui fluidi caldi e le risorse energetiche marginali-Piacenza1.10.1982.

Caputo M., Pieri L., Unguendoli M., 1970. Geometric investigation of the subsidence in the Po Delta, Bollettino di Geofisica Teorica ed Applicata, v. 12 (47), 187-207

Castellarin A., Eva C., Giglia G., Vai G.B., Rabbi E., Pini G.A. and Crestana, G., 1985. Analisi strutturale del Fronte Appenninico Padano. Giornale di Geologia, 47, 47-75.

Dalla S., Rossi M., Orlando M., Visentin C., Gelati R., Gnaccolini M., Papani G., Belli A., Biffi U. and Catrullo D., 1992. Late Eocene-Tortonian tectono-sedimentary evolution in the western part of the Padan basin (northern Italy), Paleontologia i Evoluciò 24-25, 341-362.

Dondi L. and D'Andrea M.G., 1986. La Pianura Padana e Veneta dall'Oligocene superiore al Pleistocene. Giornale di Geologia 48, 197-225.

Fontolàn G., Covelli S., Bezzi A., Tesolin U., Simeoni U., 2000. Stratigrafia dei depositi recenti della Sacca di Goro. Studi Costieri, V. 2, 65-79.

Gasperi, G., Cremaschi, M., Mantovani Uguzzoni, M.P., Cardarelli, A., Cattani, M. and Labate, D., 1987. Evoluzione plio-quaternaria del margine appenninico modenese e dell'antistante pianura. Note illustrative alla carta geologica. Mem. Soc. Geol. It., 39, 375-431.

Martinson, D.G., Pisias, N.G., Hayes, J.D., Imbrie, J., Moore, T.C. and Shackleton, N.J. (1987) Age dating and the orbital theory of the ice ages - development of a high-resolution 0 to 300,000 year chronostratigraphy. Quaternary Research, 27, 1-29.

Ori G.G., 1993. Continental depositional systems of the Quaternary of the Po Plain (northern Italy). Sedimentary Geology 83, 1-14.

Pieri M. and Groppi G., 1981. Subsurface geological structure of the Po Plain, Italy. Pubbl. 414 P.F. Geodinamica, C.N.R., 23 pp.

Pini G.A. 1999 - Tectonosomes and Olistostromes in the Argille Scagliose of the Northern Apennines, Italy. Geological Society of America, Special Paper, 335: 70 pp.

Regione Emilia-Romagna and ENI-AGIP, 1998. Riserve idriche sotterranee della Regione Emilia-Romagna. A cura di G. Di Dio. S.EL.CA., Firenze, 120 pp.

Regione Lombardia and Eni Divisione Agip, 2002. Geologia degli acquiferi Padani della Regione Lombardia. A cura di C. Carcano e A. Piccin. S.EL.CA., Firenze, 130 pp.

Ricci Lucchi F., Colella A., Ori G.G., Ogliani F., Colalongo M.L., (with the collaboration of Padovani A., Pasini G., Raffi S. & Venturi L.), 1981. Pliocene fan deltas of the Intra-appenninic Basin, Bologna. In Ricci Lucchi F. (ed.), International Association of Sedimentologist, 2nd European Regional Meeting. Excursion Guidebook: 79-138. Tecnoprint, Bologna.

Ricci Lucchi F., Colalongo M.L., Cremonini G., Gasperi G., Iaccarino S., Papani G., Raffi I. and Rio D., 1982. Evoluzione sedimentaria e paleogeografica del margine appenninico. In: Cremonini G. and Ricci Lucchi F. (eds.) Guida alla geologia del margine appenninico-padano. Società Geologica Italiana, Guide geologiche regionali, Pitagora Tecnoprint, Bologna, 17-46.

Ricci Lucchi F., 1986. Oligocene to Recent foreland basins of northern Apennines. In: Ph. Allen & P. Homewood, eds., Foreland Basins, IAS Special Publication No. 8, 105-139.

Rizzini A., 1974. Holocene sedimentary cycle and heavy mineral distribution, Romagna-Marche coastal plain, Italy. Sedimentary Geology, 11, 17-37.

Ruggieri G., 1962. La serie marina pliocenica e quaternaria della Romagna. Camera di Commercio, Industria e Agricoltura Forli. 76 pp.

Ruggieri G., 1995. Sull'età delle "sabbie di Imola". Naturalia Faventina, 2, 79-81.

Simeoni U. (2000). "Studi costieri, Dinamica e difesa dei litorali- Gestione integrata della fascia costiera", N 2, La Sacca di Goro.

Vai G.B. and Castellarin A. 1992. Correlazione sinottica delle unità stratigrafiche nell'Appennino Settentrionale. Studi Geol. Camerti vol. spec. 1992/2, CROP 1-1A, 171-185.

Back Cover:
field trip itinerary

32nd INTERNATIONAL GEOLOGICAL CONGRESS

FIELD TRIP MAP

Edited by APAT

Volume n° 2 - from B16 to B33

32nd INTERNATIONAL GEOLOGICAL CONGRESS

NEOTECTONIC TRANSECT MOESIA-APULIA

Leader: I. Mariolakos

Associate Leaders: I. Zagorchev, I. Fountoulis, M. Ivanov

Field Trip Guide Book - B26

Florence - Italy
August 20-28, 2004

Pre-Congress **B26**

The scientific content of this guide is under the total responsibility of the Authors

Published by:
APAT – Italian Agency for the Environmental Protection and Technical Services - Via Vitaliano Brancati, 48 - 00144 Roma - Italy

Series Editors:
Luca Guerrieri, Irene Rischia and Leonello Serva (APAT, Roma)

English Desk-copy Editors:
Paul Mazza (Università di Firenze), Jessica Ann Thonn (Università di Firenze), Nathalie Marléne Adams (Università di Firenze), Miriam Friedman (Università di Firenze), Kate Eadie (Freelance indipendent professional)

Field Trip Committee:
Leonello Serva (APAT, Roma), Alessandro Michetti (Università dell'Insubria, Como), Giulio Pavia (Università di Torino), Raffaele Pignone (Servizio Geologico Regione Emilia-Romagna, Bologna) and Riccardo Polino (CNR, Torino)

Acknowledgments:
The 32nd IGC Organizing Committee is grateful to Roberto Pompili and Elisa Brustia (APAT, Roma) for their collaboration in editing.

Graphic project:
Full snc - Firenze

Layout and press:
Lito Terrazzi srl - Firenze

Volume n° 2 - from B16 to B33

32nd INTERNATIONAL GEOLOGICAL CONGRESS

NEOTECTONIC TRANSECT MOESIA-APULIA

AUTHORS:
I. Mariolakos (University of Athens - Greece)
I. Zagorchev (Bulgarian Academy of Sciences, Sofia - Bulgaria)
I. Fountoulis (University of Athens - Greece)
M. Ivanov (University of Sofia - Bulgaria)

Florence - Italy
August 20-28, 2004

Pre-Congress

B26

Front Cover:
Balkan Peninsula (NASA satellite photograph)

Leader: I. Mariolakos
Associate Leaders: I. Zagorchev, I. Fountoulis, M. Ivanov

Foreword

The field trip B26 was conceived by I. Mariolakos and I. Zagorchev as a joint initiative of Bulgarian and Greek geologists with the aim of demonstrating to the international geological community the main features of the Alpine geology of the Balkan Peninsula from a standpoint of the extensional tectonics in Neogene and Quaternary times. The preparatory work had reached its final phase when it was cruelly interrupted by the sudden death of Dimitris Mariolakos, - a bright young geologist full of vitality and enthusiasm. We, the colleagues and friends of Professor Mariolakos, wish to express again to him and his family our deep sympathy. This guidebook is dedicated to the memory of Dimitris.

Introduction

The field trip aims to present a comprehensive view over the principal neotectonic features of the Balkan Peninsula. This general idea is placed within the larger setting of the Alpine structures: the Alpine fold belts (Balkanides, Hellenides) and platforms (Moesian and Apulian) in their plate-tectonic evolution. Stress is laid also on the problems of the geological and cultural heritage.The field trip starts in Sofia, following the Maritsa fault belt east to Plovdiv, and then it crosses the principal tectonic units of the Balkanides travelling northwards to the Moesian platform. Afterwards, the itinerary crosses the Balkanides again to Sofia, and from there continues south through the main units at the margin between the Serbo-Macedonian and the Rhodope (*s.l.*) massif along the Strouma/Strymon fault belt. Then it crosses the Serbo-Macedonian massif, the Vardar/Axios zone, and the principal zones of the Hellenides to the Apulian platform. Important neotectonic structures are observed and broadly discussed, including active faults and related seismic and geotechnical hazards.

Principal field references

Geological map of Bulgaria, M 1:500,000
Geological map of Greece, M 1:500,000
Geological map of Greece, M 1:1,000,000
Geological map of Bulgaria, M 1:100,000
Geological map of Greece, M 1:50,000
Road maps of Bulgaria and Greece, M 1:500,000
Zagorchev, I. 1995. *Pirin. Geological Guidebook*. Academic Publishing House, Sofia.

The geological maps are available at the geological surveys of Bulgaria (Direction of Geology and Mineral Resources, Ministry of Environment and Waters, Sofia) and Greece (I.G.M.E. – Institute for Geology and Mineral Exploration, Athens).

Regional geologic setting Alpine structure

The Balkan Peninsula has a complex geological structure made up of Precambrian, Cadomian, Hercynian (Variscan), Early Alpine (Cimmerian),and Alpine *s.s.* tectonic movements. Although the field trip mostly demonstrates the structures formed during the extensional collapse of the Late Alpine orogen in Palaeogene and Neogene times, it will demonstrate also some of the older features.

The Alpine structure of the peninsula (Figure 1), is a result of the collisions between the Eurasian and the African continental plates and the closure of the Tethyan Ocean. It is dominated by two principal elements: the metamorphic crustal fragments, and the ophiolites issued from closed oceans. The metamorphic crustal fragments (from the North to the South) are as follows: Sredna-gora crystalline block; Rhodope massif, Pirin-Pangaion unit included; Osogovo-Lisets and Lisiya fragments in the core of the Strouma unit; pre-Ordovician fragments in the Morava unit; Serbo-Macedonian massif; Pelagonian massif. These crustal fragments have mostly a Precambrian age, and were amalgamated and reworked in Cadomian times. In some of the units they are covered unconformably by Palaeozoic (Ordovician and younger) sedimentary formations, and are intruded by Hercynian and Alpine granitoids.

The Alpine structure is divided into two parts by the Axios (Vardar) suture zone.

To the ENE of this zone, the Alpine structure is characterized by pre-Alpine and Alpine continental crust of the Moesian platform and its southern margin, with the development of arc basins and rifts. Along the Axios/Vardar zone, and to the WSW towards the Apulian platform, the Alpine evolution bears a pronounced Tethyan signature, with well-preserved remnants of the Tethyan Ocean.

Alpine structure of the eastern parts of the Balkan Peninsula

(Moesia – Serbo-Macedonian massif)

I. Zagorchev

The Moesian platform is geomorphically a low

Volume n° 2 - from B16 to B33

plain (Danube plain) with Quaternary loess cover. The oldest sedimentary complexes (Precambrian, on Romanian territory, and Devonian, in Bulgaria), are crossed by boreholes. Uplift episodes and partial erosion are reflected in several regional unconformities which occur between the Upper Permian and Lower Triassic; in the Lower Jurassic; between the Lower and Middle Cretaceous; and several unconformities in the Palaeogene and Neogene. The cover consists of continental Lower Triassic red beds, followed by Middle Triassic to Norian platform carbonates, and Carnian to Norian marine red beds; terrigenous and carbonate Jurassic, the marine transgression over the deeply eroded Triassic, beginning often directly with Middle Jurassic; Middle and Upper Jurassic and Lower Cretaceous carbonate platform sequences; Upper Cretaceous shallow-marine carbonate and terrigenous deposits, and continental or marine Palaeogene; and local Badenian to Pontian Neogene marine sediments belonging to a transitional zone between the Central and Eastern Paratethys.

The Fore-Balkan (transitional zone between the Balkan fold belt and the Moesian platform) is characterized by a low degree of deformation, and by transitional Alpine facies. In the eastern parts of the zone, the Triassic and Jurassic rocks are deeply buried beneath the Cretaceous and Palaeogene (partial) cover.

The Balkan (Stara-planina) zone is characterized by north-verging thrusting and folding in pre-Late

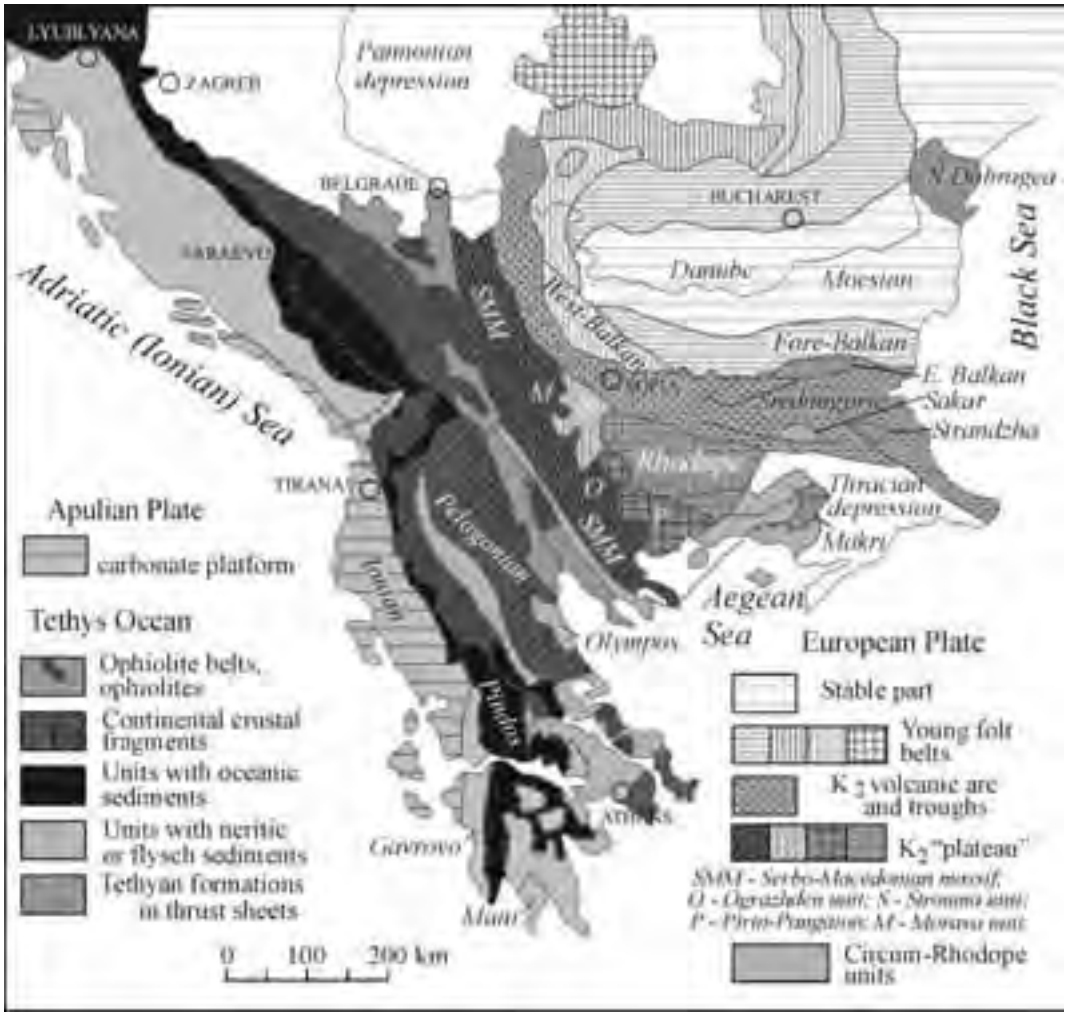

Figure 1 - Tectonic sketch map of the Balkan Peninsula (after Zagorchev, 1996, 1998)

Eocene and latest Oligocene times. The separate units (thrust sheets and anticlinoria) include fragments of units of Mid-Cretaceous and Late Cretaceous folding. The following complexes are distinguished: pre-Ordovician volcano-sedimentary complexes of oceanic (partially) and island-arc signature; Palaeozoic (Ordovician to Carboniferous) sedimentary formations intruded by Carboniferous granitoids; Permian red beds; a Triassic Peri-Tethyan sequence, ending with folding and covered unconformably by a Lower Jurassic to Kimmeridgian Peri-Tethyan sequence; an Upper Jurassic - Lower Cretaceous carbonate sequence (carbonate platform); an Upper Cretaceous shallow-water carbonate sequence; Danian to Middle Eocene continental and shallow-marine sediments; unconformable Upper Eocene molasse.

The Srednogorie zone has been set in by crustal necking and rifting in the southern edge of the Moesian platform, after the Mid Cretaceous compressive event, and developed as a volcanic island arc of Late Cretaceous age. It was transformed into an orogen by north-verging folding and thrusting in latest Cretaceous times, and later thrusted northwards over the Stara-planina zone. The Upper Cretaceous covers with unconformable depositional contact the following different complexes: slivers and rootless bodies of ultramafic (ophiolitic?) character and mantle (or oceanic crust) origin (parts of the Precambrian Prerhodopian Supergroup); the principal part of the Precambrian Prerhodopian Supergroup - a typical continental crust of granitic composition (migmatites, gneisses, metagranites); granitoid plutons of Carboniferous age (determined with Rb-Sr whole-rock isochrons), and mixed (I-type) and continental crustal signatures; Permian, Triassic and Jurassic sedimentary complexes, with Peri-Tethyan (Balkanide) signature. The Upper Cretaceous sedimentary formations are represented by coal-bearing continental to shallow-marine Cenomanian and Turonian, terrigenous to carbonate marine Coniacian, pelagic carbonates and shales, locally with radiolarites (Santonian – Campanian), and Lower-Middle Maastrichtian flysch. The Cenomanian? to Lower Maastrichtian volcanics (from pikrites and basanites to andesites and latites) form a volcano-plutonic association, with gabbro to monzonites and granodiorites of mantle signature. The Late Cretaceous folding, uplift and erosion was followed by a Danian conglomeratic formation of fluviolacustrine origin, that contains well-rounded pebbles from all older rocks. Upper Eocene and younger formations fill in syn- and post-sedimentation grabens.

The Morava-Rhodope zone embraces the tectonic units between the Srednogorie and the Axios zone. They represented in Late Cretaceous times a frontal arc ("plateau") built up of Mid-Cretaceous tectonic units. The Morava-Rhodope zone consists of several units: Rhodope *s.l.* (Rila-West Rhodope and Pirin-Pangaion subunits included), Strouma, Morava and the Serbo-Macedonian massif.

The Rhodope massif is a lenticular body of continental crust. The metamorphic complexes have been and still are the subject of discussions and controversial interpretations (Zagorchev, 1998). Two metamorphic complexes (Prerhodopian and Rhodopian Supergroup) are distinguished. The Prerhodopian Supergroup represents a continental crust of granitic composition (migmatites, gneisses, metagranites), that contains amalgamated rootless bodies of ultrabasic and basic rocks. The Rhodopian Supergroup originated from products (flysch-like sedimentary sequences, volcanogenic sequences, platform carbonates) of a Precambrian island arc. Both supergroups suffered Cadomian reworking, and were intruded by igneous bodies of granitic composition and Palaeozoic and Late Cretaceous age, in most cases bearing the signature of recycled and molten older continental crust. The metamorphic complexes are covered by non-metamorphic sedimentary and volcanic cover of Palaeogene age. Other hypotheses consider the Rhodope metamorphic complexes as having been formed during accretion of crustal and mantle fragments with Palaeozoic and Mesozoic ages that suffered Alpine deformations and metamorphism.

The basement of the *Strouma unit* consists of various gneisses, schists, and amphibolites (including orthoamphibolites) of Precambrian age and Cadomian reworking. The Neoproterozoic - Cambrian Frolosh Formation (metadiabases, schists, metapsammites), contain rootless bodies of mafics and ultramafics (lherzolite, troctolite, gabbro, and norite) and is intruded by the Strouma diorite formation (gabbrodiorite to granite). They are regarded as a volcanic arc association that contains some slices of oceanic crust or upper mantle. These Precambrian to Lower Palaeozoic rocks are directly covered by Permian red beds formed in the intramountain depressions of the Variscan orogen. The Triassic section begins over Permian or its basement with Lower Triassic mature conglomerate and sandstone, followed by Middle-Upper Triassic

Volume n° 2 - from B16 to B33

carbonates (limestones, dolomites), and Carnian – Norian marine red beds (red to purple shales, marls, and conglomerates, interbedded with oligomictic quartz sandstones and limestones). The whole unit was folded and uplifted in latest Triassic time. The gradual Early Jurassic to Bajocian transgression occurred only in the northern, in the Trun subunit. The Jurassic sedimentation ended with the Upper Jurassic – Berriasian flysch of the Nish-Troyan flysch trough (called also Perimoesian marginal flysch basin), that continued to the East, also within the future Srednogorie and Balkan zones. After the Mid-Cretaceous folding and thrusting, the unit was united with the Morava and Rhodope units into a single Morava-Rhodope superunit that represented a frontal arc ("plateau") of the complex Late Cretaceous volcanic island arc. The Late Cretaceous marine transgression of the Srednogorie basin penetrated only locally in the northeastern parts of the Strouma unit, where a trough with flysch-like sedimentation existed in Campanian and Maastrichtian times.

The Morava unit was formed as a result of Mid Cretaceous thrusting of a ridge structure (Serbo-Macedonian massif) over the Triassic to Lower Cretaceous sediments of the Nish-Troyan flysch trough. The unit consists of several thrust sheets with different lithologies. Only pre-Alpine rock units are present. The basement rocks are very similar to that of the Strouma unit, and belong to two types: pre-Cadomian high-grade gneisses, migmatites, and amphibolites intruded by Cadomian granites, and Neoproterozoic - Cambrian greenschist-facies rocks similar to the Frolosh Formation, with gabbro-diorites to diorites. Some of the thrust sheets exhibit Ordovician metasandstones and schists, Silurian – Devonian basinal schists, lydites, and limestones, and Upper Devonian flysch-like sediments.

The Ograzhden unit is a part of the Serbo-Macedonian massif. It consists of gneisses, migmatites and amphibolites, amalgamated with mantle ultrabasic and basic rocks and intruded by Cadomian granites, aplites, and pegmatites. The whole Ograzhdenian polymetamorphic and polydeformational complex was reworked in Late Cadomian times.

Alpine structure of the SW parts of the Balkan Peninsula (Macedonia – Epirus)

I. Mariolakos, I. Fountoulis

On Greek territory *(Fig. 2)* the tectonic units largely inherited former Tethyan sedimentation zones with a continuous Alpine evolution. Greece forms a very characteristic part of the Alpine System, known as the Hellenic Arc. It is one of the major mountain chains of the Alpine-Himalayan System, which resulted from the convergence/collision between the Eurasian and the African continental plates.

The morphotectonic direction of the Hellenic Arc in Continental Greece is NNW-SSE (Figure 2), bending gradually to E-W between Kythera and Crete. Eventually, the direction becomes NE-SW east of the Dodekanissa ("twelve islands") island complex up to near Turkey.

The Hellenides comprise a large number of geotectonic units (Figure 2), corresponding to individual nappes. The overall kinematics shows a west-vergent movement directed from the core of the arc in the Aegean Sea towards the periphery, in the Ionian and Libyan Seas (Figures 3, 4).

Two main orogenic cycles have been distinguished in the Hellenides, namely:

- The Palaeo-Alpine orogeny in Late Jurassic – Early Cretaceous times;
- The Alpine orogeny, which started in Late Eocene, and culminated during Oligocene and Miocene times.

However, plate movements with resulting orogenic processes are still active along the present Hellenic Arc and Trench System.

The geotectonic units of the Hellenides can be subdivided into two groups (Internal and External Hellenides). The Internal Hellenides have undergone deformations in both orogenic cycles, whereas the External Hellenides have been deformed only during the Alpine *s.s.* orogeny. The Internal Hellenides consists of the Rhodope, Serbo-Macedonian, Circum-Rhodope, Vardar/Axios, and Pelagonian zones, and the External Hellenides, of the Pindos, Gavrovo-Tripolitza, Ionian, and Pre-Apulian (Paxos) zones.

Rhodope zone. This consists of two tectonic zones, and namely, the *Pangaion (Paggaio) unit* (tectonically in a lower position), and *Sidironero unit* (in an upper position). They are separated by the SW-vergent Middle-Mesta thrust. The Paggaio unit is characterized by the extensive presence of marbles, along with amphibolites, gneisses, and mica schists. The Sidironero unit comprises gneisses (muscovitic, biotitic, augen), amphibolites, migmatites, and anatectic granites.

The *Serbo-Macedonian zone* consists, on Greek territory, of two geotectonic units: *Kerdylia* and

Vertiskos (Kockel, 1977). Their boundary is unclear, and could be considered either as a tectonic or disharmonic contact. Both units are composed of high-grade (amphibolitic facies) metamorphic rocks (mica schists, amphibolites, and migmatites) and are crossed by Hercynian and Alpine granites (schistosed or not). The boundary between the Serbo-Macedonian and Rhodope is located within the Strymon graben (Kockel and Wallther, 1965), with the Serbo-Macedonian zone tectonically overthrusting (ENE-verging Strymon thrust) the Rhodope in the area NE of Sidirokastro.

The Circum-Rhodope zone consists of greenschist facies metamorphic formations, mainly marbles and dolomites (Triassic), clastics (Jurassic), and ophiolites. They are overthrusted with a SW vergence by the Serbo-Macedonian zone. The relationship between the Circum-Rhodope zone, and the more internal parts of Axios zone (Paionia, according to Mercier, 1968), is not clear.

Figure 2 - The Hellenic Arc and Trench System. KF: Kefalonia Faul; NAF: North Anatolian Fault; PT: Plini Trench; ST: Strabo Trench.

Axios/Vardar zone. It was Mercier (1966) who divided the Axios zone into three sub-units: *Almopia* (later defined as a geotectonic unit by Papanikolaou, 1984), *Paikon,* and *Paionia*. The Paionia unit consists of marbles, crystalline limestones, clay schists. and phyllites of Triassic – Jurassic age. They are tectonically overlaid by basic magmatic rocks (but not a typical ophiolithic complex). of Jurassic age. The Paikon unit comprises neritic marbles, clastic sediments, both basic and acid volcanic rocks. and the "Phanos granite" of Jurassic

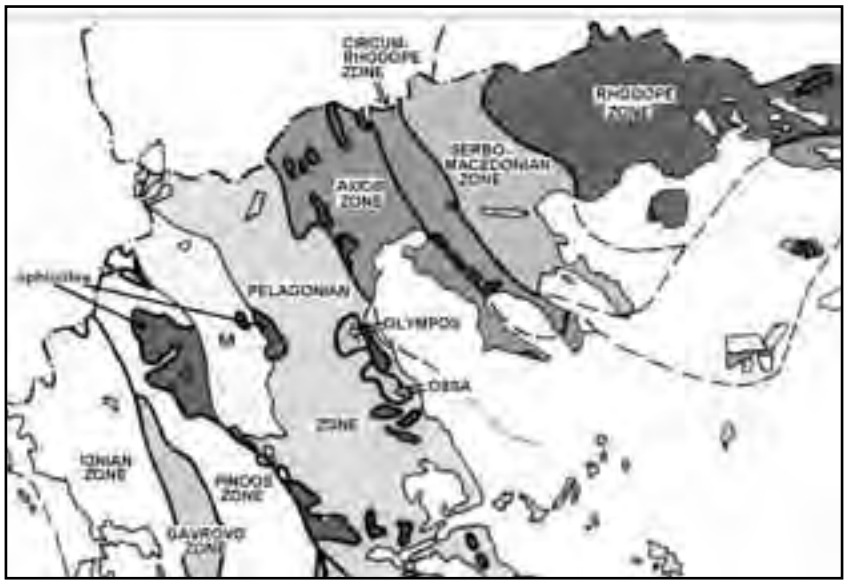

Figure 3 - Simplified map of the geotectonic units of Greece (based on Papanikolaou, 1986)

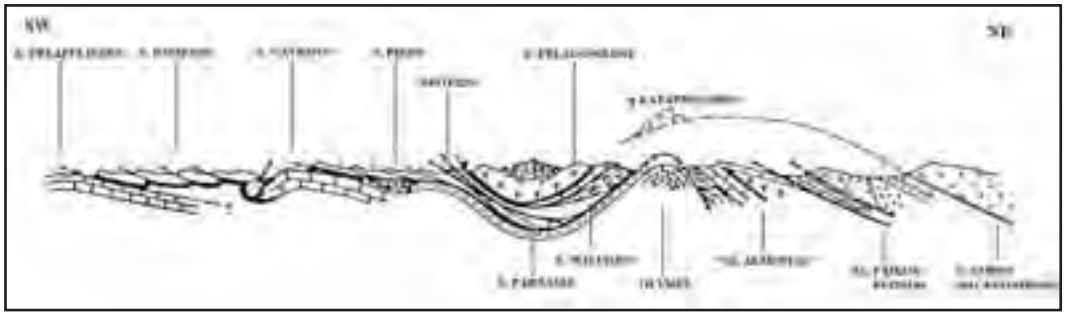

Figure 4 - Schematic cross section of the Hellenides, depicting the allochthony of the Pindos unit in relation to the Olympus window (after Aubouin et al., 1979).

age. It is a low-grade metamorphic unit in which some fossils are found. The metamorphism "disappears" in the Upper Jurassic – Cenomanian formations. The Almopia geotectonic unit was formerly considered as part of the Axios zone. It crops out as a tectonic nappe, "rising" from the Axios area, and reaches the Meso-Hellenic Trough, covering all the metamorphic units of the Northern Pelagonian tectono-metamorphic unit. The column of the unit begins with basic rocks (ophiolites), unconformably covered by Aptian conglomerate. It is followed by Upper Cretaceous carbonates and Upper Maastrichtian flysch.

The Pelagonian zone consists mostly of metamorphic rocks of Palaeozoic and Mesozoic age, and is subdivided into two major tectonic units: Flabouro and Kastoria.

The Flabouro unit is characterized by the presence of high-grade metamorphic rocks, gneisses, amphibolites, mica schists, and marbles. They have a polymetamorphic and polydeformational character, and are intruded by Hercynian (Carboniferous – Permian) granites.

Kastoria unit. The stratigraphic column of the Kastoria geotectonic unit is divided into two parts. The lower part consists of granites, mica schists etc., and the upper one, of low-grade metamorphic sedimentary formations (low-grade greenschist facies), such as phyllites, quartzites, sericite – chlorite schists and metatuffs. Older (schistose) and younger granites are distinguished.

Eastern Greece. It was deformed twice, during the Palaeo-Alpine, and the typical Alpine orogeny. A neritic Triassic – Jurassic sequence (*Sub-Pelagonian unit*) is overlain by the obducted ophiolites, and the

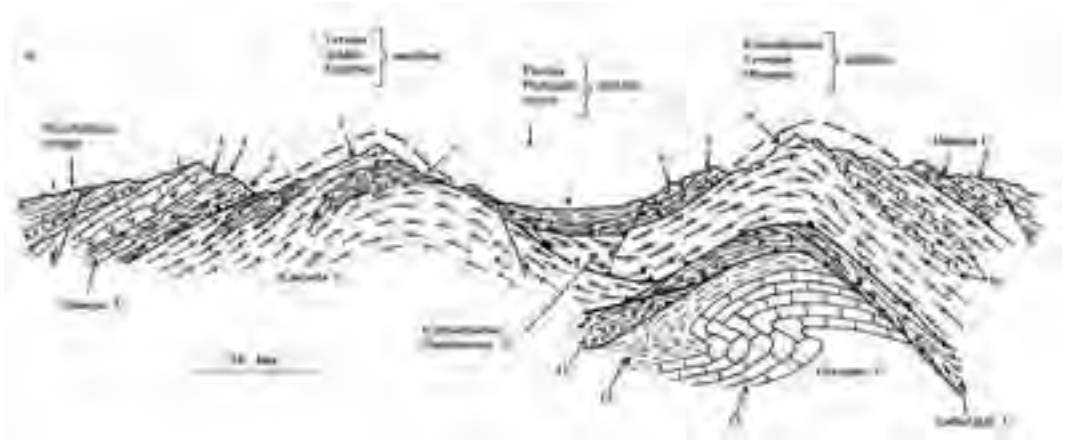

Figure 5 - Synthetic cross section in the northern part of the Middle tectonometamorphic zone (ex-Pelagonian zone) (after Papanikolaou, 1983). 1:Molasse of the Meso-Hellenic Trough; 2: sediments of the Upper Cretaceous transgression; 3: ophiolites; 4: M. Triassic - Jurassic marbles of Almopia unit; 5: phyllites, marbles and meta-volcanics of Almopia unit; 6: granites and gneisses of Kastoria unit; 8: post-Alpine deposits of the Ptolemais basin; 9: gneisses, granites, amphibolites, mica schists of Flabouro unit; 10: marbles of Flabouro unit; 11: blueschists of Ambelakia unit; 12: Eocene flysch of Mt. Olympus.; 13: Triassic – Eocene crystalline limestones of Mt. Olympus .

transgressive Upper Cretaceous limestones. The section ends with the Eocene flysch.

Western Thessalia – Beotia zone. This zone is characterized by a continuous sequence from Triassic to Eocene. It is the most internal stratigraphically continuous unit of the Hellenides. The section begins with Triassic limestone and dolomite, followed by Jurassic pelagic limestones, shales, and radiolarites. Lower Cretaceous rhythmic sandstones and limestones follow. They are covered by the Upper Cretaceous flysch that is rich in olistolites and pebbles from ophiolites and limestones of Mesozoic age. Upwards follow pelagic limestones and marls (Palaeocene), and Eocene flysch.

Parnassos zone. A thick Triassic – Lower Cretaceous neritic carbonate sequence is interrupted by 3-4 bauxite horizons. Red pelagic limestones and shales are followed by a Palaeocene – Eocene flysch.

Pindos. The Pindos zone is characterized mostly by pelagic sediments, presumably from the Tethys slope. The oldest rocks are Middle Triassic sandstones and shales, followed by Triassic - Cretaceous pelagic limestones, pelites and radiolarites (locally related to pillow-lavas), Cretaceous cherty limestones, pelites and flysch, and fine-bedded limestones (Coniacian-Maastrichtian). The section ends with the Palaeocene – Eocene Pindos flysch.

The *Gavrovo-Tripolis zone* corresponded to a neritic carbonate platform. The base of the stratigraphic column consists of Permian – Upper Triassic clastites, carbonates, evaporites, and volcanites (Tyros beds), slightly metamorphosed to slates-phyllites. The *Tripolis subzone* is characterized by neritic limestones and dolomites (Upper Triassic – Upper Eocene). The section of the *Gavrovo subzone* begins with Upper Jurassic and Lower Cretaceous shelf (oolithic, reefal, etc.) carbonates. The Upper Cretaceous is represented by limestones with rudists, and dolomites and carbonate breccia with orbitoids, and fragments of corals and rudists. Bauxite levels and sedimentation breaks are recorded. The most important breaks are referred to the Cretaceous/Palaeogene boundary and in the Palaeocene and Eocene section. The latter consists of shallow-water carbonates replaced in the Upper Eocene by shales that pass upwards into flysch.

Ionian zone. The zone is built up of Triassic breccia and evaporites, Upper Triassic neritic carbonates, the Liassic Pantokrator Limestone, red nodular limestones and black shales (Upper Lias – Lower Malm), and platy limestones and cherts (Tithonian – Turonian). Pelagic limestones (Campanian – Eocene) pass upwards into the West-Hellenic flysch.

The non-metamorphic units of Hellenides are characterized by longitudinal NNW-SSE trending *b*-folds without schistosity, mostly representing flexural-slip folding. The interlayering of competent and incompetent rock units control the geometry of folding. The rocks probably have not been subjected to a load of more than 3-5 km.

Extensional collapse of the Alpine orogens in the eastern parts of the Balkan Peninsula

I. Zagorchev

A special emphasis is laid on the extensional collapse processes in Palaeogene and Neogene times. The Late Cretaceous orogen, issued from the Srednogorie island arc, was the subject of fast uplift and erosion, already in latest Maastrichtian times, and of gradual peneplainization in the Danian (Figure 6). Exhumation of deeper levels occurred both on the former frontal arc ("plateau") of the Morava-Rhodope superunit, and in the Srednogorie itself.

A new extension occurred in Palaeocene and Early to Middle Eocene times, with local flysch basins in the Balkan area, and with continental grabens with marine ingressions in the Rhodope region. Intracontinental collision processes formed the first fold-and-thrust belt of the Balkanides. Limited thrusting probably occurred in the Rhodope area, being more important in its southern part on Greek territory.

The extensional collapse of the Middle Eocene orogen occurred in Late Eocene and Early Oligocene times, and was most prominent in the area of the "plateau" – in the heterogeneous crustal areas of Srednogorie and Morava-Rhodope. Numerous small grabens were filled in by coarse terrigenous, often coal-bearing, sediments, beginning with the Bartonian, and mostly in Priabonian times. At the end of the Priabonian, marine ingression along the Strouma/Strymon fault belt and in the East Rhodope Mountains was almost coeval with outbursts of intense volcanic activity. The volcanic activity had a different composition in the different parts of the arc. It was of a bimodal composition, probably deriving from mixed mantle and crustal sources,in the East Rhodope; of a trachyandesitic composition, with a later more acidic tendency, along the Strouma belt and in the Mesta graben complex; and with an acidic (rhyolites) character in continental conditions (on dry land or in lacustrine environments), in the Central and Western Rhodope, where the continental crust reached its

Volume n° 2 - from B16 to B33

Figure 6 - Sketch map for the Palaeocene palaeogeography (without palinspastics).
Modified after Zagorchev (1996)

maximum thickness. Thus, a complex fluviolacustrine system was drained towards the two marine gulfs. The field trip demonstrates the relationship between the Palaeogene formations and their basement in the Padesh graben (a part of the gulf along the Strouma belt), and in the continental Padala graben (a part of the fluviolacustrine system near the source area).
The marine regression in Mid- to Late Oligocene times led to a total reorganization of the fluviolacustrine

Figure 7 - Earliest Miocene transpression, thrusting and right-lateral strike-slip along the Strouma fault belt (after Zagorchev, 1992, 1996).

systems on the Balkan Peninsula. Almost all previous basins were dried out. A marine gulf became active along the eastern part of the Maritsa fault belt East of Plovdiv. In transtension conditions, a huge lake extended along the Strouma fault belt from Brezhani in SW Bulgaria (to be briefly visited), through Bobovdol, Pernik, and East Serbia, where it drained into the Pannonian sea basin, with a probable link to the East Carpathian basin. This Paratethys system gave birth to the most important coal deposits in Romania, Serbia, and Bulgaria. In earliest Miocene times, the system became reorganized, due to dramatic transpression events (Figure 7).

Molasse basins
in the Hellenic area
I. Mariolakos, I. Fountoulis

The evolution of Northern Greece, especially during the neotectonic period, has been the subject of different and often controversial opinions. This evolution is greatly defined by the activity of the North Anatolian Fault (NAF), and its prolongation towards the Aegean Sea.
Three great molassic basins are distinguished within the Hellenic area. Their activity and location cover different time spans during the Alpine evolution of the Hellenic arc. These basins are (Figure 8):

The *molassic basin* of *Rhodope* existed as a basin in the northeastern part of Greece during Eocene-Oligocene times. The molassic sediments were deposited over the metamorphic basement of Rhodope, the area of Axios, and the present-day marine area of the northern Aegean. The oldest sediments are of Early to Middle Eocene age, and span to the Oligocene/ Miocene boundary (Kopp, 1966). An Oligocene volcanic activity is most significant.
The *molassic basin* of the *Meso-Hellenic Trough* existed in the midst of continental Greece during Late Eocene – Middle Miocene times. The trough sediments were unconformably deposited over the non-metamorphic formations to the west and the metamorphic formations to the east. Along different sections perpendicular to the longitudinal axis of the trough, the consistency and the origin of the deposits vary. So, every area has its own stratigraphic column. Brunn (1956) was the first to study the Meso-Hellenic Trough sediments, and divided them into different "formations", namely (from bottom to top): the Krania Formation (Upper Eocene); Eptahori Formation (Oligocene), which consists mainly of

Figure 8 - The main molassic basins of the Hellenic Arc system. (after Papanikolaou, 1986).

marls; the Pentalofo Formation (Upper Oligocene – Aquitanian), consisting mainly of conglomerates (Meteora area) and sandstones; the Tsotyli Formation (the thickest of all, Lower Miocene), consisting of marls and sandstones; and lastly, the Odria Formation (Middle to Upper Miocene) that consists of small thickness (20-50 m) sandy – marly limestones. New research proved that the marine sedimentation continued at least up to the Early Pliocene times (Fountoulis et al., 2001). The total thickness of the Meso-Hellenic Trough deposits reaches c. 5 km.

The *molassic basin of Epirus – Acarnania* existed as a sedimentary basin in western continental Greece during Late Oligocene – Miocene times. In this particular basin it is difficult to distinguish between molasses and the underlain flysch (common formation to both Ionian and Gavrovo zones). This distinction can only be made with certainty in areas where the Lower – Middle Miocene molassic formations are in direct contact with the folded sediments belonging to the Ionian zone.

Neogene basins in the northern and eastern parts of the Balkan Peninsula

I. Zagorchev

Most of the Balkan Peninsula was dry land in Early and Middle Miocene times. The evidence about the evolution in these times is scarce. Marine basins still existed in the Hellenides, and in the Pannonian basin of the Paratethys. The central and eastern parts of the Peninsula were affected by slow motions and denudation that resulted in the formation of the principal planation surface (initial peneplain, orthoplain). Due to the balance between uplift, accumulation, and erosion, no traces of sediments formed in these times have been preserved. Only recently, palaeobotanical evidence has been published about the Ottnangian to Karpatian age of some formations which have very limited occurrence in the West Rhodopes.

Considerable changes in this regime began in the second half of Middle Miocene time. Marine and brackish basins flooded the surrounding areas: Ionian/Adriatic, Pannonian, Precarpathian, Euxinian (Black Sea) and later, the Aegean basin. Normal faulting (mostly along the older fault belts) led to relief contrasts and triggered faster erosion and denudation in the horsts and sediment deposition in the grabens, thus initiating a new pattern of fluviolacustrine systems centered on big palaeorivers along the Maritsa and Strouma/Strymon fault belts. The areas with the thickest continental crust (West and Central Rhodopes), became again involved in differential uplift and extension. Times of relative quiescence are documented by mountain steps (pediments, oroplains). The fault amplitudes changed over time, with a climax in the time span Pontian – Pliocene, when the thickest terrigenous sediments were deposited, parallel with the fast climate changes, and marked by the disappearance of savannahs and their big mammals (Pikermi faunas), and the coming of the Ice Age in the highest mountains (Rila, Olympus, Pirin, Belasitsa, Vitosha, etc.).

The existing evidence favors geodynamic interpretations of this area, centered upon the

Volume n° 2 - from B16 to B33

interference of mechanisms such as isostasy, rifting, horizontal movements along large strike-slip faults, with the formation of pull-apart basins, etc. (s. Zagorchev, 1992, 2002). These interpretations run contrary to current popular hypotheses (e.g., Dinter and Royden, 1993), which suggest the existence of a very large extension, caused by detachment systems in the Aegean and peri-Aegean regions.

Neogene basins of the Hellenic arc
I. Mariolakos, I. Fountoulis

The post-Alpine formations of Greece comprise beds unconformably deposited over the Alpine basement. They belong to the back-arc basins of the present-day Hellenic arc, and their deposition took place during Neogene and Quaternary times. These are mainly continental deposits (plus fluvial and lacustrine), and sometimes marine (coastal), deposited in neotectonic grabens.

The most important marine basins are of Late Miocene – Pliocene age, and are located mainly in the Peloponessus (Plio-Pleistocene only) and on the island of Crete, while in the rest of continental Greece, continental basins prevail. As expected, many basins show a multi-phase evolution, since continental facies alternate with lacustrine or coastal marine, and vice-versa. Especially interesting are the cases of post-Alpine (Neogene) basins formed and evolved over pre-existing molassic basins, such as in Thessaly and western Macedonia (over the Meso-Hellenic Trough) and in the Serres – Drama basin (over the Rhodope molasse).

The limited extent of marine post-Alpine sediments in Greece is due to the fact that many marine basins of Neogene age still exist today (Thassos basin).

A general observation concerning the distribution of Neogene basins is that although some characteristic trends exist, a normal spatial distribution is not present. Below, the presence of other common features, such as the sedimentary facies or their thickness, is examined.

Although the systematic study of Greece has not yet been completed, it is evident that there is a general geotectonic regime, within which some areas differ because of special tectonic conditions.

The post-Alpine (Neogene-Quaternary) basins, selected for the stops on this field trip, are the following (Figure 9): Strymon basin; Axios basin; Servia – Ptolemais basin; Meso-Hellenic Through; and the Thessaly basin.

The current geodynamic regime in the Hellenic area
I. Mariolakos, I. Fountoulis

The present Hellenic Orogenic Arc is restricted to the southern part of the Hellenic territory, in contrast to all the previous arcs, which extended throughout the whole length of the Hellenides.

During the Middle Miocene, a part of the Hellenic arc, still active today, was cut off from the Tethyan chain, and since then has followed its own evolution. To the north, this part is bounded by the prolongation of the right-lateral Anatolian fault (Figure 10). In the northern Aegean region, this fault coincides with the northern limit of the active part of the Hellenic arc, bounding an area termed “Aegean microplate” (McKenzie, 1970; 1972; 1978; Galanopoulos, 1972).

The present geometry of the Hellenic Arc has been developing since the Late Miocene. The back-arc basin and the volcanic arc are restricted in the Aegean

Figure 9 - Main Neogene basins of the Aegean region (after Dermitzakis and Papanikolaou, 1981): a) Lower Miocene, b) Lower Miocene – Pliocene, c) Miocene and Pliocene, d) Upper Miocene – Pliocene, e) Pliocene (M: marine, C: continental). 1:Meso-Hellenic Trough, 2: Epirus, 3:Cyclades, 4:Ionian islands, 5:Attica – Boeotia, 6:Thessaloniki, 7:Strymon, 8: Thrace, 9:Eastern Aegean islands, 10:Chania, 11:Rethymno, 12:Irakleio, 13:Ierapetra, 14: Karpathos, 15:Cretan basin, 16:N. Sporades, 17:Servia – Ptolemais, 18:Peloponnesus).

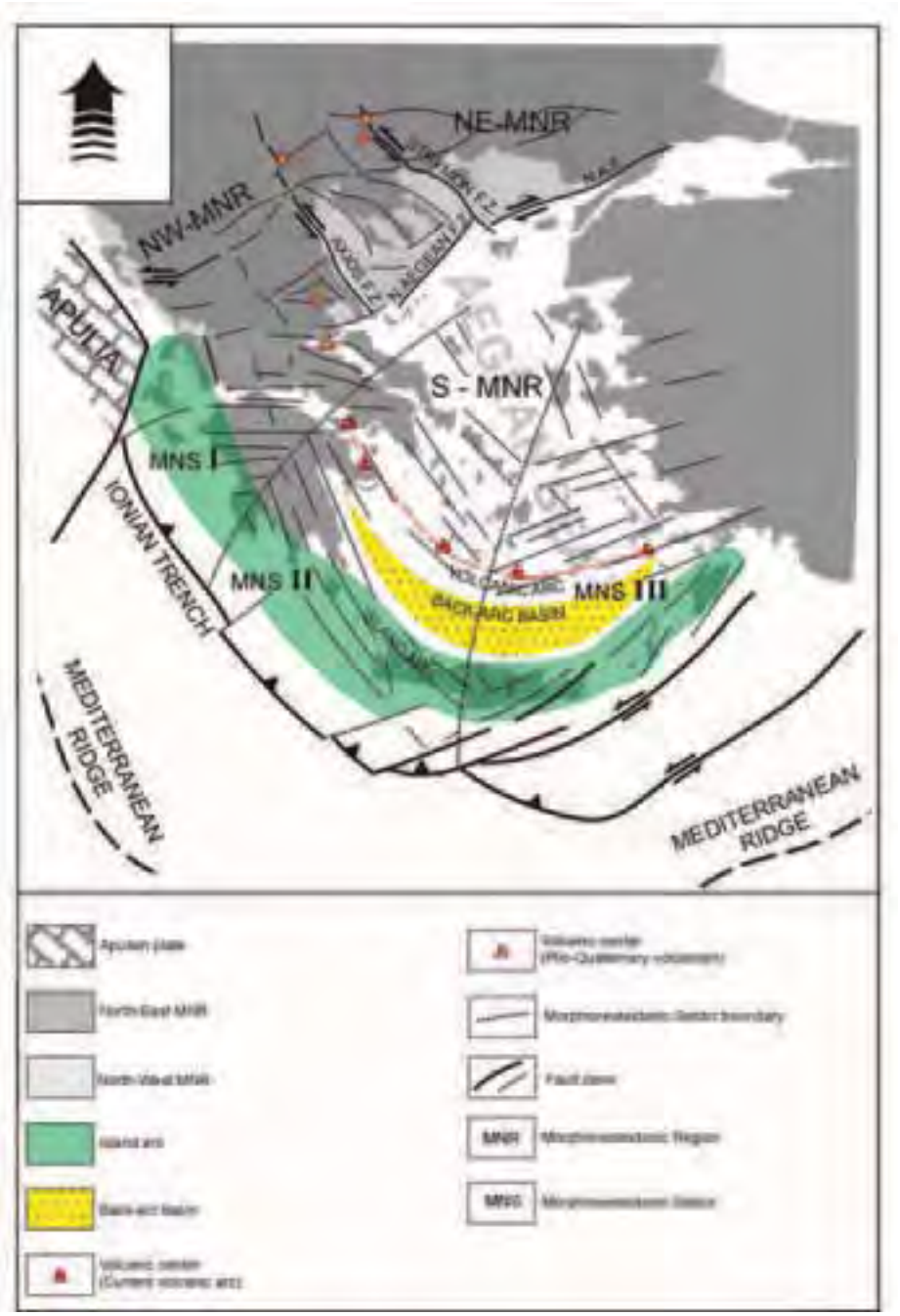

Figure 10 - Current morpho-neotectonic regime of the Greek territory.

plate region.

According to Le Pichon et al. (1981), the present geodynamic regime of the Hellenic arc is characterized by asymmetrical movement; along the Ionian trench, the subduction direction is NE-SW, and the regime is pure compression, in accordance with the fault plane solutions while, in the Pliny and Strabo trenches, the direction of movement is

Volume n° 2 - from B16 to B33

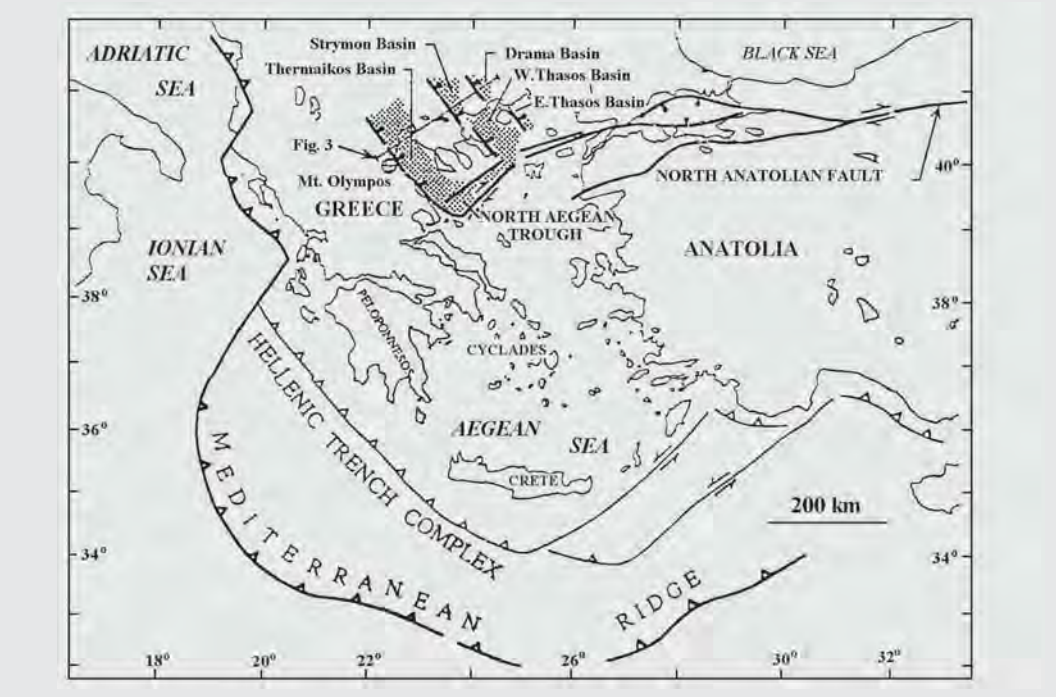

Figure 11 - Tectonic elements of NE Greek region. Subduction-related thrust contacts have barbs on hanging wall. High-angle faults bounding the modern basins have balls on downthrown side. Offshore geometry of modern depocenters (dot pattern,) north of the North Aegean trough is from Lalechos and Savoyat (1977) (after Dinter and Royden, 1993).

composite, featuring a substantial sinistral NNE-SSW horizontal component. In the back-arc area there are extensional structures, also with a significant horizontal component of movement.

According to Mariolakos et al. (1981, 2001), the Greek territory can be divided into three Morpho-Neotectonic regions (MNR) (Figure 10), and these are described below:

The Northeast MNR (NE-MNR) is bounded by the large North Aegean Fault Zone (prolongation of the North Anatolian Fault into the north Aegean Sea) to the south, and the Axios fault zone to the west. Compared to the NW-MNR, there are no intensive vertical movements affecting the whole region, resulting generally in a smooth relief, but they are localized in areas where fault reactivation occurred, mainly in Plio-Quaternary times, resulting in local incision. The majority of the high order tributaries of the drainage network come from the north (the Axios, Strymon, Nestos, and Evros Rivers). The 1st order basins strike NW-SE. In the northern margins of the present grabens, Plio-Pleistocene volcanic activity occurs (Aridaia, Sidirokastro, and Strymoniko).

The Northwest MNR (NW-MNR) is bounded by the Axios fault zone to the east, and the prolongation of the Malliakos - by the Amvrakikos gulf fault zone to the west. Intensive vertical movements (mainly uplift), affecting most of the region, resulted in intensive fragmentation (partition), high-energy relief, incision, and drainage developments, mainly within the Greek territory, and characterize this morpho-neotectonic region. The mountain ranges as well as the drainage network strike mainly NW-SE. Some other characteristics, especially for the western sector, are the absence of typical horst – graben structures, and the occurrence of E-W strike-slip fault zones. For the eastern sector, the initial strike of the horst – graben structures is NW-SE (Meso-Hellenic Trough, Ptolemais – Servia basin), and later were fractured into smaller basins by faults striking NE-SW. Plio-Pleistocene volcanics occur in the SE part of the sector.

The South MNR (S-MNR) is bounded by the large North Anatolian Fault Zone and the prolongation of the Malliakos - Amvrakikos gulf Fault Zone to the north, by the Hellenic trough to the west and south,

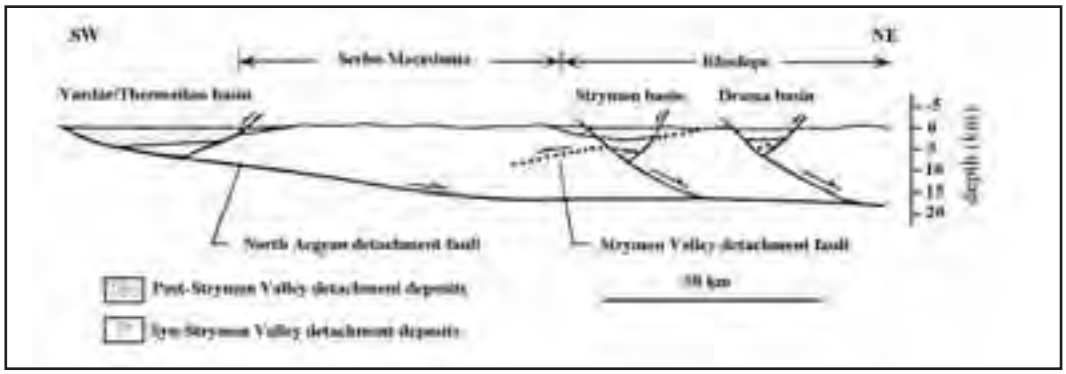

Figure 12 - Schematic cross section, showing major Upper Cenozoic extensional structures of NE Greece. Plane of section is parallel to slip on Strymon Valley detachment fault, and sub-parallel to slip on North Aegean detachment system, as proposed by Dinter and Royden(1993). No vertical exaggeration. See Figure 11 for locationand.

and by the Pliny and Strabo troughs to the south-southeast. The Strabo and Plinytroughs constitute the eastward prolongation of the southern part of the Hellenic Trough. Of course the Pliny and Strabo troughs present different kinematics to the Hellenic one, resulting in differences in (fault) brittle tectonics, karstification, and hydrogeological characteristics of the controlled areas.

Within these MNR a large number of neotectonic basins have been created, which have been mainly filled with deposits of Pliocene – Quaternary age.

Most geodynamic models proposed for the evolution of the Aegean domain during Neogene times have considered that the initiation of extension in this area is a direct consequence of the westward extrusion of the Anatolia (Minor Asia) plate away from the Arabia – Eurasia collision front.

According to Dinter and Royden (1993), and Dinter (1994), the Strymon basin detachment system accommodated at least 25 km of extension at the northern margin of the Aegean extensional province, from Middle Miocene through Early Pliocene time. Displacement ceased on the Strymon basin detachment with the Late Pliocene development of the Strymon and Drama basins. They propose that the Strymon and Drama basins, together with the other principal basins in the northern Aegean, are subsiding above an active northeast–dipping extensional detachment zone, that forms a unified kinematic system with the western offshore continuation of the dextral North Anatolian Fault, and the Northern Aegean Trough (Figures 11 and 12).

Gautier et al. (1999) suggested that regional-scale extension, with a pattern of stretching orientations similar to that of Pliocene – Pleistocene, was already strongly active in this domain before the onset of the Arabian indentation into Eurasia (Early Miocene vs. Middle or Late Miocene). This implies that the initiation of the Aegean extension did not result from the lateral extrusion of Anatolia, and they propose that the extension started due to the gravitational spreading of the continental lithosphere that had previously been thickened during the Alpine collision (Figure 13).

Moreover, many geodynamic models have been proposed for the Hellenic arc. These models accept that the latter was the result of an extensional stress field, accompanied by grabens created by normal faulting in the back arc basin (according to publications by Ritsema, 1974; McKenzie, 1978; Mercier, 1979; Le Pichon and Angelier; 1979; Dewey and Seng?r, 1979 and others: s. Mariolakos and Papanikolaou, 1981a).

Mariolakos and Papanikolaou (1981a) suggested that marginal fault zones control the configuration of Neogene basins. These fault zones create an asymmetry with the basin morphology and sedimentation. According to the above-mentioned authors, the Hellenic arc is separated into three large parts. In part I, the major fault zones have an E – W direction. In part II, the direction is NW – SE, and in part III, the direction changes to NE × SW. This arrangement shows that only parts II and III have an apparent dynamic relation to the Hellenic arc and trench system, while part I has its own peculiarity.

Data on the current deformation pattern of the Hellenic Arc have been provided by numerous researchers, and these take the form of: (i) *in situ* measurements of the stress field in shallow (<10 m) drillings (Paquin et al., 1982); (ii) Palaeomagnetic investigations of

the Neogene and Quaternary sediments (Laj et al., 1982); (iii) fault plane solutions (McKenzie 1972; 1978, Ritsema, 1974; Drakopoulos and Delibasis, 1982; Papazachos et al., 1984.) Mariolakos and Papanikolaou (1987) combined the results of various geological, seismological, and geophysical studies, and proposed a present (active) deformation model. Further data that contribute to the interpretation of the current deformation regime of the Hellenic territory, have been supplied by geodetic measurements (Billiris et al., 1991) and by the distribution of earthquake foci.

More recent investigations in the SW Peloponnessos (Messinia) showed (Mariolakos et al., 1991) that the stress field responsible for the neotectonic active deformation of the area is that of a rotational couple, which caused not only brittle but also ductile deformation structures, resulting from local transpression and transtension sectors.

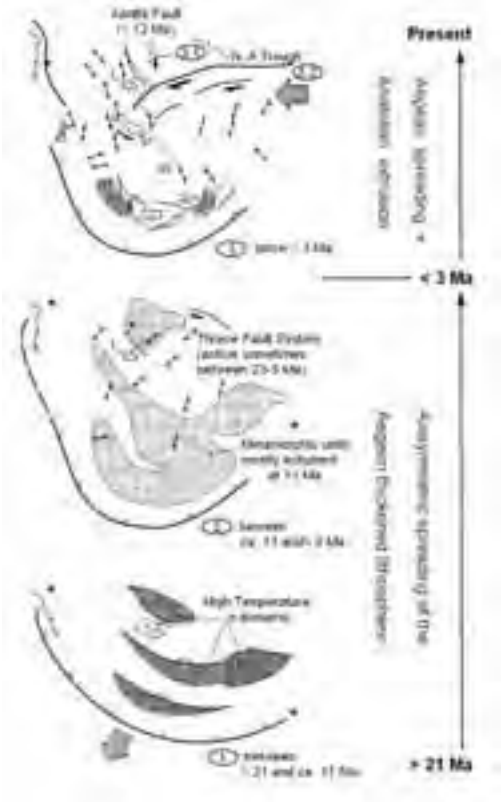

Figure 13 - Three-step scenario depicting the Neogene evolution of the Aegean (after Gautier et al., 1999).

Field itinerary

DAY 1

Sofia - Plovdiv - Starosel - Hisar - Karnare - Troyan (about 310 km)

M. Ivanov, I. Zagorchev.

The itinerary of the first day (see inside back cover) to start with follows the famous route from Rome, via Serdica, to Constantinople, along the Maritsa fault belt in the southern edge of the Srednogorie zone. From Plovdiv, it crosses towards the north the Upper Thracian plain (Neogene – Quaternary graben), the central parts of the Sredna-gora crystalline fragment, the Sub-Balkan neotectonic grabens, the Sub-Balkan normal fault, and the Central-Balkan thrust, the Balkan (Stara-planina) zone, and enters the Fore-Balkan zone.

East-Southeast of Sofia, the itinerary leaves the Sofia neotectonic graben, and follows the Maritsa fault belt in the southern edge of the Ihtiman unit, in the Srednogorie zone. The "Trayanovi vrata" (Trayan's Gates) Pass had a strategic importance in antiquity as being the only way from Europe to Constantinople.

Stop 1.1:

Quarry and road cutting: altitude 491 m; at about 70 km from Sofia

Granodiorites of the Upper Cretaceous Vurshilo pluton. Formerly believed to be of Palaeozoic age because of the superimposed schistosity, they are now referred (N. Georgiev) to the Upper Cretaceous (c. 82 Ma; A. v. Quadt). Numerous xenoliths from folded metamorphic rocks are observed. Other features exhibited at the outcrop are: vertical wrench fault, striking 118º, with striae plunging East; almost vertical dyke of granodioritic porphyrite, striking 130º, about 1.2 m thick. A superimposed, almost vertical schistosity strikes 130-135º, with striae in the schistosity planes plunging 55ºNW.

Dykes of granite-porphyries, and granodioritic, syenodioritic, and monzodioritic porphyrites are typical of the Srednogorie. Most of them have a Late Cretaceous age, and are intruded both in the Upper Cretaceous intrusive (hypabyssal to subvolcanic) bodies, and in the host Palaeozoic granites and Precambrian metamorphics. The schistosity is related to an Ihtiman shear zone, that was first a magma conductor under transtensional conditions (with mixing of magmas of mantle and crustal origin), and then developed, under transpressional conditions and right-lateral strike-slip.

Stop 1.2:

Plovdiv, Nebet-tepe Hill: 209 m

The hills of the old town are built up of syenites ("plovdivites"), with numerous xenoliths and enclaves from basic and acid rocks, hornfelses included. Moebus studied in detail the composition of the enclaves, and reported in 1959 the presence of reworked Upper Cretaceous sedimentary rocks and hornfelses. According to him, the "plovdivites" were formed through intense metasomatosis, and should not be called "syenites", this name being reserved only for rocks of purely igneous origin.

The town is more than 6000 years old, thus being older than either Rome or Constantinople. A Thracian fortified town (Eumolpia, Poulpoudeva), it was conquered in 432 BC by Phillip II of Macedonia and named "Phillipopolis" after him. The Romans called it Trimontium. In 815 the Bulgarian Kan Kroum seized the fortress. Afterwards, it was for different periods in the hands of Byzantines, Crusaders, and Turks (Filibe), and was later proclaimed by the Berlin Congress (1878) capital of the autonomous province Eastern Roumelia, and re-united with Bulgaria in 1885. Our brief visit will allow us to observe archaeological traces of this turbulent past.

>From Nebet-tepe we observe the panorama of the Plovdiv polje of the Upper Thracian depression. It is a wide graben structure, superimposed over the Srednogorie zone during Late Oligocene, Neogene and Quaternary times, along the Maritsa fault belt. to the south, the graben is framed by the complex neotectonic horst of the Rhodopes, and to the north, by the complex horst of the Sredna-gora crystalline block. The normal faults and strike-slip faults of the Maritsa fault belt strike 90-120º, and have steep to moderate dip angles. With transversal and oblique faults, they form the complex block structure of the pre-Oligocene basement. Some of the faults are still active, as witnessed by the earthquakes, the Plovdiv earthquake of 18.04.1928 (M=7) included.

Stop 1.3:

Temple of Sitalkes, Starosel: 484 m

Excavations during the last 3 years have exposed a Thracian temple complex, referred to the time of King Sitalkes (5nd Century B.C.). The principal temple is built over Precambrian biotite gneisses (often garnet-bearing) and migmatites, intruded by the biotite porphyric granites to leucogranodiorites of a Palaeozoic (c. 300–320 Ma) granite pluton. Rarely, dykes of pegmatites and aplites are observed.

The temple of Sitalkes is built with local granite blocks but the well-polished elements (columns, capitels, etc.) have been made from imported zeolitized tuffs.

Stop 1.4:

Hisar

From Starosel we continue to Hisar – first a Neolithic site and a Thracian town transformed into a fortified spa (Diocletianopolis) during the Roman rule. The well-preserved walls (2.5 km long, up to 10 m high, with 44 towers, and 15 m high main gates) are a typical Roman construction of stone, brick and mortar. The stone blocks come mostly from the local biotite porphyric granite of the Hisar pluton (c. 337 Ma, Sr_i 0.706). For some important places (key stones and thresholds at the northern gates, corner blocks of towers, etc.), huge blocks of equigranular syenites have been transported from Plovdiv. Presently, 22 mineral springs have a total debit of 4000 l/min, the temperatures ranging between 27 and 52ºC. The waters are alkaline (pH 7.6 – 9.02), sodium hydrocarbonic, with sulphate, fluorine, and more than 20 microelements.

The Hisar polje represents a peculiar irregular post-sedimentation (in respect to the Neogene) graben formed by ENE- and NNE-striking steep (60-90º) normal faults. To the south, the Starosel and Hisar grabens are separated from the Upper Thracian depression by the Krasnovo normal fault that strikes ESE. Thus, a second-order step-like graben is formed between the depression and the Sredna-gora horst. The normal faults are the conductors of the thermal mineral waters.

Stop 1.4a:

Quarry "Sveti Georgi" (St George),
Verigovo: 432 m

The young (III complex, c. 270 Ma) Sveti-Georgi granitoids are mostly biotite equigranular fine- to medium-grained granites, leucocratic, often with schlieren, due to the contamination with, and resorption of, basic enclaves and older granitoids. Xenoliths and enclaves originating from the Hisar granites (c. 337 Ma) are abundant.

Stop 1.5:

Quarry "Momina banya": 445 m

Coarse-grained biotite porphyric granite to granodiorite of the Hisar pluton, with numerous melanocratic enclaves with dioritic composition.

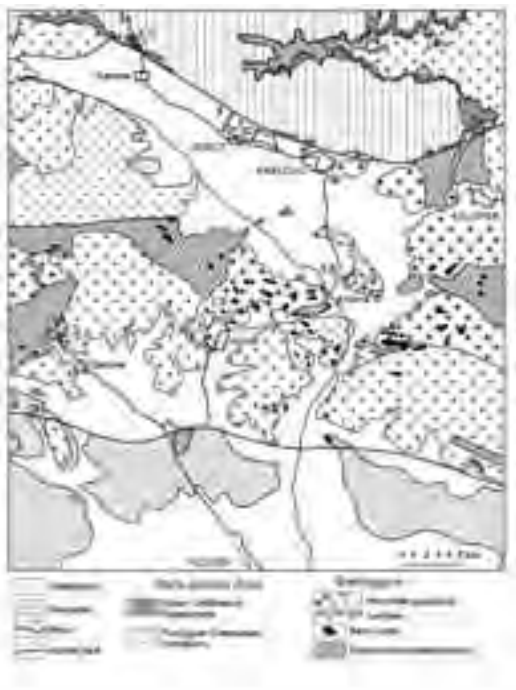

Figure 14 - Geological map of the central part of the Srednogorie zone

It possesses a clear platy parallelism of enclaves, schlieren, coarse (up to 5 cm) K-feldspar endoblasts, and biotite. The planar structure strikes 120-135º, and has a steep (about 80º) dip to NNE that indicates a steep northern contact of the pluton with the host Precambrian metamorphics. The granitoids of the Hisar pluton are intersected by dykes of fine- to medium-grained Sveti-Georgi granites. The thickest (1.5 m) dyke strikes 165º, and dips to the ESE at about 55º. Another 60-cm dyke strikes 140º and dips 55-70º NE. Whole-rock samples from the quarry defined a Rb-Sr isochrone, corresponding to 271 +/- 26 Ma and an initial Sr ratio of 0.709.

The road continues through biotite gneisses and migmatites, and the strongly weathered leucocratic granites of the Mihiltsi pluton (III complex) similar to the Sveti-Georgi granites.

Stop 1.6:

Road junction after the town of Banya: 316 m

The stop exhibits a neotectonic panorama of the Karlovo graben, the Sub-Balkan fault and the Stara-planina linear morphostructure (s. Figure 14). The neotectonic features of these parts of the Srednogorie zone are related to the formation and subsidence of a Sredna-gora swell, trending approximately west-east. The subsidence is linked to the collapse of the back parts of the Stara-planina Palaeogene orogen. As a result, two rows of Neogene – Quaternary grabens have been formed: the grabens of the Sub-Balkan poljes to the North (at the boundary between the Srednogorie and Stara-planina zones, along the Sub-Balkan fault), and the grabens along the Krasnovo fault, to the South. The internal structure of the Karlovo graben is complicated by second-order normal faults. It is filled with Neogene (Maeotian? – Romanian) and Quaternary sediments, with a total thickness of about 500 m. The sediments have been deposited in a fluvial system, and a lake (with diatomites and coal) has existed in the northernmost parts in latest Miocene – earliest Pliocene times.

The Upper Cretaceous Srednogorie orogen was uplifted and deeply denudated already at the end of the Maastrichtian. In some parts (southern edge of the Sredna-gora crystalline block) a fluvial system was formed in Danian time, being drained towards the marine gulf along the Stara-planina range (then below sea level). At the end of Middle Eocene times, the new folding within the Balkans led to the north-vergent thrusting of the Srednogorie over the Balkan (Stara-planina zone), followed by the uplift of the latter in Late Eocene and Oligocene times. During the most important Neogene – Quaternary uplift, a tectonic relief inversion favoured the formation of the numerous normal faults of the Sub-Balkan fault belt, and some of the old thrust surfaces rotated and were transformed into steep normal faults. Further on, some of the steep normal faults rotated in the extension process to low-angle (listric) normal faults.

The itinerary continues through the Karlovo graben, and at the village of Karnare, reaches the normal faults of the Sub-Balkan fault belt.

After the village of Karnare (altitude 643 m) the itinerary leaves a high mountain step built over the Neogene at the foot of the mountain, and enters the Stara-planina zone.

Stop 1.7:
Along the road North of Karnare: 666 m

The road cutting exposes tectonized Upper Cretaceous deposits. They represent an alternation of clayey limestones (locally with flint nodules), and fine- to medium-bedded marls. The limestones are mostly micritic, and the marls, clayey or slightly silty,

and fine-bedded. The two lithotypes are combined in doublets and represent periodites. They are probably climate-controlled, and represent low-order Milankovic cycles. This clayey-limestone formation has a Santonian – Campanian age. The bedding varies between 75º/35ºSSE and 120º/50ºSSW. South-vergent (opposite to the prevalent North-vergent thrusting) upthrusts are observed. The next clayey limestones exhibit also the typical North-vergent thrust surfaces.

Stop 1.8:

Parking place to the right side: 993 m

A neotectonic panorama exhibits (Figure 15) relics of the granite thrust sheet (towards the village of Christo-Danovo), the Karlovo graben, and the Sredna-gora crystalline block (a neotectonic horst). The Precambrian (Cadomian?) metamorphics (biotite migmatized gneisses) contain numerous granite veins. Prevalent foliation 80º/60ºS. Strong mylonitization and diaphthoresis.

Stop 1.9:

1143 m

Internal thrusting along a surface with 125º/35º: strongly schistified Cadomian? granitoids, intersected by basic dykes (dolerites, lamprophyres), are thrust

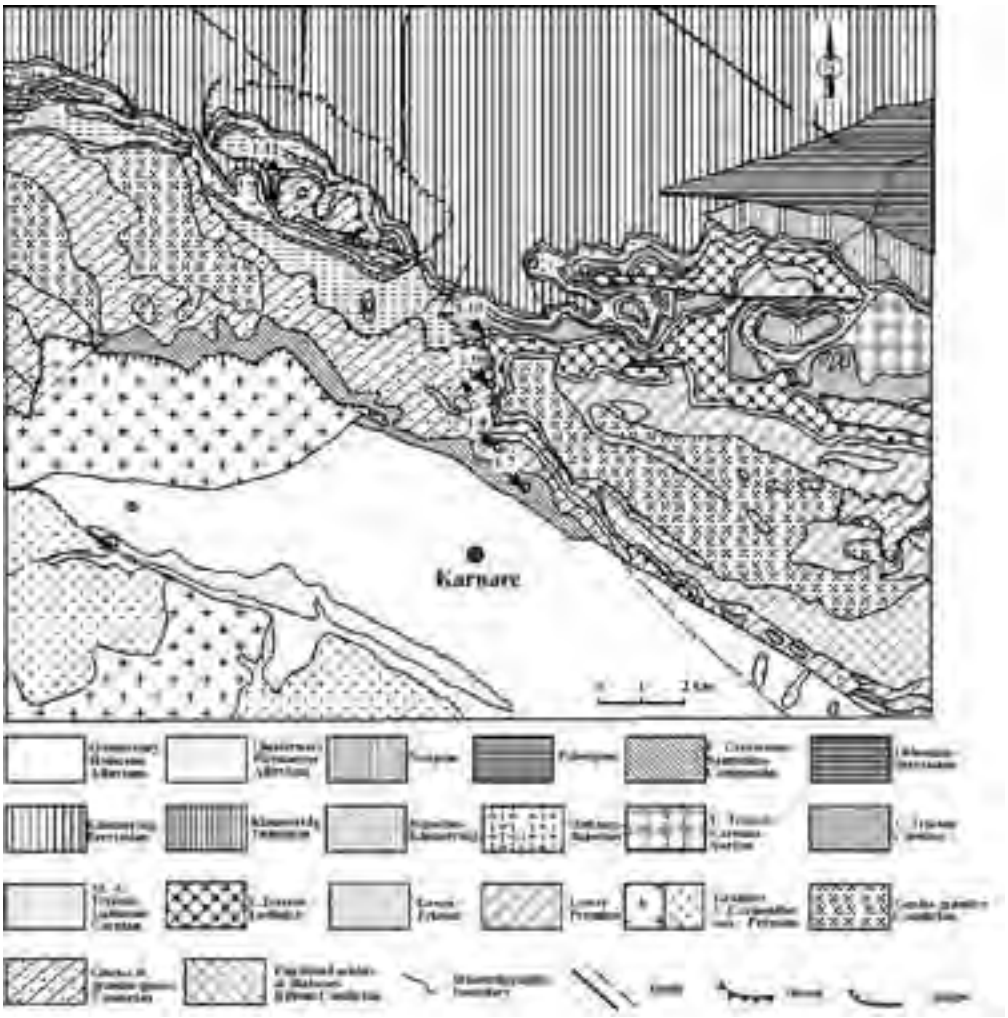

Figure 15 - Geological map of a part of the Central Srednogorie, Central Balkan and Central Fore-Balkan (after Geological map of Bulgaria 1:100000)

over Triassic dolomites, and dolomitic limestones with crinoid ossicles (Mogila and Bosnek Formation – Anisian).

Stop 1.10:

The outcrop exhibits well-bedded dark-gray to blackish limestones, with crinoid ossicles and biodetritus, locally oolithic (Vasilyov Formation, Ladinian), with bedding striking 100º/50ºN. They are covered by the Upper Triassic of the Troyan Formation: limestones, brecciated calcareous dolomites, sandstones, locally interbedded with variegated (red and greenish) clays. Rarely, badly-preserved moulds (probably, *Monotis* sp.) are visible. In the upper parts of the section, dolomites with typical weathering are observed, with bedding striking 110º/60º, changing fast to 90-110º/45-55ºNNE. The next Jurassic sequence consists (from bottom to top) of mixed continental and marine reddish-brown sandstones with coal (Bachiishte Formation - Hettangian? - Pliensbachian); quartz sandstones and quartzites (Kostina Formation, Pliensbachian); dark-gray fine-bedded limestones (Ozirovo Formation; Pliensbachian - Aalenian); and oolithic, biodetritic, and sandy limestones (Polaten Formation; Bajocian-Bathonian). Along the road, rock fragments of micritic limestones, some of them with cherty nodules, and red "ammonitico rosso" limestones, come from nearby outcrops of Callovian (Yavorets Formation) and Oxfordian-Kimmeridgian (Gintsi Formation).

Stop 1.11:

Beklemeto Pass - quarry near the mountain ridge: altitude 1399 m

The quarry exposes strongly tectonized Jurassic limestones. The klippe exhibits in an overturned position (from bottom to top): Anisian dolomite (Bosnek Formation); limestones and intraclastic limestones (Anisian Mogila Formation); sandy limestones, marls, sandstones, and fine dolomite beds (Spathian-Anisian Svidol Formation); flakey and variegated sandstones with separate quartz, quartzite,

Figure 16 - Palaeogeographic and basin reconstruction of Northern Bulgaria in the Berriasian (after Minkovska et al., 2001)

and granite pebbles (Lower Triassic Petrohan Terrigenous Group); strongly tectonized Hercynian? granite.

The neotectonic panoramic view exhibits the Neogene (Maeotian?) planation surface at 1500 - 1600 m over the Stara-planina morphostructure. To the South, the Karlovo graben, and (in the background) the Sredna-gora crystalline block (neotectonic horst). Several planation surfaces are visible, and they are clearly superimposed one upon the other due to the low-velocity uplift of the horst, in contrast with the clearly-defined planation surfaces within the Stara-planina range.

Stop 1.12:

Bridge at the entrance of the town of Troyan.

Upper Jurassic - Lower Cretaceous (in their full range - from Middle Kimmeridgian to Lower Vallanginian) flysch sediments (Cherni-Osam Formation) are exposed in the road cuttings and the picturesque cliffs. They belong to the Central-Balkan Flysch Group, deposited in the so-called Nish-Troyan flysch trough. The sedimentary sequence consists of flysch rhythms, built up of fine- to medium-bedded sandstones, siltstones and marls. Rarely, the flysch sequence is disturbed by thick turbidite beds. The flysch rhythms possess a typical texture sequence illustrative for Bouma rhythms: gradational bedding, parallel bedding, a convolution interval, and they end with marls of the background sedimentation. Some of the rhythms are incomplete. The flysch complex has been formed in the axial part of the basin (Figure 16), and shows transitions to the hemipelagic slope sediments (clayey limestones and marls) of the Salash Formation (to the west), and the coarse terrigenous sediments (conglomerates, sandstones, and marls) of the Kostel Formation (to the east). The flysch complex has a most outstanding development in the Central Fore-Balkan zone. The Nish-Troyan flysch trough had a roughly East-West trend. It is regarded as a back-arc trough, a foredeep, or else, as a wrench-type basin, with a clear asymmetry.

The journey from the ridge of the Stara-planina (Balkan) mountain range towards the Danube plain (Moesian platform), allows for almost continuous observation of the Neogene surfaces (Table 1). In contrast to the steep southern slope of the Balkan (along the Sub-Balkan fault belt), the northern slope exhibits a gradual lowering of the planation surfaces that corresponds to the flexural transition from the range towards the plain, and to a steady uplift. In Neogene times, the evolution of the relief was greatly controlled by this steady uplift, and by the draining of the fluvial systems towards the Paratethyan marine basin in the Moesian platform.

DAY 2

Lovech - Pleven - Mezdra - Sofia (about 230 km)
M. Ivanov.

Stop 2.1:

Lovech, Stratesh Hill: 224 m

Carbonate rocks of the Stratesh Limestone Formation (Upper Barremian) are exposed. They are a part of the Lovech Urgonian Group (Figure 17), that consists of four terrigenous and four carbonate formations. The limestones of the Stratesh Formation are biomorphic, bioconstructed, biodetritic, oolithic, etc. The principal reef-building organisms are corals, algae, and rudists (genera *Requienia, Toucasia, Monopleura*). The Urgonian complex is a complex biosedimentary system, formed along the northern Tethyan margin. This facies type is traced at thousands of kilometers on the territories of Europe and Asia. Carbonate

Morphostructure	initial peneplain (E.–M. Miocene)	oroplain I (Maeotian?)	oroplain II (Dacian?)	oroplain III (end Romanian?)
Danube plain	0-200			
Fore-Balkan	420-650-1250	320-550-1000	300-480	200-460
Stara-planina range	1700-1900(2200)	1400-1600	650-1250	
Sub-Balkan grabens	0-400			
Sredna-gora range	400-1400-1600	1000-1100	750-850	380-500
Plovdiv depression	(-)100 -100			
Rhodope complex horst	1700-1900	1600-1700	1400-1500	1000-1100

Table 1 - Altitudes of the Neogene planation surfaces in Central Bulgaria

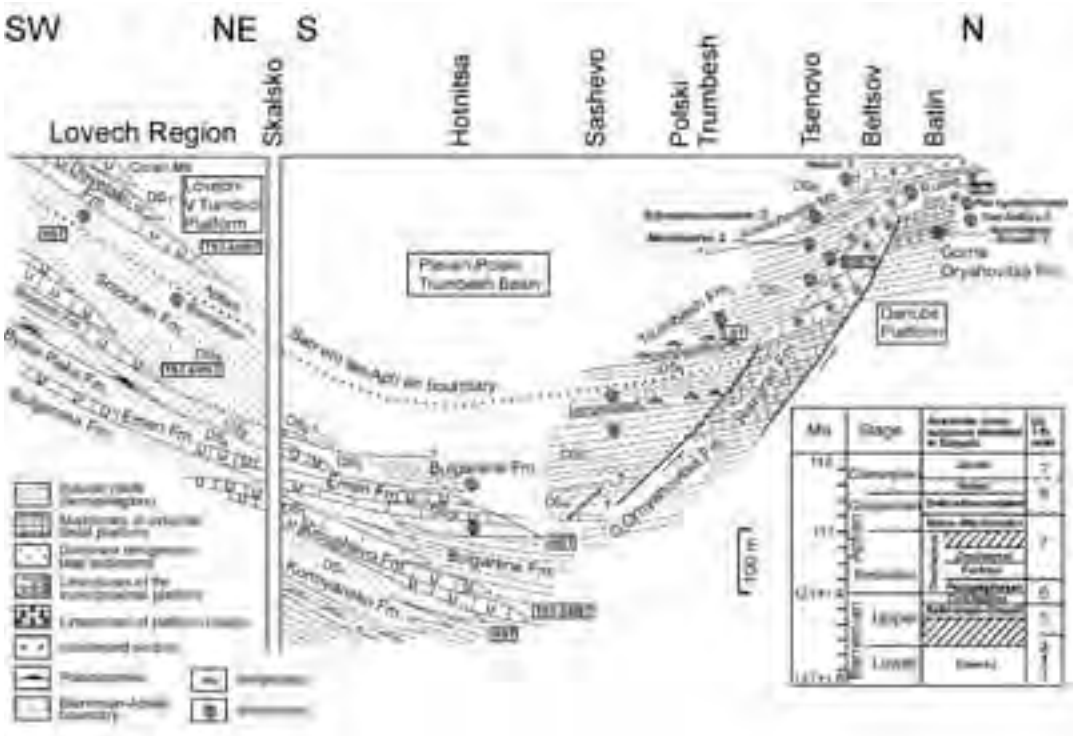

Figure 17 - Basin reconstruction of Northern Bulgaria in the interval Barremian-Aptian (after Ivanov et al., 1997)

sequences, typical both for inner and for outer carbonate platforms, are found at the Stratesh Hill. In their alternation, they form parasequences within a transgressive system tract.

The panoramic view of the town looking north exhibits the typical relief of the Fore-Balkan and the Danube hilly plain (Moesian platform) already mentioned: planation surfaces gradually dipping north, conformable to the drainage pattern of the Neogene – Quaternary fluvial system.

Stop 2.2. NW part of Lovech – road junction towards Goznitsa Suburb: 214 m

The outcrop exhibits the Smochan Terrigenous Formation (Upper Barremian). In the basal parts, it consists mostly of marls and thin layers of sandstones, and clayey and *Orbitolina* limestones. Patch reefs and biostrome bodies have been formed here. They are built of colonial corals, faceloid and dendroid, adapted to a soft substratum (clayey bottom). They are preserved in the rock in situ, the dimensions of the colonies varying from several centimeters to several tens of centimeters. Growth breaks are often visible in the big colonies, due to intense inflow of clayey material. The big colonies form the cores of isolated reefs. Massive colonies dominate the central parts, and dendroid corals, the peripheries. A high taxonomic diversity is found here, both on generic and on species level. The composition of the organisms changes in a vertical sequence. When the growth of the patch reefs is broken, the upper levels are dominated by single corals (*Montlivaultia*), in association with small bivalves and gastropods. The patch reefs and biostromes are formed at a high stand in lagoonal conditions. The rock sequence in this interval is a part of a system tract of high sea level in a third-order sequence.

Stop 2.3:

"Kayluka" Quarry near Pleven: 175 m

The quarry is situated (Figure 18) in the central part of the Moesian platform. The lower parts of the quarry exhibit the limestones of the Kayluka Formation (Upper Maastrichtian). They are biomorphic and biodetritic, and abundant in fossils: bivalves, echinids, gastropods, brachiopods, and rarely, cephalopods (ammonites and nautiloids). Its uppermost levels are dominated by biomorphic limestones. The upper boundary of the formation is marked by an wash-

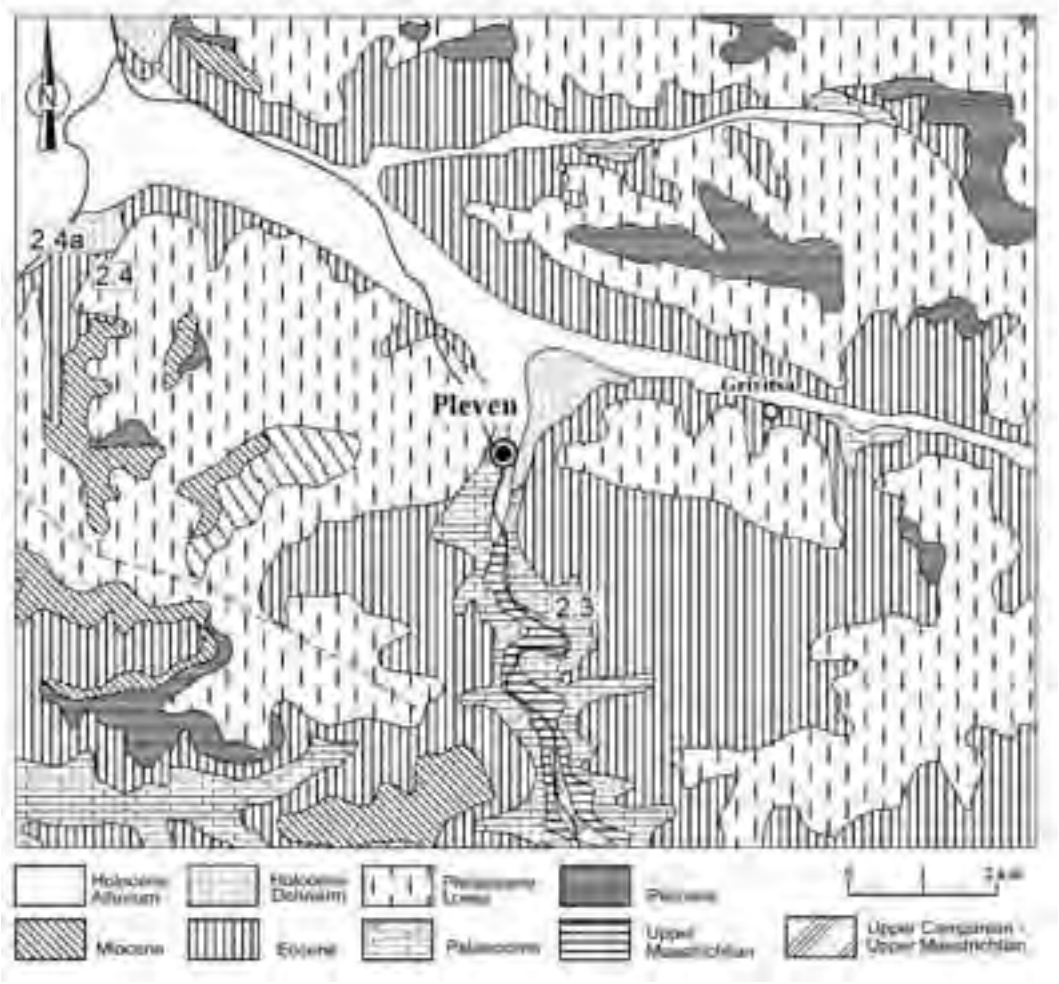

Figure 18 - Geological map of the Pleven Region (after the Geological map of Bulgaria 1:100000)

out, and unconformably covered by the Komarevo Formation (Upper Palaeocene): clayey limestones interbedded with marls. A glauconite-bearing layer (20-30 cm to 1-1.2 m thick), is situated at the base of the formation. The limestone - marl interbedding in the middle and upper parts of the formation is in doublets, and probably indicates a climatic Milankovic cyclicity. The Komarevo Formation is covered with a sharp boundary and wash-out by the marls of the Avren Formation (Lower Eocene). At the base of this formation, a glauconitic marl is observed, too, as well as nummulitoids.

The section illustrates a rock sequence typical of the geodynamic state of the Moesian platform, with low dips and without important tectonic disturbances.

Stop 2.4:

"Yasen" Quarry: 107 m

The quarry exhibits the marls of the Avren Formation, dated here in the boundary interval Lower-Middle Eocene. They represent a monotonous sequence, mostly of clayey marls in irregular interbedding with silty marls. The following gray-blueish to beige and yellowish calcareous clays of the Opanets Formation (Middle Miocene - Badenian) cover them with a sharp transgressive boundary. They contain abundant fossils of different groups (mostly gastropods and bivalves). The uppermost parts of the quarry expose Quaternary sediments: loess and palaeosoils with brown color. They cover the Neogene sediments with a sharp erosional boundary. The whole section is typical for

Photo 2.4 - Quarry "Yasen". Eocene transgressively covered by Miocene.

the interrelations of the Palaeogene, Neogene, and Quaternary cover sediments, and their interrelations, in the central parts of the Moesian platform.

Stop 2.4a:

Road junction at the destroyed bridge on the River Vit, towards the "Yasen" quarry: 75 m

This additional stop exhibits the base of the Neogene (Badenian) section that covers with wash-out and unconformity the Middle Eocene (better exposed at the principal stop).

Stop 2.5:

Quarry next to the road, exit of the village Roumyantsevo: 175 m

This quarry exposes an Upper Cretaceous (Santonian - Maastrichtian) sequence, that transgressively covers terrigenous Lower Cretaceous sediments (Roman Formation, Upper Barremian - Lower Aptian). At the base of the Upper Cretaceous, the Kalen Formation (Upper Santonian) consists of light-brownish to greenish medium-bedded to unclearly-bedded limestones. Small amounts of glauconite are irregularly distributed among them. The next Novachene Formation (Lower Campanian) follows with a sharp boundary, and often after a wash-out. It is represented by chalk-like and clayey limestones interbedded with marls. Light-gray limestones with unclear bedding, and small amounts of glauconite (Roumyantsevo Formation, Upper Campanian; holostratotype section) follow with a sharp boundary. This formation is covered with a sharp boundary by glauconitic sandstones and glauconitic sandy limestones (Durmantsi Formation, uppermost Campanian - lowermost Maastrichtian). This formation is a typical and well-traceable marker in the Upper Cretaceous section in NW and central north Bulgaria, due to the sharp boundaries and the comparatively small thickness. With a sharp boundary again, the Durmantsi Formation is covered by clayey and micritic limestones with a nodular appearance, and abundant flint nodules (maximum range Lower Maastrichtian - Danian). The limestones build layers of moderate thickness, often interbedded by very thin (less than 2 - 3 mm) clayey-silty beds. The Upper Cretaceous section ends with a thick (>200 m) limestone sequence (Kayluka Formation, Upper Maastrichtian).

The section is typical of the platform (northern) facies of the Upper Cretaceous that is widespread over the Moesian platform and the Fore-Balkan. Here it is exposed within the flexural boundary (Bresnitsa-Preslav flexure) between these two units.

Stop 2.6:

Along the motorway, after the road junction to Dzhourovo (at the sign "Sofia 70 km").

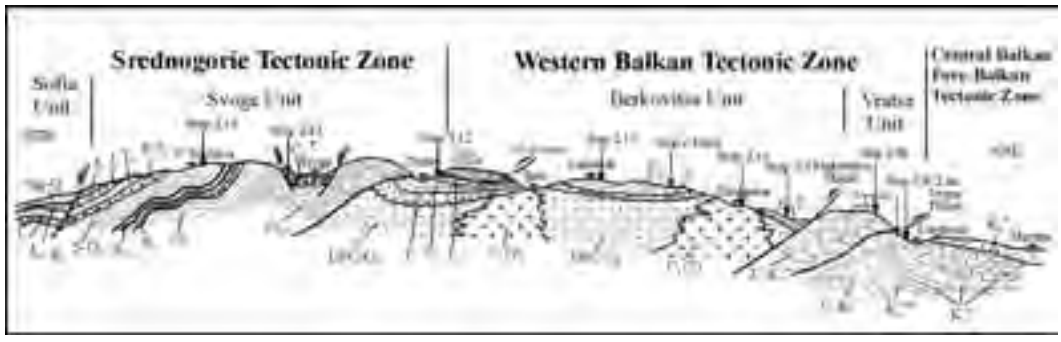

Figure 19 - Geological section along the Iskur valley (modified after the geological maps of Bulgaria 1:100000)

At the stop, a nice panoramic view of the Fore-Balkan and Balkan is afforded, with the principal planation surfaces. Farther along the road, an anoxic blackish flysch is exposed in the road cutting. It belongs to the Upper Jurassic - Lower Cretaceous Cherni-Osam Formation, deposited in the Nish-Troyan flysch trough.
The motorway crosses one of the ridges of the Balkan by a tunnel, and closely afterwards, the itinerary deviates along the road towards Botevgrad.

Stop 2.7:

To Botevgrad, before the right turn: 400 m

The stop exhibits a panoramic view of the Botevgrad graben. This is an internal depression within the Stara-planina positive morphostructure filled in by Neogene (partly) and Quaternary sediments. The graben is situated between the Rzhana horst (to the north; mostly built up of Mesozoic sediments of the Fore-Balkan), and the Mourgash horst (Palaeozoic, mostly Ordovician sediments), to the south. The Botevgrad graben itself has a basement typical of the Berkovitsa unit: Neoproterozoic-Cambrian low-grade metamorphics of the Berkovitsa Group intruded by Variscan granites. The graben is asymmetric: the steep high-amplitude Dragoy-Balkan normal fault to the north is well-expressed in the relief, and covered by steeper and narrower alluvial fans, whereas the southern edge is step-like, with large alluvial fans originating at small-amplitude normal faults.

The itinerary continues (Figure 19) to the valley of the River Iskur (at the Iskur Gorge). This is the only river that has its origin in south Bulgaria (Rila Mountain), and crosses the Stara-planina (Balkan) Range to the north to enter the Danube. The valley has an antecedent character: it existed in Neogene times, before the uplift of the Stara-planina Range, and had been gradually incised in the uplift process.

Stop 2.8:

Lyutibrod: 289 m
(after "Ritlite" - a geomorphic geosite).

Sediments from the upper parts of the Urgonian complex (Vratsa Urgonian Group, Lyutibrod Formation: Lower Aptian) are exposed. They are detritic, oolithic, orbitolina-bearing, and other limestones, in alternation with terrigenous-carbonatic packets (interbedding sandy limestones, calcareous sandstones, and marls). They are typical of the external carbonate platform or marginal

Photo 2.8 - "Ritlite", Iskur Gorge. Boundary between the West-Balkan and Fore-Balkan units.

environments. Tempestites are often present. Detailed observations prove the presence of retrogradational and progradational tendencies and sequences. In combination they form 3rd order sequences with eustatic genesis. Both limestones and marls contain abundant and various fossils (bivalves, gastropods, corals, brachiopods, and orbitolinas). The Urgonian complex along the Iskur valley, between the Cherepish Monastery and Lyutibrod, is near the boundary between two tectonic units: the West-Balkan and the Central-Balkan – Fore-Balkan ones. The boundary between them has a thrust or upthrust character. Consequently, the packets of the Lyutibrod Formation are in an upright position, the soft rock intervals are eroded, and the vertical limestone packets form the natural phenomenon (geomorphic geosite) "Ritlite".

Stop 2.8a:

After the tunnel: 289 m

The sediments of the Cherepish Formation (Lower – Upper Barremian) are a part of the Vratsa Urgonian Group. They are mostly limestones in thick packets, divided by terrigenous-carbonate packets. Pachiodont and bioclastic limestones are dominant. Oolithic and micritic limestones are frequent in the carbonatic packets, whereas the terrigenous-carbonatic packets are dominated by the sandy limestones and calcareous sandstones. They often contain structures typical for shallow environments: cross and oblique bedding by oolithites and the detritus, and HCS in tempestites, situated at several levels in the formation. The rhythmic sediments, with high fossil content and participation of clayey rocks, are the result of storm phenomena. Ripple-marks in the hanging wall of sandstone layers, and strong bioturbation in marls and sandstones, are also typical. Carbonatic and

terrigenous-carbonatic sediments are genetically related to transgressive–regressive cycles. Several 3rd-order sequences are distinguished in this stratigraphic interval of the Vratsa Urgonian Group (Cherepish and Lyutibrod Formation). Palaeogeographically, the Urgonian complex was formed in a basin already closing in Late Barremian and Aptian times, as a typical carbonate platform probably of a ramp type, and without a well-expressed shelf margin.

Stop 2.8b (photostop):

291 m.

The stop exhibits the Cherepish Monastery and the meanders of the Iskur River around cliffs built up of light-gray to white massive limestones (Brestnitsa Formation, Upper Jurassic - Lower Barremian). Micritic and biomorphic varieties are dominant. Less frequent are biomorphic (rudist) limestones (*Diceras* sp.). The limestones of the Brestnitsa Formation are typical of the internal carbonate platform. It is an element of the chain of carbonate platforms situated along the northern margin of the Tethys in the Callovian – Vallanginian time span.

Stop 2.9:

281 m

After a fault structure, the itinerary leaves the Fore-Balkan, and enters the West-Balkan (Berkovitsa) unit of the Balkanides. Permian red conglomerates and sandstones, with pebbles of granite and lydite, are exposed. The bedding is 125-135º/50-60ºNE.

Stop 2.10:

Eliseyna, facing the railway station: 316 m

The outcrops in the road cuttings exhibit Permian andesites (porphyrites) from the core of the Berkovitsa unit.

Stop 2.10a:

349 m

In this outcrop, the basal parts of the Lower Triassic Petrohan Terrigenous Group are exposed. They cover the Carboniferous – Permian volcanics. Two formations are distinguished: lower (sandstone) and upper (sandstone-marly) formation.

In its basal parts, the sandstone formation consists of fine- to medium-grained oligomictic to polymictic sandstones, interbedding with siltstones and marls. These three rock types form cycles with different thickness. Fine and moderate rhythmicity prevail. The sandstones contain also pebbles, intraclasts (from sandstones and claystones), and extraclasts (from red Permian sedimentary rocks). The red color is dominant, beige to whitish beds are also present. Cross and oblique bedding are typical. Internal erosional surfaces, and discordant layering of some packets are frequent. The sediments of the group were formed in a fluvial environment and arid climate. They build the base of a transgressive cycle with progressive retrogradation.

Stop 2.10b:

North of Bov (panorama of the Triassic): 373 m

The section exhibits the base and the sequences of the Triassic System of the western Balkanides. The Triassic covers with angular and regional unconformity different Palaeozoic complexes. It is subdivided into three groups.

The Lower Triassic Petrohan Terrigenous Group consists of clastic rocks: conglomerates and coarse- to fine-grained sandstones, interbedded with siltstones, and dark- to light-red shales. It is formed in fluvial systems: in an alluvial plain, in alluvial fans and under aeolic conditions, in an arid to semi-arid climate.

The Iskur Carbonate Group (uppermost Lower Triassic - Upper Triassic) contains carbonatic sequences formed in shallow marine environments. Its formal lithostratigraphy, as delineated by D. Tronkov, consists of 6 formations and several members. The lower boundary represents a fast transition from the Petrohan Terrigenous Group, and marks the marine transgression. The transition interval has a terrigenous-carbonate character, with the presence of fine-grained clastic or clayey rocks, and gray limestones and yellowish dolomites. Upwards in the sequence follow: rhythmic rocks (alternation of bioclastic micritic limestones and dolomites) formed in sublittoral and littoral environments; massive micritic and bioclastic limestones (with a carbonate bank geometry); and nodular and bioclastic limestones (formed on a carbonate ramp – submarine slumps and storm products, tempestites and tsunamites are observed). The group ends with massive dolomites.

The Triassic section ends at most places with the Moesian Group: marine red beds that correspond to a regressive sequence. It consists of various varicolored rocks: from boulder breccia-conglomerate and conglomerate, polymictic to oligomictic sandstones, siltstones, to shales, marls, limestones, and evaporites. The beginning of the Moesian Group is dated at different places as lowermost Carnian, Upper Carnian, Lower or Middle Norian. It ends also

diachronously, and is followed by a significant hiatus (due to the Late Triassic orogeny), and erosion.

Stop 2.11:

Karst spring "Zhitolyub": 377 m

The cliffs on the left bank of the River Iskur near the karst spring (near the railway station of Lakatnik), exhibit an almost full section of the Iskur Carbonate Group, which was thoroughly studied by D. Tronkov. The lowermost parts of the section close to the spring are built up of cyclic sediments (Opletnya Member of the Mogila Formation; Lower Anisian). Each cycle consists of 3 components, in a regular alternation, and an almost constant bed thickness. The first component is a gray allochemic limestone, the second, micritic limestone, and the third one, a dolomite (that becomes yellowish to beige with weathering). Allochems are represented by ooids, bioclasts of different marine fossils, and lithoclasts. Boundaries between the adjacent cycles have often the character of a wash-out (inundation) surface. The member was formed in littoral to sublittoral environments with a varying hydrodynamic regime: dynamic medium in the lower parts of each cycle, and quiet in the upper ones. The tendency is retrogradational, and typical of a transgressive regime. Low-order cyclicity shows all signs of a climatic control, and probably represents a Milankovic cyclicity.

Stop 2.12:

Tserovo, junction to Zimevitsa: 476 m

The hill Cherni Kamak east of the river exhibits a panoramic view of the contact (Vidlich tectonic zone) between the Berkovitsa and Svoge units. West of the

Photo 2.12 - Panorama of the thrust at Tserovo (s. Figure 20).

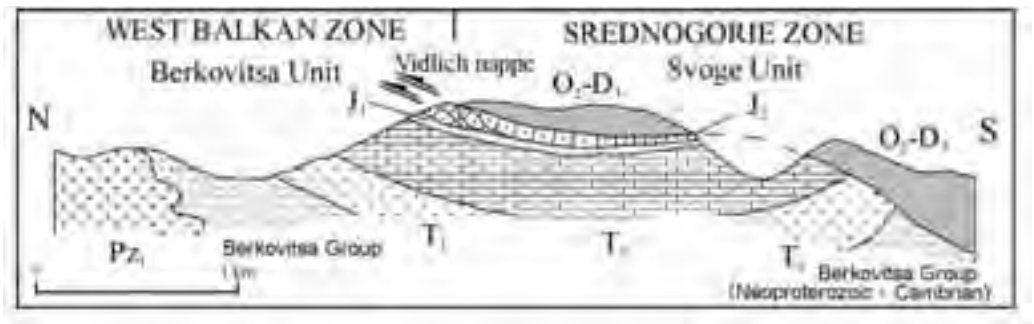

Figure 20 - Simplified sketch of the contact zone between the Svoge and Berkovitsa tectonic units near Tserovo (the Cherni Kamak hill)

Iskur, it is a steep upthrust, whereas to the east, it passes into an overthrust. The allochthon is built up of pre-Mesozoic complexes of the Svoge unit, and the autochthon, of Triassic and Jurassic formations of the Berkovitsa unit.

The basement of the Berkovitsa unit consists of a Neoproterozoic - Cambrian diabase-phyllitoid complex, intruded by Lower Carboniferous granitoids. The Mesozoic cover contains Triassic (Petrohan Terrigenous Group, and lower parts of the Iskur Carbonate Group – not higher than the Anisian Mogila and Babino Formation), unconformably covered by Lower Jurassic (Kostina and Ozirovo) and Middle Jurassic formations. The allochthon (Svoge unit) is strongly tectonized, and consists of sandstones and siltstones of the Ordovician (Grohoten Formation). Jurassic sediments from the autochthon have been also involved in thrusting as parautochthonous lamellae (thrust horses) in the frontal parts of the thrust (*Figure 20*).

Stop 2.13:

South of Svoge: 548 m

The road cuttings exhibit a part of the Carboniferous sequence of the Svoge coal basin. The continental sediments have been formed in different (fluvial, lacustrine, and paludal) environments. They cover discordantly a varied basement: Ordovician, Silurian, and Devonian formations. The lowermost Carboniferous sediments are coarse terrigenous sequences (Namurian Tsarichina and Svidnya Formation). Comparatively finer-grained (sandstones, siltstones, and shales) coal-bearing sediments follow (coal measures between 0.2 and 8 m thick) (Westphalian A: Drumsha and Svoge Formation). The uppermost parts of the section are built up again of coarser terrigenous sequences of Westphalian B (Berovdol Formation), and Westphalian B – C, and (partly) Westphalian D (Chibaovtsi Formation) age. The section exhibits several wash-out and erosional boundaries. The internal architecture often exhibits a cyclic character, forming cyclothems with parasequences. The abundant fossil megaflora has been thoroughly taxonomically studied and published by Y. Tenchov.

The road cuttings expose rocks of the Svoge Formation: sandstones and conglomerates that cover an alternation of medium-bedded sandstones and shales. They are polymictic to oligomictic, with parallel or oblique bedding, typical of fluvial sediments. Huge (decimetric to metric) fragments of branches and trunks of megaflora (*Lepidodendron* and *Calamites*) are abundant. They are in allochthonous position, and possess a preferred orientation, indicating a fluvial transport. A part of the fragments are carbonized, and others changed into coal. It has been proposed to add this outcrop to the geosite list under State protection.

Stop 2.14:

Along the road NE of Vlado Trichkov: 585 m

Ordovician and Silurian sediments from the Svoge tectonic unit (Figure 21) are exposed in the road cuttings. Several formal lithostratigraphic units have been introduced and thoroughly studied by Y. Tenchov and V. Sachanski. The Tseretsel Formation (Ordovician) consists of gray-green shales with non-distinct bedding. The Upper Ordovician (Sirman Formation) is represented by interbedding of dark-gray to black sandstones and shales with graptolites. Further upwards, fine-bedded black and gray shales, gray chertified shales, and banded shales are interbedded with black or gray lydites (Saltar Formation; uppermost Ordovician - Lower Silurian). They contain rich graptolite fauna that allows the exact positioning of the Ordovician/Silurian boundary. The next Mala-Rechka Formation (Silurian) consists of monotonous (but rich in graptolites) fine-bedded black shales.

The uppermost Ordovician and the Silurian of the Svoge unit contain event markers that have been well-correlated with the event stratigraphy schemes of Europe. Such a marker is represented by the sandstones of the Sirman Formation, probably formed at a low sea stand. The interbedding of light- and dark-colored sedimentary packets is explained with climatic cyclicity.

At the town of Novi Iskur, the route enters the Sofia neotectonic graben. The northern boundary of the graben is a steep Neogene-Quaternary fault that is now also the surface expression of the boundary between the Svoge unit, and the central part of the Srednogorie zone.

DAY 3

Sofia - Doupnitsa - Rila - Rila Monastery - Padesh - Blagoevgrad (about 190 km)

Sofia graben and Vitosha unit south of Sofia

I. Zagorchev.

The route South of Sofia crosses the southern part of the Upper Cretaceous Srednogorie superunit. The

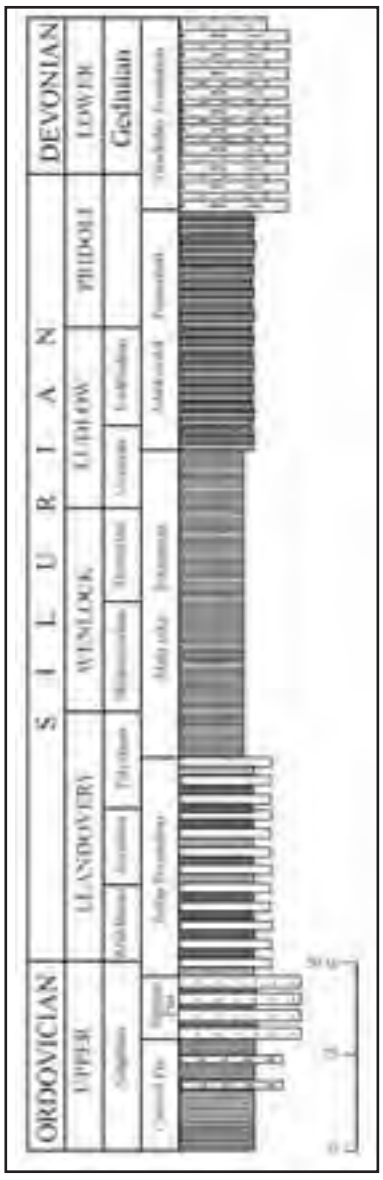

Figure 21 - Simplified section of a part of the Palaeozoic in the Svoge tectonic unit

Vitosha Mountain itself constitutes the principal part of the Vitosha unit. It consists mostly of Coniacian – Santonian volcanic rocks (mainly andesites), and their tuffs intruded by the Vitosha pluton. The Vitosha pluton is built up of three consecutively intruded magmatic phases, that illustrate the development of a deeper source in the upper mantle or depleted lower crust (low initial $^{87}Sr/^{86}Sr$ ratio – about 0.704!) of the Srednogorie zone. The first phase consists of gabbro and gabbro-monzonite, the second, - of different varieties of monzonites, and the third one, - of granosyenite in dykes or small bodies.

The mountain represents a neotectonic horst uplifted at more than 1.5 km above the Sofia neotectonic graben (Figure 22). The graben has a heterogeneous

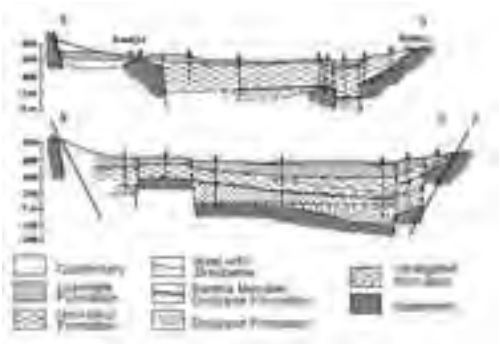

Figure 22 - Cross sections through the Sofia graben (after Kamenov and Kojumdgieva, 1982)

basement: the Neogene deposits (with a total thickness of up to 1000 m) cover with depositional, unconformable contacts different rock units in small pre-Middle Miocene internal blocks: Upper Cretaceous volcanics or sediments, Jurassic and Triassic carbonate or terrigenous rocks, and even (in a very few localities), the pre-Alpine basement.

The Neogene section of the Sofia graben begins with a variegated terrigenous formation, referred to the Maeotian Stage. The second local cycle (Pontian) is related to a lacustrine environment, and is represented by the coal-bearing Gnilyane and Novi-Iskur formations. The cycle begins with a slight local unconformity over an eroded surface. A similar unconformity is even better expressed at the bottom of the last, Lozenets Formation (Dacian – Lower Romanian). It consists of well-sorted yellowish to whitish conglomerates and sands. The whole sedimentary filling of the graben is intersected and displaced by neotectonic (Quaternary) faults, some of them even displacing the Quaternary river terrace sediments.

The itinerary follows the road E-79 and crosses the westernmost periphery of the Pernik Palaeogene basin (Upper Oligocene – lowermost Miocene), which is made up of lacustrine coal-bearing sediments. The basin is a graben (Figure 23), situated over the southernmost parts of the Srednogorie superunit. In

Volume n° 2 - from B16 to B33

Figure 23 - Sketch map of the Palaeogene and Neogene formations in SW Bulgaria (after Zagorchev, 1995)

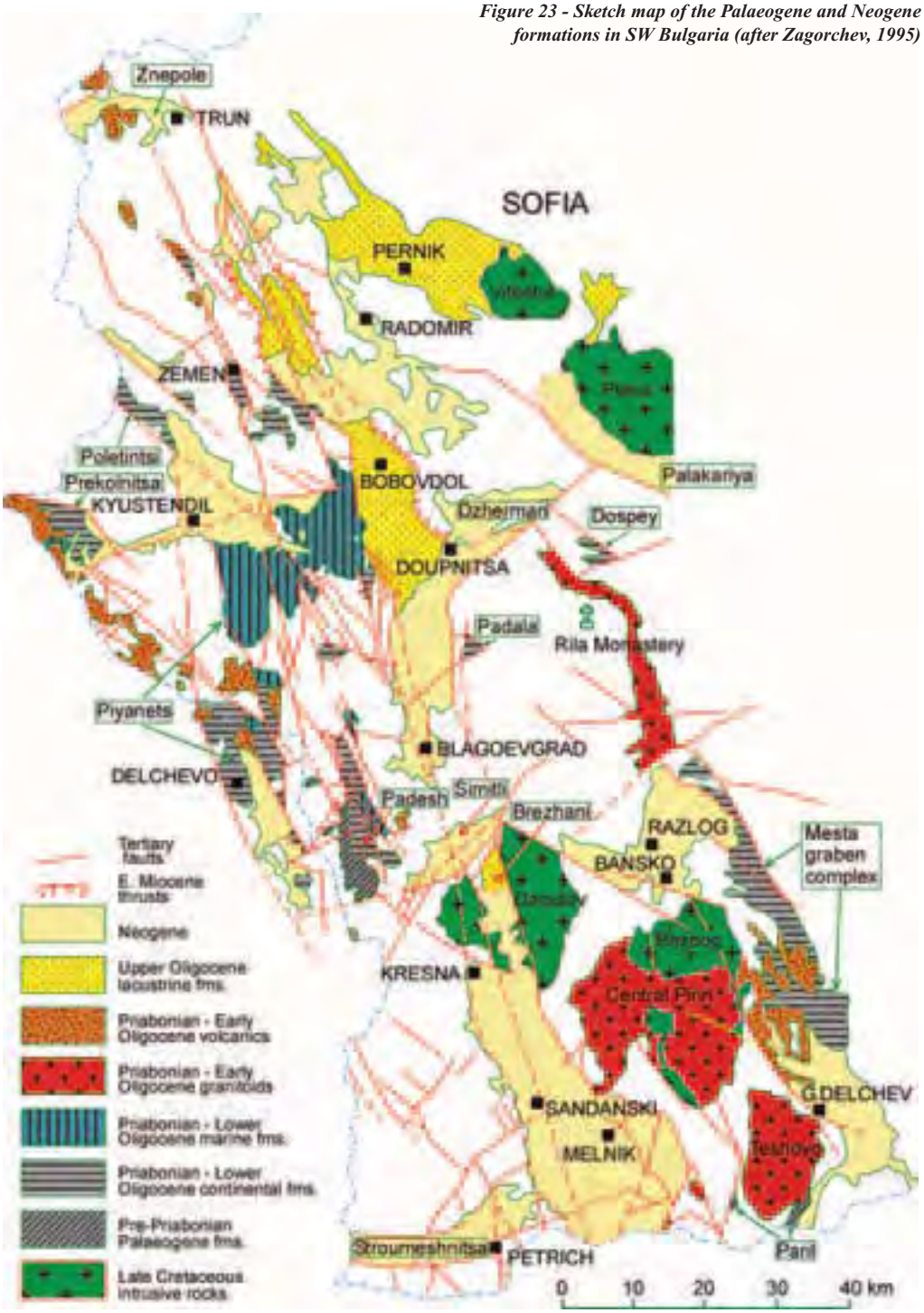

the new road cuttings, varicoloured (gray, green, and red) conglomerates, sandstones, and shales may be observed. At Stoudena, the road enters the Verila unit of the Srednogorie: mostly Triassic carbonate beds (Iskur Carbonate Group) that dip monoclinally south. The road cuttings exhibit dolomites of the Anisian Bosnek Formation, well-bedded nodular dark-gray limestones with shaly interbeds (Ladinian; Radomir Formation), and dolomites and dolomitic limestones (Carnian; Rousinovdel Formation). The latter is covered with unconformable depositional contact by the Middle Jurassic (not exposed).

Stop 3.1:

Staro selo: altitude 784 m

The road cutting exhibits Tithonian flysch: rhythmic interbedding of shales, siltstones, sandstones, and (rarely) conglomerates. The beds are striking about 140º, and dip SW at an angle of 35-40º. They are referred to as the Upper Jurassic – Lower Cretaceous Kostel Formation, and have been deposited in the Nish-Troyan flysch trough, strongly folded and displaced in Mid-Cretaceous, Late Cretaceous and Palaeogene times. Sediments of the same trough have already been observed in the Troyan area.

Stop 3.2:

Near Doupnitsa, 557 m: panorama of the Rila horst

The Rila horst has been uplifted relative to the Blagoevgrad and Dzherman grabens, with an upthrow of more than 3 km since Late Miocene times. The moderately inclined, to steep bounding Klisoura normal fault (Figure 24), strikes NE, and has an angle of dip between 30º and 70º to NW. It has an outstanding geomorphic expression.

The stop is situated over a planation surface that represents a part of the Lower – Middle Miocene peneplain. It gradually lowers to the South, and is subsided in the Dzherman graben to altitudes about and below sea level, being uplifted to more than 2500 m in the Rila horst.

Blagoevgrad basin

The stratigraphy of the Neogene and Eopleistocene filling of the Blagoevgrad graben has been studied in detail. Here it is schematically outlined.

The section begins locally with red polymictic conglomerate that covers unconformably Palaeogene and older rock units and structures. It is followed by proluvial polymictic conglomerate, interbedded with sand and sandy clay (Pokrovnik Formation). The

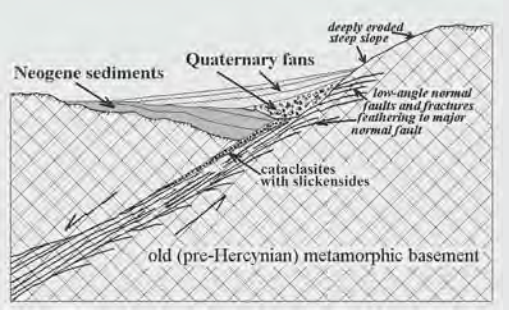

Figure 24 - Schematic section across the Klisoura fault

next Dzherman Formation (Maeotian to Pontian? after mammal fauna) consists of alluvial greenish, whitish, or yellowish sand and clay interbedded with pebble gravel lenses. The Barakovo Formation (Pontian? - Pliocene) is composed of well-sorted alluvial to proluvial whitish or yellowish pebble gravels or sands, with cross or gradational bedding. It covers the washed-out erosional surface on the older Neogene or pre-Neogene rocks. In the western slope of the Rila Mountain, an erosional surface built over the Dzherman and Barakovo Formation is covered by thick unsorted or chaotically deposited Eopleistocene to Pleistocene reddish, brownish to yellowish pebble gravel, sand, and sandy clay, all containing pebble fragments. The road cutting near the small town of Kocherinovo exposes well-sorted conglomerate and sandstone of the Barakovo Formation (Pontian? – Pliocene).

See Table 2 at pag. 32

Stop 3.3:

At the village of Porominovo: 394 m

Panorama (to the SE) of the very young (Quaternary) NE-striking fault along the river Rilska and the lowermost terraces of the river; in the background – erosion forms in the Neogene and Pleistocene, with the high terrace over the two formations. The West-Rila fault zone between the Rila horst and the Blagoevgrad graben is visible to the NE.

In the town of Rila, we cross a narrow horst, built up of rocks of the Cadomian Strouma diorite formation (diorites and quartz-diorites cut by dolerite dykes). At the eastern exit of the small town, south of the "Krusta" hill (the Cross), we enter the post-sedimentary Padala graben. Several stops (Figure 25) are briefly described.

Volume n° 2 - from B16 to B33

Morphostructure	initial peneplain (E.–M. Miocene)	oroplain I (Maeotian?)	oroplain II (Dacian?)	oroplain III (end Romanian?)
Rila horst	2200-2600	1900-2400	1400-1800	1050-1350
Simitli graben	(-)1200?			
Lisiya horst	200-1450-1600	1200-1400	950-1200	650-900
Padezh graben	610-850			600-750
Ograzhden horst	250-1700-1800	1250-1620	900-1200	650-1000
Sandanski graben	(-)1000	380-520	?	750-1070
Pirin horst	2200-2600	1950-2250	1500-1800	1000-1300

Table 2. Altitudes of the planation surfaces in SW Bulgaria

Figure 25 - Simplified map for the itinerary of the third day

The Padala graben (Figure 26) is filled in by the 350 -400 m thick Padala Formation. It consists of coarse breccia and conglomerate interbedded by sandstone with abundant coalefied plant debris (parts of leaves and stems). The pebbles in the conglomerate come from the typical basement rocks that occur in the Rila Mountain: biotite gneisses and migmatites, amphibolites, marble, granite, pegmatite, quartz, and diorite. These basement rocks have been attributed to the Tertiary age as early as in 1844 by Ami Boue, and in 1912, G. Bonchev reported for the first time the presence of a coal lens. An Early Oligocene age has been proven by S. Chernyavska with typical palynomorphs. Thus, the Padala Formation was formed in a part of the alluvial to lacustrine system feeding the Early Oligocene gulf. The graben has a post-sedimentary character. However, some of the normal faults at its northern periphery have pre-dated the sedimentation, and others were active during the sediment deposition. Some syn-sedimentary faults are

Stop 3.4:

Exit of the town of Rila (sign) on the road to Rila Monastery: 531 m

Panorama of beautiful erosion forms: the “Krusta” hill and adjacent hills formed in the Palaeogene conglomerate and sandstone of the Padala Formation are the majestic natural gates towards Rila Monastery.

Photo 3.4 - Town of Rila. Palaeogene Padala Formation.

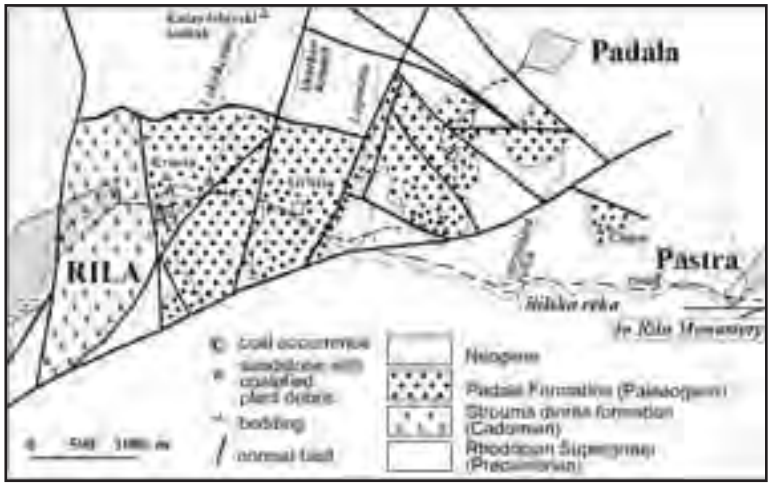

Figure 26 - Geological map of the Padala graben (after Zagorchev et al. 1999)

filled in by neptunian clastic dykes. Post-sedimentary steep, moderately-inclined and low-angle normal faults, are observed to the east and within the sediments of the graben.

Stop 3.5:

At 150 m after the Metoh (monastery branch) "Ortlitsa", near the road junction for Padala, altitude 567 m

The metoh was first mentioned in 1378 in the Chrysovoul (Charter) of the Tsar Ivan Shishman.

The conglomerate is built up mostly of gneiss, schist and amphibolite pebbles, coming from the adjacent basement rocks. The pebbles are chaotically situated in the sandy matrix. Several steep normal faults are visible, with slickensides striking east (90º) (with a dip of 80ºS and subhorizontal striae) and north (360º). Two-mica gneisses, affected by diaphthoresis, follow.

The road enters deeply into the Rila Mountain (West-Rila unit of the Central-Rhodope superunit). It follows the River Rilska-reka, crossing biotite gneisses and amphibolites of the Precambrian Rhodopian Supergroup (Rupchos Group), intensely folded and intersected by the granitoids (granodiorite, granite, quartz-monzonite) of the Kalin pluton. Traditionally, the pluton has been referred to the Upper Palaeozoic, but it is highly probable to be of Alpine age.

Stop 3.6:

Near the confluence of the Rivers Manastirska and Iliyna: 897 m

This stop exposes in the road cuttings the Chepelare Formation of the Rhodopian Supergroup (Proterozoic). Migmatized amphibolites (probably at least partially of ortho-origin), with a clear foliation, are intersected by pegmatite dykes (coarse-grained muscovite pegmatite). The amphibolites are interbedded with biotite gneisses (often graphite- and garnet-bearing). The foliation strikes 155-170º, and dips at 60º to the west. Late quartz veins. A significant post-pegmatite deformation is observed, with partial diaphthoresis in gneisses and amphibolites, gliding along the contacts of the pegmatites, with the formation of thin schistified zones, and fracturing inside the pegmatites.

Stop 3.7:

Rila Monastery: 1103 m altitude

Rila Monastery is the biggest monastery in Bulgaria, and the most important national spiritual center in the Middle Ages and the National Revival in the 18th and 19th centuries. It was founded in the 10th Century by Saint Ivan Rilski (St. John of Rila), and has been ravaged and set on fire several times. The oldest building preserved is the Hrelyu Tower (1335), built by a local feudal lord. The other buildings are dated from the first half of the 19th century. Important manuscripts, treasures, and frescoes can be seen in the church and the museum.

Photo 3.7 - Rila Monastery

Volume n° 2 - from B16 to B33

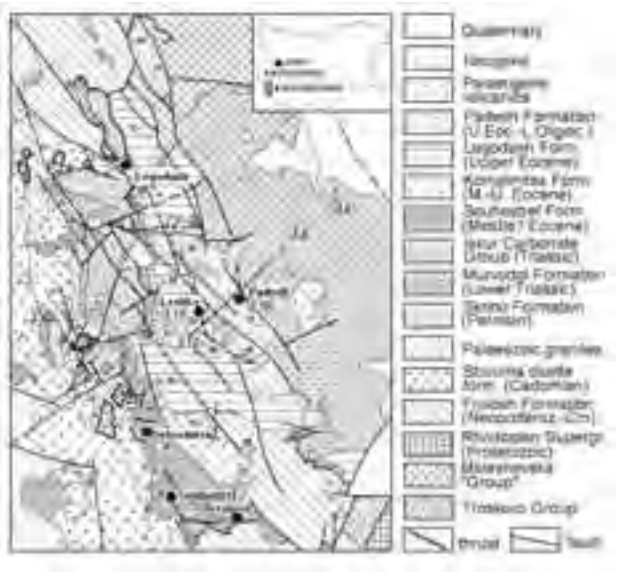

Figure 27 - Geological map of the Vlahina and Lisiya horsts and the Padesh graben (Zagorchev, 2001)

From Rila Monastery the itinerary follows back to the main road, and from there, to Blagoevgrad and Padesh (Figure 27).

Stop 3.8:

After the village of Pokrovnik: 409 m

Cross-bedded fluvial sediments (loose yellowish and whitish sandstone and conglomerate) of the Pontian – Pliocene Barakovo Formation. They belong to the western periphery of the Blagoevgrad graben, partially covering the eastern part of the Lisiya horst.

Stop 3.9:

529 m

The road cutting exhibits amphibolites, and hornblende-biotite and biotite gneisses, of the Troskovo Group, Ograzhdenian Supergroup. The foliation strikes NE (45º), and dips at 25º to NW. Interbeds of leptitoid (quartzo-feldspathic) gneisses are also observed. Numerous coarse-grained dykes of muscovite pegmatite have been prospected for feldspar in the past.

Stop 3.10:

At the entrance of Padesh: 614 m

Panorama of the Padesh graben, with the post-sedimentary Vlahina horst at the background.

The Lisiya horst is built up of gneisses and amphibolites of the Ograzhdenian Supergroup. The Padesh graben is separated from this horst by the Lisiya normal fault zone, that was first activated in Late Eocene time, during the sedimentation if the Logodash Formation. Tongues of coarse conglomerate and breccia, built up exclusively of rocks of Lisiya-horst provenance, are interfingering with sandstones and shales of the formation. The Logodash Formation covers coal-bearing and flysch-like sediments of Middle to Late Eocene age, and is covered with a sharp depositional contact by Upper Eocene – Lower Oligocene pyroclastic and sedimentary rocks of the Padesh Formation. The initial peneplain, built over the Padesh Formation, is covered unconformably by Neogene deposits.

The Vlahina horst is built up of Cadomian diorites, covered by Permian and Triassic sedimentary formations. Outcrops of Palaeogene deposits are preserved over the horst, thus pointing at its post-sedimentary (after deposition of the Padesh Formation) character.

Stop 3.11:

On the road Leshko - Gorno Leshko: 627 m

Layers (up to 100 – 120 m thick) of coarse conglomerate and breccia, built up exclusively of gneiss, amphibolite, and pegmatite pebbles and boulders, are interbedded with sandstones, siltstones, and clays (Logodash Formation). Some of the thin (5 cm) interbeds are rich in carbonate matter, with interwoven ichnofossils. Coalefied plant debris is present, too.

Stop 3.12:

On the road Padesh - Gabrovo: 588 m

Along an interval of about 200 m, the road cuttings exhibit the boundary between the Logodash and Padesh Formation. The Logodash Formation is represented by the typical fine-pebble conglomerates, sandstones, siltstones, and shales, interlayered with coarse to boulder breccia and conglomerate. It is covered with sharp depositional contact by lithoclastic, crystaloclastic, and vitrocrystalloclastic phenodacitic tuffs of the Padesh Formation. They are followed by sandstones and conglomerates, and by the Ovnarska-chouka marker bed (Eocene-Oligocene boundary), built here of carbonatic fossil-rich

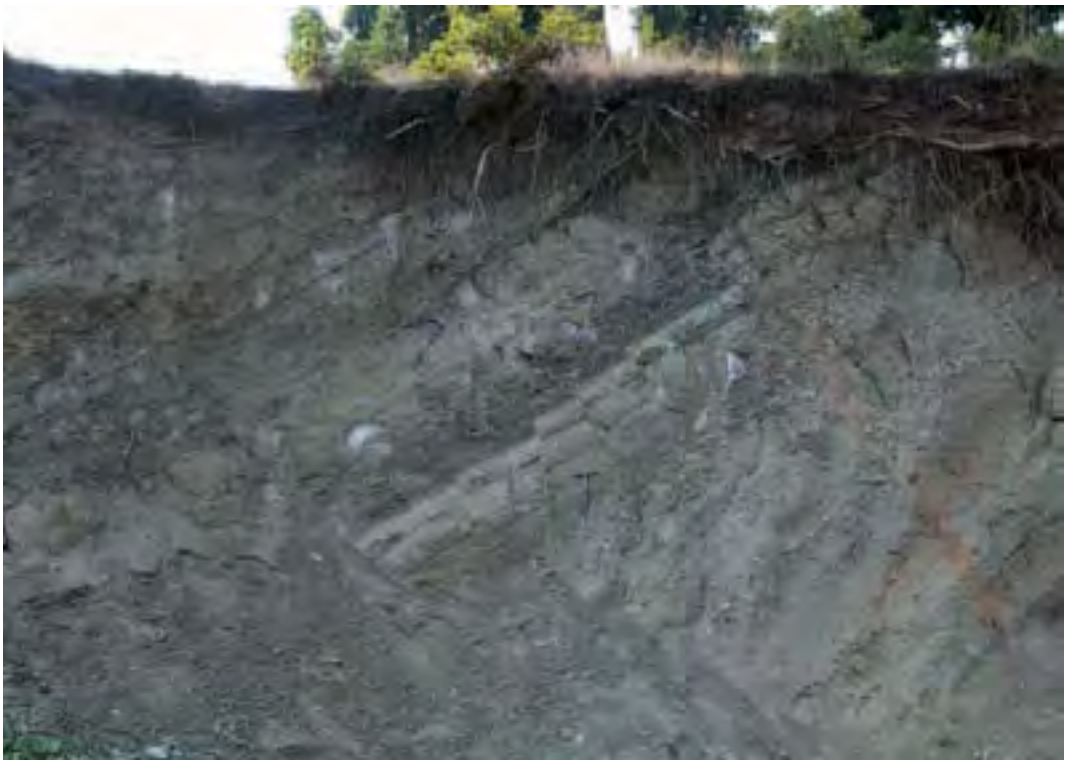

Photo 3.12 - Neotectonic normal faults in Lower Oligocene sediments, road towards Gabrovo.

sandstone. Further on, sandstones and conglomerates, rich in weathered, rounded pebbles of volcanics and tuffs follow. The bedding is almost monoclinal, with beds striking 135-155º, and dips between 30 and 40º to NE. Numerous steep (70-80º) neotectonic normal faults strike 145-165º.

DAY 4

Blagoevgrad - Brezhani - Kresna - Mikrevo - Ilindentsi - Melnik (about 160 km)
I. Zagorchev.

Stop 4.1:

Bridge above the main road: 308 m

A panorama of the Kroupnik active normal fault is exhibited. It bounds at the South the Neogene asymmetric Simitli graben (Figure 28). The total vertical offset is estimated at about 3 km. The fault strikes NNE-SSW, and crosses the NNW-SSE Strouma fault in the northernmost part of the Kresna Gorge of the river Strouma. The two fault zones form a peculiar seismotectonic fault knot that

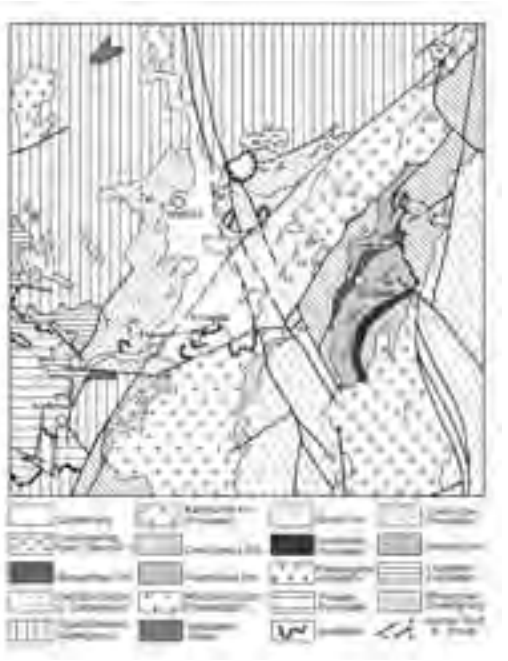

Figure 28 - Geological map of the Simitli graben (modified after I. Zagorchev and N. Dobrev)

Volume n° 2 - from B16 to B33

Photo 4.1 - Panorama of the Kroupnik fault

was the site of several devastating earthquakes in historic time, the earthquake (4.04.1904) with the highest magnitude (7.83) on the Balkan Peninsula included. To the South, the narrow Kachovska horst divides the Simitli graben from the Palaeogene of the Brezhani graben. In the background, the faults of the West-Pirin fault zone form the western boundary of the Pirin horst. The uppermost planation surface in Pirin (at an altitude of about 2600 m) and some of the lower surfaces (at c. 2000-2200, and 1500-1600 m) are visible in the far background, too.

Stop 4.2:

Road to Brezhani:
537 m

The road cutting displays the active neotectonic Kroupnik fault as a slickenside with thin mylonites. It strikes about 25º (NNE) and dips 65-70ºWNW, and is traced well in the morphology of the terrain, with the faceted slopes of the footwall. Further northeast, the fault strike changes gradually to nearly 50º, and the dip angle, to 40ºNW. The striae on the slickensides point to a normal fault character, with a slight (about 10% of the vertical component), left-lateral strike-slip.

The footwall is built of amphibolites of the Vucha Formation (Rupchos Group, Rhodopian Supergroup). They are intensely fractured and mylonitised, and the older structures (foliation, lineation, folds) are hardly visible. The hanging wall is built up of conglomerates of the Kalimantsi Formation (Pontian–Romanian). The conglomerates consist of well-rounded pebbles of equigranular granites of the Upper Cretaceous North-Pirin (Dautov) pluton. Some pebbles situated near the slickenside of the fault display shear fractures with slight (one to several millimetre) displacements, with the same sense as the master fault.

The Kroupnik fault has been active since Sarmatian time, with a total neotectonic (Upper Neogene and Quaternary) vertical offset of the order of 3500 m, and a mean velocity of 0.25 mm a^{-1}. Most of this offset (more than 3000 m), refers to the Neogene times, with two major epochs of activity (Sarmatian - Maeotian and Pontian - Romanian). The recent activity is gauged with a station that measures the relatively slow recent movements on either side of the fault. The fault was particularly active in the years 1901 – 1910. Fourteen earthquakes with epicenters along the fault trace had a magnitude exceeding 4.5, and the total number of tremors was more than 1700. The seismic foci migrated gradually from the NNE towards SSW. The strongest earthquake (M estimated at 7.83!) occurred on 4.04.1904 with an epicenter near Kroupnik.

Stop 4.3.:

Road towards Brezhani: 540 m
Panorama of the Brezhani graben

The Brezhani graben is a post-sedimentary structure, formed mostly in earliest Miocene times. It is limited by the West-Brezhani fault to the west (from the Kachovska horst), and the faults and a west-vergent thrust belonging to the West-Pirin fault zone, to the east. The Palaeogene filling of the Brezhani graben has been studied by B. Kamenov et al. in 1956, and S. Cernjavskadetermined the Late Oligocene age by using palynomorphs. A formal lithostratigraphy was introduced by M. Vatsev in 1984 based on all previous published and unpublished research. The section is subdivided into 5 formations, with a total thickness of 1000 - 1200 m. It consists (from bottom to top) of polymictic gray conglomerate, with sandstone

and siltstone interbeds (Kachovska Formation); interbedding of bituminous shales, siltstones, sandstones, and some coal seams (Goreshtichka Formation); sandstones with conglomerates and siltstones (Rakitnishka Formation); bituminous shales, sandy shales, siltstones, and coal seams (Loulevska Formation); and the topmost conglomerate and sandstone (Dermirishka Formation). The sediments are correlatable with the other coal-bearing Upper Oligocene – lowermost Miocene (Egerian) formations in western Bulgaria (Krasava, Pernik, Stanyovtsi, Bobovdol) and eastern Serbia, and are relics of a large lake. The sediments of the graben and the border thrust are sealed by Pliocene sediments of the Kalimantsi Formation.

Stop 4.4:

Entrance (road sign) of Brezhani: 546 m

The West-Brezhani normal fault strikes NNE-SSW, and dips at an angle of about 55ºW. It displaces with small amplitude the amphibolites (Vucha Formation) of the Kachovska horst from the basal conglomerates of the graben.

Stop 4.5:

Kresna Gorge, after the first tunnel and bridge: 232 m

Entering the picturesque Kresna Gorge, the itinerary crosses the Upper Cretaceous North-Pirin (Dautov) pluton. The biotite granites to quartz-monzonites exposed are equigranular, medium- to fine-grained, locally with numerous small (from several to 10 - 20 mm) segregation biotite inclusions. Thin aplite veins are also observed, as well as (rarely) pegmatoid nests, with cavities filled with adularia feldspar, quartz, and epidote crystals. Whole-rock samples gathered near the tunnel yielded a Rb-Sr isochron, corresponding to 92 +/- 22 Ma. The initial Sr isotopic ratios of the Upper Cretaceous and Palaeogene igneous rocks of SW Bulgaria, show that magmas within the thickened continental crust of the Rhodope massif (Pirin horst included) had a crustal source (anatexis), whereas magmas in the southern parts of the massif exhibit a mixed character, and the Upper Cretaceous magmas of the Srednogorie (e.g., Vitosha pluton), an upper mantle origin. The pluton is intruded both into the Ograzhdenian metamorphics of the Ograzhden unit, the northern branches of the NE-vergent Mid-Cretaceous Strymon thrust, and the Rhodopian Supergroup and Palaeozoic Kroupnik pluton of the Pirin unit.

Intense faulting and fracturing are related to the Palaeogene and Neogene development of the Strouma Lineament. Typical associations of several fault sets and the fault surface morphology and sculpture, may be observed in many outcrops along the gorge. In the outcrop, intense fracturing defines two sets of faults, striking 115-145º, and dipping 35-40º and 55-75º, with striae plunging c. 70º at angles of 30-40º. A late strike-slip fault of the Strouma fault belt strikes 150º and dips East at about 80º.

Stop 4.6:

Tunnel S of Yavorov RW station: 209 m

This stop enables observation of the rocks of the gneiss-migmatitic complex of the Ograzhdenian Supergroup (from the Ograzhden unit) West of the Strouma fault zone. The serpentinite (serpentinized harzburgite with talc, tremolite and asbestos in the peripheral zone) is preserved as a rootless lenticular body parallel to the foliation in the two-mica and biotite gneisses and amphibolites. Some desillicified pegmatitic veins cross-cut the serpentinite. A dyke of granodioritic porphyrite crops out in the vicinity. The road cutting exhibits also a case of boudinage, when biotite gneisses are boudinaged within the rich in leucosome biotite and two-mica migmatites. Obviously, the relative viscosity of the gneisses was higher than this of the “migma”, and they reacted in a semi-brittle manner to the stress during the synmigmatic folding.

Ultrabasic rocks are widespread in the Ograzhdenian Supergroup. They occur usually as rootless bodies throughout the section, their emplacement pre-dating the amphibolite-facies regional metamorphism. Their origin is considered to be related to pre-metamorphic Precambrian processes of obduction of the oceanic crust, or to penetration of mantle material in the continental crust, and their further amalgamation.

Stop 4.7:

Mikrevo: 222 m

This observation point is situated on the sinuous road from Mikrevo towards Tsaparevo, and exposes also the rocks of the upper parts of the Ograzhdenian Supergroup (Maleshevska “group”) from the eastern margin of the Ograzhden unit. These are biotite and two-mica gneisses and migmatites interlayered with amphibolites and biotite schists. In the locality the biotite schists contain tiny tourmaline crystals. After folding, the schists were intruded by pegmatites (with tourmaline) and aplites, that underwent afterwards a new deformation event (again in amphibolite-facies conditions), together with the host rocks, with intense

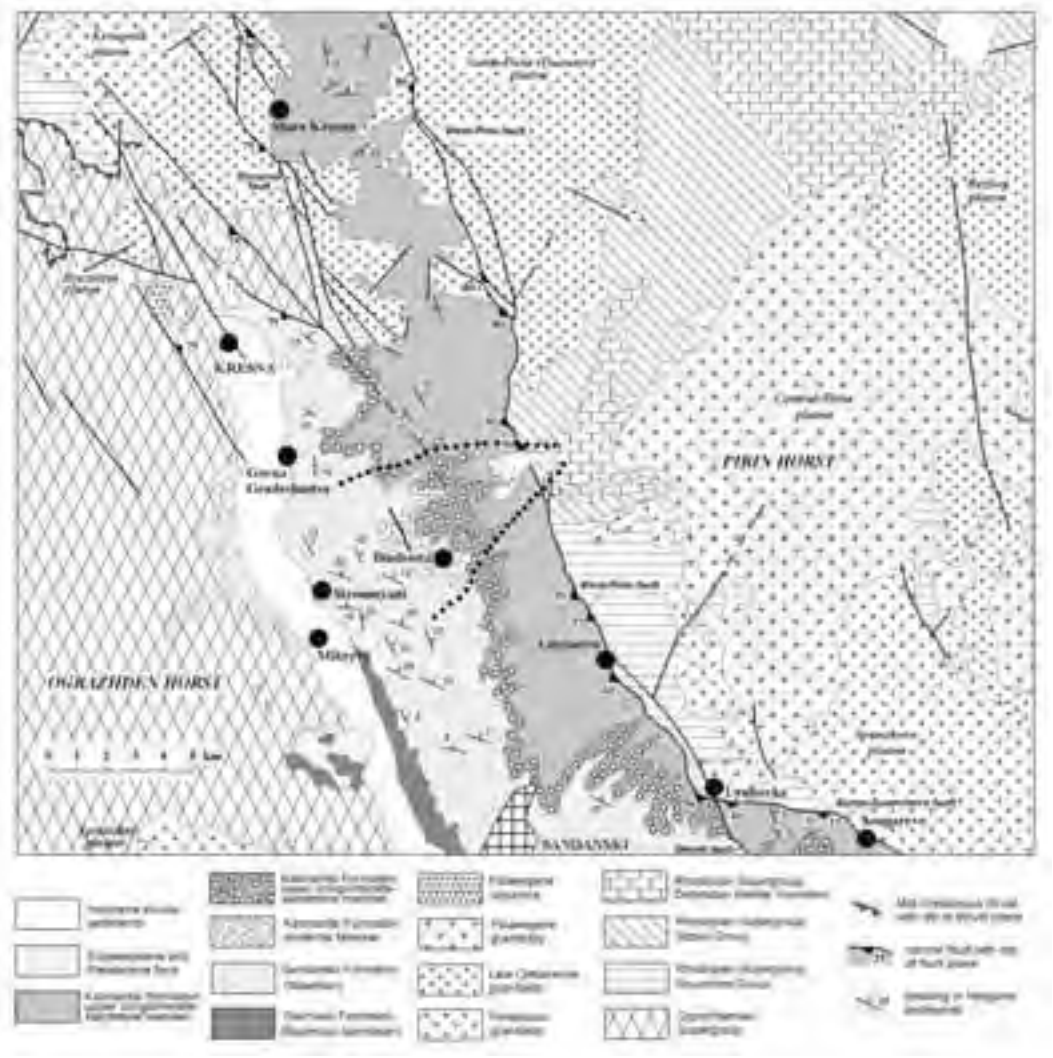

Figure 29 - Geological map of parts of the Sandanski graben and Pirin horst

schistification (aplites and pegmatites transformed into quartzo-feldspathic gneisses) and folding in two episodes.

The Sandanski graben is an asymmetric structure, with maximum (3000 - 3500 m) vertical displacement along the eastern margin (West-Pirin fault zone), and a small (150 - 500 m) offset along the western margin (Ograzhden fault zone). The stop displays a panoramic view (Figure 29) of the Pirin horst with the highest peak Vihren; the initial (Lower - Middle Miocene) peneplain (orthoplain) at ca. 2600 m, and the planation surfaces (oroplains) at 1950 - 2200 m and 1500 - 1600 m; the tilted section of the Sandanski graben, with the marble breccia of the Ilindentsi Member; and the post-Neogene surfaces (pediments) built over the tilted Neogene section (and partially, over the West-Pirin fault zone itself) at altitudes of 650 - 900, 500 - 600, 320 - 360, and 220 - 270 m.

Stop 4.8:

Road to Ilindentsi: 244 m

Some outstanding features of the neotectonics of the Sandanski graben (for details, Zagorcev, 1992, 1995) are visible along the road from Stroumyani towards

Ilindentsi.

The Sandanski graben is filled in with Neogene sedimentary formations with a total thickness exceeding 1600 m. They are clearly divided into three parts.

The basal parts (Delchevo Formation, with Badenian to Sarmatian - Maeotian age, and a thickness exceeding 200 m) are represented by silty and shaly, reddish or greenish sandstones, interbedded with fine-pebble conglomerates, siltstones and shales. Rarely, they contain tuffite (or tephra) material, and single limestone beds. In the upper parts of the Formation, internal wash-outs are clearly visible, with thin (from centimeters to a few meters) rhythmic repetition of conglomerate or coarse sandstone over the wash-out surface of siltstone or clay (locally with coalefied plant debris), and becoming finer-grained, with graded bedding, upwards. These features are observed on the main road near Sandanski (Stop 4.7).

The next formation (Sandanski Formation, of Maeotian age, or more precisely, from uppermost Sarmatian to lowest Pontian; 180 - 1000 m thick); is built up of medium- to coarse-grained sands and sandstones, locally with cross or graded bedding, with silty or clayey interbeds (at the village of Hotovo, with the Hotovo coal seam), and some conglomerate.

At the village of Ilindentsi, the uppermost, Kalimantsi Formation (Pontian - Romanian; 200 - 600 m thick) begins over the washed-out surface of the Sandanski Formation with the 50 - 80 m thick Ilindentsi Member. It is built up of huge fragments and blocks of Dobrostan marbles coming from the nearby outcrops of the Pirin horst, in the area of the peaks Sinanitsa and Sharaliya. The breccia is well-cemented by carbonate cement, and has a sharp and sinuous lower surface. Locally, the lower surface is sharp and planar, and has the character of a slickenside with striae. The upper surface is also uneven, and numerous fractures into the breccia are filled in (neptunian clastic dykes) by sandstones of the next member of the formation. The breccia is displaced by normal faults that belong to the Strouma fault zone (mostly sealed by the sediments of the graben). Laterally, the Ilindentsi Member passes from the monomictic marble breccia into polymictic (with amphibolite fragments) breccia-conglomerate, and thins out at a distance of a few kilometers. The next two members of the Kalimantsi Formation are built mainly of whitish to yellowish conglomerate (well-rounded granite pebbles coming from the Palaeogene Central-Pirin pluton) and sandstone. They are separated by a thin reddish layer that may represent a lateritic palaeosoil.

The whole Neogene section described was tilted against the West-Pirin fault zone, and dips east at an angle of 5 - 20º. The post-Neogene planation surfaces (pediments), beginning with the Eopleistocene one, truncate this structure, and are inclined west, towards the Strouma valley at an angle of 2 - 5º. Locally, Eopleistocene pebble gravels with the same dip cover the Eopleistocene pediment.

The marble breccia of the Ilindentsi Member (now at an altitude of about 500 m above sea level) is correlated with the destruction of the planation surface (oroplain I) situated now at an altitude of 1950

Photo 4.8 - Pontian coarse breccia (fragments from Precambrian marbles, Pirin horst).

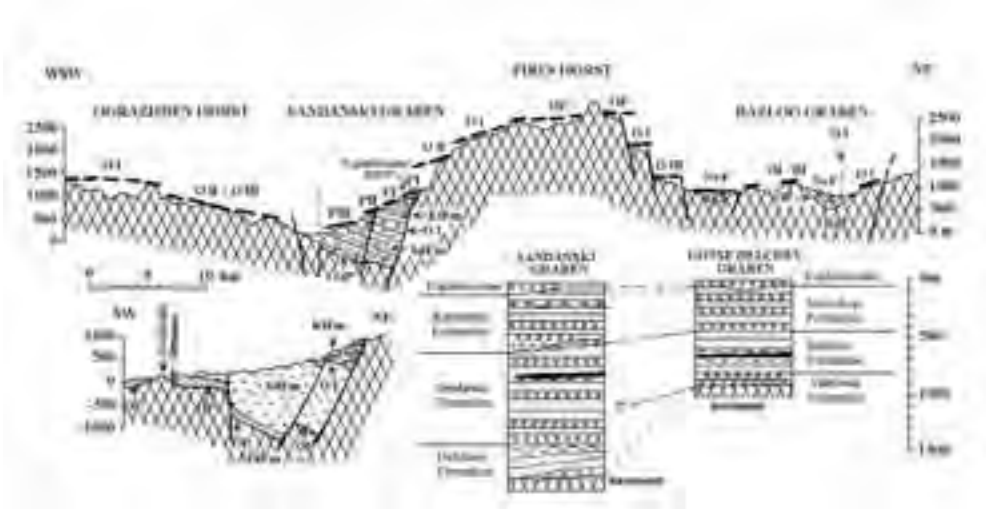

Figure 30 - Schematic neotectonic section through the Pirin horst and the adjacent grabens

- 2250 m in the Pirin horst (Figure 30). Therefore, two main epochs of relative uplift of the horst may be distinguished in Neogene times, the second one embracing most of the Pontian, and the Dacian and Romanian. Correspondingly, the vertical amplitudes along the West-Pirin fault zone may be calculated at 1500 - 2000 m for the Badenian to Maeotian, 1300 - 1500 m for the Pontian - Dacian (and Romanian), and 100 - 200 m, for the post-Pliocene times. Another important feature is the first mass occurrence of pebbles from the Palaeogene granitoids in the Kalimantsi Formation, that determined the time of exhumation of these granitoids not earlier than the Pontian.

Stop 4.9:

Pediment over Kalimantsi Fm: 863 m

Crossing the whole section of the Kalimantsi Formation, the itinerary arrives at this Pleistocene pediment, which is situated at an altitude of 850 – 1050 m, and truncates both the tilted section of the Neogene, and the border normal faults of the West-Pirin fault zone. The zone itself is covered by Pleistocene pebble gravels – the Pleistocene part of the Ilindentsi fan. Along the road on the way back, sandstones and conglomerates of the Kalimantsi Formation are visible. Some of the conglomerate layers are richer in marble fragments, whereas in others, abundant granite pebbles and boulders from the Palaeogene Central-Pirin pluton are related to the fast exhumation (unroofing) of the pluton in Pontian and Pliocene times.

Stop 4.10:

Above Ilindentsi: 411 m

Marble breccia over interbedding sandstones and conglomerates, with marble and granite pebbles. The panorama exhibits at least two thick layers of marble breccia of the Ilindentsi Member, partially displaced by faults of the Strouma fault belt (the most important faults of the belt are sealed by the Neogene section!). Many of the big cliffs are in fact due to landslides.

Stop 4.11:

Ilindentsi: 396 m

At this stop, the lowermost parts of the lower breccia layer of the Ilindentsi Member cover the sandstones of the Sandanski Formation. The panorama of the Ograzhden horst, west of the Sandanski graben, exhibits polyfacial and polychronous planation surfaces of Neogene age, the older truncated by the younger, and gradually lowering towards the small-amplitude Ograzhden fault. The latter is marked by a facetted slope.

Stop 4.12:

On the main road after the Ploski junction and before the railway bridge:134 m

The road cutting exhibits the Delchevo Formation (Badenian-Sarmatian), which is covered by the basal parts of the Sandanski Formation (Maeotian). The Delchevo Formation consists of reddish and greenish siltstones and sandstones, often with graded bedding and small calcareous concretions. In this

outcrop, a fine cyclicity can be observed, consisting of an occurrence of wash-outs over the finest sediments, covered with sharp depositional contacts by well-sorted whitish small-pebble conglomerate or coarse sandstone, and continuing into greenish and reddish siltstone. This cyclicity is typical of the transition towards the Sandanski Formation.

Stop 4.13:

Melnik: Neogene sediments of the Sandanski graben

The "Melnishki piramidi" (Melnik Pyramids) are erosion forms that are included in the list of natural sites protected by the Bulgarian state. They developed within the loosely cemented rocks of the Kalimantsi Formation (Pontian - Romanian). The whole section is gently dipping (5 - 20º) ENE, towards the West-Pirin fault zone.

The Sandanski Formation consists mainly of whitish or yellowish sandstones, interbedded with some clays and coal clays (also a thin coal seam at the village of Hotovo), and fine-pebble conglomerate. It is covered by similar (whitish to yellowish) conglomerates, with sandstone interbeds, that belong to the Kalimantsi Formation. The principal diagnostic feature of the Kalimantsi conglomerates, is the abundance of well-rounded pebbles coming from the Palaeogene granitoids that were unroofed in Pontian time. Graded bedding and cross bedding are often observed.

The rocks of the Sandanski Formation are well exposed at the crossroad to Vinogradi, 2 km West of Melnik. Typical sandstones, interbedded with clay and coal clay crop out, and the gentle dip towards east is clearly visible.

Stop 4.14:

Rozhen Monastery: erosion forms in the Kalimantsi Formation

The Rozhen Monastery was built in the beginning of the 13th century. Ruined several times during the Turkish occupation, it is now one of the most beautiful Bulgarian monasteries. Pyramids, capped pillars, and other picturesque erosion forms are typical for the badlands between the monastery and Melnik. They are observed at their best from a point situated at about a 15-minute walk above the monastery.

Photo 4.14 - Neotectonic fault in Maeotian (Sandanski Formation)

DAY 5

Melnik - Popovi livadi - checkpoint Koulata/ Promahon

I. Zagorchev.

From Melnik the itinerary crosses the Neogene of the Sandanski graben, and enters, in the Pirin horst, the Precambrian metamorphics of the Rhodopian Supergroup. At the highest point of the pass (Popovi Livadi), the itinerary enters the Palaeogene Teshovo pluton. A full section of the Rhodopian Supergroup (Figure 31) is exposed, and is briefly described hereafter, although the concentrated programme makes thorough observations impossible. This

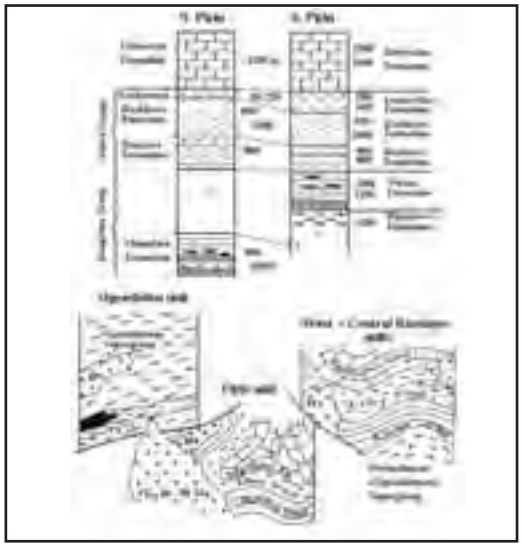

Figure 31 - Schematic columnar sections and interrelations between the Ograzhden, Pirin, and Rhodope units

section is in an inverted position (upside down), and from the Popovi livadi pass, the itinerary follows the succession downwards (although upwards in the geometric section).

Stop 5.1:

Contact of the Teshovo pluton with the Dobrostan Marble Formation: altitude 990 m

The Dobrostan Marble Formation consists of gray or white, massive, or banded calcite marbles, locally interlayered with gray fine-grained dolomite marbles, hornblende schists, biotite schists, and quartzo-feldspathic gneisses. In the schists and impure marbles, a prominent mineral lineation parallel to synmetamorphic fold hinges is observed. In the road cutting, in very rare cases, the observations reveal that there are two generations of synmetamorphic mineral lineations and fold hinges. The earlier lineation and fold hinges are deformed (folded) and/or obliterated by the second fold generation. The second generation lineation and hinges are usually situated at a very small angle (5 - 10º) to the first generation, and very rarely, at high (50 - 80º) angles.

The Palaeogene Teshovo granitoid pluton is built up of biotite or hornblende-biotite equigranular (locally with porphyric feldspar) fine- to medium-grained granites to granodiorites. The road cutting displays (Figure 32) complex interrelations between the pluton and the marbles. The intrusive contacts often follow normal faults, and locally suggest a subsidence of the pluton host rocks into the magma chamber. Subparallel apophyses intrude the marbles along the foliation

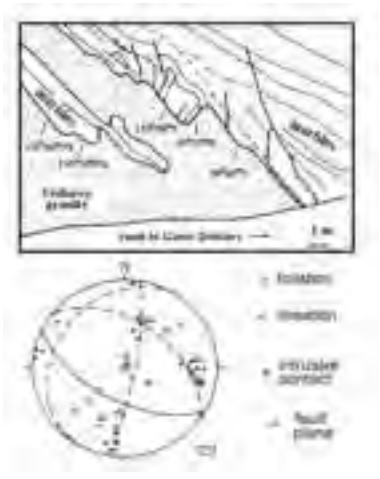

Figure 32 - Contact of the Teshovo pluton with the Dobrostan marbles (after Zagorchev, 1995)

Photo 5.1 - Extensional intrusive contact of the Palaeogene Teshovo granite (s. Figure 32)

planes. The overall impression is that of extension conditions during the pluton intrusion.

Stop 5.2:

Near the Popovi Livadi pass: 1399 m
Granites of the Teshovo pluton

Stop 5.3:

Boundary between the Dobrostan Marble Formation and the Loukovitsa Formation 1272 m

The contact between the two formations is marked by the disappearance of the gneiss and amphibolite layers. The foliation strikes 170º and dips steeply (70º) west, and has a polydeformational character (composite foliation). The Loukovitsa Formation consists of biotite gneisses and schists, amphibolites, calcareous schists, and marbles. Tight folds with axial planes striking about 175º and dipping 70ºW or E are abundant.

Stop 5.4:

Parking lot at the monument to Yane Sandanski: 1190 m

Banded gneisses with porphyroblastic feldspars of the Boykovo Formation, and quartzo-feldspathic gneisses (also with occasional feldspar porphyroblasts) of the Bachkovo Formation (both of the Sitovo Group, Rhodopian Supergroup) are exposed by the road cutting. They are characterised by a strong S/L structure, with prominent foliation and lineation. The sense of shear corresponds to top-to-southwest.

Stop 5.5:

Vucha Formation: 1079 m

The Vucha Formation consists of biotite gneisses (mostly garnet- and graphite-bearing), amphibolites (both ortho- and para-), schists, calcareous schists, and marbles. They are all present in the outcrops in the road cuttings. The foliation strikes 130-140º and dips at 35º to SW; a lineation plunges 10º to NW (320º). Tight folds are visible in the marble layers. The rocks are intersected by pegmatite dykes. Mylonitization along foliation surfaces and related diaphthoresis are due to late deformations.

Stop 5.6:

Granitoids of the Spanchevo pluton: 712 m

The Spanchevo granite pluton is intruded into the rocks of the Bogoutevo and Vucha Formation from the core of the Petrovo anticline. The southern part of the anticline has now an eastern to SE vergency. The whole structure, the Spanchevo granites and their planar structures included, has been deformed with the formation of the Belyovo conical fold (Figure 33).

The Spanchevo granitoid pluton is built up of biotite and two-mica coarse-grained or porphyric granites to granodiorites. The heterogeneous internal structure is demonstrated by the frequent occurrence of schlieren and melanocratic enclaves. In the road cutting, the granites exhibit also a clear superimposed schistosity (strike 160º/35ºSW; lineation 200º/22º), that intersects also the numerous pegmatite and aplite dykes within the granitoids. The pegmatites and aplites are often folded. The superimposed schistosity intersects the dykes, and is roughly parallel to the axial planes. Late normal faults strike 115-120º/60-65ºNNE.

The pre-Palaeogene structure of the Pirin unit has a complex and polydeformational character. The following sequence of events has been described (Zagorchev, 1994): (1) Neoproterozoic(?) deposition of a thick (8 – 10 km) sequence of flyschoid island-arc deposits with basic volcanism (Chepelare, Bogoutevo, and Vucha Formation), a mostly psammitic sequence (Boykovo and Bachkovo Formation), another varied sequence of psammites, pelites, marls, and limestones (Loukovitsa Formation) and thick limestones and dolomites (Dobrostan Formation); (2) intense folding in Cadomian(?) times, with the formation of two synmetamorphic fold generations; the first generation F_1 consists of isoclinal folds, and the second one (F_2), of tight to isoclinal folds; a single planar structure is observed, and it is a foliation of a probable multiphase development (composite foliation). The hinges of the isoclinal F_1 folds and the mineral lineation L_1 trend nearly N-S, and plunge at 5 – 20º South. Mostly in the marbles of the Dobrostan Formation of the Orelek syncline, the foliation and the F_1 hinges are deformed by F_2 folds. The principal folds (Petrovo anticline and Orelek syncline) were formed during the second phase. (3) Intrusion of the Spanchevo granitoid pluton (Hercynian?) approximately in the core of the Petrovo anticline; (4) Compression and formation of a superimposed schistosity in the Spanchevo granitoids, roughly parallel to the older composite foliation – this event probably coincided with the Mid-Cretaceous thrusting (Strymon thrust) of the Ograzhden over the Pirin unit; (5) Deformation of the older structures (composite foliation included) into the Belyovo conical fold; (6) Intrusion of the Upper Cretaceous Dautov and Bezbog plutons during an extensional event coinciding with the extension within the Srednogorie zone North of the Morava-Rhodope superunit; (7) Extension and deposition of thick Palaeocene? – Middle Eocene? terrigenous sediments in the southern parts and around the Pirin unit; (8) Folding; (9) New Palaeogene extension, deposition of thick volcanic and sedimentary deposits in depressions around

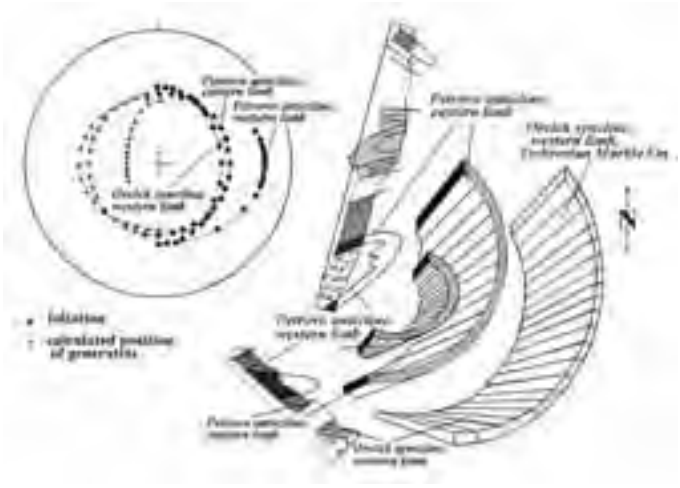

Figure 33 - Bloc-diagram for the structure of the Belyovo conical fold. After Zagorchev (1981, 1995)

Volume n° 2 - from B16 to B33

the unit, and Upper Eocene – Lower Oligocene intrusion of granitoids in the Pirin unit; (10) Late Oligocene deposition of coal-bearing sediments (Egerian fluviolacustrine system Pernik – Bobovdol – Brezhani); (11) Thrusting of the Pirin horst over the Brezhani graben, related to the transpression along the Strouma fault belt; (12) Extension (after Lower - to Upper Miocene planation) and rifting with the formation of the neotectonic horsts and grabens, and of the new Strouma/Strymon fluviolacustrine system.

Stop 5.7:

Gorno Spanchevo neotectonic fault: 599 m

East of the village of Gorno-Spanchevo, the West-Pirin fault zone is represented by a low-angle (25 - 30º) normal fault (Figure 34), that displaces the folded and mylonitized gneisses and amphibolites (with pegmatite veins) of the Vucha Formation (footwall) from the conglomerate of the Kalimantsi Formation (hanging wall). The displacement occurred in latest Pliocene or Eopleistocene time, since the Kalimantsi Formation belongs to the time interval from Pontian (or latest Maeotian) to Romanian.

The folded rocks of the Vucha Formation exhibit several fold generations (recumbent folds included), and a last compressive event with mylonites and east-vergent movement. This structure is intersected and displaced by numerous minor normal faults dipping South-West at angles from 25 - 30º (parallel to the master fault) to 60 - 70º. The master (Gorno-Spanchevo) fault is a normal fault with a very narrow gauge along the fault surface.

The Kalimantsi Formation is represented by the typical conglomerate, built up predominantly of granite pebbles coming from the Palaeogene Central-Pirin and Teshovo plutons.

Towards the south and southeast, a large Eopleistocene pediment (mountain step), gently-dipping towards the west, is beautifully exposed. It truncates the metamorphic rocks of the Pirin horst, the tilted conglomerate beds of the Kalimantsi Formation, and the bounding Gorno-Spanchovo low-angle fault, and is partly covered by proluvial and alluvial Eopleistocene sediments.

Stop 5.8:

Roupite – Kozhoukh: 103 m

Neogene volcanics of Kozhoukh, and the Neogene Delchevo Formation; Roupite church

The hills of Kozhouh and the Roupite locality are famous as being the site of the home and church of the sybil Vanga, who died a few years ago, and was the most popular prophetess and woman saint in the area. Something magnetic exists in that place: the pathetic hills in the flat and wide valley near the confluence of the Stroumeshnitsa River into the Strouma River; the steep northern slope of Belasitsa to the south; the ghosts of Samouil and his warriors defeated by the Byzantines in 1014, and the ghosts of thousands of dead men of different tribes that lived in the ancient and now destroyed town of Petra, and worshipped the forgotten gods of the Thracians in the nearby sanctuary. The migratory birds fly along the *Via Aristotelis* twice each year, and find a temporary refuge at that place, too.

The hills are built up of volcanic rocks of alkaline trachydacitic composition. They form an oval body about 1800 m long, and 350 - 500 m wide, with a height of 200 m above the plain. The volcanics are strongly hydrothermally altered, and the host rocks of the Ograzhdenian Supergroup and the nearby Neogene (Delchevo and Sandanski Formation) bear also traces of the hydrothermal activity. The hydrothermally-

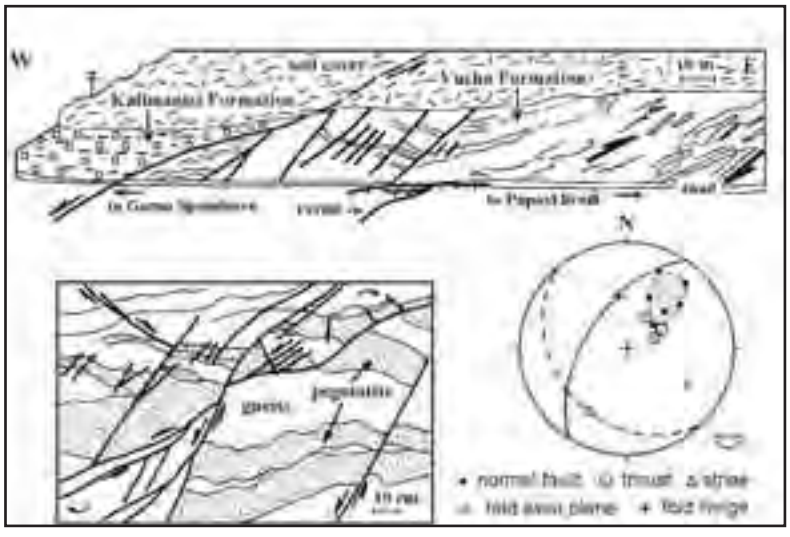

Figure 34 - Road cutting near Gorno Spanchevo. After Zagorchev (1995, Figure 25)

altered rocks contain opal, and are limonitized and kaolinized. The palaeohydrothermal activity is marked also by the irregular masses of hydrothermal carbonates (calcite and aragonite) that have been prospected as ornamental stone, due to their beautiful layered structure. They are situated at the northern side of the body, and dip steeply south. The thickness of these masses reaches up to 150 m.

The thermal mineral waters possess a sodium hydrocarbonate character, and a temperature reaching up to 67÷ °C at the surface. Several other natural springs are known at the nearby villages of Levounovo (temperature from 44 to 82÷ °C), and Marikostinovo (with more than 50 springs with temperatures between 42 and 61.5÷ °C). The springs have been prospected with boreholes, and are only partially used for cures and greenhouses.

Kozhouh has a probable latest Miocene or Early Pliocene age. As far as no other volcanics of this age have been recorded in Southwest Bulgaria, it has an exceptional position at the crossing of the Strouma and Stroumeshnitsa fault zones. Similar volcanics of Neogene and Quaternary age, and even more alkaline composition, are known at the southern side of the Belasitsa (Kerkini) Mountain, on Greek and Macedonian territories. The age problem is still under discussion, as far as no direct contacts with Neogene rocks are observed, and the "tuffites", known from the Neogene sedimentary succession, are determined by other scientists as hydrothermally-altered sediments (due to the mineral waters), or else their source is being sought in volcanoes outside Bulgarian territory.

At the checkpoint Koulata/Promahon the itinerary leaves Bulgarian territory and enters Greece.

Itinerary in Northern Greece (Macedonia and Epirus)

I. Mariolakos, I. Fountoulis

DAY 5

Checkpoint Koulata/Promahon - Verria

Strymon Basin

The Basin of Strymon lies between the Bulgarian/ Greek border to the NNW, and the Strymon Gulf, to the SSE. The basin covers an area of 2700 km^2 of eastern Macedonia.

The onset of the Strymon basin was in Middle Miocene times. The basin is a typical postorogenic graben, trending NW-SE (Lalechos, 1986), which is still active. The basin has been formed between the Serbo-Macedonian massif to the SW, and the Rhodope massif to the NE. Based on drilling data (Figure 12), the total thickness of the post-Alpine sediments (Table 3) is estimated at about 3500 meters. The discrimination of facies is based on palynological analyses of the cores. Miocene sediments originated from N-NW, through delta type deposition. Later on, lacustrine sedimentation takes effect, periodically interrupted by sea ingressions or continental depositions.

The travertine – lignite zones show the deposition of sediments in coastal areas near the carbon-rich basement, under favorable climatic conditions.

Table 3. Stratigraphy of the Strymon basin.

Pleistocene formations:	**Clays, coarse grain sands, quartz gravels, sandstones, siltstones**
Pliocene formations:	**Alternations of clastic clays**
Continental facies:	Alternations of red clays, red sandstones, and dolomite sands. Intercalation of siltstones, sandstones, and micro-conglomerates. Travertine limestone with lignites and chalk limestone
Brackish facies:	Sandstones, siltstones, travertines and lignite layers
Miocene formations:	**Alternations of lacustrine and marine facies of sediments from bottom to top**
Marine facies:	Alternations of clastic clays, siltstone, sandstone, with intercalation of microbreccia and lignite layers
Lacustrine facies:	Alternations of sandstones, siltstone, dark brown marl, which eventually change to petroliferous limestone
	Breccia with gravels from fine grain sandstone or hard conglomerates

Many faults cross the basin sediments. Faults parallel to the initial marginal fault zones of the basin, and younger than the Alpine deformation, have created a gradual antithetic tectonic graben within the basin sediments, at the center of the basin. Within this graben, low angle normal faults are observed, creating strata bending and anticline structures. This case is similar to the marine area of the Thrace Sea, but is limited to a smaller scale.

The geothermal gradient for the Strymon basin has been estimated to fluctuate from 25 to 36°C/km, to depths of over 2000 m. These values are above the normal geothermal gradient.

In the Strymon basin, several geothermal

Volume n° 2 - from B16 to B33

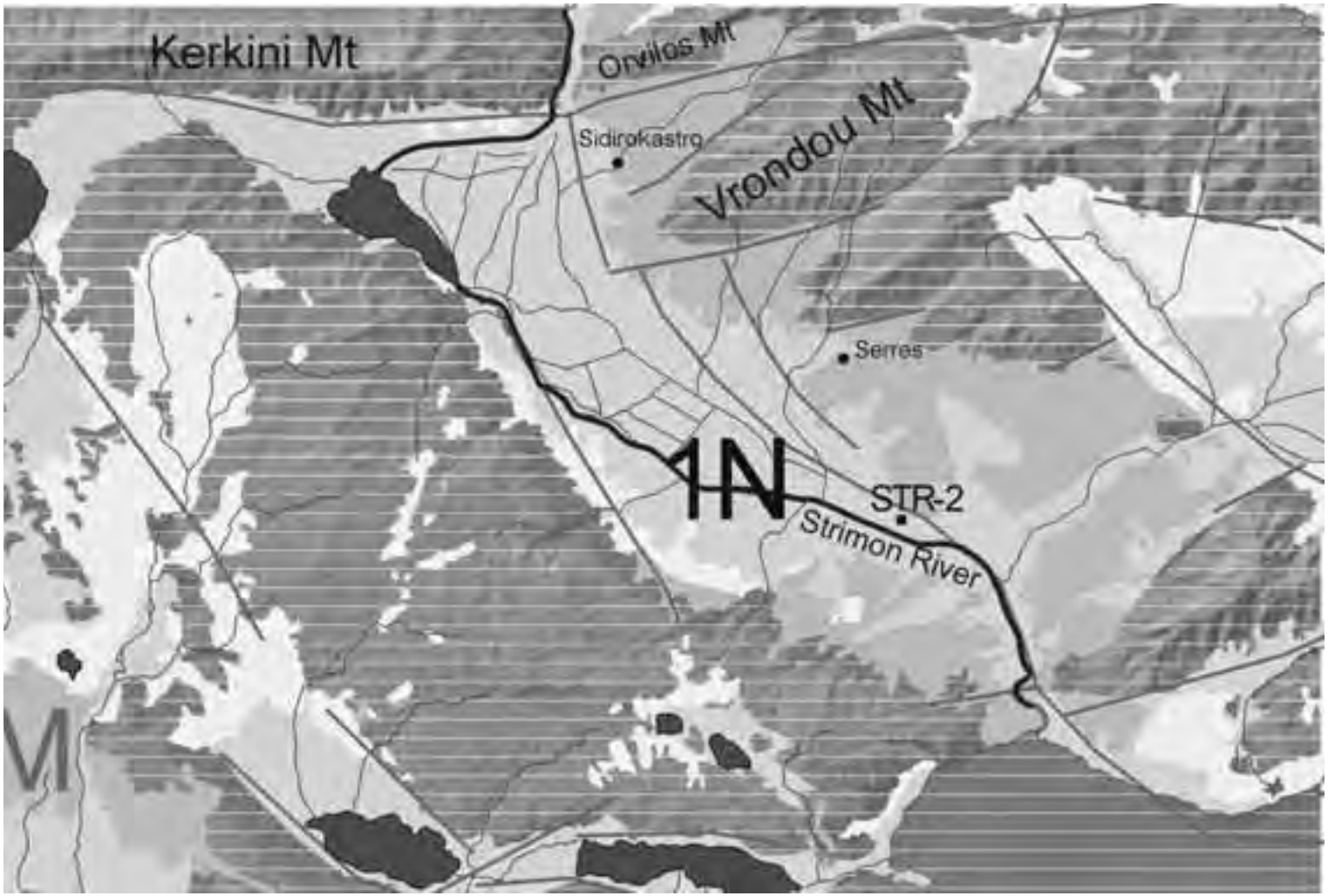

Figure 35 - Map of the Strymon basin: Neogene sediments (dark gray), Quaternary (light gray) and major faults

Figure 36 - Stratigraphic column of the well STR-2 (after Lalechos, 1986).

manifestations occur (at the thermal springs of Therma Nigrita, Loutra Sidirokastro, Loutra Angistro), and geothermal fields (the known fields of Therma-Nigrita, Sidirokastro, Irakleia-Lithotopos, etc.).
At the eastern margin of the basin, two minor basins, trending E-W (Sidirokastro basin and Serres basin), are located (Figure 37).

Stop 5.9:

Strymon Straits

It is the narrowest site between the Kerkini (to the west) and Orvilos (to the east) mountains, where the Strymon River passes through. The contact between the Kerkini gneisses and amphibolites (equivalent to the Ograzhdenian Supergroup, Serbo-Macedonian massif), and marbles and schists of the Pirin-Pangaion unit (Rhodope massif) is here a steep fault. Thick travertines are locally observed.

Stop 5.10:

Sidirokastro - Kirikos and Ioulitis Monastery

Sidirokastro Basin

The basin of Sidirokastro is a part of the greater Strymon basin, and lies between the mountains of Orvilos (to the north) and Vrondou (to the south), with an E-W trend, which means that it is transversal with respect to the Strymon basin that trends NNW-SSE (Figure 38).
The Quaternary deposits of the Sidirokastro basin consist of olisthothremata (huge blocks) and breccias, originating exclusively from marbles of the Pirin-Pangaion unit. The breccias are well cemented with carbonate cement, and overlay uncomformably the Pliocene deposits. They have a very impressive relief. The main outcrops

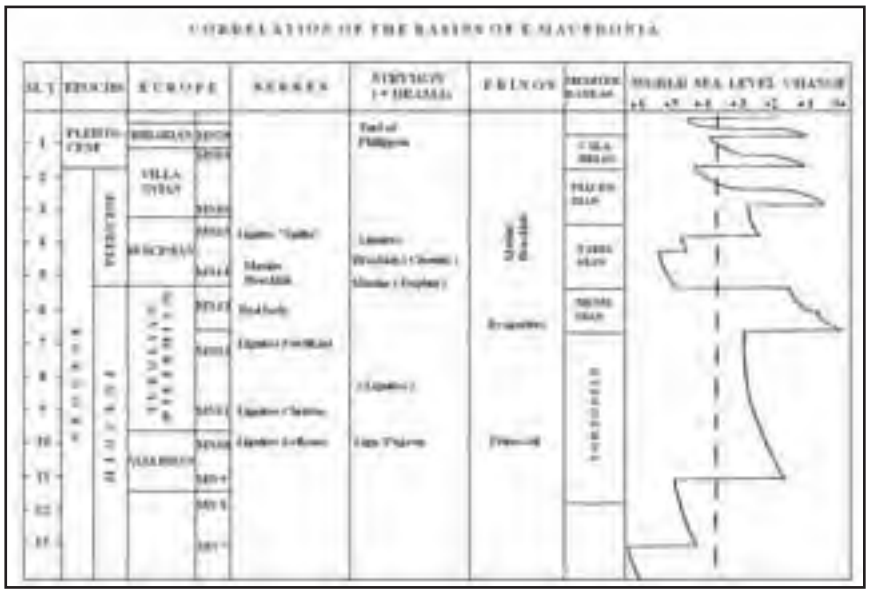

Figure 37 - Correlation of the Strymon, Drama, Serres and Prinos basins, and the global sea level changes (after Karistineos and Georgiades-Dikeoulia, 1986).

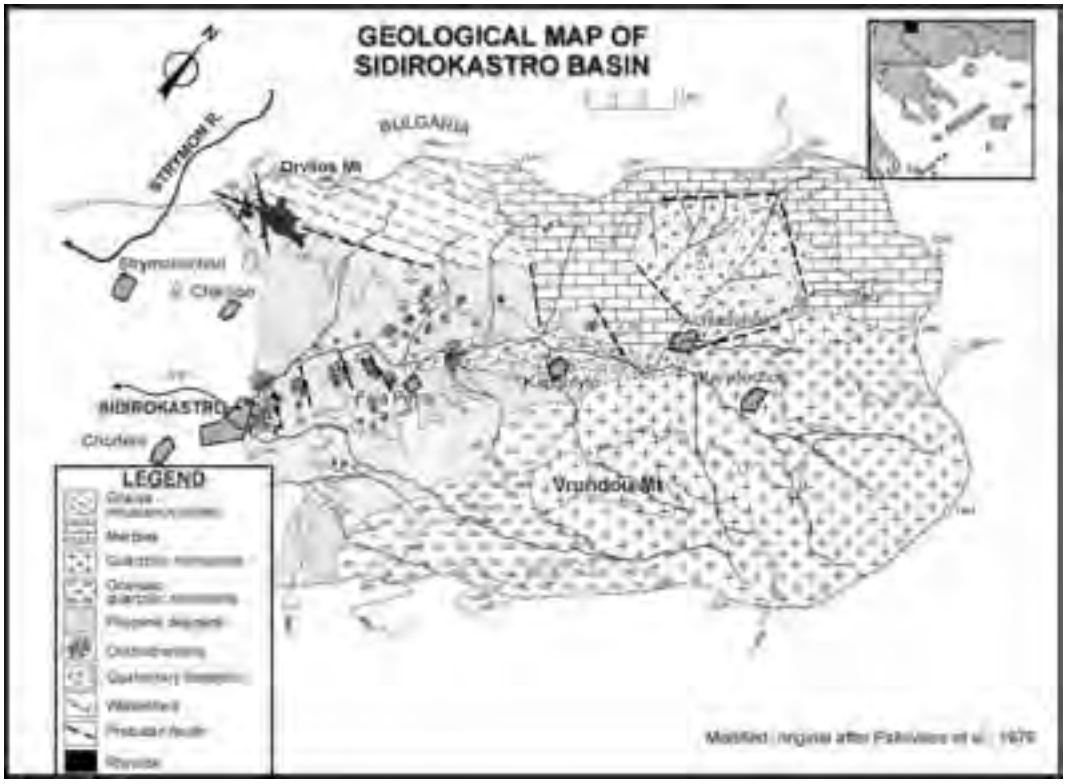

Figure 38 - Geological sketch map of the Sidirokastro basin (modified after Psilovikos et al., 1979; data for the volcanics after Maratos, 1966).

Photo 5.10 - The characteristic relief of Quaternary olisthothremata at Sidirokastro hill (View from SW)

are situated along the valley of the Achladitis River. Similar rocks occur in Bulgaria, but they have been dated as Neogene (Pontian – Romanian) (at the base of the Kalimantsi formation).

Some travertine deposits also occur in the western part of the basin, under the alluvial Strymon deposits, with a thickness that varies between a few and 40 meters (Maratos, 1966).

Volcanic rocks outcrop in the northern part of the basin (towards Mt. Orvilos), at the margin between the metamorphic formations and the post-Alpine Pliocene deposits. Rhyolites cross the Pliocene deposits, and appear on top of them (Maratos, 1966). Within these deposits, no rhyolithic pebbles occur. This fact, combined with the intense topography of the volcanic cone, the presence of hydrothermally-altered metamorphosed blocks of the Alpine basement, the volcanic bombs originating from the sedimentary formations, and the obvious thermal alteration of the surrounding deposits, points to the conclusion that the volcanic activity took place during Quaternary times (Maratos, 1966). The Neogene formations consist of conglomerates, with pebbles originating from the pre-Alpine basement (granites, gneisses), followed by lacustrine and fluvial deposits which consist of alternations of marls, sandstones, micro-conglomerates with lignite intercalations. Their thickness reaches 300 m. (Kavouridis and Karydakis, 1989).

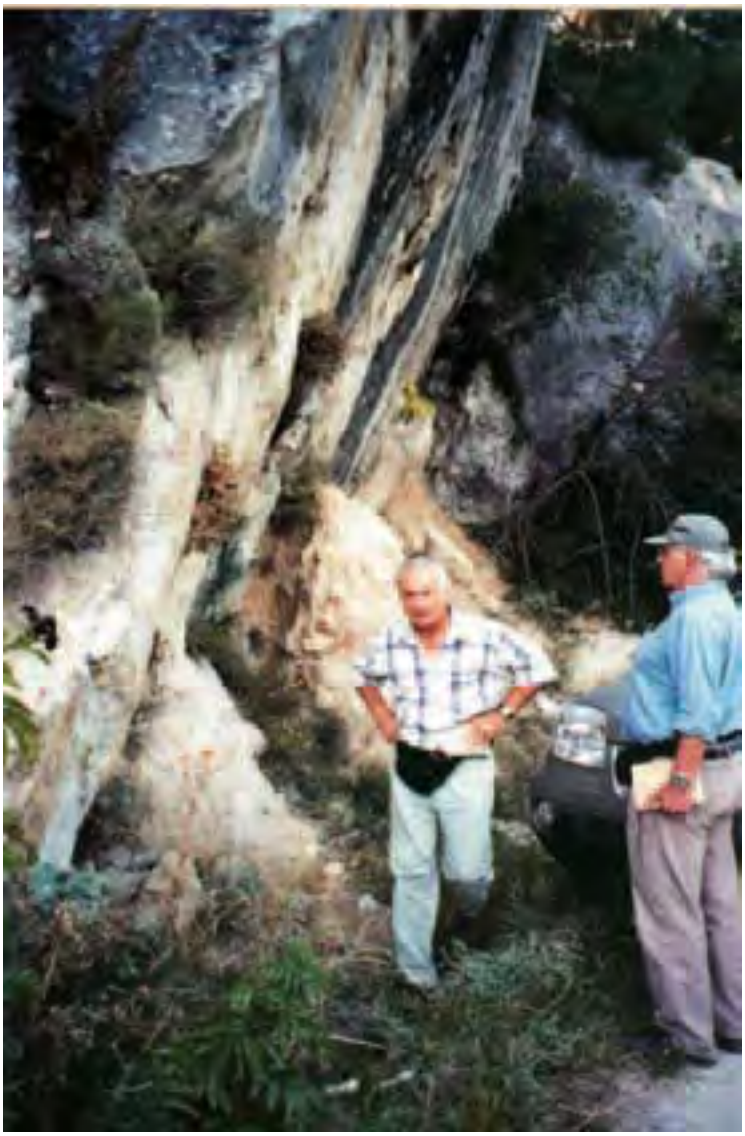

Photo 5.10a - Strike-slip fault crossing the Quaternary and Pliocene deposits. Location 100 m east from the entrance of the Kirikos and Ioulitis Monastery.

The paleogeographic evolution of this basin follows the general characteristics of the Strymon basin evolution during the Neogene, with the important difference that there is no marine influence (Sotiriadis, 1966). This means that the deposition of fluvial-lacustrine sediments in the lowermost parts of the basin must not have been interrupted from the Early - Middle Miocene to the end of Pliocene. The exact time of the end of the Neogene deposition is not known, but it is very likely that at the Pliocene – Pleistocene boundary, a phase of intense tectonic movements was activated.

The Kirikos and Ioulitis Monastery

In this area, coarse breccias occur, with fragments and olisthothremata (hill-size blocks) originating exclusively from marble. These breccias overlay unconformably a packet of generally fine-grained sediments (marl, sandstone, and occasional intercalations of conglomerate, whose pebbles originate exclusively from the Vrondou granite). The age and facies of the underlying formations is not known. However, in the eastern-northeastern adjacent areas, the olisthothremata and breccias are reported to be of Quaternary age.

A strike–slip fault occurs in both the underlying formation, as well as in the marble olisthothremata.The fault strikes N246º, dip 75º, with striation 20º to342º). More striations (284º/60º, 174º/30 º) of this fault surface were also observed in different outcrops, and so their relative dating is not possible. Near the entrance of the Monastery, another fault (50º/60º), also with striations (92º/60º, 110º/35º), can be observed. As in the previous locations, marl and sandstone, with polymictic conglomerates (pebbles exclusively from the Vrondou granitoids), underlie the monomictic breccias.

Stop 5.11:

Village of Vyronia: Kerkini boundary fault

Aggistro western margin

A major fault zone separates Kerkini Mt. and the reddish-brown clay and conglomerate of the plains.

The marginal fault zone of Kerkini, trending E-W, outcrops at the Aetovouni (abandoned village) location (past Nea Petritsi village, the entrance of Vyronia village). At the local amphibolite abandoned quarry, ankerites outcrop along the fault zone (amphibolite schistosity dipping 40º to 132º, ankerite dip 45º to150º, fault surface dipping 70º to150º).

Impressive talus cones of varying size occur along the front of the Kerkini fault zone. The larger of these cones occur at the foothill of the highest areas of the Kerkini Mountain.

Pliocene deposits dip towards the NW in the area between Sidirokastro and the Kerkini marginal fault zone. The watershed between the Kerkini and Doirani lake basins develops over lacustrine sandy deposits, while no fans occur in the western part of the basin margin. At this location, the Quaternary asymmetry of the Strymon River is very obvious.

Kerkini lake through time

After many geological and climatic changes, at the end of the last European glacial episode, that marked

Photo 5.11 - Panoramic view of the E-W striking Kerkini fault zone. View from SW.

the beginning of Holocene times about 20,000 years ago, a vast lake, fed by the melting glaciers that had covered the higher elevations of the Rhodope Mountains, occupied the lower parts of the Serres/ Strymon basin. During Classical and Hellenistic times, the huge interglacial lake had been reduced to two smaller, separate ones. Historians of that era first mention the name Kerkini, calling the large lake to the south "Kerkinitis" (although this name was known in mythology, Bartzoudis, 1993), and the much smaller one in the northwestern corner of the basin, "Prassias". Several Thracian tribes inhabited the wild lands of the Serres/Strymon basin, until they were subjugated or displaced by the expanding Macedonians in the 5th century BC. Among them, the Visalds lived in the valleys of Mount Dysoron, the Edones to the east of Strymon, and several clans of the Peones in the interior, around Siris (latterday Serres), Lake Prassias and the upper Strymon basin (Petrou, 1995). Since then, many historians and writers have made references to this area and to its rich flora and fauna. The lakes and marshes of Strymon were fabled for their wildfowl. A coin of the Visaltes, depicting a crane, has been found, and the wild goose was a common emblem of Edonian coinage. Fish was so plentiful that the locals "...gave them for fodder to their horses and beasts of burden". Herodotus mentions two kinds of fish in Lake Prassias "paprakes" and "tilones", both so abundant that "... if a man lets an empty basket down by a line into the lake, it is no long time before he draws it up full of fish...".

For long periods of time, the people lived in harmony with the wetlands. The lake and the river provided fish and wildfowl, various raw materials, and water for crop irrigation. Human intervention was always small-scale, and the lack of technical knowledge meant that their influence on the landscape and habitats was negligible. Continuing active deposition by the Strymon River further reduced the size of the lakes, creating large expanses of marshes and occasionally flooded areas. The northern lake was quite small, occasionally drying out completely. During the years of Ottoman occupation, it became known as "Lake Butkovo" and was later renamed "Kerkini"; the southern lake was named "Achinos".

By the turn of the 20th century, a complex unstable system of small lakes and extensive freshwater marshes covered most of the lower parts of the Serres basin. The River Strymon entered the basin from the north, through the narrow ravine of Klidi (Ruppel). Upon exiting the defile, it formed a large alluvial fan, covering an area of 180 km^2. There it spread out, with several channels meandering towards the southeast, supplying water to lake Kerkini. Downstream from Kerkini, the river turned to the east, forming a permanent bed, until finally, it emptied into the shallow lake of Achinos.

Both lakes, but mainly the larger Achinos, trapped the floodwaters and almost all of the suspended materials carried by the river. This explains the inability of the Strymon to form a delta at its mouth in the bay of Orphanos, in marked contrast to all the other rivers in eastern Greece.

The river served as a virile, undisciplined, sometimes violent, artery of life to the ecosystem, causing constant habitat modification in accordance to changes in its water level. During flood periods, the lakes increased in size, and the marshes often extended to the foot of the hills. Surrounding meadows and forests were flooded, and the water found or cut new channels, and aquatic vegetation spread and grew in profusion. During periods of drought, the lakes diminished in size, water flow was restricted to a few beds and the marshes dried out, leaving behind fertile soils.

The boundary between the Circum-Rhodope belt (situated SW of the Serbo-Macedonian and the Rhodope massif) and the Axios zone, is situated in the eastern parts of Thessaloniki, and will not be visited due to limited time and poor exposure. The Alpine Axios (Vardar) zone grossly coincides with a Neogene – Quaternary fault belt and the Thermaikos gulf.

Stop 5.12:

Kalohori: the problem of Kalohori subsidence

Kalohori is a town within the industrial area west of Thessaloniki. It is situated in the delta of Gallikos River, close to the sea. In ancient times the area was part of the sea, but the rivers accumulated enormous quantities of soil, so that they formed this part of land. According to the ex-mayor of Kalohori, "after the second world war, the local Thessaloniki authorities started to pump out water from the area for the needs of the population of the city". This pumping was more intensive year after year, because the population and the need for water were constantly increasing. The first signs of subsidence appeared in 1955, and the municipal authorities protested and tried to slow down the water pumping. The Water Company of Thessaloniki, which was under the authority of the Ministry of Macedonia-Thrace, continued the drillings in the area, resulting in further subsidence.

Photo 5.12 - The subsidence is well obvious from the fact that the old road lies beneath the water surface, as it can be seen along the telephone line poles. This happened due to the intensive water groundwater pumping, soil subsidence has occurred and embankments were constructed to prevent seawater intrusion. 8 years ago, one of the dams broke and the sea flooded a large part of the area.

The ground water level reached a depth of 40-45 meters from the 20 meters that it was at the beginning. Two textile factories in the area contributed to this evolution, each of them pumping 8,000 m^3 per day. As a result of this subsidence, there were several floods from the sea. In 1969 the sea reached the center of the town. By that time the department responsible for these matters from the Ministry of Public Works built a small dam to protect the town. However water pumping was still going on, resulting in further subsidence, and a bigger dam was built in 1976-77. Due to the subsidence and this construction work, the lagoon of Kalohori was formed. The subsidence went on, despite the protests of the people, their appeals to the Court, and the political interventions of local representatives. Finally, in 1995, the Water Company of Thessaloniki decided to quit its activity under the engagement of the local authorities, to allow for supplementary pumping only during July and September, and whenever it was necessary. The water company also took the responsibility to carry

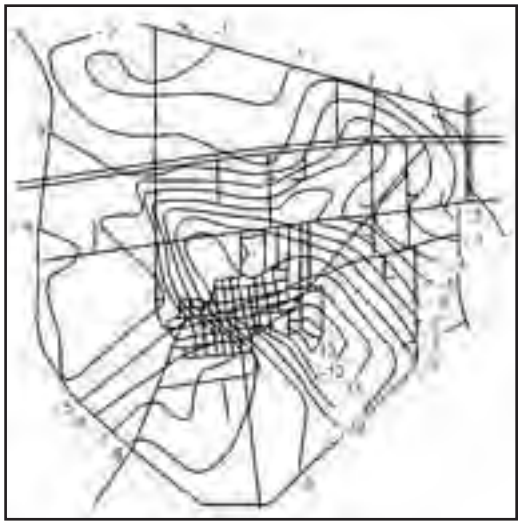

Figure 39 - The rate of subsidence in the Kalohori area, as measured by the Laboratory of Geodesy of Aristotle University of Thessaloniki for the period 1996-1998.

out research every year, to record the sinking which is still going on today at a rate of 3-4 cm every year.

Research on the ground settlements in the area of Kalohori west of Thessaloniki

Ground settlements have been observed for the last 35 years in Kalohori, a village and industrial area west of Thessaloniki. These settlements have been continuously monitored by the Laboratory of Geodesy (AUTH) since 1992, with the help of a leveling network. As it was found, the settlements have a 5 cm/year rate in the south-east part of the area (Figure 39), and can be attributed to the intense water pumping.

DAY 6

Verria – Kozani – Grevena

Verria is situated close to the western boundary of the Axios with the Pelagonian zone. Along the itinerary, ophiolites and Upper Cretaceous flysch sediments are exhibited in the road cuttings, as well as some low-grade metamorphic rocks (mostly of carbonate composition) of Triassic and Jurassic age, that belong to the Subpelagonian mantle. These rocks continue west of Kozani, where they are in tectonic contact with the Vourinos ophiolite. Towards Grevena, the itinerary enters the Palaeogene and Neogene sediments of the Meso-Hellenic trough.

Axios basin and Thermaikos Gulf

The Axios basin is extended onto the onshore to the Thessaloniki-Katerini plain, to FYROM in the North, and is connected to the Thermaikos Gulf in the South. It is bounded by the mountains of Pieria-Vermio in the west, and in the east by Chortiatis. East of Thessaloniki, it is covered with molassic Tertiary sediments. Older formations occur in the borders of the basin (Figure 40).

The Tertiary sediments are unconformably deposited over the metamorphic basement. In Early Eocene times, a basin was formed by faults, and filled in with sediments up to the present time (Figure 41). The basin has not been continuously active, but during

Figure 40 - Geological sketch map of the Axios basin (after Lalechos, 1986).

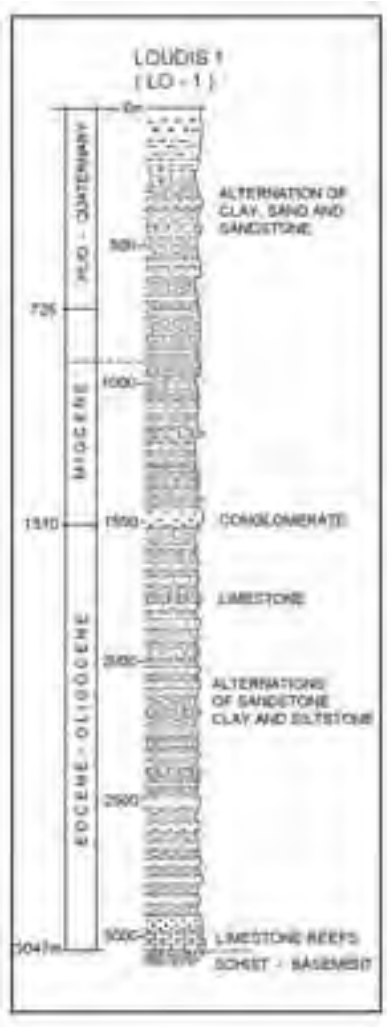

Figure 41 - Stratigraphic column of the well Loudias 1 in the Axios basin. Well location on Figure 40 (after Lalechos, 1986).

Middle Miocene and Oligocene times is indicated by the change from marine to lacustrine facies. The Miocene formations are lacustrine and brackish, and are transgressively situated over the older formations. The Pontian-Pliocene deposits cover unconformably lacustrine facies. It is emphasized that the thickness distribution of the sediments lacks symmetry along the E-W and N-S axes of the basin.

Table 4. Stratigraphy of the Axios basin

Plio-Quaternary	**Sandstone – marls, coarse sandstone, and gravels on the upper section.**
Miocene formations:	**Lacustrine and continental marls and sandstones of variable thickness**
M.–Upper Miocene	Sandstones, blue marls, yellow sand, red clay.
Lower Miocene:	Conglomerate and intercalation of siltstone, followed by thin layers of lignite (age: L. Miocene, palynology analysis).
Unconformity	
Eocene-Oligocene formations:	**Marine sediments, alternations of marine and continental facies**
U. Eocene – L. Oligocene:	Marls, sandstones, hard clays.
Upper Lutetian:	Marine and continental facies, marls and conglomerates (Cassandra area, thickness approx. 400 m.)
Middle Eocene:	Limestone reefs, horizon of lacustrine marls, horizon of marine facies, sandstone and conglomerates. Thickness: 50-100 m. (Vassilitsa, Kastro areas)

The modern structure of the basin is controlled by the combination of the previous tectonic deformation stages, the resulting continuous sedimentation or unconformities, or changes in the facies of the sediments. Middle – Upper Eocene marine sediments were deposited on the paleorelief of the subsiding basement. From the existing onshore and offshore wells, an increase of the thickness of the Miocene formation (422 m) can be observed, indicating that the basin in the southern part has subsided in depth. On the contrary, the thickness of the Eocene-Oligocene formations is smaller in the Thermaikos, and larger in the Thessaloniki basin. This indicates that the center of the sedimentary basin was on land, with then a rise of the south section, which then dropped during Miocene times, resulting in the considerable thickness of Miocene formations.

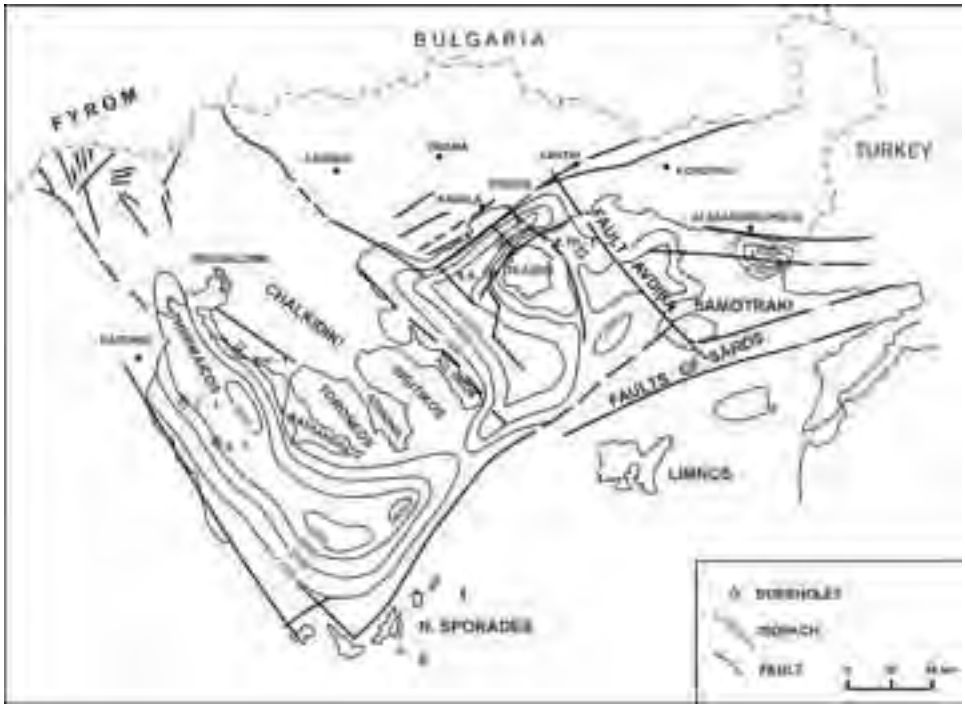

Figure 42 - Extension of the Axios and Strymon basins towards the Aegean Sea since Miocene times. Contours show Miocene isopachs (after Lalechos, 1986).

Stop 6.1:

Pella

Shoreline displacements often occur without the contribution of a seismic event. These cases are mainly present in large river deltas, being thus connected to the suspended material transported by rivers and deposited at their estuary. Nevertheless, even in these cases, shoreline displacements are connected to continuous tectonic uplift. There are many examples in Greece, such as the broader area of Pella. In Figure 43, the stages of evolution of the Thermaikos gulf and Salonica plain are shown. It is evident that, in this case too, an important role has been played by the large rivers such as Aliakmon, Loudias, Axios, and Gallikos, depositing their sediments in the northern and western parts of the Thermaikos Gulf. At the end of the 5th, and beginning of the 4th century B.C., Pella became the capital of the Macedonian kingdom. Excavations have revealed parts of the earlier city, including the cemetery and scanty architectural remains in the area of the modern drainage canal. The city was organized and expanded during the reign of Philip II and Cassander, and flourished in the middle of the 4th and during the 3rd and 2nd centuries B.C. It was captured by the Romans in 168/167 B.C., and was finally destroyed by an earthquake, possibly in the first decade of the 1st century B.C.

The first excavations (between 1957 and 1963-64) brought to light the houses with the mosaic floors and part of the Palace. A second campaign was undertaken in 1976, and is still in progress. So far it has revealed the Agora, part of the Palace, other houses, sanctuaries, and cemeteries. The most important monuments on the site are: (i) the private houses; (ii) house with mosaic floors of the Abduction

Photo 6.1 - Mosaic depicting a hunting scene from the archeological site of Pella.

Volume n° 2 - from B16 to B33

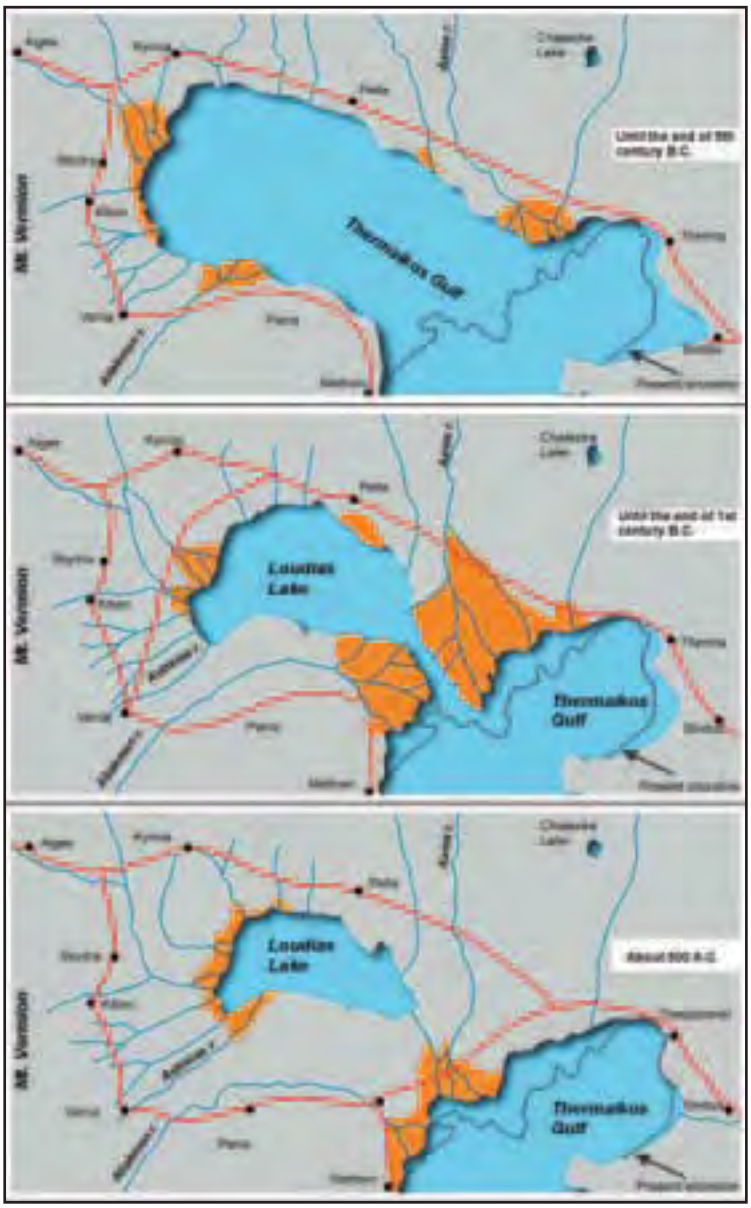

Figure 43 - Stages of evolution of the Thermaikos Gulf since 5th Century BC (modified after Struck, 1908, 1912).

of Helen, the Stag Hunt and Amazonomachy; (iii) the Palace; (iv) the Agora; and (v) the Sanctuaries, which consist of Thesmophorion, Sanctuary of Aphrodite, the Mother of the Gods, and Sanctuary of Darron, the curing god (identified by an inscription).

Stop 6.2:

Vergina

The ancient city situated on the northern slopes of the Pierian Mountains is securely identified as Aigai, the capital of the kingdom of Lower Macedonia. Archaeological evidence proves that the site was continuously inhabited from the Early Bronze Age (3rd millennium BC), while in the Early Iron Age (11th-8th centuries BC), it became an important center, rich and densely inhabited. The city reached its highest point of prosperity in the Archaic (7th-6th centuries BC), and Classical periods (5th-4th centuries), when it was the most important urban center of the area, the seat of the Macedonian kings, and the place where all the traditional sanctuaries were established. Moreover, it was already famous in antiquity for the wealth of its royal tombs, which were gathered in its extensive necropolis. The finds from the excavations are exhibited in the protective shelter over the royal tombs of Vergina, and in the Archaeological Museum of Thessaloniki.

The first excavations on the site were carried out in the 19th century by the French archaeologist L. Heuzey, and were resumed in the 1930s, after the liberation of Macedonia, by K. Rhomaios. After the Second World War, in the 1950s and 1960s, M. Andronicos, who investigated the cemetery of the tumuli, directed the excavations. At the same time, the Palace was excavated by the University of Thessaloniki, and a part of the necropolis, by the Archaeological Service

of the Ministry of Culture.
In 1977, M. Andronicos brought to light the royal tombs in the Great Tumulus of Vergina (Megale Toumba). The most remarkable of these was the tomb of Philip II (359-336 B.C.), and its discovery is considered to be one of the most important archaeological events of the century.
The most important monuments on the site are the following: (i) the royal tombs in the Great Tumulus; (ii) the royal tombs to the NW of the city; (iii) the cemetery of the tumuli; (iv) the Palace and the Theatre; (v) the temple of Eukleia; (vi) the acropolis and the city walls.
A major marginal fault zone, trending NNW-SSE, occurs along the southern bank of the Aliakmon River and exits at Mt. Vermion (bridge).

Figure 44 - Map of the Ptolemais - Servia - Florina Neogene-Quaternary basin showing the main faults. Equal-area projection of measured striated faults (after Mountrakis et al., 1998).

Stop 6.3:

Mavropigi (Ptolemais)

Ptolemais - Servia basin

The Kozani – Servia basin is part of the larger Florina – Vegoritis - Kozani Neogene basin, which extends northwards to FYROM in the Bitola plain, and presents a total length, from Servia to Bitola, of about 100 km. Its average width is about 15 km. It trends in a NW-SE direction, and is divided by ridges and hills trending NE-SW (Figure 44). The basin was filled in with sediments from the Late Miocene to the Quaternary. The Neogene sediments are exclusively of lacustrine origin and contain lignites. The Quaternary ones are usually fluviolacustrine and terrestrial. It is worth mentioning that there is no evidence of marine influence in the Neogene and Quaternary deposits of the basin.
The marginal fault zones trend NW-SE. Within the Plio-Quaternary deposits, a lot of NE-SW normal faults occur. Apart from these normal faults, there are some reverse faults striking NE-SW (Pavlides, 1985). To the south, the basin is bounded by the impressive Servia fault zone, which is an active one, as it affects Holocene deposits (Mountrakis et al., 1998). This kind of deformation is responsible for the Basin-and-Range type of morphology that has developed across these faults, and appears to be still active.

Mavrodendri - Pontokomi - Mavropigi fault zone

The Mavrodendri - Pontokomi - Mavropigi fault zone is the west marginal fault zone of the Ptolemais – Servia basin. It consists of almost parallel NW-SE striking faults, which are dipping 60°- 80° towards ENE (Figure 45). This fault zone bounds the Triassic-Jurassic carbonates of the Pelagonian unit with the Plio-Pleistocene deposits of the Ptolemais – Servia basin. The normal faults, occurring within the basement of the Pelagonian unit at Mt. Askion, present the same geometry (NW-SE) with the faults that constitute the fault zone.
The Mavrodendri - Pontokomi - Mavropigi fault zone is mostly covered by the young Pleistocene and Holocene deposits (scree), and only in some

Figure 45 - Lower hemisphere projection of the average fault surfaces occurring at Mavropigi village of the Mavrodendri - Pontokomi - Mavropigi fault zone.

Photo 6.3 - View from NE of the northern part of the Mavrodendri - Pontokomi - Mavropigi

locations, occasional fault surfaces (slickensides) can be observed. The faults can be distinguished into two sets, according to the striations observed on their surfaces. The first set (A), presents a pitch 50-80° south, whereas the pitch for the second set (B) is 50-80° north. The second one is observed on almost all fault surfaces (Mountrakis, 1996). Secondary antithetic faults exhibit analogous kinematics to the main ones. The length of the fault zone is estimated to be more than 12 km. Mountrakis et al. (1996), characterized this fault zone as inactive because they assumed that there is no compatibility with the current stress field trending NNW-SSE, which is recognizable in W. Macedonia.

It is worth to mention that during the May 13, 1995 earthquake, the Mavrodendri village suffered damages, although the epicentral area was located far from the village.

Stop 6.4:

Aliakmon terraces

Below the structural surface of the Plio-Quaternary deposits, which are located at a mean altitude of 624-630 m, the valleys that have been created due to the incision of the Aliakmon River and its tributaries, show usually four terraces (Brunn, 1956). A typical example is the area of Asprokampos (NE of Grevena). Terraces are found at 8, 35, 55, and 100 m above the present-day river bed, the high surface being at 150 m.

Neotectonic movements determine the drainage network of the Aliakmon River. From its source, it probably flowed northwards into Albania, but was barred by the uplift of the transverse Koritsa fault. To the south, it was barred from flowing south by the uplift of the Vounassa, Khassia Krastovon transverse accident, and was forced eastwards through the marginal Pelagonian range, where it has incised deep gorges (e.g. Zavorda gorge).

Stops 6.5 and 6.6:

Pramoritsas River

Marine Pliocene sediments

The stratigraphic structure of the Meso-Hellenic trough, presented by Brunn (1956), is the hitherto most complete analysis of the mollassic deposits. Brunn (1956) accepts that marine sediments filled the NW-SE trending Meso-Hellenic trough, from Upper Eocene (Krania Formation) till the Middle-Upper Miocene boundary (Ontria Formation). More specifically, for this particular location, Brunn suggests that: a) the youngest marine sediments date back to the Upper Miocene (Tortonian); b) the transition from the Miocene to the Pliocene consists of fluvial deposits, something observed only in Albania; c) north from Grevena town towards Neapoli, the Pliocene and Lower Pleistocene deposits are sandy and contain numerous mammal fossils of Villafranchian age; d) the Upper Quaternary deposits are lacustrine, containing; west of Servia village; numerous *Planorbis*, *Lymnaea,* etc.

Eltgen (1986) doubted the fluvio-lacustrine origin of the Pliocene deposits in the area south of Neapoli, proposing that they are marine, while sometimes there is evidence of brackish facies. His views were based on petrographic observations and paleontological findings; including benthic and planktonic foraminifera genera, but he did not determine any species. More specifically, he suggests that marine sedimentation in this part of the Meso-Hellenic trough continues throughout the Pliocene, without reference to specific species or locations.

Fountoulis et al. (2001), after a detailed lithostratigraphic study of the deposits on the banks of the Pramoritsa River (a tributary of Aliakmon River) north of the town of Grevena, and discovering numerous pelagic and benthic foraminifera and nannoplankton species determinations, have proven that marine sedimentation did not stop in the Late Miocene, but continued until at least the Early

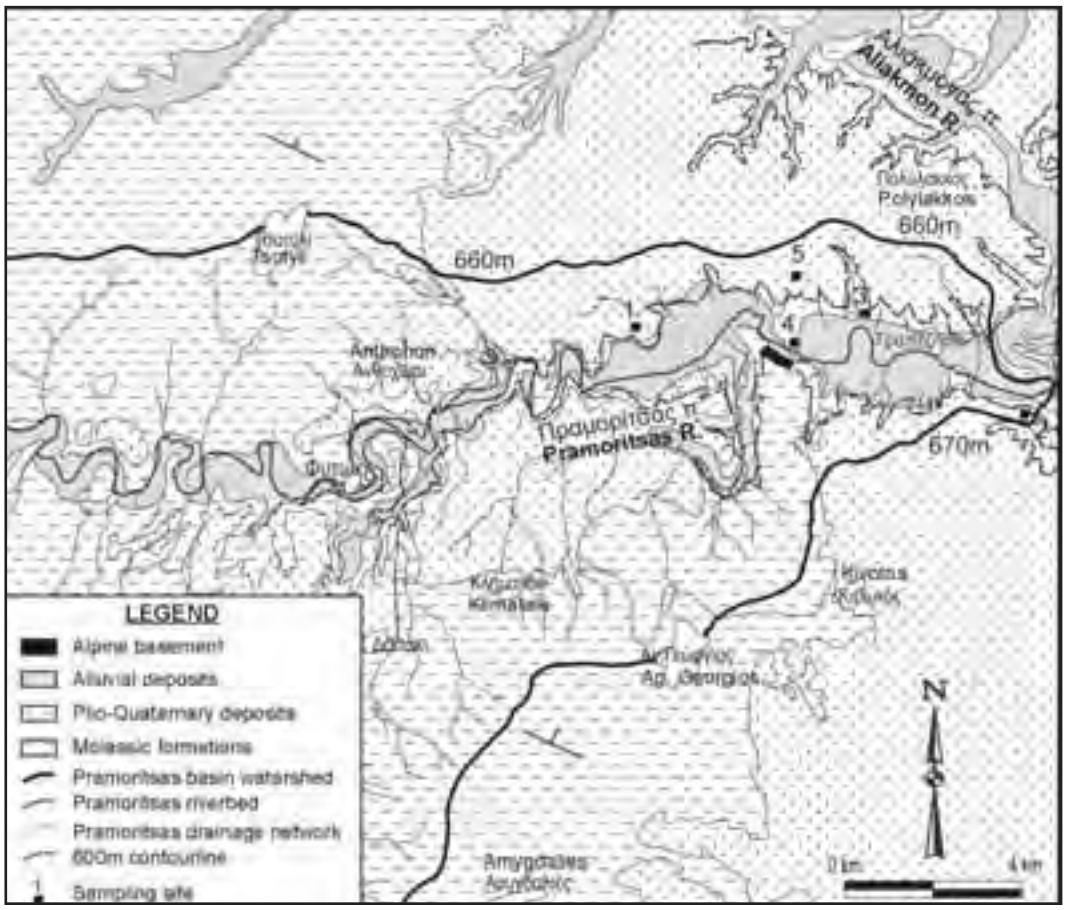

Figure 46 - Geological sketch map of the broader area of occurrence of Pliocene marine deposits in the Meso-Hellenic Trough (after Fountoulis et al., 2001).

Pliocene (Biozone NN13) times (Figures 46 and 47). The discovery and determination of these marine sediments of Pliocene age is very important, because it means that the sea north of Grevena communicated with the Mediterranean sea of that time. Thus, the question arises, through which routes did this communication occur?

East of the marine Pliocene basin, lie the Askion and Vourinos Mts and further to the east, the Kozani-Servia basin, filled with lacustrine Pliocene deposits. Moreover, no marine Pliocene deposits have been found to the south. To the west, the basin is bounded by the Pindic Cordilliera, and further to the west, the Ioannina and Konitsa basins develop, in which no trace of Pliocene marine deposition has been documented. This leaves a single possible exit through the northwest to the Ionian Sea, which has to be thoroughly investigated. All these data lead to the conclusion that most of the uplift movements in the broader area have taken place in the Quaternary (the last 1.6 Ma). Moreover, Bourcart (1922), as well as Brunn (1956), reported that during Villafranchian times, the Aliakmon river had to be flowing inversely to its present direction, that is, to the northwest.

The Pramoritsa strike-slip fault zone

The neotectonic structure of the broader Grevena area is characterized by the presence of two large-size tectonic structures, the common boundary of which is the Pramoritsa fault zone. The two macrostructures are: (i) the *Tsotili neotectonic structure* bounded by the Aliakmon river bed to the north, northeast, and east, and by the Pramoritsa fault zone to the south; (ii) the *Grevena neotectonic structure,* bounded by

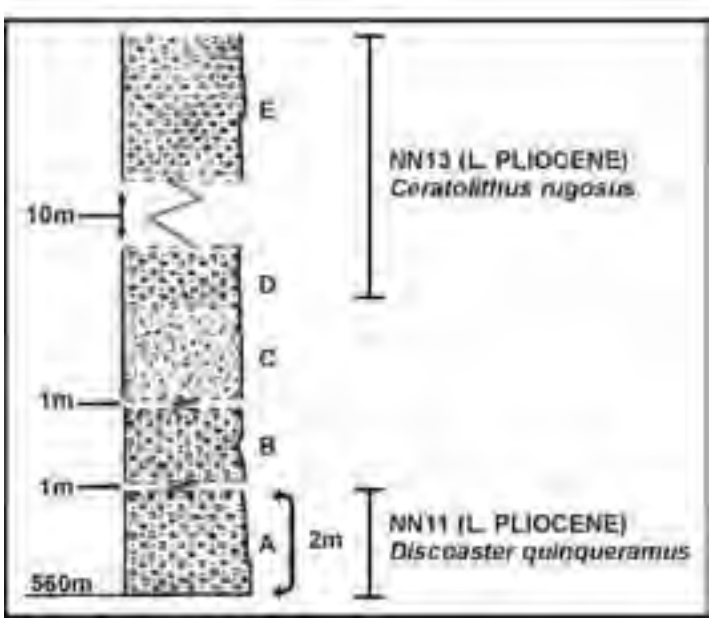

Figure 47 - Representative stratigraphic column of the Pliocene marine deposits on the banks of the Pramoritsa river in the Meso-Hellenic Trough (after Fountoulis et al., 2001).

the Pramoritsa fault zone to the north, the Aliakmon river to the east and west, and by the Venetikos River to the south.

The Tsotili neotectonic structure presents the following characteristics (Figure 47): (i) In this block, occur the younger formations of the Meso-Hellenic Trough [Tsotili (Lower Miocene) and Ondria (Middle to Upper Miocene) formations]. (ii) The beds of the sediments possess constant dip direction towards the NE. (iii) The main tributaries of the drainage networks strike SW-NE and flow from SW to NE. (iv) The majority of the planation surfaces created on the molassic sediments dip towards NE. (v) The faults and fault zones occurring in the area strike mainly SW-NE and SE-NW, that is the same strike as the strike of the tributaries of the drainage networks. (vi) At the southern part of the block, and in the Pramoritsa riverbed, folded beds of molassic sediments of Tsotili Formation occur (scale of some meters), the axes of which trend NW-SE.

The *Grevena neotectonic structure* presents the following characteristics: (i) In this neotectonic structure, occurs mainly the Pentalofon (Upper Oligocene – Aquitanian) Formation and there is no evidence of Tsotili (Lower Miocen) and Ondria (Middle to Upper Miocene) formations; (ii) The beds of the sediments do not have a constant dip direction× the beds dip either towards NE, or towards NW and SW; (iii) There is no sufficient geometry for the distribution of the planation surfaces, nor sufficient dip direction; (iv) The drainage network has no sufficient geometry ×– locally (e.g. the Amygdalies area), it presents a radial arrangement; (v) The faults and fault zones occurring in the area strike mainly E-W and N-S, and occasionally occur in pairs of conjugate faults striking NNW-SSE and NNE-SSW; (vi) In the northern part of the block, and close to the Pramoritsa river-bed folded beds of the molassic sediments of the Pentalofo Formation occur in various scales, the axes of which strike NW-SE and NE-SW. Locally, the fold axes plunge in a radial way.

As already has been described, the Pramoritsa fault zone is the boundary between the Grevena and Tsotili neotectonic structures. It occurs at the southern banks of the Pramoritsa River, and has the same (E-W) mean strike. The fault surface dips at steep angles (70-80º) towards north-northeast (25º) or towards south-southwest (210º). Almost horizontal striations (126º/20º) can be observed on the fault surface. In other words, the Pramoritsa fault is a typical left-lateral strike-slip fault. The fault surfaces occur at the Pentalofo conglomerates, but it is difficult to observe the fault continuation in the marls.

Stop 6.7:

Paleokastro - Mt. Vourinos

Basal conglomerates of the molasse deposits are exhibited at the eastern margin of the Meso-Hellenic trough. The conglomerates consist of pebbles and cobbles, that come exclusively from the metamorphic rocks mostly located to the east, northeast, and southeast of the occurrence. There are no pebbles coming from the underlying marbles of Mt. Askion.

The broader area has been evidently inhabited since

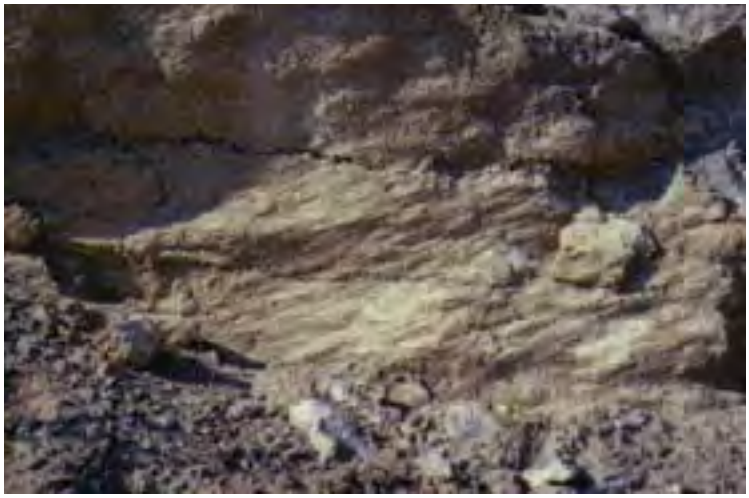

Photo 6.7 - Fault surface with striations of the Pramoritsa fault zone. View from the North.

the Paleolithic times, continuously until today. Human presence is verified by the oldest (for the Hellenic area) Paleolithic findings in Paleokastro area, while it shows dense population in Neolithic times.

Stop 6.8:

Dafnero

Dafnero fault zone

At the area of Dafnero, located at the NW edge of Mt. Vourinos, there is an impressive occurrence of an E-W trending fault zone (DFZ) (Figure 48). The outcrops there consist of Plio-Quaternary deposits that form well-expressed sub-horizontal planation surfaces throughout the eastern part of the Grevena basin and comprise: (i) a lower member (visible thickness more than 50 m.) of cohesive monomictic (ophiolitic) conglomerates (well-rounded pebbles) with sandy matrix, bearing intercalations of soil horizons, and (ii) the upper member of fairly sorted loose polymictic conglomeratic breccias, with a thickness of 10-30 m. All studies so far have left the two members undifferentiated and the age assigned to them is Plio-Pleistocene, according to Faugeres and Vergely (1974), and Mavridis and Kelepertzis (1994), or Villafranchian, (2.0 Ma BP) according to Koufos and Kostopoulos (1993) and Rassios *et al.* (1996). The Dafnero fault zone (DFZ) has a steep 70°° northern dip, and striations measured on some of its constituent surfaces were very slightly inclined (plunge 10-13°°), yielding a dextral character with a slight reverse component. It cuts the monomictic conglomerates, as well as the lower part of the overlying upper member. The reverse component of DFZ is clearly shown: (i) at the slopes of the stream running to the east of the village, where the polymictic horizon is displaced

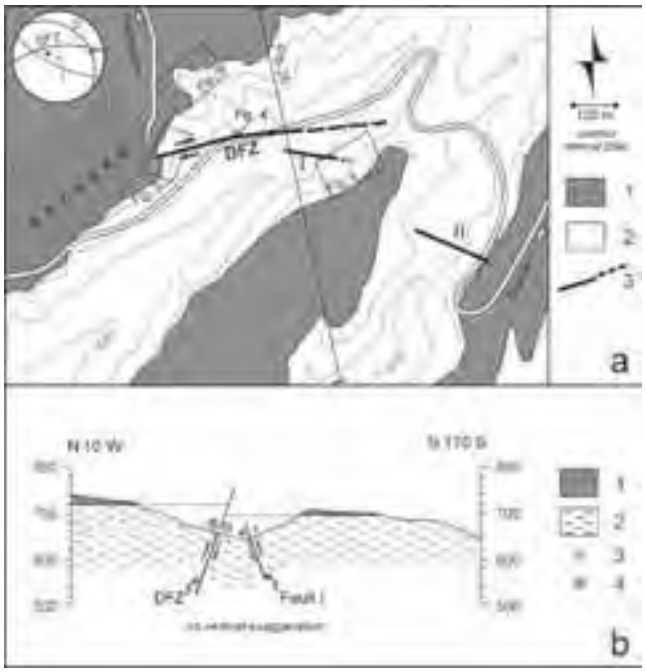

Figure 48 - (a) Geological map of Dafnero: 1: upper member, 2: lower member (see text for description), 3: faults; DFZ: Dafnero fault zone. Inset: stereographic projection (Schmidt projection, lower hemisphere) of the three mapped faults; the displacement vectors of DFZ and fault I also shown. Approximate locations of figs 3-6 - rectangles. (b) Cross section- relationship of DFZ with the outcropping Plio-Quaternary deposits: 1: upper member, 2: lower member, 3: fault displacement towards reader, 4: fault displacement away from reader. Note that fault I does not displace the upper member (polymictic conglomeratic breccias) (after Fountoulis et al., 2000).

by approximately 0.50 m (northern-side up); and (ii) at a natural cut normal to DFZ, where between two shear surfaces the two-generation gouge developed to follow the reverse slip component. The latter is also evidenced by the deep incision at the hanging-wall, while in the footwall incision is almost absent, if existing at all. Also, a set of veins, formed parallel to DFZ has developed at the hanging-wall for a width of about 30 m. Similar observations can be made elsewhere in Greece, where rocks of ophiolitic origin are faulted.

Another fault occurs about 200 m to the southeast; its has a NE (40°°) strike and dips SW at 70°°. The fault displaces the monomictic conglomerates, but not the overlying polymictic ones. Striation measured on it (220°°/36°°) showed a reverse character with a significant right lateral component.

No earthquake fractures could be found in the immediate area of DFZ.

DAY 7

Grevena - Kalambaka - Ioannina

The itinerary is concerned mostly with the Palaeogene, Neogene, and Quaternary sediments and tectonics of the Meso-Hellenic trough. After that, it crosses the Upper Cretaceous wild flysch of the West-Thessalia zone. The oceanic sediments of the Pindos zone are not exhumed along the road, and the itinerary enters directly the Palaeogene flysch of the Ionian zone. Then we continue to the picturesque town of Ioannina on the shores of the Ioannina Lake.

Stop 7.1:

Servia

The Ptolemais – Servia basin is bounded to the south with the impressive active Servia fault zone, that affects Holocene deposits (Mountrakis et al., 1998). This kind of deformation is responsible for the Basin-and-Range type of morphology that has developed across these faults.

The Servia area has been inhabited since Prehistoric times, and tombs, pottery and Neolithic tools were recovered in settlements, a major part of which is most of the time covered by the lake surface.

Stop 7.2:

Samara Rahi

During the recent seismic activity (Ms=6.6; 13.05.1995), few faults and fractures bearing signs of reactivation were found. Phenomena such as landslides, settlement damages as well as local distribution of damage that developed in a linear pattern, may mark the reactivation of some faults. One of these cases was the Chromio – Varis fault zone. Few *en-echelon* (right lateral) arranged fractures (E-W strike) were found at the location of Samara Rahi. These were the longest soil fractures created during the earthquake. Their total length was approximately 1 km. Vertical displacement of 20-40 cm was measured, as well as left-lateral displacement of 10-20 cm.

Photo 7.1 - Panoramic view from NW of the Servia fault zone.

Photo 7.2 - Seismic-fracture created during the Grevena earthquakes (13-5-1995, Ms=6.6). View from the south.

Stop 7.3:

Paleohori

Recent Movements of the Upper Crust due to Creep Deformation based on GPS Measurements in W. Macedonia (NW Greece)

This is the location where the greater GPS measured subsidence was recorded for the years 1995 - 2000. In the broader area north of Paleohori, no drainage pattern has developed on the mollassic sediments, but a soft morphological lowering occurs instead. The area has been previously characterized as inactive by the seismologists, and thus one of the safest areas in Greece. The unexpected destructive seismic activity in western Macedonia (NW Greece) in May 1995, afforded the opportunity to study (Fountoulis et al., 2002) the current deformation processes using GPS measurements.

Between the years 1995 and 2000, a number of measurements were carried out at a network of observation pillars, most of them belonging to the Hellenic Triangulation Network. The coordinates were determined by terrestrial geodetic methods. The use of these pillars permits us to compare the results of satellite geodesy methods to their known coordinates on the Hellenic Geodetic Reference System 1987 (HGRS 87). The epoch of the HGRS 87 coordinates is assumed to be in the early 1980s, since the 1st order measurements were done in the period 1975 – 1979, and the 2nd order measurements, in the period 1982 – 1985.

In May 1995, a week after the main shock, 91 pillars were measured. These triangulation pillars were occupied without prior knowledge of the location of the earthquake epicenter. Further measurements took place on September 1995, May 1996, May 1998, and September 2000, where 37, 39, 56, and 59 sites were measured respectively, in order to check the aftershock behavior of the affected area. 53 of the 59 last measured (September 2000) sites belong to the Hellenic Triangulation Network. The whole network consists of 120 sites observed within 5 years. This high number of sites allowed us to draw some conclusions concerning the movements that took place due to the seismic activity, as well as the movements that took place in the period 1998 – 2000

Photo 7.3 - Panoramic view from northwest of the western part of the Paleohori-Sarakina fault zone. In this area is very characteristic the incision on the uplifted block.

without seismic activity.
The accuracy of the GPS results is estimated to be better than 1 cm for the horizontal components, and of the order of 2 cm for the vertical component.
For the time period May (?) 1980 – May 1995, there were 91 common sites, and the mean displacement was calculated to be 11 cm, and the mean velocity, 0.7 cm/y. This period includes 9 earthquakes before the main shock of the May 13, 1995, and 79 aftershocks with M>4 R.
For the time period May 1995 – May 1996, there were 19 common sites, the mean displacement being calculated to be 1.5 cm. This value is very high in comparison with the previous ones. This period includes 56 aftershocks with 4<M<5 R and only one (1) shock with M>5 R.
For the time period May 1996 – May 1998 there were 29 common sites, and the mean displacement was calculated to be 0.6 cm, and the mean velocity 0.3-cm/y. This period includes only 5 aftershocks with 4<M<5 R.
For the time period May 1998 – September 2000, there were 31 common sites and the mean displacement was calculated to be 0.8 cm, and the mean velocity 0.4 cm/y. This period includes only 3 earthquakes with 4<M<5 R. All epicenters located outside the mezoseismal area.
For the time period May 1995 – September 2000, there were 21 common sites and the mean displacement was calculated to be 2.8 cm and the mean velocity 0.5 cm/y.
It is known that a comparison of heights can be done between GPS coordinates only, since the heights in HGRS 87 are orthometric, and heights derived from GPS measurements are geometrical. So we present a comparison of heights between May 1995 and September 2000. The value of subsidence was calculated at 5 cm, and the mean subsidence velocity 1 cm/y, whereas the highest value of uplift was calculated at 4.8 cm, and the mean uplift velocity at 0.96 cm/y.
In conclusion (Figure 49), (i) The kinematics of the blocks resulting from the GPS measurements, are in good relation with the kinematics of the fault zones. (ii) Areas that are under a subsidence regime according to GPS measurements coincide with the areas that have been filled in with Plio-Quaternary

Figure 49 - Horizontal and vertical displacements of the distinguished blocks, based on GPS measurements for the period May 1995 - September 2000 (after Fountoulis et al., 2002).

sediments. The only exception is the area located NW of Grevena, which has suffered a complicated brittle-ductile deformation. (iii) For the 1996-1998, as much as for the 1998-2000 periods, there is a significant displacement of the blocks, without any important seismic activity. In W. Macedonia, the deformation processes in the moment is not only due to seismic activity, but even aseismic activity ("creep").

Paleohori – Pontini and the Paleohori-Sarakina Fault Zone (PSFZ)

On the hills SW of Paleohori, a morphological scarp has been created by the activity of the Paleohori – Sarakina fault, trending E-W. The fault throw increases from east to west, while in the western area (at Kentro village), incision is very high on the uplifting block. This fault creates an intermediate tectonic block between the latter and the Aliakmon River, which is uplifting slower than the south margin of the Kamvounia Mts. This ENE-WSW striking fault zone is discernible through the topographic escarpment it has created in the Miocene deposits of the molassic Tsotyli Formation, while no actual fault break can be observed. The kinematics of this fault zone still remain to be clarified, as no surface kinematic indicator could be found. Therefore, it is probable that the Paleohori – Sarakina fault zone (PSFZ) is of analogous character to DFZ, so that the scarp created by it is less prominent than it should be for a normal fault.

A set of approximately E-W trending fractures was found about 500 m. before the northern entrance to Sarakina. The main fracture had a N 110°° trend, cut the asphalt road, and continued into the adjacent slope. It had no vertical displacement; however, most of the fractures had a 1 mm - 1 cm "heave". The fracture set was *en echelon* arranged, and the fractures had a slight dextral offset.

Along the road that passes through the hills south of Paleohori, we have found a series of small-scale landslides. Two hundred meters after the road junction to Deskati, we found fractures cutting the tarmac and continuing into the soil. They are *en echelon* arranged, along an overall E-W trend, and a small 'graben' has been created between two sets.

Stop 7.4:

Karpero

Aliakmon drainage divide

Brunn (1958) suggests that the halting of the Aliakmon River flow towards Thessaly plains (to the south) may be explained by the transverse accident built by the Servia fault zone (which affects the Quaternary), and the Vounassa flexure. This transverse accident is prolongated westwards across the Meso-Hellenic Trough by the Kratsovon and the southern end of Krania paleogulf (Figure 50). A drainage divide between Aliakmon and Pinios drainage basins has been created on the Plio-Quaternary deposits. It has to be mentioned the opposite direction of flow of the two rivers: Aliakmon flows towards east-northeast, while Pinios flows towards west and then south.

Stop 7.5:

Meteora

Meteora is located at the northwestern boundary of the Thessalian basin, and at the southeastern limits of the Meso-Hellenic deposits. Meteora is among the biggest and most important groups of monasteries in Greece, after those in Mount Athos. The first evidence of the monasteries' history can be traced back to the 11th century, when the first hermits settled there. The rock monasteries are characterized by UNESCO as a unique phenomenon of cultural heritage, and they form one of the most important sites on the cultural map of Greece.

The most important monasteries of Meteora are as described below:

The Holy Monastery of Great Meteoron is the biggest of the Meteora monasteries. The church "Katholikon", dedicated to the "Transfiguration", was erected in the middle of the 14th century and from 1387 to88, and decorated in 1483 and 1552. The old monastery is used as a museum nowadays.

The Holy Monastery of Varlaam is the second biggest monastery. The church, dedicated to three bishops, is of the Athonite type (cross-in-square, with dome and choirs), with a spacious "esonarthex" (litesurrounded by a dome. It was built in 1541/42, and decorated in 1548, while the esonarthex was decorated in 1566. The old refectory is used as a museum, while North of the Church, we can see the "parekklesion" (chapel) of the Three Bishops built in 1627, and decorated in 1637.

The Holy Monastery of Rousanou is dedicated to "The Transfiguration", but in honour of Saint Barbara. The "Katholikon" (church) in the Athonite type, was founded in the middle of the 16th century, and decorated in 1560. Both the Katholikon and the reception halls are in the ground floor, while the "archontariki" (?), cells, and subsidiary rooms are scattered in the basement and the first floor.

Figure 50 - Schematic geological map showing the area of the drainage divide between the Aliakmon and Pinios drainage basins. B: Alpine basement, E,m-l: Upper Eocene marls and limestones, Ol-M, m-s-c: Oligocene - Miocene marls, sandstones, conglomerates, M, m-s-c: Miocene marls, sandstones, conglomerates, Pl-Q, s-m: Pliocene-Quaternary sands, marls, Q: Quaternary deposits

The Holy Monastery of St. Nicholas Anapausas is the first we meet on our way from Kastraki to Meteora. The "Katholikon", dedicated to St. Nicholas, is a single-nave church with a small dome, built in the beginning of the 16th century. It was decorated by the Cretan painter, Theophanis Strelitzas or Bathas, in 1527.

The Holy Monastery of St. Stephen is one of the most visited, and can be reached without climbing innumerable stairs. The small single-nave church of St. Stephen was built in the middle of the 16th century, and decorated in 1545 or a little later. The "Katholikon", in honour of St. Charalambos, was built in the Athonite type, in 1798. The old refectory of the convent is used as a museum nowadays.

The Monastery of the Holy Trinity is very difficult to reach. The visitor has to cross the valley and continue high up through the rock before arriving at the entrance. The church is in the cross-in-square type, with the dome based on two columns, built in 1475-76, and decorated in 1741. The spacious barrel - vaulted esonarthex was founded in 1689, and decorated in 1692. A small skeuophylakeion (explain what it is) was added next to the church in 1684.

A great part of the monasteries (Katholika, cells, other buildings) have been restored and the rest of them are in restoration. Conservation of the frescoes has been fulfilled in most of the monasteries, too.

Stop 7.6:

Theopetra

The Theopetra Cave is located on the NE slope of the rocky limestone bulk of a hill, at whose foot lies the community of the same name. Its entrance is apsidal and large (17 x 3 m. approximately). The interior of the cave measures about 500 sq m. and small conches are formed in its periphery.

The Theopetra limestone has been dated to the Upper Cretaceous (100 – 65 Ma before present). The creation of the cave is consequently later than

the above-mentioned date. The cave started being inhabited from the Middle Paleolithic period (which started at about 100,000 years before present).

The excavation started in 1987, under the direction of the prehistorian/archaeologist Catherine Kyparissi-Apostolika. The cave has been excavated for nine years now, and the excavations are still in process. Stone tools of the Paleolithic, Mesolithic, and Neolithic periods have been found, as well as Neolithic pottery, bone, and shell objects.

It is the first excavated cave in Thessaly, and the only one for the moment in Greece with deposits that start at the Middle Paleolithic, and last until the end of the Neolithic (3000 B.C.), without gaps.

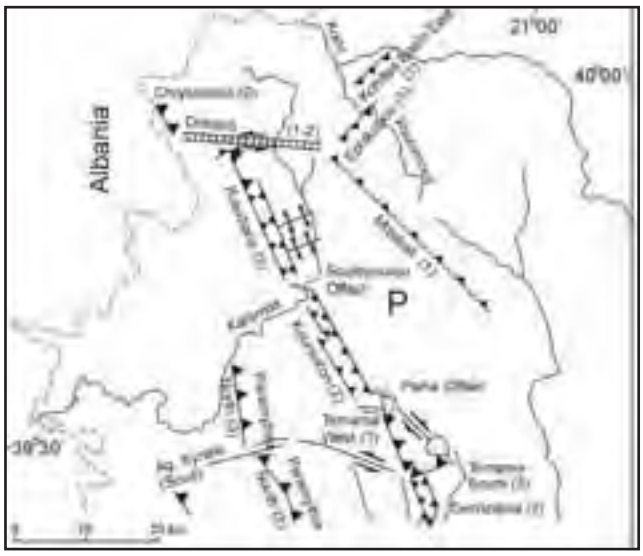

Figure 51 - Major tectonic features of northern Epirus (after Karageorgi et al., 2002).

DAY 8

Ioannina - Konitsa - Dodona - Ioannina

Fault zones in Epirus (NW Greece)

Epirus consists of a series of anticlines, formed and dominated by a sequence of Tertiary thrusts. These thrusts separate the land between the Ionian coast in the west, and the Pindos mountains in the east, into regions of different relief and rock types, and are dominated by Mesozoic carbonates, ranging in elevation between 1200 m to 1700 m, with some peaks at 2000 m. The highest ridges, striking NW (335º), are Mitsikeli in the east, and Paramythia, Kourenton and Kassidiaris in the west. The carbonate Ioannina plateau (P) lies in between. The eastern and western boundaries of the area have Oligocene flysch at outcrop, and are known as the Zagoria (Z) basin, and Botzara (B) synclines, respectively (Figure 51). The NW-SE fold-and-thrust trend is laterally shifted by East-West transverse faults (arrows); the Petousi-Souli (or Agia Kyriaki) to the South, the Soulopoulou fault in the plateau, and the Doliana fault zone northwest, in the Delvinaki (D) well area. Several large NE-SW trending normal faults truncate the fold and- thrust belt of N. Epirus. These include the Konitsa, Pogonianni and Doliana faults.

Stop 8.1:

Konitsa marginal fault zone

Normal faulting with a NE-SW strike extends most of the way from Aridea to the fold-and-thrust belt of Epirus and coastal Albania. In particular, the Pogonianni and Doliana faults cut across the lines of anticlines that are associated with the continental collision between the Adriatic (Apulia) platform and Albania-Greece, though there is insufficient earthquake data to see how these structures are related at depth. The NE-SW normal faults cannot be traced continuously between Konitsa and the Ptolemais or the Grevena regions, but the intervening area consists mostly of flysch, in high, steep ground that is prone to landsliding. The faulting may be more continuous than it appears, but there is no historical seismicity to guide us.

The zone of NE-SW normal faults seems to cut across and mark the southern limit of the N-S normal faulting in eastern Albania and western FYR Macedonia. However, the well-constrained mechanism of the earthquake of 1 May 1967 at 39.5ºN 21.2ºE, showing normal faulting with a NNW-SSE strike, is an apparent anomaly that casts some doubt on this conclusion (Figure 52).

Both along the Konitsa and Pogonianni faults the footwall blocks (built up of Mesozoic limestones) have generated a relief of 500–1000 m. They are characterized by steep, relatively undissected ridges and exposed fault surfaces along the tops of a nearly continuous apron of scree, similar to faults in limestone elsewhere in Greece. Corrugated and striated slip surfaces along the 10 km long Konitsa fault, indicate

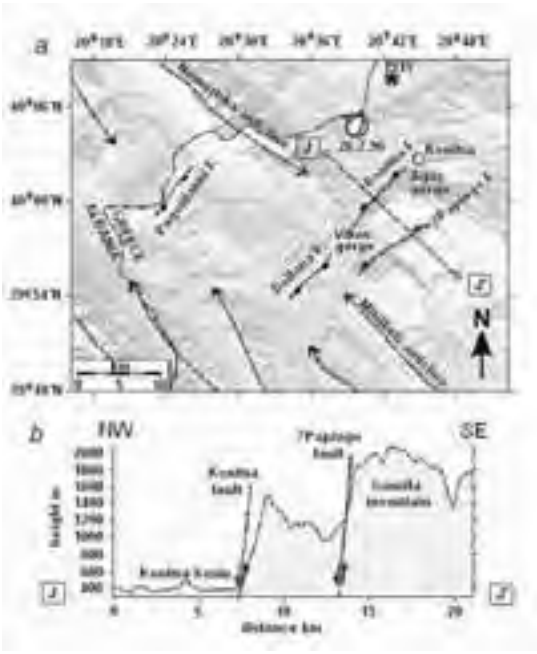

Figure 52 - (a) Major faults and earthquakes in the Konitsa region of northern Epirus. (b) Topographic profile across the Konitsa and possible Papingo faults (after Goldsworthy et al., 2002).

slip vector azimuths of 295÷ in the central section, and 330÷ at the SW end. An earthquake of Mw 5.3 in the Konitsa region in 1996 had a focal mechanism with a slip vector of 290÷ and may have ruptured part of the Konitsa fault. The Konitsa fault controls the northern limit of the Gamila limestone plateau, which rises up to 2400 m above sea level, and is drained by two rivers (the Aoos and Voidomatis), that cut deep gorges into the rising footwall block. The Doliana fault is much less pronounced, forming a minor ridge to the west of the Konitsa fault.

Palaeolithic human presence

The complex relief of the mountainous area of Konitsa, which is dominated by the drainage basins of the Aoos and Voidomatis Rivers, formed a pole of attraction for hunter-gatherer groups during the Late Palaeolithic period. In an environment rich in natural resources - raw materials, flora and fauna - the earliest evidence of human activity goes back to 17,000 A (years before the present, uncalibrated dates), and continues uninterrupted down to 10,000 A, when the local glaciers of western Pindos began to retreat and climatic conditions gradually improved. Based on natural refuges such as Klidi, Megalakkos, and Boila, groups of hunters systematically exploited the mountain biotopes. In these rock shelters, used as occasional/seasonal campsites, are preserved the remains of a way of life based on the consumption of natural available resources, rather than the growing of foodstuffs.

Flint, a hard stone procured from river beds, was used by people of the Palaeolithic period to manufacture their weapons and tools: arrows and spearheads, and a variety of cutting, scraping, and piercing tools with which to work other materials such as wood, hide and bone. They engaged in organized forays to hunt wild animals (caprines and deer), set traps for hares and birds, fished the rivers and gathered plants and fire-wood.

Although humble at first sight, this evidence is unequivocal testimony to a complex, organized society that adapted to palaeoclimatic and ecological fluctuations by exploiting the collective experience of a long cultural and biological history.

Although human presence may logically be inferred in the surrounding area of Konitsa from the Upper Palaeolithic to the 2nd millennium BC, with settlement centers being in accordance with the productive needs of Neolithic hunters-stockbreeders, there is no direct archaeological evidence for this. An indication of human presence in the river valley of the Aoos, at the end of the 2nd millennium BC, is furnished by the two bronze swords from Mesoyephyra. About the 13th-12th century BC, the mountainous area of the central and west Pindos was settled by the Molossoi, one of the most important tribes in the area of Epiros in terms of its political strength. Evidence for their arrival has recently been discovered on the Liatovouni hill in the Aoos valley, near its confluence with the Voidomatis.

From 1200/1100 to 730/700 BC, Epiros was isolated; a circumstance associated with the general upheavals and invasions in the Greek world. About the middle of the 8th century BC, peace was established, leading to a demographic growth that can also be seen in the cemetery of Liatovouni.

Stop 8.2:

Kalpaki - Delvinaki - Doliana

The outcrop of Triassic anhydrite formations and evaporites in relation to the thrust structure and the Doliana fault zone will be demonstrated.

Stop 8.3:

Vikos

The Vikos Gorge, 900 metres deep and 12 kilometres long, regarded as the grand canyon of Greece, is a

unique geological marvel. It is covered with lush vegetation, composed of various trees and flowers. The healing herbs, used by the renowned "quack" herbalists who worked in former centuries, were mostly collected from the Vikos. Many wild animals including the rare wild goat, still live in the gorge. Moreover, in the whole region of Zagori, th many kinds of wild animals still survive, such as wild boar, bears, wolves, ferrets, roe, deer, etc.

Vikos, and a part of Aoos, have been regarded since 1973 as the biggest national forest of Greece, covering an area of 126,000 square miles. Another well-known national forest, the one of Valia Kalnta, lies in Eastern Zagori, north of Vovousa. The national forest is considered to be one of particular natural beauty.

Photo 8.3 - Vikos gorge

It takes seven hours to explore the Vikos, which extends from the bridge of Voidomatis, to the village of Koukouli. Beginning the exploration from Vitsa village (from the site called "Skala"), it takes about 20 minutes to get to the river Voidomatis, where the explorer can take a look at the Misios bridge, and the fantastic view. A path, passing between the two riverbanks, leads to the ravine, which is formed of perpendicular rock faces reaching a peak of 950 m. The width of the gorge, at riverbed level, fluctuates between 30 and 100 m. Because of its great length, some visitors do not intend to explore the Gorge. For them, it is possible to enjoy it from one of several viewpoints. We suggest three sites, which offer the best possible views into the Gorge, and namely: a) The Monastery of St. Paraskevi in Monodendri; b) Oxya above Monodendri on the mountain; c) Beloi, a view point about half an hour walk beyond Vradeto.

Stop 8.4:

Dodona

The ancient site of Dodona is located 22 km south of Ioannina, in the narrow valley between mounts Tomaros and Manoliassa. The first remains on the site date from the prehistoric period, and the first deity worshipped here was the Earth goddess. The cult of Zeus and the sacred oak tree was brought to Dodona by the Selloi, a branch of the Thesprotian tribe, between the 19th and 14th centuries B.C., and soon became the prevalent cult of the sanctuary. The first offerings from southern Greece date from the end of the 8th century B.C., and building activity began in the 4th century B.C. The sanctuary reached the highest point of its prosperity in the 3rd century B.C., but was destroyed by the Aetolians in 219 B.C.. It was rebuilt shortly thereafter, and continued to be in use, until its destruction by the Roman invaders in 167 B.C.. In the Roman period, it had a different function, and its end came in the 4th century A.D., during the reign of Theodosius the Great. The area of the sanctuary was then covered with Christian basilicas. Today the theatre is used for performances.

The first excavations on the site, carried out by N. Karapanos in 1873-75, confirmed the location of the sanctuary and revealed a great quantity of finds. The following excavation campaign was undertaken shortly after 1913, by the Archaeological Society, under the direction of G. Soteriades but was stopped by the events of 1921 (which events?). The site was investigated again by D. Evangelides, in the period from 1929 until 1932, and systematic excavations started in the 1950s, under the direction of D. Evangelides and S. Dakaris (after Evangelides' death, they were continued by S. Dakaris). Since 1981, the excavations have been carried out under the auspices of the Archaeological Society, with the financial support of the University of Ioannina.

Systematic restoration work in the theatre, the stadium, and other monuments of the site started in 1961, and was based on the study by the architect B. Charissis. The whole project was financed by the Archaeological Society and the Program for Public Investments. Until 1975, the greatest part of the theatre had been restored, except for the third diazoma.

The most important monuments of the site are: (i) the Sacred House (early 4th century B.C.); (ii) the Theatre, which is one of the largest in Greece, seating 18,000 people (3rd century B.C.); (iii) the Bouleuterion (end

of the 4th century B.C.); (iv) the Stadium (late 3rd century B.C.); (v) the Acropolis (4th century B.C.); (vi) the Prytaneum (4th century B.C.).

DAY 9

Ioannina - Igoumenitsa

The itinerary of the last day crosses through the Ionian zone towards the Apulian platform. Mesozoic and some Cenozoic sediments are exhibited in tight folds and imbrications along the road.

Stop 9.1:

Petousi

A left lateral strike-slip fault zone forms the southern boundary of the Ioannina basin, Mt, Tomaros.

Stop 9.2:

Arillas

This stop displays the thrusting of the Ionian unit over Pliocene marine deposits.

Acknowledgments

The field work on Bulgarian territory was carried out thanks to the financial support by the Ministry of Environment and Waters under the project "Trans-border Sections and Itineraries". The assistance of the Bulgarian Academy of Sciences is also gratefully acknowledged.

I. Mariolakos and I. Fountoulis are grateful to their colleagues, E. Anderadakis and E. Kapourani. Without their skilful help, the Greek part of the present guidebook could not have been accomplished under the painful circumstances mentioned in the Foreword.

References cited

Armour-Brown, A., De Bruin, H., Maniati, C., Siatos, G. and Niesen, P. (1977). The geology of the Neogene sediments north of Serrai and the use of Rodent faunas for biostratigraphic control. Proc. VI Coll. Geology Aegean Region, Athens 1977, II, 615-622.

Aubouin, J., Le Pichon, X., Winterer, E. and Bonneau, M. (1979). Les Hellenides dans l'optique de la tectonique des plaques. Proc. VI Coll. Geol. Aegean Region, Athens 1977, Proc., III, 1333-1354.

Brunn, J.H. (1956). Contribution a l' etude geologique de Pinde septentrionale et de la Macedoine occidentale. Ann. Geol. Pays Hellen., VII, 1-358.

Burchfiel, C. B., Nakov, R., Tzankov, Tz. andRoyden, L. H. (2000). Cenozoic extension in Bulgaria and northern Greece: the northern part of the Aegean extensional regime. in: Bozkurt, E., Winchester, J.A., Piper, J. D. (eds.) Tectonics and Magmatism in Turkey and the Surrounding Area. Geol. Soc., London, Spec. Publ. 173, 325-352.

Dabovski, C., Boyanov, I., Khrischev, K., Nikolov, T., Sapounov, I., Yanev, Y. andZagorchev, I. (2002). Structure and Alpine evolution of Bulgaria. – Geologica Balcanica, 32, 2-4; 9-15.

Dinter, D. and Royden, L. (1993). Late Cenozoic extension in northeastern Greece: Strymon valley detachment system and Rhodope metamorphic core complex. Geology, 21, 45-48.

Dinter, D. (1994). Tertiary structural evolution of the southern Rhodope metamorphic province: A fundamental revision. Proc. 7th Congress, Geol. Soc. Greece, Bull. Geol Soc. Greece, XXX/1, 79-89.

Eltgen, H., (1986). Feinstratigraphisch - Fazielle Untersuchungen an Pliozän - Sedimenten im Tertiarbecken Südlich Neapolis/Kozani, Nordgriechenland. ….G.M.E. Geol. Geoph. Res., Special Issue, 107-115.

Faugeres, L. and Vergely, P., (1974). Éxistence de deformations en compression d'âge quaternaire ancien (Villafranchien superieur) dans le Massif du Vourinos (Macedoine occidentale, Grèce). C.R. Acad. Sc. Paris, 278, Ser. D, 1313-1316.

Fountoulis, I. and Bakopoulo A. (1999). Morphotectonic observations in Pramoritsa River basin (Grevena, Greece). Proc. 5th Geographical Congress Geographical Soc. Greece, 94-100 (in Greek).

Fountoulis, I., Kranis, H., Lekkas, E., Lozios, S. and Skourtsos, E. (2000). Quaternary deformation in Grevena (W. Macedonia, Greece): Importance of shear and compressional strain. Ann. Geol. Pays Hellen. 38, Fasc C, p. 123-132.

Fountoulis, I., Marcopoulo-Diacantoni, A., Bakopoulo, A., Motaiti, E., Mirkou, M.R., and Saroglou, H. (2001). The presence of Pliocene marine deposits in the Meso-Hellenic Trough (Pramoritsa river banks, Grevena, Greece). Proc. 9th Congress, Geol. Soc. Greece, Bull. Geol Soc. Greece, XXXIV/2, 603-612 (in Greek).

Fountoulis, I., Paradisis, D., Veis, N. and Tsagaroulias, V. (2002). Recent Movements of the Upper Crust due to Creep Deformation based on GPS measurements in W. Macedonia (NW Greece). In WEGENER 2002 Proceedings.

Gautier, P., Brun, J.P., Moriceau, R., Sokoutis, D., Martinod, J. and Jolivet, L. (1999). Timing, kinematics and cause of Aegean extension: a scenario based on

a comparison with simple analogue experiments. Tectonophysics, 315, 31-72.
Goldsworthy, M., Jackson, J. and Haines, J. (2002). The continuity of active fault systems in Greece. Geophys. J. Int., 148, 596-618.
Gramann, von F. and Kockel, F. (1969). Das Neogen im Strimonbecken (Griechicsh-Ostmazedonien). Geol. Jb., 87, 445-484, Hannover.
Kahle, H.G., Straub, C., ReilingerR., McClusky, S., King, R., Hurst, K., Veis, G., Kastens, K., and Cross, P. (1998). The strain rate field in the eastern Mediterranean region, estimated by repeated GPS measurements. Tectonophysics, 294, 237-252.
Karageorgi, E., Watts, M. and Savvaidis, A. (2002). Integration and correlation of Geophysical data in NW Greece. EAGE 64th Conference and Exhibition – Florence May 2002, E-39.
Karistineos, N. and Gergiades-Dikeoulia, E. (1986). The marine transgression in the Serres Basin. Ann. Geol. Pays Hellen. 33/1, p. 221-232.
Karydakis, G. and Kavouridis, TH. (1988). Geothermal research of low enthalpy in Agia Varvara – Thermopigi Sidirokastrou (Serrai prefecture). Report Institute of Geology and Mineral Exploration.
Kavouridis, TH. and Karydakis, G. (1989). Geothermal research of low enthalpy in Sidirokastron area (Serres prefecture). Report E 5968 Institute of Geology and Mineral Exploration.
Kockel, F. and Walther, H.W. (1965). Die Strimonlinie als Grenze zwischen Serbo-Mazedonischen und Rila-Rhodope Massiv in Ost-Mazedonien. Geol. Jb., 83, 576-602.
Kockel, F. and Walther, H.W. (1967). Der Rhyolith von Strimonikon, sein tektonischer Rahmen und die junge Laggerstattenbildung in seiner Umgebung (Zentral – Mazedonien, Griechenland). Bull. Geol. Soc. Greece, VII/1, 1-16.
Kockel, F., Mollat, H. and Walther, H.W. (1977). Erlauterungen zur geologischen Karte der Chalkidiki und angrenzender Gebiete 1/100.000 (nord Griechenland). Bund. Fur Geowiss. V. Rohstoffe, 110 p. Hannover.
Kopp, K.O. (1966). Geologie Thrakiens III: Das Tertiar zwischen Rhodope und Evros. Ann. Geol. Pays Hellen., 16, 315-362.
Koufos, G.D. and Kostopoulos, D.S. (1993). A stenonoid horse (Equidae, Mammalia) from the Villafranchian of Western Macedonia, Greece. Bull. Geol. Soc. Greece, XXVIII/3, 131-143, Athens.
Koukouzas, K. (1972). Le chevauchement de Strymon dans la region de la frontiere greco-bulgare. Z. Deutsch. Geol. Ges., 123, 343-347, Hannover.
Lalechos, N. and Savoyat, ED. (1977). La sedimentation Neogene dans le fosse Nord Egeen. VI Coll. Geology Aegean Region, II, 591-603.
LE Pichon, X. and Angelier, J. (1981). The Aegean sea. Phil. R. Soc. London, A 300, 357-372.
Lekkas, E., Kranis, C., Fountoulis, I., Lozios, S. and Adamopoulo, E. (1996). Spatial distribution of damage caused by the Grevena -Kozani earthquake (May 13, 1995, W. Macedonia, Greece). In proceedings of Intern. Meeting on results of the May 13, 1995 earthquake of W. Macedonia: One Year after, Abstract p. 89-95, Kozani.
Lekkas, E., Lozios, S.G., Fountoulis, I.G., Kranis, H.D. and Adamopoulo, E.I., (1995). Investigation -Correlation of the geodynamic hazards at the earthquake stricken areas of Kozani - Grevena: Proposals for safe reconstruction. Unpublished Applied Research Project, Athens.
Makropoulos, K., Kassaras, I., Tzanis, A., Ziazia, M., Louis, J. andDiagourtas, D. (1996). The 13 May 1995 M-6.6 Kozani-Grevena aftershock sequence: towards understanding its dynamics and rupture processes, Proc., International Meeting: On results of the May, 13, 1995 earthquake of West Macedonia: One year after, p. 99-103, Kozani, Greece.
Maratos, G. (1967). The Sitsi-Kamen volcano on the Angistron mountain. Age and relation with the metallogenesis and the hot springs. Bull. Geol. Soc. Greece, VII/1, 93-106.
Mariolakos, I. and Papanikolaou, D. (1981). The Neogene basins of the Aegean Arc from the Paleogeographic and the Geodynamic point of view. Proc. Int. Sym Hell. Arc and Trench HEAT, I, 383-399, Athens.
Mariolakos, I. and Papanikolaou, D. (1987). Deformation pattern and relation between deformation and seismicity in the Hellenic arc. Bull. Geol. Soc. Greece, … , 59-76 (in Greek).
Mariolakos, I., (1975). Thoughts and viepoints on certain problems of the Geology and tectonics of Peloponnesus Greece. Ann. Geol. Pays Hellen.. 27, 215-313 (in Greek).
Mariolakos, I., Fountoulis, I., Logos, E. andLozios, S. (1991). Methods to study the torsional neotectonic deformation: the case of Kalamata area (SW Peloponnesus, Greeece), in C. Qingxuan (Ed.) Proceedings of IGCP Project 250" Regional Crustal Stability and Geological Hazards, 3, 15-21, UNESCO-IUGS/ "Seismological Press" publications.
Mariolakos, I., Papanikolaou, D., andLagios,

E. (1985). A neotectonic geodynamic model of Peloponnesus based on morphotectonics, repeated gravity measurements and seismicity. Geol. Jb., B-50, 3-17.

Mavrides, A., and Kelepertsis, A. (1993). Geological map of Greece 1: 50,000, "Knidi" quadrangle, I.G.M.E., Athens.

Mc Kenzie, D. (1970). Plate tectonics in the Mediterranean region. Nature, 226, 239-243.

Mc Kenzie, D. (1972). Active tectonics of the Mediterranean region. Geoph. J. R. Astron. Soc., 30, 109-185.

Mc Kenzie, D. (1978). Active tectonics of the AlpineHimalyan Belt. the Aegean Sea and surrounding regions. Geophys. J. R. Astron. Soc., 55, 217-254.

Mercier, J. (1966). Paleogeographie, orogenese, metamorphisme et magmatisme des zones internes des Hellenides en Macedoine (Grece): vue d'ensemble. Bull. Geol. Soc. France, 8, 1020-1049.

Mercier, J. (1968). Etude geologique des zones internes des Hellenides en Macedoine centrale (Grece). Ann. Geol. Pays Hellen., 20, 1-792 (1973).

Mountrakis, D. (1994). Introduction to the Geology of Macedonia and Thrace. Aspects of the geotectonic evolution of the Hellenic Hinterland and Internal Hellenides. Proc. 7th Congress, Geol. Soc. Greece, Bull. Geol Soc. Greece, XXX/1, 31-46.

Mountrakis, D., Pavlides, S., Zouros, N., Astaras, T., and Chatzipetros, A. (1998). Seismic fault geometry and kinematics of the May 1995 western Macedonia (Greece) earthquake. J. Geodynamics, 26/2-4, 175-196.

Papanikolaou, D. (1984). Introduction to the Geology of Greece: The pre-Alpine Units. In: I.G.C.P. No 5, 1984 Field meeting in Greece, Field guide, Part, I, 3-35.

Papanikolaou, D. (1984). The three metamorphic belts of the Hellenides: a review and a kinematic interpetation. Geol. Soc. London, Spec. Publ. 17, 551-561.

Papanikolaou, D. (1986). The geology of Greece 240 p. (in Greek).

Papanikolaou, D., Sassi, F.P., and Skarpelis, N. (1982). Outlines of the Pre-Alpine Metamorphisms in Greece. In Sassi and Varga (editors), I.G.C.P. No 5, Newsletter, 4, 56-62 and Ann. Geol. Pays Hellen., 31/1, 16-31.

Papazachos, B.C., et al. (1995). Focal properties of the 13 May 1995 large (Ms=6.6) earthquake in the Kozani area (N. Greece), Publ. Geophys. Lab., Aristotle Univ., 4, Thessaloniki.

Pavlides, S. (1985). Neotectonic evolution of the Florina-Vegoritis- Ptolemais basin (W. Macedonia, Greece). Ph.D. Thesis, University of Thessaloniki, 265 p. (in Greek).

Pavlides, S., Zouros, N.C., Chatzipetros, A.A., Kostopoulos, D.S. and Mountrakis, D.M. (1995). The 13 May 1995 western Macedonia, Greece (Kozani - Grevena) earthquake; preliminary results, Terra Nova, 7, 544-549.

Psilovikos, A., Sotiriadis, E., and Vavliakis, E. (1979). Quaternary tectonics and morphological differentiation of Sidirokastron basin. Ann. Geol. Des Pays Hellen., XXX/1, 588-601.

Struck, A. (1912). Zur Landeskunde von Griechenland, Frankfurt.

Tzankov, Tz., Angelova, D., Nakov, R., Burchfiel, B. C. and Royden, L. H. (1996). The Sub-Balkan graben system of Central Bulgaria. Basin Research 8, 125-142.

Yordanova, M., and Donchev, D. (eds.) (1997). Geography of Bulgaria. Academic Publishing House "Marin Drinov". Sofia, 730 pp (in Bulgarian).

Zagorchev, I. (1992). Neotectonics of the central parts of Balkan Peninsula: basic features and concepts. Geologische Rundschau 81, 3, 635-654.

Zagorchev, I. (1992). Neotectonic development of the Struma (Kraistid) Lineament, south-west Bulgaria and northern Greece. - Geological Magazine 129, 2, 197-222.

Zagorchev, I. (1996). Late Alpine (Palaeogene - Early Miocene) tectonics and neotectonics in the central parts of the Balkan Peninsula. Z. geol. Wiss., 24, 1/2, 91-112.

Zagorchev, I. (1998). Pre-Priabonian Palaeogene formations in Southwestern Bulgaria and Northern Greece: stratigraphy and tectonic implications. Geological Magazine 135, 1, 101-119.

Zagorchev, I. (2001). Geology of SW Bulgaria: an overview. Geologica Balcanica 21, 1-2, 3-52.

Zagorchev, I. (2002). Neogene fluviolacustrine systems in the northern Peri-Aegean Region. – Geologica Carpathica, Special issue (CD), 53.

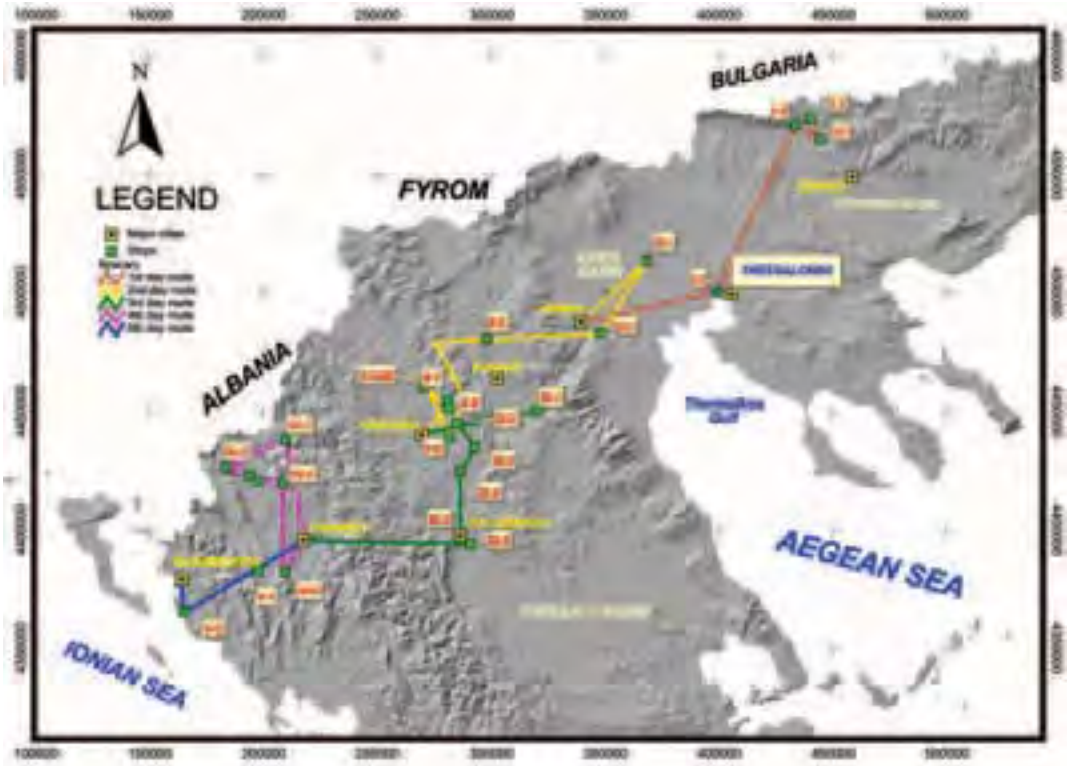

Field itinerary in Northern Greece

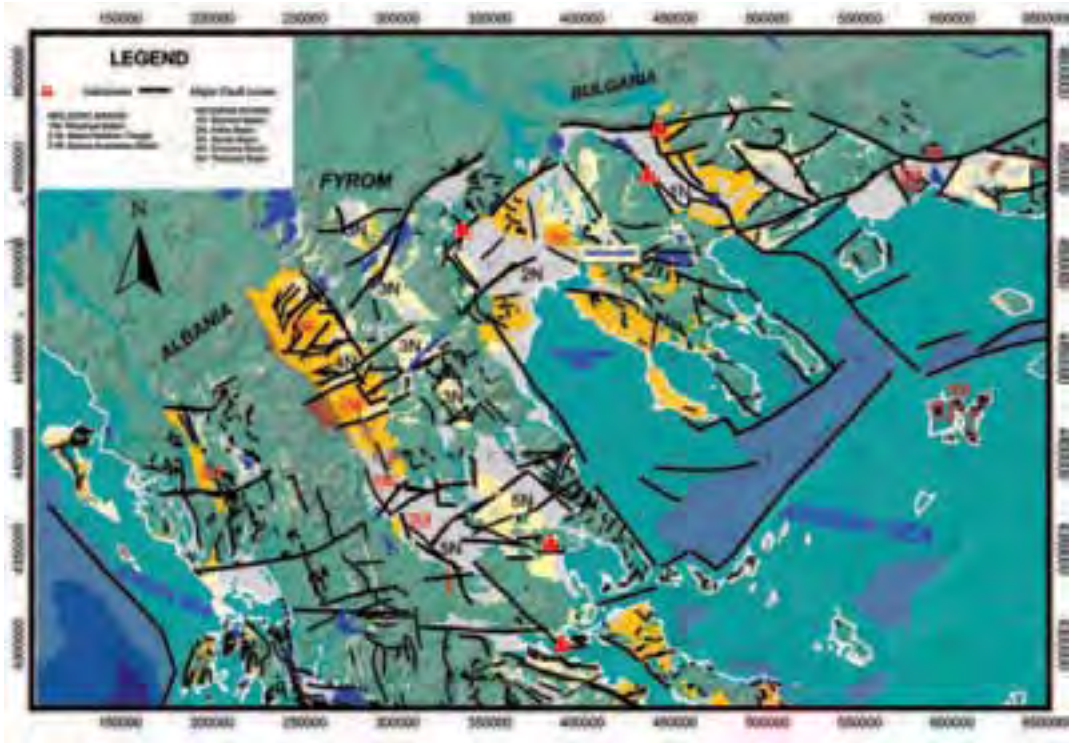

Alpine molassic basins and Neogene and Quaternary basins in Northern Greece

Back Cover:
field trip itinerary on Bulgarian territory

32nd INTERNATIONAL GEOLOGICAL CONGRESS

FIELD TRIP MAP

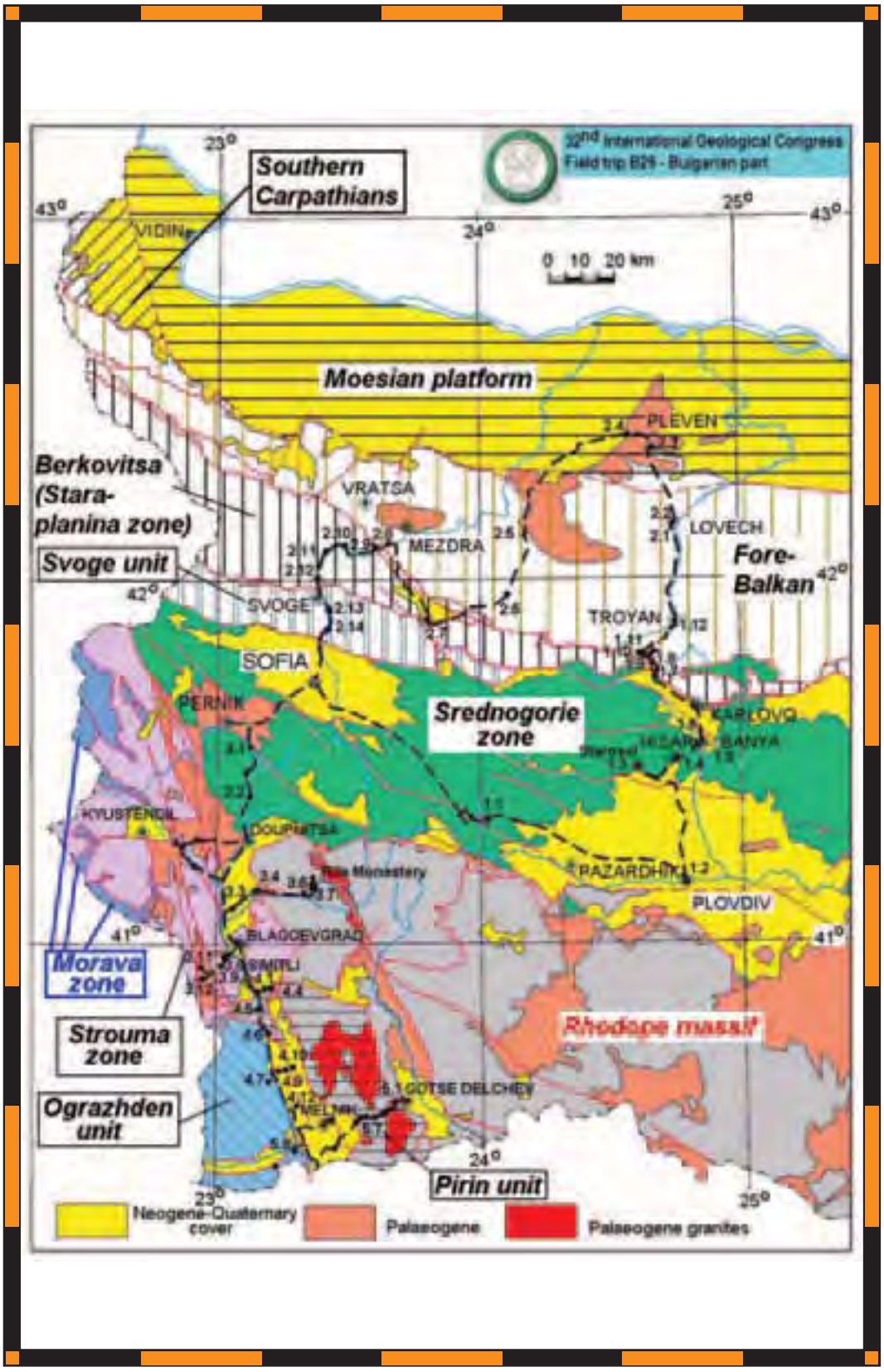

Edited by APAT